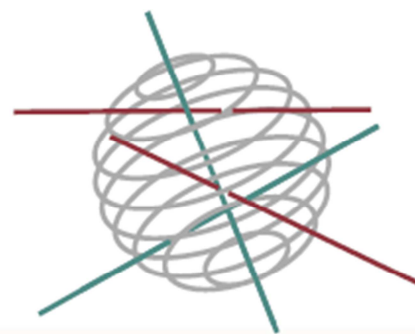


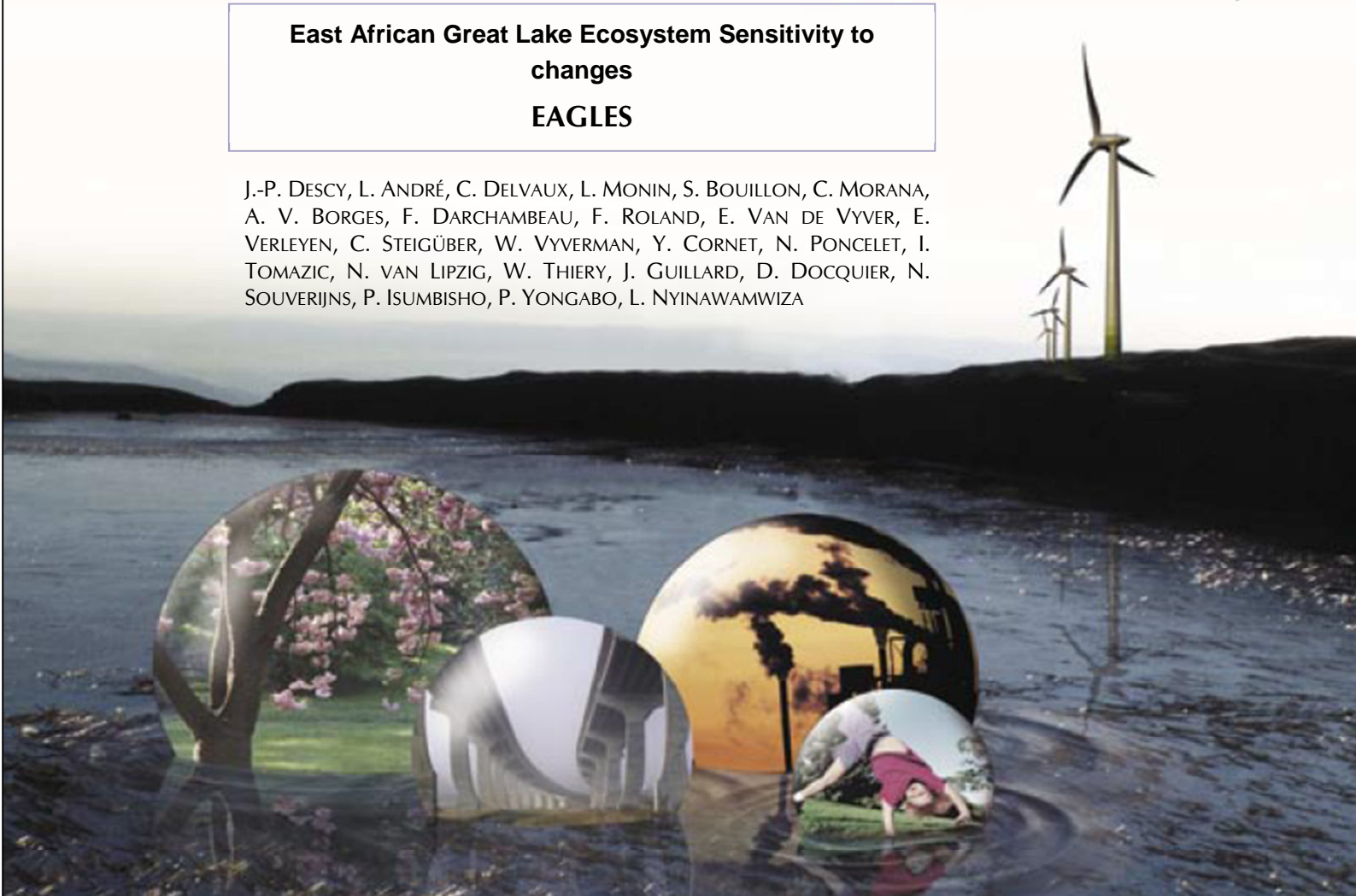
# SSD

SCIENCE FOR A SUSTAINABLE DEVELOPMENT



**East African Great Lake Ecosystem Sensitivity to changes**  
**EAGLES**

J.-P. DESCY, L. ANDRÉ, C. DELVAUX, L. MONIN, S. BOUILLON, C. MORANA, A. V. BORGES, F. DARCHAMBEAU, F. ROLAND, E. VAN DE VYVER, E. VERLEYEN, C. STEIGÜBER, W. VYVERMAN, Y. CORNET, N. PONCELET, I. TOMAZIC, N. VAN LIPZIG, W. THIERY, J. GUILLARD, D. DOCQUIER, N. SOUVERIJNS, P. ISUMBISHO, P. YONGABO, L. NYINAWAMWIZA



ENERGY 

TRANSPORT AND MOBILITY 

AGRO-FOOD 

HEALTH AND ENVIRONMENT 

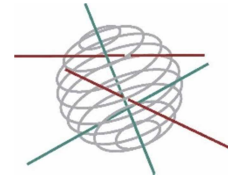
CLIMATE 

BIODIVERSITY   

ATMOSPHERE AND TERRESTRIAL AND MARINE ECOSYSTEMS   

TRANSVERSAL ACTIONS 





***Biodiversity - Terrestrial ecosystems***

FINAL REPORT

**East African Great Lake Ecosystem Sensitivity to changes**

**EAGLES**

**SD/AR/02A**

Promotors

Jean-Pierre Descy, University of Namur  
Luc André, Royal Museum for Central Africa  
Steven Bouillon, K U Leuven  
Alberto Borges, University of Liège  
Wim Vyverman, Ghent University  
Yves Cornet, University of Liège  
Nicole van Lipzig, KU Leuven  
Jean Guillard, UMR CARTELE France

Authors

Claire Delvaux, Royal Museum for Central Africa  
Laurence Monin, Royal Museum for central Africa  
Cédric Morana, KU Leuven  
François Darchambeau, University of Liège  
Fleur Roland, University of Liège  
Elie Verleyen, Ghent University  
Evelien Van de Vyver, Ghent University  
Claas Steigüber, Ghent University  
Nadia Poncelet, University of Liège  
Igor Tomazic, University of Liège  
Wim Thiery, KU Leuven  
David Docquier, KU Leuven  
Niels Souverijns, KU Leuven  
Pascal Isumbisho, ISP-Bukavu, DR Congo  
Parfait Yongabo, University of Rwanda  
Laetitia Nyinawamwiza, University of Rwanda





Published in 2015 by the Belgian Science Policy  
Avenue Louise 231  
Louizalaan 231  
B-1050 Brussels  
Belgium  
Tel: +32 (0)2 238 34 11 – Fax: +32 (0)2 230 59 12  
<http://www.belspo.be>

Contact person: Georges Jamart  
+32 (0)2 238 36 90

Neither the Belgian Science Policy nor any person acting on behalf of the Belgian Science Policy is responsible for the use which might be made of the following information. The authors are responsible for the content.

No part of this publication may be reproduced, stored in a retrieval system, or transmitted in any form or by any means, electronic, mechanical, photocopying, recording, or otherwise, without indicating the reference:

J.-P. Descy, L. André, C. Delvaux, L. Monin, S. Bouillon, C. Morana, A. V. Borges, F. Darchambeau, F. Roland, E. Van de Vyver, E. Verleyen, C. Steigüber, W. Vyverman, Y. Cornet, N. Poncelet, I. Tomazic, N. van Lipzig, W. Thiery, J. Guillard, D. Docquier, N. Souverijns, P. Isumbisho, P. Yongabo, L. Nyinawamwiza. ***East African Great Lake Ecosystem Sensitivity to changes***. Final Report. Brussels : Belgian Science Policy 2015 – 151 p. (Research Programme Science for a Sustainable Development)

**COORDINATOR:**

**P1.** Jean-Pierre Descy, Laboratory of Freshwater Ecology, URBE, Department of Biology, University of Namur, rue de Bruxelles 61, B-5000 Namur. Belgium. [jdescy@unamur.be](mailto:jdescy@unamur.be)

**OTHER PARTNERS:**

- **P2.** Luc André, Royal Museum for Central Africa (RMCA), Leuvensesteenweg, 13, B-3080 Tervuren, [luc.andre@africamuseum.be](mailto:luc.andre@africamuseum.be)
- **P3.** Steven Bouillon, Katholieke Universiteit Leuven (KU Leuven), Department of Earth and Environmental Sciences, Celestijnenlaan 200E, B-3001 Leuven, [steven.bouillon@ees.kuleuven.be](mailto:steven.bouillon@ees.kuleuven.be)
- **P4.** Alberto Borges, Université de Liège, Chemical Oceanography Unit, Institut de Physique (B5a), B-4000 Liège, [alberto.borges@ulg.ac.be](mailto:alberto.borges@ulg.ac.be)
- **P5.** Wim Vyverman, Ghent University, Ghent University, Krijgslaan 281-S8, B-9000 Ghent, [wim.vyverman@ugent.be](mailto:wim.vyverman@ugent.be)
- **P6.** Yves Cornet, Geomatics Unit, University of Liège, Allée du 6 Août, 17 (B5a), B-4000 Sart-Tilman, Belgium, [ycornet@ulg.ac.be](mailto:ycornet@ulg.ac.be)
- **P7.** Nicole van Lipzig, KU Leuven, Department of Earth and Environmental Sciences, Celestijnenlaan 200E, B-3001 Leuven. Belgium. [nicole.vanlipzig@ees.kuleuven.be](mailto:nicole.vanlipzig@ees.kuleuven.be)
- **P8.** Jean Guillard, UMR CARTELE France, 75, avenue de Corzent, F-74203 Thonon-les-Bains cedex, [jean.guillard@thonon.inra.fr](mailto:jean.guillard@thonon.inra.fr)

**AUTHOR(S):**

Jean-Pierre Descy<sup>1</sup>, Luc André<sup>2</sup>, Claire Delvaux<sup>2</sup>, Laurence Monin<sup>2</sup>, Steven Bouillon<sup>3</sup>, Cédric Morana<sup>3</sup>, Alberto V. Borges<sup>4</sup>, François Darchambeau<sup>4</sup>, Fleur Roland<sup>4</sup>, Evelien Van de Vyver<sup>5</sup>, Elie Verleyen<sup>5</sup>, Claas Steigüber<sup>5</sup>, Wim Vyverman<sup>5</sup>, Yves Cornet<sup>6</sup>, Nadia Poncelet<sup>6</sup>, Igor Tomazic<sup>6</sup>, Nicole van Lipzig<sup>7</sup>, Wim Thiery<sup>7</sup>, Jean Guillard<sup>8</sup>, David Docquier<sup>7</sup>, Niels Souverijns<sup>7</sup>, Pascal Isumbiso<sup>9</sup>, Parfait Yongabo<sup>10</sup>, Laetitia Nyinawamwiza<sup>10</sup>

Numbers in superscript refer to partner institution (1: Coordinator, 2: Partner 2, etc), except for:

- 9: Subcontracting 1 – Pascal Isumbiso, ISP-Bukavu, DR Congo, [isumbiso@yahoo.fr](mailto:isumbiso@yahoo.fr)
- 10: Subcontracting 2 – Laetitia Nyinawamwiza, College of Agriculture, Animal Sciences and Veterinary Medicine (CAVM), University of Rwanda, [nyinawamwiza@yahoo.fr](mailto:nyinawamwiza@yahoo.fr)

**PROJECT WEBSITE(S): [www.eagles-kivu.be](http://www.eagles-kivu.be)**



**TABLE OF CONTENT**

<b>SUMMARY</b> .....	<b>9</b>
Context .....	9
Objectives .....	9
Main conclusions.....	10
Output for sustainable development .....	13
Keywords.....	14
<b>1. INTRODUCTION</b> .....	<b>15</b>
1.1 Context .....	15
1.2 Objectives .....	15
1.3 Expected outcomes.....	16
<b>2. METHODOLOGY AND RESULTS</b> .....	<b>19</b>
<b>2.1. Exploitation of existing data</b> .....	<b>19</b>
2.1.1. Data base management .....	19
2.1.2 Data mining .....	19
2.1.3. Sediments.....	20
<b>2.2. In situ studies (2011-2014) and acquisition of new data</b> .....	<b>20</b>
<b>2.2.1. Water column monitoring of physical, chemical, biological variables</b> .....	<b>20</b>
2.2.1.1 Mixolimnion monitoring.....	20
2.2.1.2 Greenhouse gas distribution in the water column of Lake Kivu .....	23
2.2.1.3. Complementary measurements.....	26
2.2.1.4 Water geochemistry, Biogenic silica, incubation experiments and Silicon isotopes in the water column.....	28
2.2.1.5 Remote sensing .....	49
2.2.1.6 Fish surveys.....	60
<b>2.2.2. Carbon pathways through the planktonic food web</b> .....	<b>74</b>
2.2.2.1. Characterization of the different organic matter pools .....	74
2.2.2.2. Significant production of DOC by phytoplankton in Lake Kivu and its uptake by heterotrophic prokaryotes .....	78
<b>2.2.3. Carbon and nutrient cycling in the redoxcline of Lake Kivu</b> .....	<b>78</b>
2.2.3.1. Aerobic methanotrophy .....	79
2.2.3.2. Anaerobic methanotrophy .....	80
2.2.3.3. Chemoautotrophic and anoxygenic photoautotrophic pathways of CO <sub>2</sub> fixation in the redoxcline of Lake Kivu .....	82
2.2.3.4. Denitrification, anaerobic ammonium oxidation and dissimilative reduction of nitrate to ammonium .....	84
2.2.3.5. The importance of methanotrophy and chemoautotrophy in the ecosystem functioning of Lake Kivu.....	86
<b>2.2.4. Sediment core retrieval – new cores and analyses</b> .....	<b>87</b>
2.2.4.1. Materials and methods.....	87
2.2.4.2. Results and discussion .....	90
<b>2.3. Laboratory studies (2011-2014)</b> .....	<b>99</b>
<b>2.3.1 Diatom cultures</b> .....	<b>99</b>
<b>2.4. Data analysis and modeling</b> .....	<b>101</b>
<b>2.4.1 Statistical data analysis</b> .....	<b>101</b>
<b>2.4.2 Modelling of present conditions</b> .....	<b>104</b>
2.4.2.1 Climate simulations for the period 1999-2008.....	104

- 2.4.2.2 Lake hydrodynamics and ecological simulations for the period 2002-2013 ..... 119
- 2.4.3 Past changes .....120**
  - 2.4.3.1 Past climate and ecology ..... 120
- 2.4.4 Prediction of future changes & ecosystem responses .....121**
  - 2.4.4.1 Climate projections..... 121
  - 2.4.4.2 Effects of methane exploitation ..... 125
- 3. POLICY SUPPORT.....127**
- 4. DISSEMINATION AND VALORISATION.....133**
- 5. PUBLICATIONS .....135**
  - 5.1 Publications of the teams.....135**
    - 5.1.1 Peer review (published and in press) ..... 135
  - 5.2 Co-publications.....136**
    - 5.2.2 Others ..... 136
- 6. Acknowledgements.....141**
- 7. References.....143**
- ANNEXES .....151**

## ACRONYMS and ABBREVIATIONS

AATSR Advanced Along-Track Scanning Radiometer  
aer\_opt Aerosol option for atmospheric correction in SeaDAS  
AGL: African Great Lakes  
Aqua NASA Earth Observing Satellite (EOS/ PM-1) launched 2002  
AVHRR Advanced Very High Resolution Radiometer  
AWS: Automatic Weather Station  
BT Brightness temperature  
chl-a Chlorophyll-a  
CMIP5: Coupled Model Intercomparison Project Phase 5  
CORDEX: CO-ordinated Regional Downscaling EXperiment  
COSMO: COnsortium for Small-scale MOdelling numerical weather prediction model  
COSMO-CLM: COSMO model in CLimate mode  
COSMO-CLM<sup>2</sup>: COSMO-CLM<sup>2</sup> coupled to the Community Land Model  
COST733: Weather type classification software  
CTL: COSMO-CLM<sup>2</sup> control simulation (reanalysis downscaling)  
ENVISAT ENVIRONMENT SATellite from European Space Agency  
FUT: COSMO-CLM<sup>2</sup> future simulation (GCM downscaling)  
HIS: COSMO-CLM<sup>2</sup> historical simulation (GCM downscaling)  
HPLC High Performance Liquid Chromatography  
K490 Diffuse Attenuation Coefficient at 490 nm wavelength  
LakeMIP: Lake Model Intercomparison Project  
LSWT Lake Surface Water Temperature  
LwWater-leaving radiance  
MCSST Multi-Channels Sea Surface Temperature  
MODIS Moderate Resolution Imaging Spectroradiometer  
MUMM Management Unit of the North Sea Mathematical Models  
NASA National Aeronautics and Space Administration  
NIR Near Infrared  
NLSST Non Linear Sea Surface Temperature  
NOL: COSMO-CLM<sup>2</sup> no-lakes simulation (reanalysis downscaling)  
OBPG Ocean Biology Processing Group  
OC Ocean Color  
REE Rare Earth Elements  
Rrs Remote sensing reflectance  
RS Remote Sensing  
RTM Radiative Transfer Model  
SeaDAS Software suite developed by NASA for the processing visualization, analysis and quality control of ocean color data  
SST Sea Surface Temperature  
Terra NASA Earth Observing Satellite (EOS/ AM-1) launched 1999  
TOA Top-Of-Atmosphere  
TS Time Series  
UTC Coordinated Universal Time



## **SUMMARY**

### **Context**

Large East African Rift lakes have been changing rapidly during the last decades. They typically have a relatively high productivity compared to large temperate lakes and sustain active fisheries providing local populations with a relatively cheap source of proteins. However, human-induced changes, including climate change, can have significant negative effects on primary production of these lakes, as shown for Lake Tanganyika. It is likely that these decreases in primary production have affected secondary producers and fisheries, but, before being able to predict the extent of the primary productivity changes and how they affect whole ecosystem production, an improved understanding of ecosystem function and food web processes is required.

Lake Kivu, despite its relatively small size (2370 km<sup>2</sup>) among the East African Great Lakes, is of particular interest for several reasons : on the one hand, the lake mixolimnion responds to the same atmospheric forcing as the other Rift lakes, with a relatively weak thermal stratification, so that a great sensitivity to changes in the regional climate is expected; on the other hand, the deep waters of the lake, separated from the surface by a salinity gradient, present a unique structure due to geothermal inflows, with increases of temperature and salinity by steps, and very large amounts of dissolved carbon dioxide and methane, particularly below 270 m depth. Nowadays methane harvesting appears as a means for reducing the risk of gas eruption while producing energy for the surrounding countries, but the extraction should be made in such a way as to avoid harmful consequence for the other lake resources, including fisheries. It is then relevant to complete studies on the lake ecosystem, in order to understand its present functioning and how and why it changed in the past, and to predict future changes as a result of natural changes (climatic, volcanic,...) and of anthropogenic impacts, as those which may result from large-scale methane exploitation.

### **Objectives**

The general objective of the EAGLES project was to understand, monitor and forecast how the ecosystem of a large African lake, Lake Kivu, responds to human-induced changes, in order to predict the effects of environmental changes on the goods and services provided by the ecosystem.

The first objective, exploitation of existing data, consisted mainly in the synthesis of the data acquired in the period 2002-2010 in previous research and cooperation projects. It resulted in a database including limnological variables, plankton, fish abundance and meteorological data that allowed a very good view of the knowledge on Lake Kivu, unique for an East African great lake. In relation with this work, a synthesis of the knowledge of Lake Kivu limnology and biogeochemistry was published in a book printed by Springer in its "Aquatic Ecology Series".

The second objective – acquisition of new data – was completed by undertaking new *in situ* studies, with a substantial contribution of the African partners in Rwanda and DR Congo, which were in charge of monitoring of the mixolimnion variables (limnology and plankton) and of fisheries surveys. Regular acquisition of mixolimnion data was carried out in the two

monitoring sites - Gisenyi, Rwanda) and Ishungu (DR Congo) – from 2011 to mid-2014 on a monthly basis at least. In addition, we organised six field campaigns including several Belgian and foreign teams, in July 2011, February 2012, October 2012, May 2013, September 2013, and August 2014. During these field cruises, sampling and field experiments took place in both study sites. The main activities were devoted to detailed process orientated investigations on carbon and nutrient pathways in the mixolimnion and in the chemocline, such as on the carbon pathways in the microbial food web, methane oxidation, the nitrogen cycle, complementing the monitoring of variables. Sediment core collection was also carried out, in order to allow paleolimnological studies based on several proxies, and fresh diatom algae were collected for laboratory culturing in Belgium. Also a new state-of-the-art automatic weather station was installed on an offshore platform. This objective was largely fulfilled and the data were organised into several data bases: a CTD data base and a phytoplankton pigment data base, combining the data acquired during the project with those from the previous studies, allowing investigation of the changes that have occurred in the lake mixolimnion since 2002 (Ishungu) or since 2005 (Gisenyi).

A third objective was to determine ecophysiological requirements of key diatoms isolated from Lake Kivu by conducting laboratory studies on isolated taxa in pure cultures, under conditions mimicking those prevailing in the lake (light, temperature, nutrient concentration). These cultures would also allow the study of Si isotopic fractionation by different species

The final step was devoted to data processing and modeling, in order to:

- link atmospheric variability and lake physics: two-way interaction between atmospheric conditions on the one hand and lake temperature and water column structure on the other hand, aiming to understand/simulate the regional climate and variability of seasonal mixing processes, and to forecast long term changes,
- link physical processes with biological and ecological (e.g. nutrient availability) processes: diversity and biomass of plankton, fate of primary production in the planktonic food web, CH<sub>4</sub> fluxes, fish abundance and fisheries yield,
- predict future changes of ecosystem processes and resources, as a result from fisheries management, exploitation of methane from the deep waters, and climate change (linking global climate to regional climate).

Finally, we examined how the methodologies used and developed in the research project could be applied to other large African lakes, particularly Lake Tanganyika.

## **Main conclusions**

The exploitation of the existing data and the acquisition of new data have led to several key insights on various components and processes of the ecosystem of Lake Kivu. Among the most notable results is a general view of the carbon transfer through the food web, including the microbial food web and the estimates, on an annual basis of the main flows of organic matter. This allowed to show that:

- contrary to the assumptions made from a planktivore introduction in the pelagic zone of the lake, the efficiency of the planktonic food web is in a range comparable to that of the other East African great lakes of similar trophic status;

- the relatively low fish yield in Lake Kivu stems from a low efficiency at the zooplankton-fish interface.

The study of the ecological processes, based on experiments conducted in the field, showed that Lake Kivu is net autotrophic, which is a quite different view of the functioning of an oligotrophic lake from that presented in the current limnological literature. This conclusion may be applicable to other tropical large lakes where nutrient availability is mainly governed by internal loading. The interannual variability of phytoplankton production can be high, probably explaining variations at the consumer level, including fish. This variability is greatly influenced by the regional climate, as shown by teleconnections with indices determined in the tropical ocean. Another key result pertaining to the fate of primary production in tropical oligotrophic lakes is that a large fraction of phytoplankton production occurs as dissolved production (excretion of organic molecules) which are used by heterotrophic bacteria, thereby fuelling the microbial food web. In Lake Kivu, this fraction amounts to ~50 % of the total primary production. Complementary measurements using sediment traps allowed investigating the fate of particulate primary production: the average percentage of this production exported to the deep waters was ~8 %, with substantial variation (2.7 – 22.2 %), and all phytoplankton groups contributed to the sediment flux.

Another result, more specific to Lake Kivu, is that the emissions of CO<sub>2</sub> and CH<sub>4</sub> to the atmosphere are low, despite the very large amount of dissolved CH<sub>4</sub> and CO<sub>2</sub> in the deep waters. This paradox stems from the fact that microbial transformation of the CH<sub>4</sub> diffusing upward occurs in the oxycline. Chemoautotrophic processes are also significant in the lake's carbon budget: notably, the nitrogen fluxes to the surface waters is largely dependent on microbial activities and in the balance between nitrification and denitrification in the oxycline.

The geochemical studies in the surface and deep waters yielded several results pertaining to the mineral composition of the lake waters and to the diatom productivity and its control by phosphorus availability. For instance, they confirmed that most of the solutes of the Lake Kivu waters are mainly controlled by the hydrothermal alteration of the volcanics along the northern shoreline, the most probable recharge source for these hydrothermal fluids being the surface water of the lake itself, locally mixed with magmatic-derived and meteoritic-derived fluids. The annual quick changes in Ba distribution and P/Na as well as the rapid  $\delta^{30}\text{Si} - D_{\text{Si}}$  re-equilibration of the upper chemocline after the diatom mineralization demonstrate that the lake water mixing is more dynamic than previously thought. The strong P limitation that controls the diatom productivity throughout the year is dependent of a "bathtub ring" oxic-anoxic precipitation at the mixolimnion-chemocline interface. The strong Si-Ba correlation and the strong Ba depletion of the surface waters when the diatom productivity was larger indicate that the Ba cycle is partly controlled by the Barite precipitation and dissolution consecutive to the decay of diatom biomass. The changes in  $\delta^{30}\text{Si}$  vs  $D_{\text{Si}}$  are very sensitive to the global seasonal diatom productivity and mineralization in Lake Kivu.

The use of remote sensing, through the processing of MODIS data, was extensively tested on Lake Kivu, in order to assess surface chlorophyll a (ocean color products) and water surface temperature (LSWT). Due to high and very frequent radiometric alterations of the signal in the case of Lake Kivu, the optimization of the computation of these products has

been based on a dataset from Lake Tanganyika. Several constraints (on stray light, cloudiness) had to be reduced in the filtering of the computed values; consequently, the final time series and the validation of the results were not directly representative of the *in situ* measurements. However, the spatio-temporal aggregation of the computed chlorophyll a values greatly reduced the effect of local highly inaccurate values. Such temporally aggregated time series can efficiently be exploited for analysis with other environmental factors, particularly to assess variations at a seasonal scale.

Similar uncertainties were encountered when determining lake water surface temperature from the MODIS products. The model was adjusted using daily data with low radiative perturbation, resulting in high uncertainty in situations of high radiative perturbation. The results from our model were affected by the same anomalies than ARC-Lake dataset, with lower spatial and temporal amplitude than the reality. However weekly aggregated time series provided results that are in the range of the *in situ* measurements.

The fishery survey conducted in the Rwandese part of the lake showed that *Limnothrissa miodon*, the “Tanganyika sardine” remains the major species caught in the pelagic zone of Lake Kivu, despite the recent introduction of *Lamprichthys tanganicanus*. If *Limnothrissa* and *Lamprichthys* adults do compete for large zooplankton and have significant niche overlap, it seems that *Lamprichthys* did not invade the pelagic zone but preferred the littoral zone. The fishery survey, together with the hydroacoustic surveys, show that seasonal variations of the catches may be related to resource-dependent variations in the sardine stock, rather than resulting from overexploitation. The fact that the catches are greatest at the beginning of the rainy season, after reduced catches in the dry season months, may result from greater abundance of large zooplankton following the phytoplankton peak, allowing growth to the young fish. Hence, the variation of the catches over the year should be seen as a natural phenomenon depending on the lake functioning, and not a result of poor fishery management. The hydroacoustic surveys, completing those conducted in 2008 and those from the “Biological baseline of Lake Kivu”, show that is little seasonal variation of the fish stock and that no significant change of the sardine stock occurred since the end of the 1980's.

Geochemical, fossil diatom and fossil pigment analyses were carried out on sediment cores. Although there is significant uncertainty regarding the age of the sediment layers, the upper 27 cm of the cores showed that substantial changes of productivity occurred in a period of about 150 years BP, depending on changes in nutrient supply, most likely driven by changes of the stratification/mixing regime in the mixolimnion. The peaks of diatom productivity and changes in their community structure are neither triggered nor boosted by the hydrothermal activity. Between 5 and 3 cm an increase of magmatic-related elements as well as carbonate deposition is evident which is related to hydrothermal activity. Given the uncertainties on the age of these layers, it is not possible to detect a change that could be related to the introduction of the Tanganyika sardine.

Modelling lake hydrodynamics and ecology, in the present conditions (period 2002-2012) was an important component of the project. Lake hydrodynamics were simulated using the one-dimensional lake model FLake, which was extensively evaluated and tested over two African Great Lakes. Careful forcing data correction and model configuration allowed for the

correct representation of mixed layer depths and water temperatures of Lake Kivu. However, while lake surface temperature predictions are robust, bottom temperatures appear very sensitive to perturbations in the external parameters and meteorological driving data. Constraints on the applicability of the model are therefore identified: while this model is a suitable tool for lake surface temperature parameterizations in climate models, it cannot be used to study climate change influences on lake stratification and hydrodynamics. In addition, the skill of the FLake model is benchmarked against six other lake models. FLake demonstrates good predictive skill relative to the other models in terms of water column temperatures and lake enthalpy change, but its limitations in terms of representing stratification and hydrodynamics are confirmed by sensitivity experiments. Finally, a process study established the primary control of dry-season evaporative-driven cooling on seasonal mixed layer dynamics.

Evaluation of the COSMO-CLM<sup>2</sup> regional climate model simulation with optimized configuration reveals good performance compared to both in situ and satellite observations, notably for lake surface temperatures and precipitation. Comparison to a no-lakes simulation indicates that the four major African Great Lakes nearly double the annual precipitation amounts over their surface, but hardly exert any influence on precipitation beyond their shores. Most of the lakes also cool the annual mean near-surface air, this time with pronounced downwind influence. The lake-induced cooling happens during daytime, when the lakes absorb incoming solar radiation and inhibit upward turbulent heat transport. At night, when this heat is released, the lakes warm the near-surface air. The comparison also reveals the profound lake influence on atmospheric dynamics and stability: the example of Lake Victoria shows how lakes induce circular airflow with over-lake convective inhibition during daytime, and the reversed pattern at night.

The coupled one-dimensional hydrodynamic-ecosystem model DYRESM–CAEDYM was used as a platform for developing ecological and biogeochemical modeling of Lake Kivu ecosystem. The model reproduced the seasonal stratification of the mixolimnion in the lake during the period 2002-2013 and the seasonal nutrient upwelling, as well as the seasonal alternation between cyanobacteria and diatoms. Simulations of the operation of a methane power plant were also carried out: it showed that the oxic layer of the lake would be reduced, as result of a substantial increase of chlorophyll a, and that a shift phytoplankton composition would occur.

## **Output for sustainable development**

The first key output of EAGLES is relevant to the lake's monitoring and management in a context of environmental changes driven by climate change and aquatic resources exploitation. We provide a compilation of data (prior and from the project) and insight on the status of the lake ecosystem, that is developed in the top 60 m of the water column.

Regarding fisheries yield and management, the status of the fishery was so far incompletely known, based on studies carried out decades ago and in parts of the lake. The results of the EAGLES project suggest that the sardine fishery is sustainable, but that, the fish production may vary strongly depending on variations in the regional climate that drives plankton productivity. Hence, the regulation of the fishery, on both parts of the lake, should take into

account those natural, climate-related, variations, by adapting the fishing effort to the fish production that could be predicted from monitoring the planktonic resources. Therefore we recommend to conduct fisheries surveys over the whole lake, in parallel with periodic hydroacoustic surveys. Moreover, as effects from variations of climate-driven plankton productivity are expected, the data from the fish surveys should be examined together with the data on weather, limnology and plankton. Such analyses could be useful to achieve predictions of the fish yield and for regulating the sardine fishery in order to ensure its sustainability.

In addition to variations of the lake's productivity related to climate variability, an impact of the large-scale methane exploitation is expected, as demonstrated by model simulations, with severe alteration of water quality and ecosystem status. Therefore, we recommend to carry out long-term monitoring of limnological and planktological variables around the power plants and at reference lake sites.

Remote sensing (RS) can also be recommended for monitoring future changes affecting seasonal cycles and trends. Aggregated time series (weekly for the whole lake) of ocean color (providing estimates of surface chlorophyll a) and LSWT (allowing estimates of the surface temperature of the lake) clearly show the seasonal cycles. Therefore, RS could be used for assessing long term trends under several conditions.

The strong imprint of the lakes on the hydrological cycle additionally highlights the vulnerability of local communities to lake-induced precipitation and storm activity. On the short term, we therefore recommend the installation of early warning systems for over-lake thunderstorms (or their improvement at locations where they are already present). This may, for instance, be achieved through operational numerical weather prediction systems capable of accounting for the relevant lake-atmosphere interactions. Such prediction systems should moreover operate at sufficiently high resolution to resolve the relevant mesoscale atmospheric processes. Insights from our analyses may thereby provide useful information for improving the skill of these predictions systems.

The climate model projections for the end-of-the-century underline the major role for Lake Victoria in modulating precipitation changes. Under a high-emission scenario (RCP8.5), over-lake extreme precipitation may intensify up to three times faster towards 2071-2100 relative to 1981-2010 compared to the projected change over the surrounding land (after isolation from the mean change). In the context of climate change and lake-induced weather hazards, we therefore strongly recommend the development of climate change adaptation strategies in the African Great Lakes region, in particular measures aiming at enhanced navigation safety for the fishermen operating on their surface.

For defining adaptation measures aiming at conserving present-day ecosystem functioning in the context of climate change (and methane exploitation in the case of Lake Kivu), rigorous testing through model simulations and case studies is required before any implementation can be considered.

## **Keywords**

Environmental changes, great lakes, monitoring, resources, ecological processes, modelling.

## 1. INTRODUCTION

### 1.1 Context

Large East African Rift lakes have been changing rapidly during the last decades. They typically have a relatively high productivity compared to large temperate lakes and have active fisheries providing local populations with a relatively cheap source of proteins. However, human-induced changes, including climate change, can have significant negative effects on primary production of these lakes, as shown for Lake Tanganyika (Verburg et al., 2003 ; Stenuite et al., 2007 ; Tierney et al., 2010). It is likely that these decreases in primary production have affected secondary producers and fisheries, but, before being able to predict the extent of the primary productivity changes and how they affect whole ecosystem production, an improved understanding of ecosystem function and food web processes is required.

Lake Kivu, despite its relatively small size (2370 km<sup>2</sup>) among the East African Great Lakes, is of particular interest for several reasons : on the one hand, the lake mixolimnion responds to the same atmospheric forcing as the other Rift lakes (e.g. Sarmiento et al., 2006), with a relatively weak thermal stratification (Spigel and Coulter, 1996), so that a great sensitivity to changes in the regional climate is expected; on the other hand, the deep waters of the lake, separated from the surface by a salinity gradient, present a unique structure due to geothermal inflows, with increases of temperature and salinity by steps, and very large amounts of dissolved carbon dioxide and methane, particularly below 270 m depth (see Schmid and Wuëst, 2012). Nowadays methane harvesting appears as a means for reducing the risk of gas eruption while producing energy for the surrounding countries (e.g. Nayar, 2009), but the extraction should be made in such a way as to avoid harmful consequence for the other lake resources, including the fishery (Wüest et al. 2012). All this makes it even more relevant to complete studies on the lake ecosystem, in order to understand its functioning and how and why it changed in the past, and to predict future changes as a result of climate change and other anthropogenic impacts, as those which may result from large-scale methane exploitation.

### 1.2 Objectives

The general objective of the EAGLES project is to understand, monitor and forecast how the ecosystem of a large African lake, Lake Kivu, responds to human-induced changes, in order to predict the effects of environmental changes on the goods and services provided by the ecosystem.

In this project, we exploited the important database acquired in the period 2002-2010 (WP1). The existing database includes limnological variables, plankton records (diversity, biomass and production of phyto- and zooplankton), surveys of fish abundance based on

hydroacoustics, meteorological data and sediment archives (biogeochemical and biological proxies).

Data time series have been extended by new datasets of the same variables acquired during the period of the project (2011 – mid 2014) (WP2). New *in situ* studies were also conducted in order to increase our present understanding of ecosystem biodiversity and functioning (WP2). This part of the project includes monitoring of the mixolimnion by regular sampling and measurements, field experiments for determining the carbon and nutrient pathways within the planktonic food web, studies of past and present plankton productivity using, respectively, sediment and water column proxies, and surveys of fish stocks and of fisheries yield.

Laboratory studies (WP3) have been undertaken to determine ecophysiological requirements of key diatoms isolated from Lake Kivu and for studying Si isotopic fractionation by different species under conditions mimicking those prevailing in the lake (light, temperature, nutrient concentration).

The final step was devoted to data processing and modeling (WP4), in order to:

- link atmospheric forcing and the lake physics: relation between atmospheric conditions and lake temperature and water column structure, aiming to understand/simulate the variability of seasonal mixing processes and forecast long term changes,
- link physical processes with biological and ecological (e.g. nutrient availability) processes: diversity and biomass of plankton, fate of primary production in the planktonic food web, fish abundance and fisheries yield,
- predict future changes of ecosystem processes and resources, as a result from fisheries management, exploitation of methane from the deep waters, and climate change (linking global climate to regional climate).

Finally, we examined how the methodologies used and developed in the research project could be applied to other large African lakes, particularly Lake Tanganyika.

The objectives of WP5 (Network coordination and dissemination) were 1) to organise the general project planning and the coordination among the various work packages, 2) to establish contacts with other relevant national and international programs, 3) to ensure data and information exchange among the partners and other national and international scientific communities, and 4) to valorise and disseminate the project outputs.

### **1.3 Expected outcomes**

- Historical databases (acquired by some partners on other projects and from data mining/rescue) on water column and sediment chemistry and biology
- New datasets and databases on chemistry and biology of the water column and sediments, including paleo-reconstructions
- Remote sensing reconstructed time series (surface temperature, Chla and K490 raw)
- Statistics on fish stocks and fisheries (2011 to 2013)

- Coupled hydrodynamic-ecosystem Kivu model on present day functioning and analysis of future impacts (climate change, CH<sub>4</sub> extraction)
- Advice for sustainable management of fisheries and CH<sub>4</sub> extraction in L. Kivu
- Web-site (<http://www.eagles-kivu.be/>)



## 2. METHODOLOGY AND RESULTS

### 2.1. EXPLOITATION OF EXISTING DATA

#### 2.1.1. Data base management

The Lake Kivu EAGLES database has been created and uploaded to the main EAGLES web site (<http://www.eagles-kivu.be>). It presently contains the following items:

- The EAGLES logo
- The original proposal (i.e. the full text of the project)
- The presentations of the different partners at the first African and European follow-up committees organized at Kigali in July 2011 and at BELSPO office in Dec 2011 and March 2013
- All data (vertical CTD casts and measurements on samples from different depths) from the monitoring at the two sites sampled by the African subcontractants, as well as of the six field campaigns of the Belgian network (July 2011, January 2012, September-October 2012, May 2013, August-September 2013, and July-August 2014)
- All data on vertical profiles from previous Belgian projects (CAKI, supported by FNRS, and ECOSYKI project, supported by CUD)
- All data on phytoplankton biomass and composition as determined from the analysis of marker pigments by HPLC, from 2002 to 2010, to which the data collected till mid-2014 were subsequently added
- A collection of “grey literature” (MSc and PhD theses and reports from students who participated in studies on Lake Kivu)
- A collection of published papers by members of the EAGLES teams

All data were checked for units, headings and major errors (quality check level 1).

#### 2.1.2 Data mining

Data and metadata from 5 previous field campaigns (CAKI project, 2007-2010) were compiled and were made available from the project web page with a restricted access (1.1). These data include CTD casts and biogeochemical data, as well as data on fish stocks from two hydroacoustic campaigns carried out in 2008. The restricted page also provides pdfs of available grey literature documents (PhD thesis and Master thesis), and previous publications on Lake Kivu from members of the EAGLES consortium. Meteorological data in the Lake Kivu area were compiled from the Rwanda meteorological agency, the ISP-Bukavu weather station and weather stations from RMCA.

The gathering of the existing data in the database has allowed a synthesis on various components and processes of the ecosystem of Lake Kivu. Whenever needed, statistical methods have been applied for data processing. These syntheses allowed submission of manuscripts to international journals (Borges et al. 2011, Masilya et al. 2011, Guillard et al. 2012, Stoyneva et al. 2012, Sarmiento et al. 2013, Darchambeau et al. 2013a, Loiselle et al.

2014) as well as the edition as a peer-reviewed book of a synthesis on the limnology and biogeochemistry of the lake (Descy et al. 2012).

### **2.1.3. Sediments**

The dataset obtained from a previous paleolimnological analysis of a 40-cm sediment core (Knops 2009) has been stored in the Kivu database. The data include the relative abundance of diatom taxa, pigment concentrations (Chla and derivatives from *in situ* degradation, carotenoids, bacteriochlorophylls), concentrations of organic matter, carbonates, total nitrogen and phosphorus concentrations, and fossil invertebrate remains.

## **2.2. IN SITU STUDIES (2011-2014) AND ACQUISITION OF NEW DATA**

### **2.2.1. Water column monitoring of physical, chemical, biological variables**

#### **2.2.1.1 Mixolimnion monitoring**

The monitoring of the water column has been carried out on a monthly or fortnightly basis in the Ishungu basin (28.9775°E, 2.3374°S; RD Congo) and in the main basin off Gisenyi (29.23745°E, 1.72504°S; Rwanda), the two monitoring sites located respectively in the southern and northern part of the lake. The main limnological variables have been recorded by vertical CTD profiles, and samples for phytoplankton pigments analysis were collected every 5 m from 0 to 20 m, and every 10 m from 20 to 60 m. In the regular monitoring performed by the local subcontractors, sampling for nutrient analysis has been limited to one fixed mixolimnion depth (10 m), whereas detailed nutrient profiles have been obtained during the field campaigns of the Belgian network. For the analysis of phytoplankton pigments, the techniques have been described in Sarmiento et al. (2007). HPLC analysis allows to obtain an estimate of total phytoplankton biomass (chlorophyll a concentration) with a great precision, as well as the concentrations of specific marker pigment (chlorophylls other than chlorophyll a and carotenoids), which allow an estimate of the biomass of major phytoplankton groups. The CHEMTAX software (Mackey et al., 1996) was used to process the pigment data and to calculate the contribution of these groups (phyla or classes) to chlorophyll a, following a procedure described in Sarmiento et al. (2007).

The results from the analyses of the samples collected in 2011 and 2014 have been stored in the EAGLES database. The database includes limnological data (CTD casts, concentrations of nutrient and dissolved gases), biological data (phytoplankton biomass and composition at the class level, zooplankton biomass, ...), and ecological (primary production, CH<sub>4</sub> oxidation rates, ...) and biogeochemical ( $\delta^{13}\text{C-DIC}$ ,  $\delta^{13}\text{C-POC}$ , ...) variables.

The CTD vertical profiles acquired during the project at the two sites allow to assess the physical status of the water column, depending mainly on the seasonal cycle. Figure 1 provides an example extracted from the data base, showing how temperature and oxygenation changed in the water column between the rainy season (March) and the dry season (August). In the rainy season, the water at the top of the mixolimnion was warmer and less dense, which created a stratification affecting the distribution of dissolved substances (oxygen, nutrients). As shown in fig. 1, the oxic layer was reduced to the top 30

m (or less) in the rainy season (blue line), as vertical mixing was reduced to this top layer. The conditions changed dramatically in the dry season: as a result of cooling of the top surface layers, the density difference between the surface and deep layers of the mixolimnion disappeared, allowing deeper vertical mixing that enabled re-oxygenation down to 50 m or deeper. The deeper mixing also affected nutrient and plankton distribution, as well as the biogeochemical cycles (see 2.1.2, 2.2 and 2.3). Seasonal variations of conductivity and pH were relatively limited compared to temperature and oxygen, but varied vertically within the chemocline, creating contrasting conditions for the microbial communities involved in the biogeochemical cycles (see below).

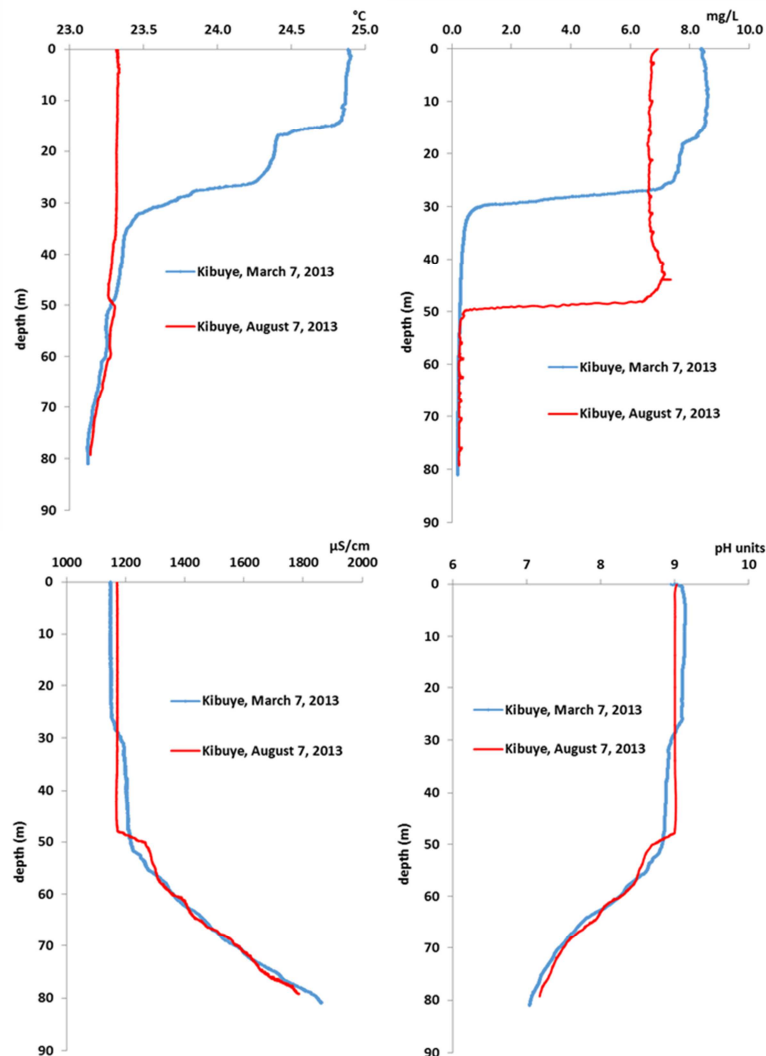


Fig. 1. Examples of vertical profiles of limnological variables, extracted from the CTD data base. Top left: water temperature; top right: dissolved oxygen; bottom left: specific conductivity at 25°C; bottom right: pH. Red line: dry season conditions; blue line: rainy season conditions. Note the change in oxycline position between rainy and dry seasons.

Phytoplankton responded to the seasonal changes, with peaks of biomass (as measured by chlorophyll a concentration) during the dry season, when deeper mixing allowed greater nutrient availability, but also presented large variations depending on the year (fig. 2).

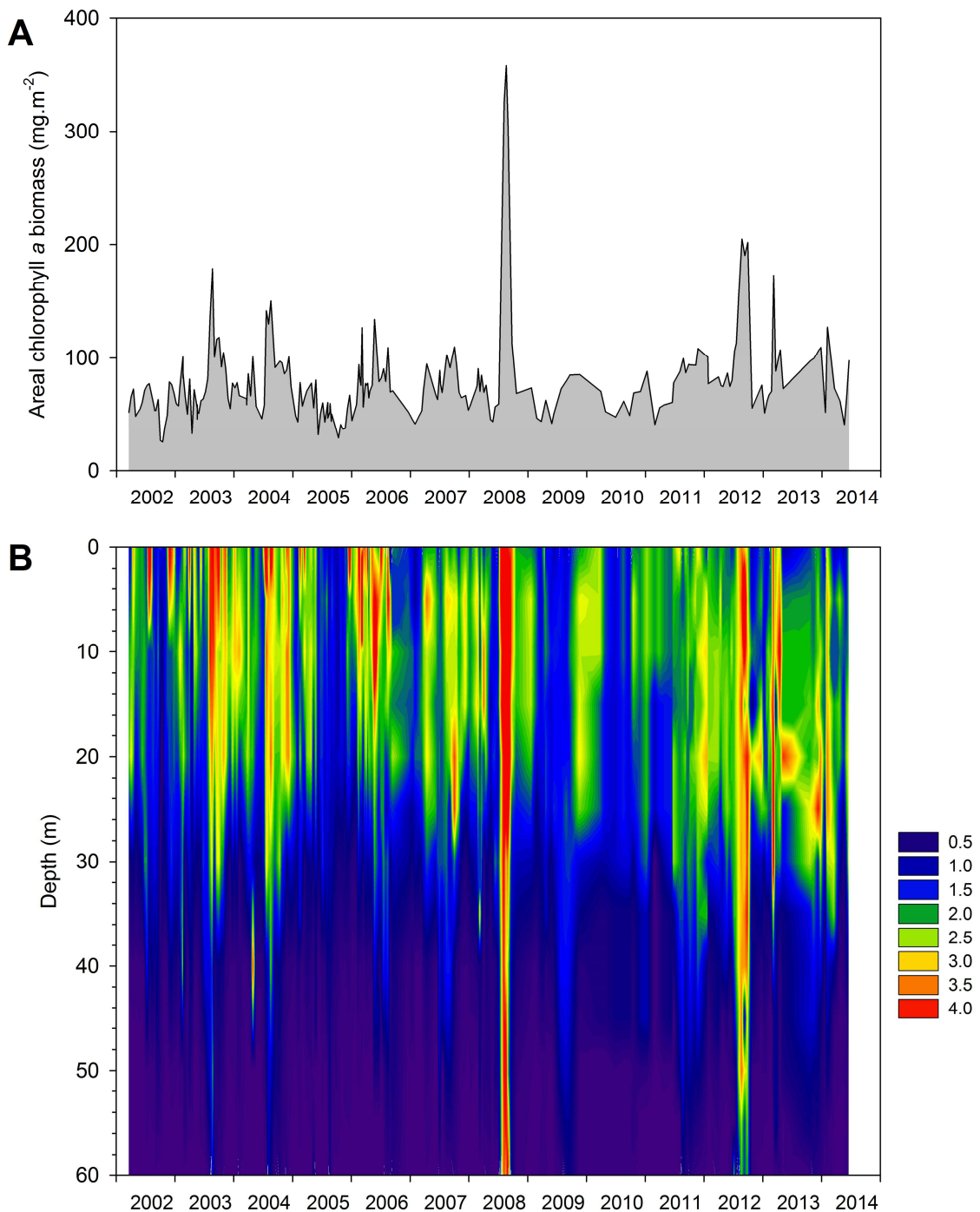


Fig. 2: Example of a variable stored in the EAGLES database. (A) Areal phytoplankton biomass (mg chlorophyll *a* m<sup>-2</sup>) and (B) vertical distribution of phytoplankton biomass (mg chlorophyll *a* m<sup>-3</sup>) in the Ishungu basin from 2002 to 2014

Phytoplankton composition also exhibited seasonal and interannual variations during the study period, as described in Sarmiento et al (2012), but remarkable changes occurred in the lake since the beginning of 2012, as shown in fig. 3. Cyanobacteria had a median biomass near 40 mg m<sup>-2</sup> in the north basin of the lake in the period 2005-2008 (Sarmiento et al., 2012), which was reduced to 16 mg m<sup>-2</sup> in the period 2012-2014. Their seasonal variation was also reduced. By contrast, an important increase of green algae has occurred in recent years, as illustrated in fig. 3. Microscope examination allowed identification of these green algae as

desmids that were present before in the lake (*Cosmarium laeve*, considered as rare in the lake by Sarmento et al., 2007). These are relatively large, non-motile cells, which need turbulence to remain in suspension: accordingly, they tended to increase in the dry season, like diatoms.

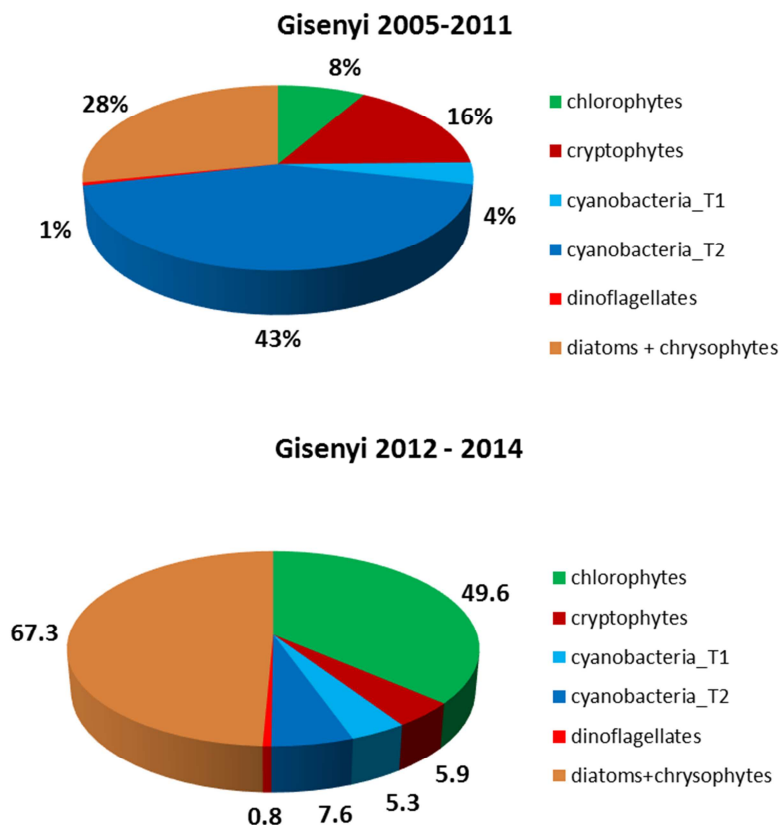


Fig. 3. Relative contribution of the phytoplankton groups to chlorophyll a in the north basin of Lake Kivu, averaged for the period 2005-2011 (top) and for the 2012-2014 period.

### 2.2.1.2 Greenhouse gas distribution in the water column of Lake Kivu

The monitoring of Lake Kivu was performed in the Southern Basin, at the station of Ishungu (-2.3374 °N, 28.9775 °E), from February 2012 to October 2013. As mentioned above (see 2.1.1) Analysis of the vertical and seasonal variability of temperature and dissolved O<sub>2</sub> concentrations allows to divide the annual cycle into two distinct limnological periods. Rainy season conditions resulted in a thermal stratification within the mixolimnion (October-June) while the dry season was characterized by deeper vertical mixing of the water column down to the upper part of the permanent chemocline at 65 m (July-September) (Fig. 4). The vertical position of the oxycline varied seasonally: the oxic-anoxic transition reached its deepest point (65 m) during the dry season, then became gradually shallower after the re-establishment of the thermal stratification within the mixolimnion at the start of the following rainy season to finally stabilize at approximately 35m, corresponding to the bottom of the mixed layer during the rainy season (Fig. 4).

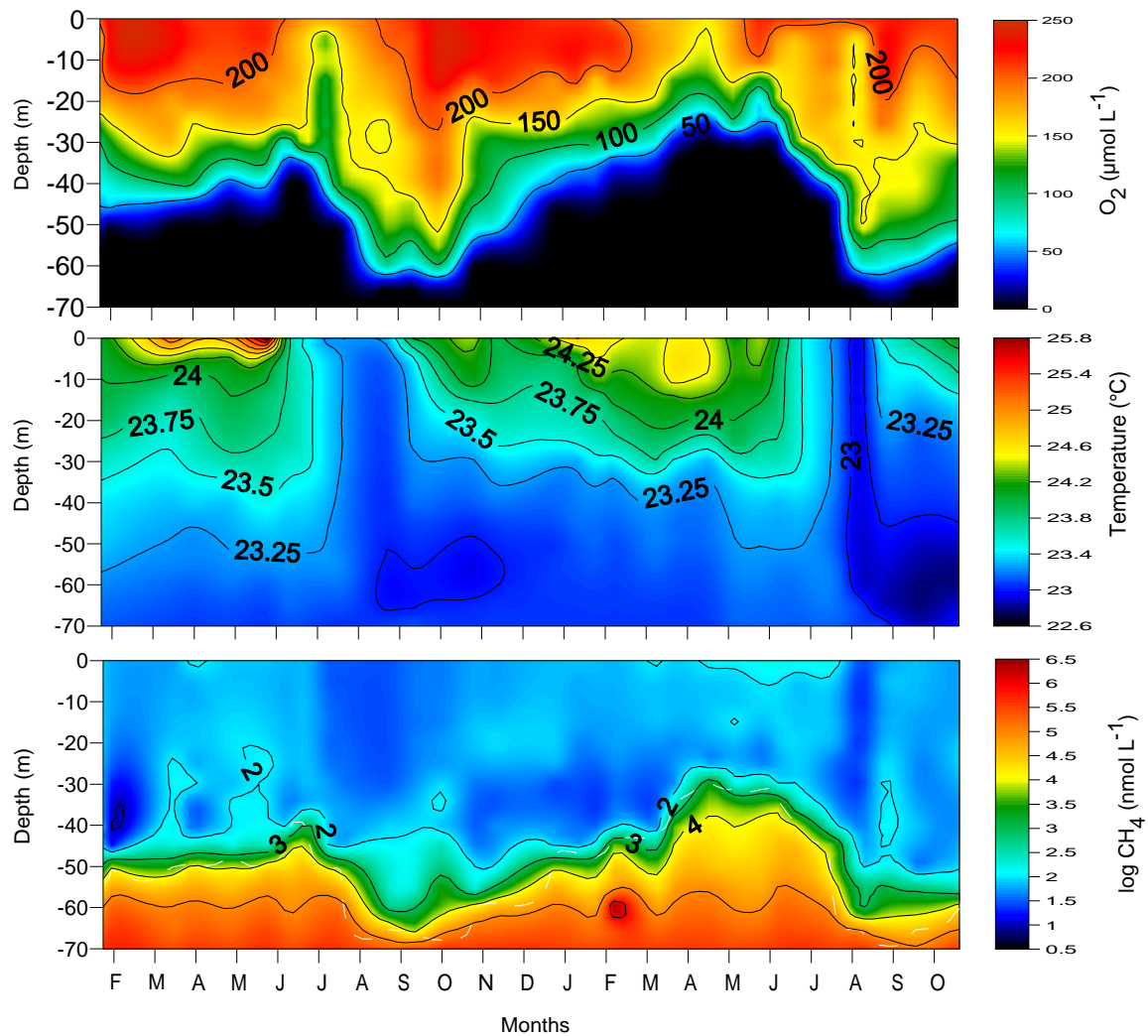


Figure 4: Dissolved  $O_2$  concentrations ( $\mu\text{mol L}^{-1}$ ; a), temperature ( $^{\circ}\text{C}$ ; b) and  $\log CH_4$  concentrations ( $\text{nmol L}^{-1}$ ; c) along the vertical profile from February 2012 to October 2013, at the station of Ishungu (South Basin).

The temporal variability of the vertical distribution of  $CH_4$  corresponded well with the seasonal variation of the oxycline. The  $CH_4$  concentrations were very high in the monimolimnion throughout the year (maximum of  $\sim 500 \mu\text{mol L}^{-1}$ ) but sharply decreased at the oxic-anoxic transition, to reach on average  $62 \text{ nmol L}^{-1}$  in surface waters.

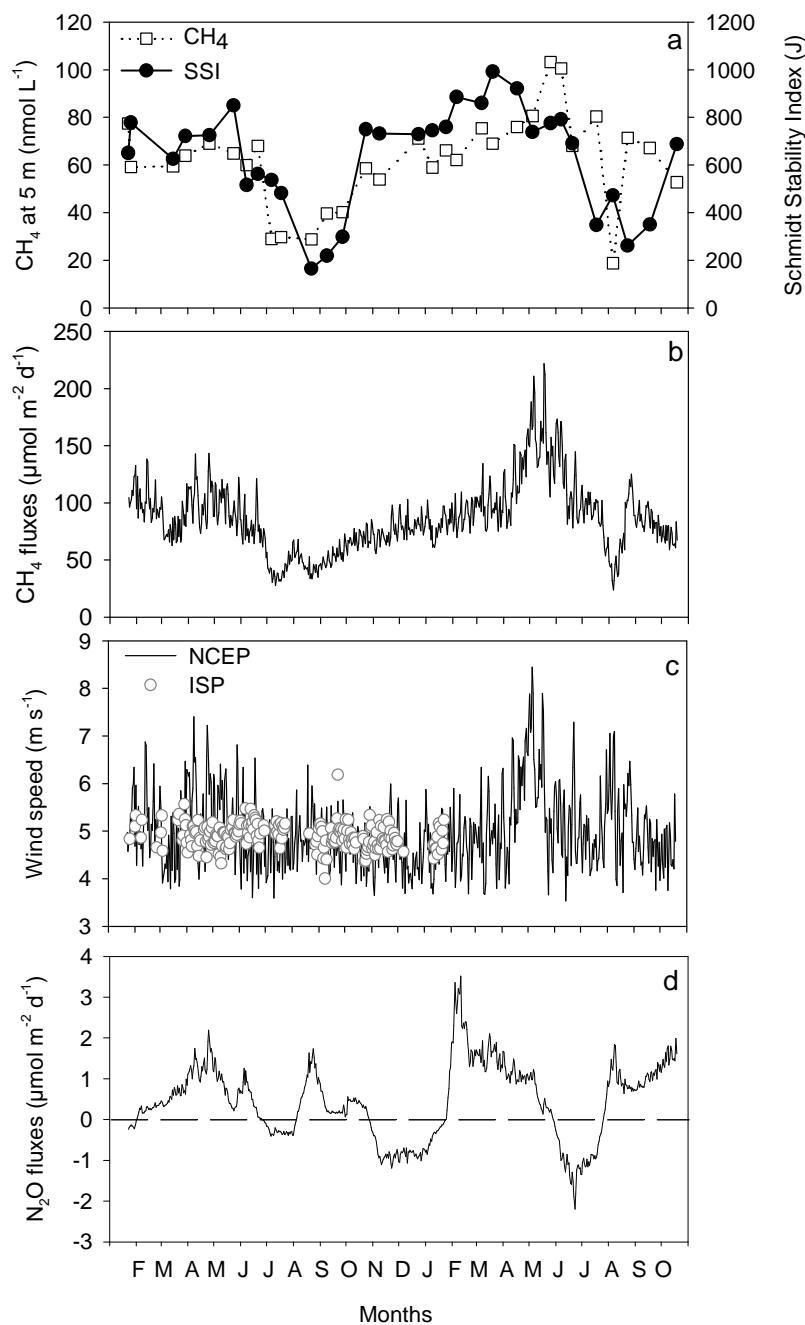


Figure 5: CH<sub>4</sub> concentrations at 5 m (nmol L<sup>-1</sup>) and SSI (a), CH<sub>4</sub> fluxes (μmol m<sup>-2</sup> d<sup>-1</sup>; b), wind speed (m s<sup>-1</sup>; c) and N<sub>2</sub>O fluxes (μmol m<sup>-2</sup> d<sup>-1</sup>; d) from February 2012 to October 2013, at the station of Ishungu (South Basin)

CH<sub>4</sub> concentrations at 5 m perfectly followed the Schmidt Stability Index (SSI) seasonal cycle (Fig. 5a), which illustrates the direct influence of the water column stratification on the C dynamics. This suggests that more CH<sub>4</sub> diffuses to surface waters when anoxic waters, rich in CH<sub>4</sub>, are closest to surface waters (high SSI, i.e. rainy season). Linked to this, CH<sub>4</sub> fluxes to the atmosphere (calculated based on wind speed and CH<sub>4</sub> concentrations) were higher during the rainy season (Fig. 5b), especially in late rainy season, where higher wind speeds (Fig. 5c) were observed, due to the accentuation of the turbulence. However, in August and September 2012 and 2013, we observed lower atmospheric CH<sub>4</sub> fluxes, independently of high wind speeds. This observation can be related to lower CH<sub>4</sub> concentrations at 5 m observed when vertical mixing is maximal, suggesting that CH<sub>4</sub> diffusing from anoxic waters

cannot reach surface waters. This may be due to the occurrence of CH<sub>4</sub> oxidation (see section "2.3.1 Aerobic methanotrophy" below). Lake Kivu is a source of CH<sub>4</sub> to the atmosphere throughout the year, but the net flux is small compared with literature data from other lakes globally, despite its exceptionally high CH<sub>4</sub> content in deep waters. Concerning N<sub>2</sub>O fluxes (Fig. 5d), it seems that Lake Kivu alternates between a source and a sink for atmospheric N<sub>2</sub>O. N<sub>2</sub>O can be produced by both nitrification and denitrification. Nitrification is a source of N<sub>2</sub>O, while denitrification is usually a sink but can act as a source in presence of O<sub>2</sub> at low concentrations. Denitrification rates have been quantified during different field campaigns (see 2.2.3.5).

### 2.2.1.3. Complementary measurements

Six scientific field campaigns took place, including several teams of the Belgian network, as well as, on some instances, international scientists, from June-July 2011 August-September 2014.

#### *Sediment trap deployment:*

Sediment traps were installed during the third field campaign, in September 2012. The traps were deployed at 90 m depth from floating platforms till September 2014 in two sites in the main basin: off Gisenyi (1.0742°S, 29.2260°E) and off Kibuye (2.0972°S, 29.2028°E). Retrieval of collected material was performed on a monthly basis by the local Rwandese subcontractor. Analysed variables in the sediment trap material were phytoplankton pigments, POC, TN and TP content. In order to prevent organic matter degradation within the traps, their bottom was gently filled with a saline solution added with mercury chloride, to inhibit microbial activity. At trap retrieval, the particulate matter accumulated was collected and resuspended in a known water volume (usually 400 ml). At return to the local laboratory, the suspension was filtered on pre-combusted glass-fiber filters, dried and weighed. Further analyses were carried out in Belgium at UNamur (HPLC pigment analyses) and at KUL (PIC: particulate inorganic carbon; POC: particulate organic carbon; PON: particulate organic nitrogen; POP: particulate organic phosphorus). Those analyses allowed to estimate the downward fluxes (as daily rates per square meter) of inorganic and organic carbon, nutrients, phytoplankton (as chlorophyll a), and the contribution of the main phytoplankton groups to sedimentation. Finally, a calculation of primary production in the water column based on chlorophyll a concentration, light penetration and average photosynthetic parameters (see Darchambeau et al., 2014) allowed the estimate of the "export ratio", which is the ratio POC sedimentation rate : daily C fixation by photosynthesis..

Considering the data from both sites, the total sedimentation rate varied between 213 and 3911 mg DW m<sup>-2</sup> d<sup>-1</sup>, with an average of 683 mg DW m<sup>-2</sup> d<sup>-1</sup>, which compares well to the estimate of 786 mg DW m<sup>-2</sup> d<sup>-1</sup> at Ishungu in 2007 (Pasche et al., 2010). The wide range of variation depended largely on a single PIC sedimentation peak in March-April 2013 (Fig. 6), corresponding to an event of calcium carbonate precipitation. The POC sedimentation varied by a factor of ~5 at both sites and tended to be higher in the rainy season than in the dry season. The mean value was 63 mg C m<sup>-2</sup> d<sup>-1</sup>, i.e. lower than that estimated by Pasche et al. (2010) at Ishungu (113 mg C m<sup>-2</sup> d<sup>-1</sup>). Phytoplankton production followed a typical seasonal pattern with maxima in the dry season, particularly in 2014. The export ratio also followed a

seasonal pattern, logically related to that of POC sedimentation rate, with maxima in the rainy season (up to 22.2 %) and minima (up to 2.7 %) in the dry season. The mean export ratio for both sites is 8.1 %, indicating that most of the organic carbon resulting from phytoplankton particulate production was recycled in the mixolimnion.

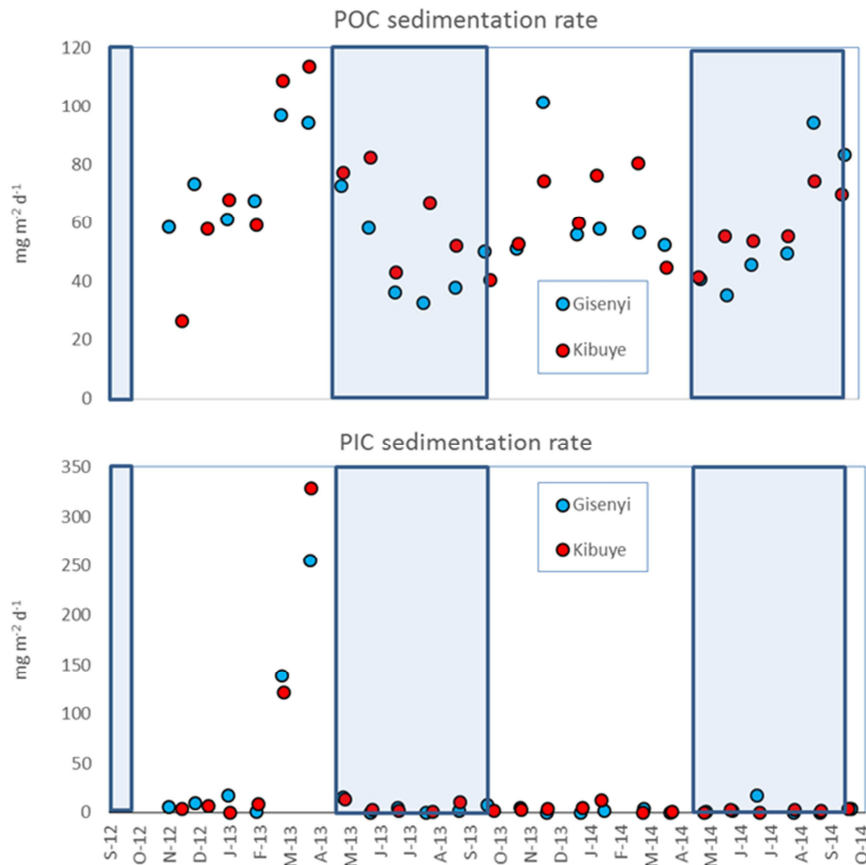


Fig. 6. Variations of the sedimentation rate of particulate organic matter (POC) and of particulate inorganic matter (PIC) in Lake Kivu at both sites during the monitoring period. The frames indicate the dry season in 2013 and 2014.

As sedimenting POC is essentially composed of settling phytoplankton, it is expected that chlorophyll a followed a pattern similar to that of POC. However, chlorophyll a sedimentation rates were weakly related to that of POC, as a result of degradation processes occurring in the water column during sedimentation. The proportion of chlorophyll a degradation products (phaeophytins a and phaeophorbides a) in the trap material varied widely over time: this indicates that the chlorophyll a degradation processes varied greatly and did not follow a clear pattern. The data for the main carotenoid pigments, markers of the phytoplankton classes, were well correlated to chlorophyll a, indicating the contribution of diatoms, green algae, cyanobacteria and cryptophytes to sedimenting phytoplankton, as expected from the abundance of these classes in the water column.

The elemental ratios (C:N and C:P) obtained from PON and POP measurements in the trap material are shown in fig. 7. C:N and C:P ratios of Kibuye site were significantly higher than those of Gisenyi site (Mann-Whitney's U test,  $p < 0.001$ ). It indicates different nutrient (N and P) recycling at the two monitoring sites, with a more efficient recycling in the water column at Kibuye than at Gisenyi. This phenomenon might be related to the stability of the water

column and to the development of the microbial plate in the redoxcline. We still know very little about the community ecology of this microbial plate and this should be the focus of future research (Llirós et al. 2012).

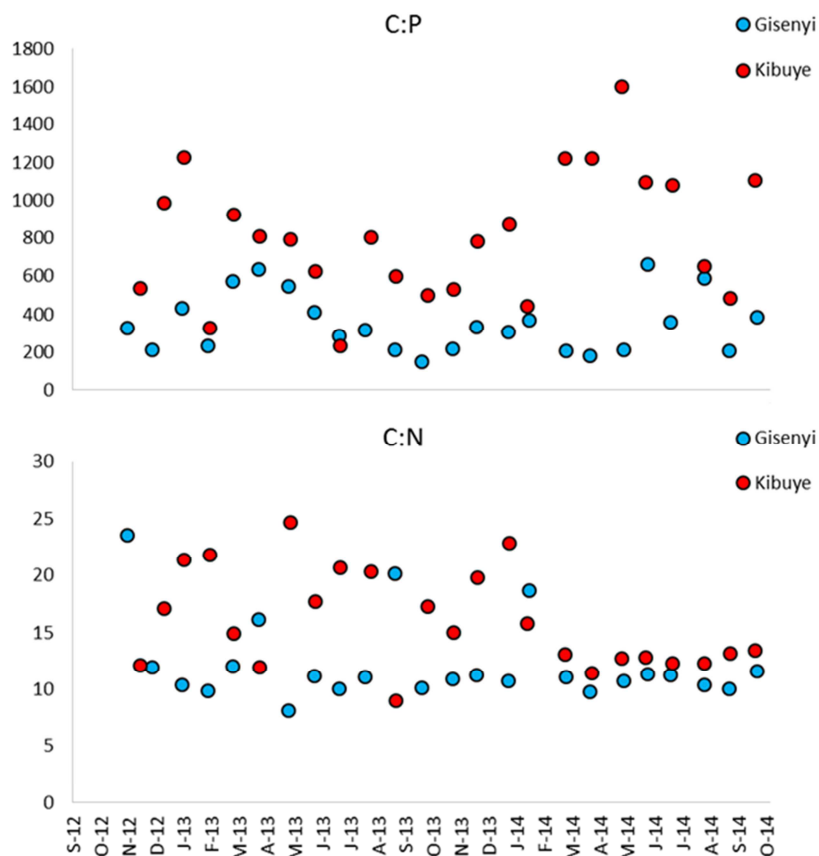


Fig. 7. Variation of the elemental ratios in the particulate matter collected the sediment traps deployed in Lake Kivu at both sites in 2012-2014..

#### 2.2.1.4 Water geochemistry, Biogenic silica, incubation experiments and Silicon isotopes in the water column

The Silicon (Si) budget within those water layers has been long recognized to be influenced by uptake and mineralization of diatoms and inputs through subaquatic springs (e.g. Pasche et al., 2009, and references therein), but the intensity and origin of these fluxes remain poorly known. Vertical profiles of biogenic silica ( $B_{Si}$ ), dissolved silicon ( $D_{Si}$ ) and Si isotopic composition ( $\delta^{30}Si$ ) were therefore determined in three locations in order to (1) quantify the diatom uptake in the mixolimnion and the diatom mineralization in the intermediate water mass; (2) investigate the composition and origin of the intermediate and deep water inflows linked to the subaquatic springs. The vertical distribution of conservative cations ( $Na^+$ ,  $K^+$ ), nutrient (P), and cations sensitive to precipitation dissolution ( $Mg^{2+}$ , S,  $Ca^{2+}$ , Mn,  $Sr^{2+}$ ,  $Ba^{2+}$ ,  $REE^{3+}$ ) was used as reference to constrain the source and mineralization processes. Several

incubation experiments were performed on the three sites to quantify the diatom production and dissolution rates.

The water profilings were carried out at the closure (September 18 – October 16 and August 20-September 6) of the dry season in 2012 and 2013 respectively to capture the end of the diatom productivity in response to the lake oscillation between the dry (May-September) and the rainy season (October-April) when deeper mixing supply the nutrients from the monimolimnion. They were focused on:

- (a) a restricted basin (The Kabuno Bay, 48km<sup>2</sup>) which is shallower (maximum depth: 110 m) and isolated from the main deep Kivu Basin (2322km<sup>2</sup>) by a narrow shallow (~10m deep) connection. This location was chosen because there seems to be characterized by a much larger contribution of internal geothermal and meteoric water inputs to the whole water column than the main basin (Borges et al., 2011).
- (b) At Ishungu and Gisenyi to compare the southern and northern parts of the main basin.

### **Methodology**

At Kabuno, the sampling (down to 65 m in 2012 and 100 m in 2013) was mostly concentrated in the first 12 m to cross the very stable oxycline at about 10.5 m. At Ishungu, the profiling range from 0 to 100 m depth to look after the Si fluxes between the mixolimnion and the upper chemocline (every 5 m between the surface and 30 m depth, and every 10 m deeper). Off Gisenyi, the 5 major water masses were sampled continuously in 2013 from 0 to 350 m (every 5 meters between the surface and 30 m depth, and every 10 m deeper). In 2012, the sampling was continuous from 0 to 100 m, but discontinuous deeper with 7 stations (170, 230, 240, 250, 280, 310, 350 m).

At each depth, 155 ml of water were sampled. A water sample (125 ml) was immediately filtered through 0.2 µm PES membrane to separate the biogenic silica (B<sub>Si</sub>) from the dissolved silica (D<sub>Si</sub>). The membranes were dried and the filtrates were stored in polypropylene bottles. These samples will be used later for (i) natural biogenic and dissolved silicon isotopic composition and (ii) major cations analysis. Another water sample (30 ml) was stored unfiltered in polypropylene bottles and 70 µl of HNO<sub>3</sub> were added. These samples will be used later for trace element analyses.

For each depth within the mixolimnion another 500ml sample aliquot was stored in polycarbonate bottle and was spiked with <sup>30</sup>Si in the form of Na<sub>2</sub>SiO<sub>3</sub> solution, in a proportion usually minimum 15% of the ambient D<sub>Si</sub> concentration. This minimized the perturbation on the natural D<sub>Si</sub> contents and provided sufficient sensitivity for the isotopic measurement (Fripiat et al. 2009). After the <sup>30</sup>Si spiking and mixing, we realized an in-situ incubation: each labeled bottles was attached along a rope at its specific depth and then put in the lake for a 24h-period. At the end of the incubation period, the samples were filtered. The membranes were dried and the filtrates were stored in the polycarbonate bottles for further isotope dilution analyses.

*Major cations, Dissolved silica (DSi) and Rare Earths (REE)*

The concentrations of major cations and  $D_{Si}$  were measured by inductively coupled plasma optical emission spectrometry (ICP-AES). REE and Y concentrations were analysed by HR-ICP-MS (Element 2) in low-resolution mode with indium (In) as internal standard. Detection limits were about 25ppt for La, Ce and Nd, 5ppt for Pr, Sm, Gd, 3ppt for Eu, Dy and 1ppt for Ho, Er, Yb. Specific BaO interference on Eu and PrO and CeOH interferences on Gd were corrected based on the percentage of U oxides. When the Ba contents was too high ( $>2 \mu\text{mol l}^{-1}$ ), the Eu concentrations could not be accurately determined due to a too large BaO interference which significantly increase the detection limit. Typical accuracy is better than 5% for Y, Ba, La, Ce, Pr, Gd, Tb, Dy, Ho, Er, and Yb and below 10% for Nd, Eu, Sm and Lu. Normalized Ce and Eu anomalies were calculated as:  $\text{Ce/Ce}^* = (\text{La}^* \text{Pr})^{1/2}$ ;  $\text{Eu/Eu}^* = (\text{Sm}^* \text{Gd})^{1/2}$ .

*Silicon isotopic composition ( $\delta^{30}\text{Si}$ )*

The water samples were first treated by photoozonolysis following the method described in Hughes et al. (2011) to mineralize the dissolved organic matter. Cation exchange resins (BioRad's DOWEX 50W-X12) were then used to remove cations from sample solutions. Si isotopes were measured with a Nu Plasma MC-ICPMS (Nu Instruments) at the Université Libre de Bruxelles, operating in dry plasma mode with a Cetac Aridus II desolvating nebulization system. The mass bias was corrected through external Mg doping (Cardinal et al., 2003), and the long-term instrumental drift was corrected with the sample standard bracketing technique relative to the NBS28 silica sand standard (National Institute of Standards and Technology, RM #8546) or an equivalent in-house standard (Pro Analysis Quartz from Merck). All results presented in this study are reported relative to NBS28 following:

$$\delta^{30}\text{Si} = \left[ \frac{\left( \frac{^{30}\text{Si}}{^{28}\text{Si}} \right)_{\text{sample}}}{\left( \frac{^{30}\text{Si}}{^{28}\text{Si}} \right)_{\text{standard}}} - 1 \right] * 1000$$

It was recently shown that anionic species, which are not removed by the cation exchange resin, could cause significant matrix effects (Hughes et al., 2011). In order to solve this issue, both samples and bracketing standards were doped with acids in large excess compared to the naturally occurring anion concentrations thereby hiding any natural variations of the anion matrix following the method of Hughes et al. (2011). The isobaric interference of  $^{14}\text{N}^{16}\text{O}$  on the  $^{30}\text{Si}$  peak is resolved by using the pseudo-high resolution that consists of measuring on the low mass side of the peak, which is free of interference (Abraham et al., 2008). All replicates are total procedural replicates. The accuracy of the  $\delta^{30}\text{Si}$  measurements was checked on a daily basis by measuring a diatomite reference material of known isotope composition. The long-term average analytical reproducibility and accuracy on this reference material for  $\delta^{30}\text{Si}$  were of  $\pm 0.141$  ( $\pm 2\text{rSD}$ ,  $n = 11$ ). All results of the Si isotope measurements are in agreement with a mass dependent equilibrium fractionation line ( $\delta^{30}\text{Si} = 1.93 \delta^{29}\text{Si}$ ).

*Biogenic silica ( $B_{Si}$ )*

The difficulty of the  $B_{Si}$  measurement resides not only in the extraction efficiency of  $B_{Si}$ , but also in the correction for the dissolution of co-existing aluminosilicates ( $Al_{Si}$ ). In order to solve this issue, we measured  $B_{Si}$  and correction for  $Al_{Si}$  interference following the method of Ragueneau et al (2005). It consists of a double wet-alkaline digestion where the filter sample is submitted to a first digestion (0.2 M NaOH, pH 13.3) at 100°C for 40 min. At the end of this first leach, all the  $B_{Si}$  and part of the  $Al_{Si}$  have been converted into  $Si(OH)_4$ . Si and Al concentrations ( $[Si]_1$  and  $[Al]_1$ ) in the supernatant are analyzed. After rinsing and drying, the filter is submitted to a second digestion, exactly identical to the first one, leading to the determination of the  $(Si:Al)_2$  ratio that is characteristic of the silicate minerals present in the sample. A third digestion step was added to the original method to verify that no  $B_{Si}$  was left after the second leach. The corrected biogenic silica concentration is thus given by  $[B_{Si}] = [Si]_1 - [Al]_1 (Si:Al)_2$ .

*Incubation experiments*

Measurements of  $B_{Si}$  production and dissolution rates were determined to better understand the Si cycle. The change in isotopic composition of the biogenic silica is used to estimate the production rate by measuring the enrichment in  $^{30}Si$  of the particulate phase. The dissolution rates were measured through the increase in  $^{28}Si$  in the dissolved phase due to the dissolution of initial biogenic silica. We followed the method of Fripiat et al (2009) for the simultaneous determination of the rates of production and dissolution of biogenic silica, using the  $^{30}Si$ -isotopic dilution technique with a high-resolution sector field inductively coupled plasma mass spectrometer (HR-SF-ICP-MS). Relative analytical precision of the isotopic measurement is better than 1%. To calculate the flux rates (production and dissolution of biogenic silica, respectively,  $\rho_P$  and  $\rho_D$ ) we use the linear one-compartment model described for production and dissolution (Cf. Fripiat et al., 2009). Measurements of real Si production rates were determined with an average relative precision of 10%. Due to the very high  $D_{Si}$  (especially in Kabuno), the ratio between the dissolved silicon and the added spike was inadequate and the estimates of the  $B_{Si}$  dissolution rates were frequently below the detection limit.

**Results***Dissolved Cations ( $Na^+$ ,  $K^+$ ,  $P$ ,  $Mg^{2+}$ ,  $S$ ,  $Ca^{2+}$ ,  $Mn$ ,  $Sr^{2+}$ ,  $Ba^{2+}$ )*

The main basin is chemically stratified, with 6 stepwise levels of concentrations for Na, Mg, K, Ca, Sr, P in agreement with previous studies (e.g. Schmid et al., 2005; Tassi et al., 2009; Pasche et al., 2009). In particular, our  $K^+$  data for Kisenyi [2012: 2.1-8.1  $\mu mol l^{-1}$ ; 2013: 2.0-8.0  $\mu mol l^{-1}$ ] fits very well with those of Tassi et al. 2009 [2.1-8.3  $\mu mol l^{-1}$ ]. The very stable Na/K molar ratio (2.09-2.27), at all depths, in 2012 and 2013, and at both locations of the main basin (Ishungu and Gisenyi) points to vertical concentration patterns driven by subaquatic springs inputs issued from similar sources with physical mixing at low depths and dilution by surface runoff.

Non-biogenic, conservative elements like  $Na^+$  and  $K^+$  are excellent tracers of the water source. The slight difference between the surface and both intermediate and deep waters (>180m) may therefore indicate that the Na/K ratio of the water runoff and intermediate

subaquatic springs could be slightly lower than that of the deep subaquatic springs. This difference between surface and deep waters was also observed in the 2004-07 sampling by Tassi et al. (2009), which recorded more scattered Na/K and Na/Mg molar ratios than ours in both Gisenyi and Ishungu, essentially due to larger contents in Na [2012: 4.5-18.0 mmol l<sup>-1</sup>; 2013:4.2-17.8mmol l<sup>-1</sup>; Tassi et al.: 4.7-20.4 mmol l<sup>-1</sup>]. These small but significant time-related changes in the Na/K and Na/Mg suggest that despite its permanent stratification, the lake is chemically dynamic on a relatively short term decadal basis.

A strong difference of cation sources between the Kabuno Bay is and the main Basin is very well illustrated in the Na/Mg versus Na/K with deep Kabuno water displaying low Na/Mg (<0.8) and Na/K (<1.7) compare to the Gisenyi and Ishungu Basins (Na/Mg>1.4; Na/K>2.05). With intermediate values (Na/Mg~1.2; Na/K~1.77), the 2013 surface water from the Kabuno Bay (<12m) is a mixture in roughly equal proportions between the deep Kabuno water layers and waters with chemical features very similar to those found in the surface of the main basin. In 2012, a similar picture was observed even if the proportion of the Kabuno deep water in the mixture was a bit larger.

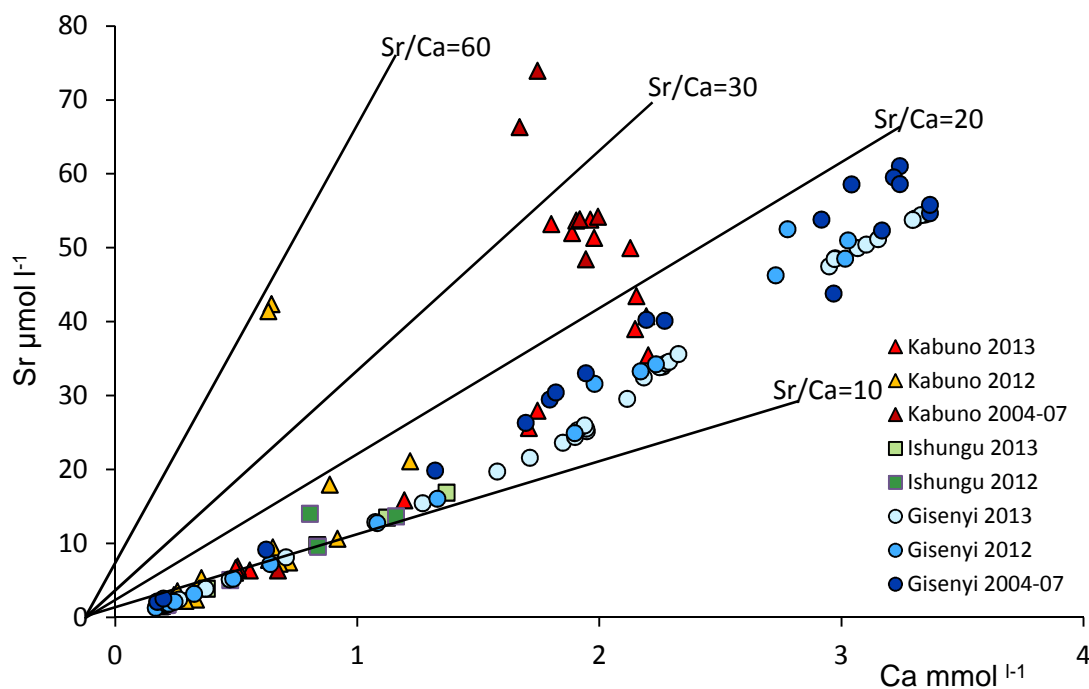


Figure 8. Sr vs Ca behavior at Gisenyi, Ishungu and Kabuno (the 2004-07 data are from Tassi et al., 2009).

Ba does show most of the stepwise levels except the last two ones, the Ba content being stable at 3.85 µmol l<sup>-1</sup> below 260 m. The 2012 Ba profiles from the 3 localities differ from the 2013's ones by their much lower Ba contents in the mixolimnion (In Gisenyi: 0.036-0.066 µmol l<sup>-1</sup> vs 0.14-0.24 µmol l<sup>-1</sup>, respectively) and their higher Ba contents in the deepest layers (In Gisenyi: 4.19-4.39 µmol l<sup>-1</sup> vs 3.80-3.87 µmol l<sup>-1</sup>, respectively).

In the main basin, Sr, whose geochemical behavior is intimately associated with Ca-bearing minerals, shows a strong positive correlation with Ca (Figure 8) because  $\text{CaCO}_3$  precipitation at the surface and its dissolution in the deepest strata control both element contents. The slight decoupling between Sr and Ca with depth (increase in Sr/Ca from 8 to 20, Figure 8) cannot be attributed to the carbonate dissolution in the deepest parts because all carbonates present higher mineral-water partition coefficient for Ca than Sr ( $D_{\text{Sr}} < D_{\text{Ca}}$ ). In the Kabuno Bay, these two cations are even more strongly decoupled below the mixolimnion ( $\text{Sr/Ca} > 20$ , Figure 8) in accordance with the difference of cation source between the Kabuno deep water and the main basin waters.

The high N:P ratio in Lake Kivu compared to Lake Malawi and Tanganyika indicates that phytoplankton suffers of a strong P limitation throughout the year (Pasche et al., 2009; Darchambeau et al., 2014). So it is interesting to have a look to the P data normalized to a conservative cation like Na (Figure 9) to get rid of most of the variability linked to the long-term cation accumulation in the water column in order to accurately evaluate the recent change in P availability and remineralisation.

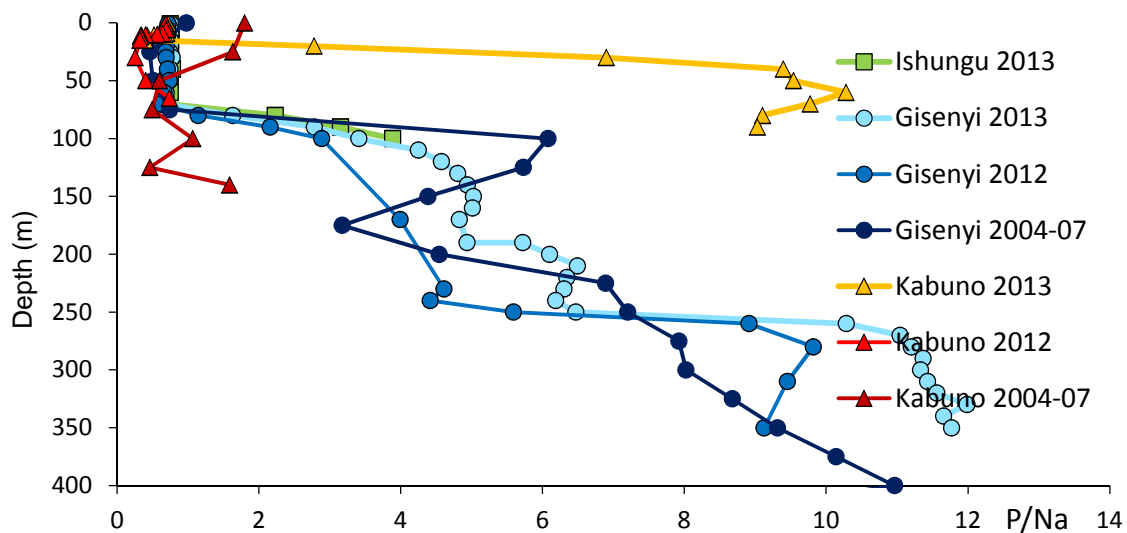


Figure 9. Depth profiling of the P/Na molar ratio in Lake Kivu.

At Gisenyi on a decadal perspective, the P/Na significantly fluctuates especially in the upper chemocline and the deepest reservoirs, showing that the P reservoir has dynamically changed through time. Likewise, in Kabuno, the P/Na profiles strongly differ from one year to another. In 2004-07, there is a relative P enrichment at the surface with depletions in depth. In 2012, P is quite depleted relative to Na at all depths. The 2013 profile contrasts strongly with the two previous ones since P/Na quickly growth below 12 m, showing that a high P reservoir has been generated in one year in the anoxic deep water.

The Mn and S depth profiles differ completely from those of other elements since they are strongly depending of the redox conditions. Mn is depleted in the surface waters at the 3 locations due to its precipitation as manganese oxy-hydroxides ( $\text{MnOOH}$ ) and carbonates ( $\text{Fe, MnCO}_3$ ). Below the oxyclines, the concentrations peak between 3,5, 8 and 23  $\mu\text{mol l}^{-1}$  at

Ishungu, Gisenyi and Kabuno respectively, due to the re-dissolution of the settling Mn-rich minerals. Below 180m, the concentration is stable around  $5 \mu\text{mol l}^{-1}$ . Three water layers with very low dissolved Mn content were detected during the high resolution profile sampled in 2013: at 90 m, 120 m and 190 m depth. These low values were also recorded in 2012 at 70-80 m and 170 m depth, but were not detected by the survey by Tassi et al in 2004-07. These 3 depths correspond to 2 among the 6 depths at which subaquatic springs enter the lake, on the basis of one-dimensional diffusive-advective model for salinity (Schmid et al., 2005):  $\sim 100$  m and  $\sim 180$  m. So, we suspect that these low Mn values trace these hydrothermal inflows in the lake in 2012 and 2013. This dilution by Mn-poor water may explain the drastic decrease in dissolved Mn from 2004 ( $\sim 7 \mu\text{mol l}^{-1}$ ) to 2013 ( $\sim 5 \mu\text{mol l}^{-1}$ ).

#### *Rare Earth (REE)*

At Ishungu and Gisenyi, REE are depleted in the epilimnion showing a significant negative Ce anomaly ( $\text{Ce}/\text{Ce}^* < 0.7$ ) but relatively enriched in the upper chemocline with no or slight positive Ce anomalies ( $0.9 < \text{Ce}/\text{Ce}^* < 1.1$ , Figures 10-11). The REE enrichment at the chemocline level is higher in Ishungu than in Gisenyi as shown by the Dy and Y concentration peaks at 50-60m. Below the chemocline, the REE contents decrease and the Ce anomaly is again present at roughly the same level than those observed in the surface water ( $0.7 < \text{Ce}/\text{Ce}^* < 0.8$ , Figure 11). It has been long established that (1) among the REEs only Ce is reported to be present as a tetravalent species under ambient environmental conditions; (2) Mn oxides sorb  $\text{Ce}^{3+}$  and oxidize it as  $\text{Ce}^{4+}$  during the sorption process; (3) Ce is more tightly associated with Mn oxides than its neighboring REEs of La and Pr, resulting in the Ce positive anomaly in the REE patterns. So, the change in the intensity of the Ce anomaly and the coincidence of low and strong dissolved Mn and REE concentrations gradient between the mixolimnion and the upper chemocline reflects the Mn oxide precipitation in the surface water and their dissolution at the oxic-anoxic interface. Below the 255-261 m chemocline, the REE contents are very low under the detection limits. We could expect a fourfold decrease in the REE contents at the light of the Y changes which mimic the heavy REE behavior (especially Dy).

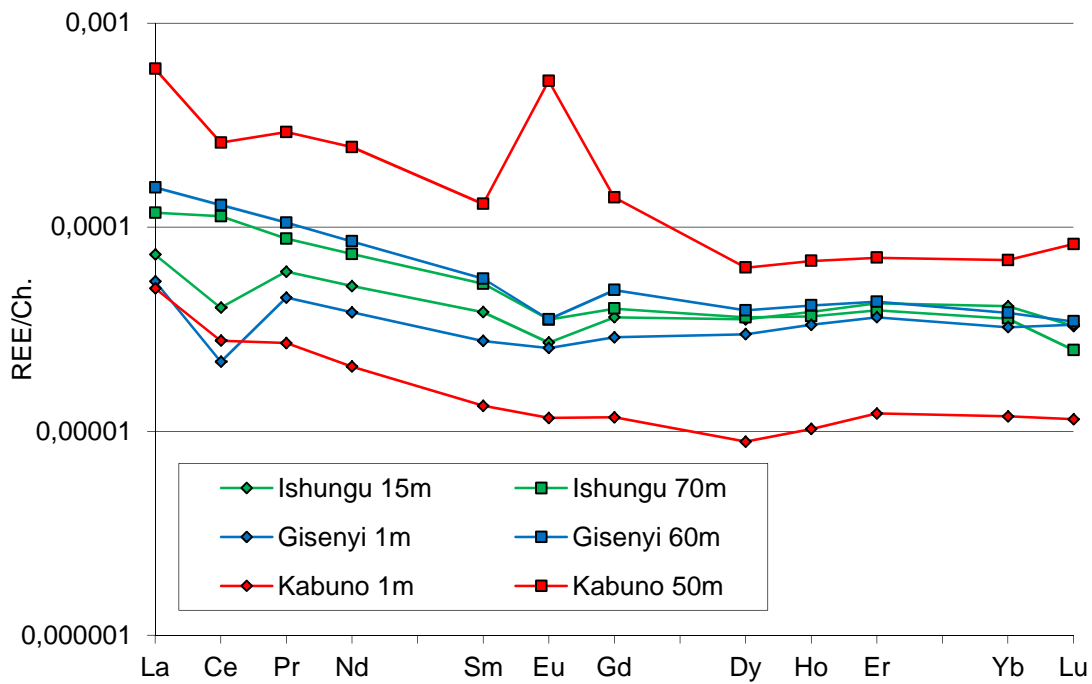


Figure 10. Chondrite normalized rare earth (REE) patterns for a selection of surface and upper chemocline waters

In the Kabuno Ba mixolimnion, the REE contents and Ce anomalies are quite similar but lower than those observed in the main basin. The REE contents decrease with depth to reach a minimal value at 10 m, at a level where a minimal temperature is maintained by a cold inflow (Katsev et al., 2014). Interestingly, deep waters are ten- to twenty-fold enriched in REE relative to the surface waters with the appearance of a major positive Eu anomaly coupled to a small negative Ce anomaly (Figure 11). This REE enrichment with a prominent positive Eu anomaly is a well-known salient feature of the high temperature magmatic-derived fluids. This is consistent with the D-O isotopic data that point to a hot spring origin for the Kabuno deep water (Katsev et al., 2014).

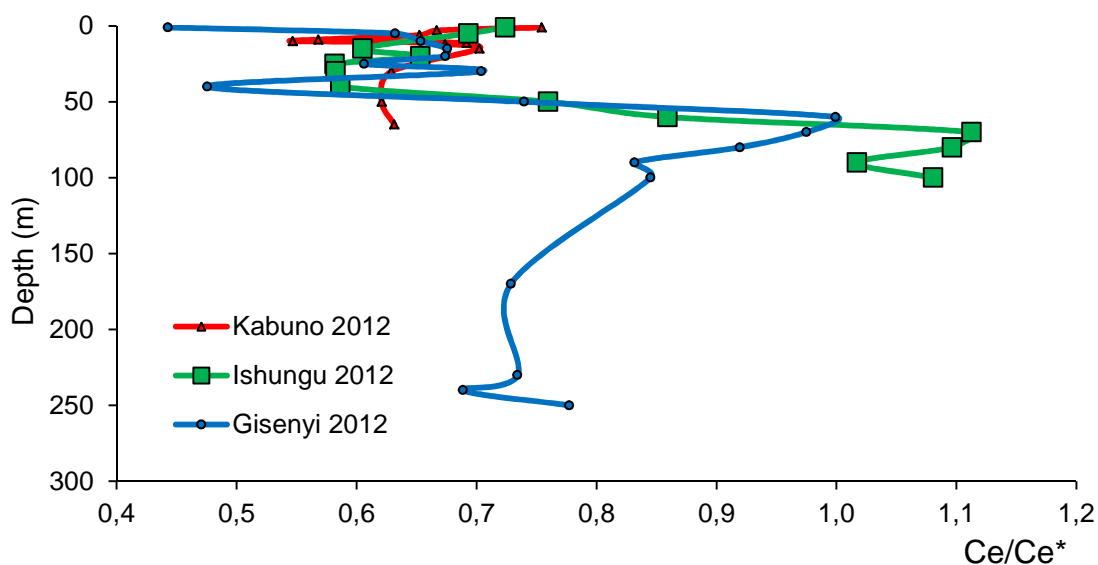


Figure 11. Depth profiling of the Ce anomaly in late September –October 2012.

*Dissolved silica ( $D_{Si}$ )*

The threshold saturation indices, at the thermal and pH conditions of Lake Kivu (23-26°C, 6<pH<9) can be easily calculated for SiO<sub>2</sub> minerals (quartz, chalcedony and amorphous silica) using the PHREEQC thermodynamic database (Parkhurst, 1995). They are about 1000  $\mu\text{mol l}^{-1}$  for quartz, 2800  $\mu\text{mol l}^{-1}$  for chalcedony and 18 mmol l<sup>-1</sup> for amorphous silica. With  $D_{Si}$  ranging below 900  $\mu\text{mol l}^{-1}$ , all surface water from the main basin (0-250m) are undersaturated for all SiO<sub>2</sub> minerals. In contrast, the deep water from the main basin and the restricted Kabuno bay (1000< $D_{Si}$ <2700  $\mu\text{mol l}^{-1}$ ) are saturated for quartz but remains undersaturated for opals. So the “rainfall” of dead diatoms could be dissolved at all depths.

For the oxic mixolimnion, the southern (Ishungu) and northern (Gisenyi) parts of the main basin display very similar  $D_{Si}$  concentrations ranging from 123  $\mu\text{mol l}^{-1}$  to 130  $\mu\text{mol l}^{-1}$  and from 127  $\mu\text{mol l}^{-1}$  to 132  $\mu\text{mol l}^{-1}$  respectively in 2012, and from 123  $\mu\text{mol l}^{-1}$  to 120  $\mu\text{mol l}^{-1}$  and from 126  $\mu\text{mol l}^{-1}$  to 128  $\mu\text{mol l}^{-1}$  in 2013 (Figure 12). These values are much higher than the concentrations recorded in Lake Tanganyika at the same depth (39 to 41  $\mu\text{mol l}^{-1}$ ). They are a bit lower than those observed (133-134  $\mu\text{mol l}^{-1}$ ) by Schmid et al (2005) in 2004, but much lower than those recorded by Degens et al in 1973 (231  $\mu\text{mol l}^{-1}$ ). This suggests that the mixolimnion of the main basin has been affected during the last 5 decades by a continuous decrease of Si concentrations in the range of about 1.5 to 3  $\mu\text{mol l}^{-1} \text{ y}^{-1}$ , demonstrating higher Si export than inputs. This is very well in agreement with the recent observation by Pasche et al. (2009) that the nutrient uptake by primary production is three times higher than nutrient upward fluxes. In Kabuno Bay (0-9.5m), the  $D_{Si}$  is much higher, fluctuating between 481 to 588  $\mu\text{mol l}^{-1}$  in 2012 and 418 and 472  $\mu\text{mol l}^{-1}$  min 2013. These higher contents most likely reflect that the  $D_{Si}$  is controlled by local Si inputs (hydrothermal and meteoritic).

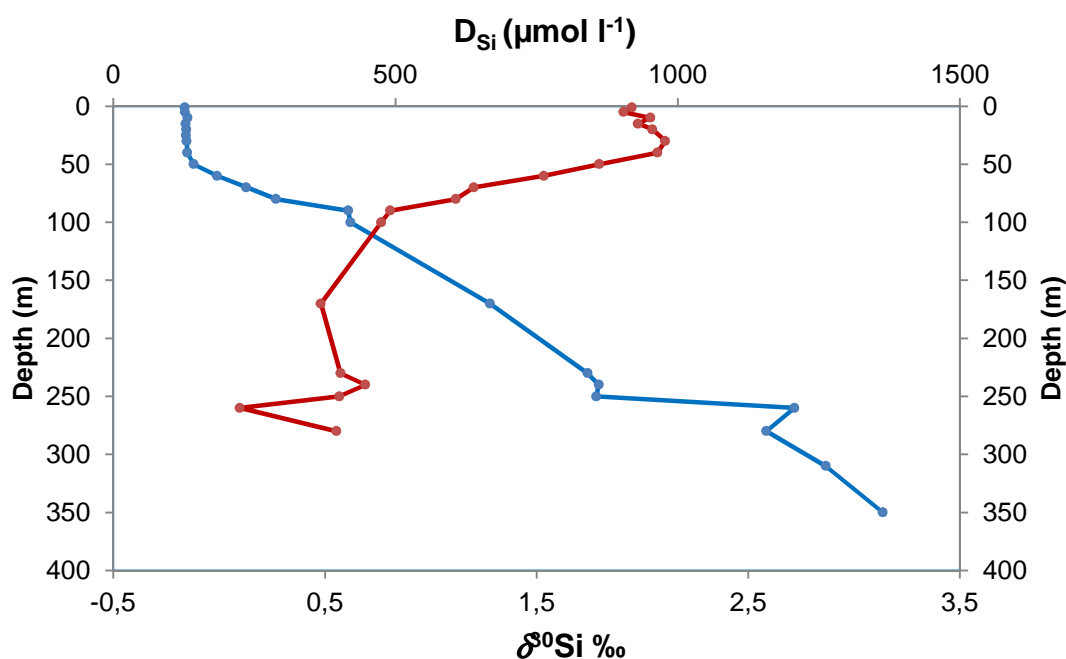


Figure 12. Depth profiling of the dissolved Si Contents ( $D_{Si}$  in blue) and isotopic composition ( $\delta^{30}\text{Si}$  in red) in Lake Kivu at Gisenyi in late September –early October 2012.

Within the upper chemocline (down to 100 m), the southern (Ishungu) and northern (Gisenyi) parts of the main basin display very similar dissolved Si concentrations ranging from 140  $\mu\text{mol l}^{-1}$  to 521  $\mu\text{mol l}^{-1}$  and from 236  $\mu\text{mol l}^{-1}$  to 420  $\mu\text{mol l}^{-1}$  respectively in 2012, and from 166  $\mu\text{mol l}^{-1}$  to 459  $\mu\text{mol l}^{-1}$  and from 211  $\mu\text{mol l}^{-1}$  to 430  $\mu\text{mol l}^{-1}$  in 2013 (Figure 12). At Kabuno Bay (below 10 m), the  $D_{\text{Si}}$  is much higher, fluctuating between 742 to 2353  $\mu\text{mol l}^{-1}$  in 2012 and at 938 to 2705  $\mu\text{mol l}^{-1}$  in 2013. Again these very high concentrations reveal that the Si budget is there controlled by local Si-rich hydrothermal and meteoritic inflows.

Below the upper chemocline, the Gisenyi intermediate water mass (130-250 m) displays  $D_{\text{Si}}$  ranging from 668  $\mu\text{mol l}^{-1}$  to 860  $\mu\text{mol l}^{-1}$  in 2012 and from 603  $\mu\text{mol l}^{-1}$  to 843  $\mu\text{mol l}^{-1}$  in 2013 (Figure 12). These values are within the range of those observed (590-825  $\mu\text{mol l}^{-1}$ ) by Schmid et al (2005) in 2004 but much higher than those recorded by Degens et al in 1973 (428  $\mu\text{mol l}^{-1}$ ). The lower chemocline (255-261 m) displays  $D_{\text{Si}}$  at 1207  $\mu\text{mol l}^{-1}$  in 2012 and 1154  $\mu\text{mol l}^{-1}$  in 2013 (Figure 12). These concentrations are within the range of those observed (1196  $\mu\text{mol l}^{-1}$ ) by Schmid et al (2005) in 2004. The deep water mass (270-350 m) has  $D_{\text{Si}}$  ranging from 1157  $\mu\text{mol l}^{-1}$  to 1364  $\mu\text{mol l}^{-1}$  in 2012, and from 1199  $\mu\text{mol l}^{-1}$  to 1343  $\mu\text{mol l}^{-1}$  in 2013 (Figure 12). These concentrations are within the range of those observed (1283-1413  $\mu\text{mol l}^{-1}$ ) by Schmid et al (2005) in 2004 but much higher than those recorded by Degens et al in 1973 (1056  $\mu\text{mol l}^{-1}$ ).

The Si data were normalised to a conservative cation like Na (Figure 13) to get rid of most of the variability linked to the long term cation accumulation in order to evaluate the recent change in Si availability and remineralisation. At Ishungu and Gisenyi, the 2004-07, 2012 and 2013 Si/Na depth profiles displayed quite similar parallel patterns, but the older measurements present a systematic offset towards higher Si/Na at all depths. In 2012 to 2013, the Si/Na is very stable at the surface (~28-30) and deep waters (~70-80) increasing gradually between these two plateau at medium depths (50-150 m, figure 13). In Kabuno, the Si/Na is higher at all depth, showing that Si is there strongly enriched relative to Na at all depths. This may suggest that Kabuno Bay, being smaller is more affected by sublacustrine inflows.

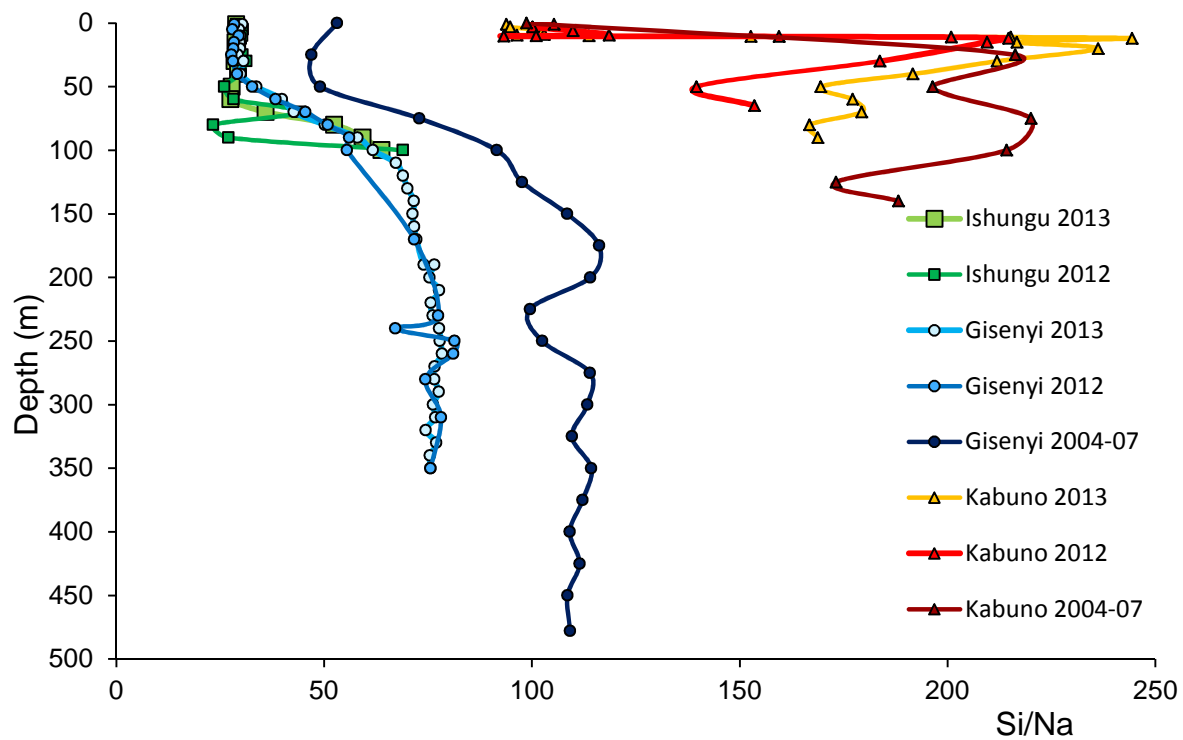


Figure 13. Depth profiling of the Si/Na molar ratio in Lake Kivu.

In Lake Kivu the biological-type behavior of Ba turns out to be significantly affected by Mn redox cycling in the anoxic water column since the peak of the Barite particulates (BaPart) occurred in parallel to the peak of MnPart between 50 and 60 m. Below the BaPart decreases while accordingly the Ba content is going to step up at a depth of about 80-90 m, just below the peak of the release of Mn and Ce between 60 and 80 m. Below 80 m the Ba dissolved content increases in a stepwise manner most likely in response to the salinity gradient which are expected to change the barite saturation properties. The strong positive correlation observed in 2012 and 2013 between the dissolved Ba and Si (Figure 14) underlines the close link between the diatom productivity-mineralization and the Ba cycle in Lake Kivu.

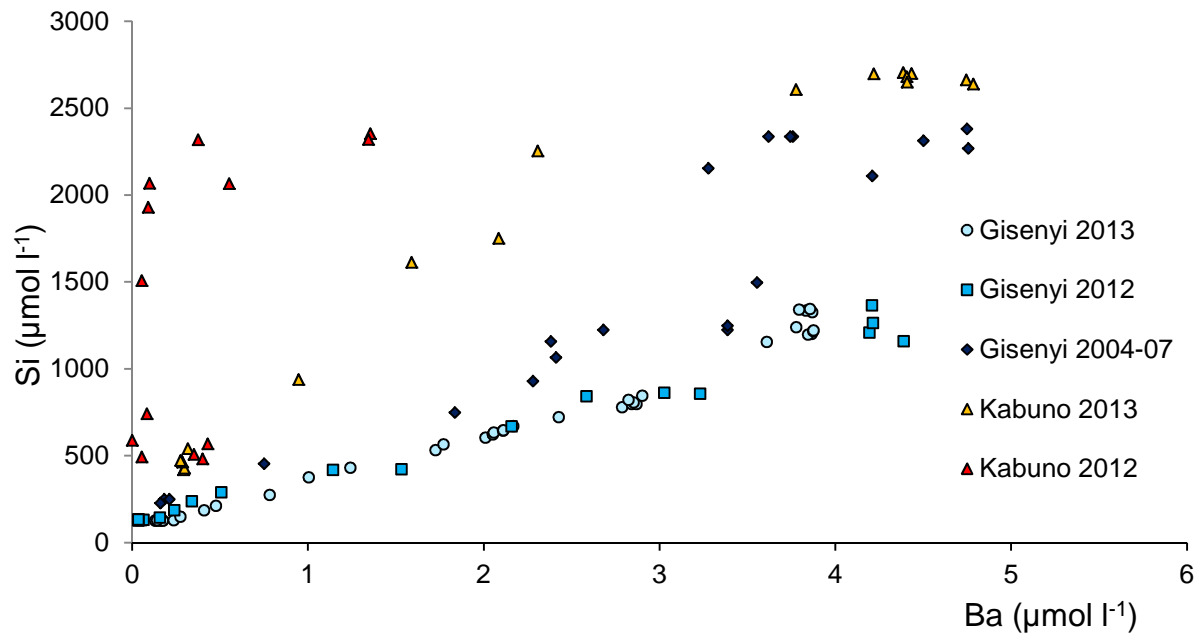


Figure 14: Si-Ba changes in the Gisenyi and Kabuno water columns (the 2004-07 data are from Tassi et al., 2009).

#### *Silicon Isotopic composition ( $\delta^{30}\text{Si}$ )*

The oxic mixolimnions at Ishungu and Gisenyi display very similar  $\delta^{30}\text{Si}$  range from +1.96 ‰ to +2.19 ‰ and from +1.91‰ to +2.11‰ respectively in 2012, and from +1.96 ‰ to +2.17 ‰ again in Ishungu in 2013 (figure 15). These isotopic signatures are actually much heavier than those recorded for Lake Tanganyika between 0-40m (+1.38 to +1.95 ‰, Alleman et al., 2005). At the Kabuno Bay, the  $\delta^{30}\text{Si}$  is different in 2012 and 2013. In 2012, it is stable between +1.4 and +1.52 ‰ from 0 to 6 m depth but it strongly varies in the range +0.54 to +2.19 ‰ between 9 m and 12 m, becoming much heavier (+2.32 ‰) at depth (65 m). In 2013, the  $\delta^{30}\text{Si}$  was constant (+1.44 to +1.60 ‰) all over the whole mixolimnion (0-9.5m). The 2012 isotopic oscillation most likely reflects the incomplete water mixing occurring during the dry season while the 2013 isotopic homogeneity traces the stable thermal stratification installed during the rainy season.

The upper chemocline (60-100m) at Ishungu and Gisenyi display very similar  $\delta^{30}\text{Si}$  decreasing from +1.23 ‰ to +0.71 ‰ and from +1.20 ‰ to +0.77 ‰ respectively in 2012, and +1.72‰ to +1.00 ‰ and +1.33 ‰ to +1.23 ‰ respectively in 2013. Below, in the Gisenyi intermediate water mass (130-250 m)  $\delta^{30}\text{Si}$  ranges from +0.48 ‰ to +0.69 ‰ in 2012 and from +0.98 ‰ to +0.62 ‰ in 2013 while the lower chemocline (250 -261 m) is characterized by very light silicon isotopic compositions at +0.10 ‰ in 2012 (260 m) and -0.06‰ in 2013 (at 250 m). In contrast, the deep water mass (270-350 m) shows a wide range of variation of  $\delta^{30}\text{Si}$ : +0.48 to +2.99 ‰ in 2013.

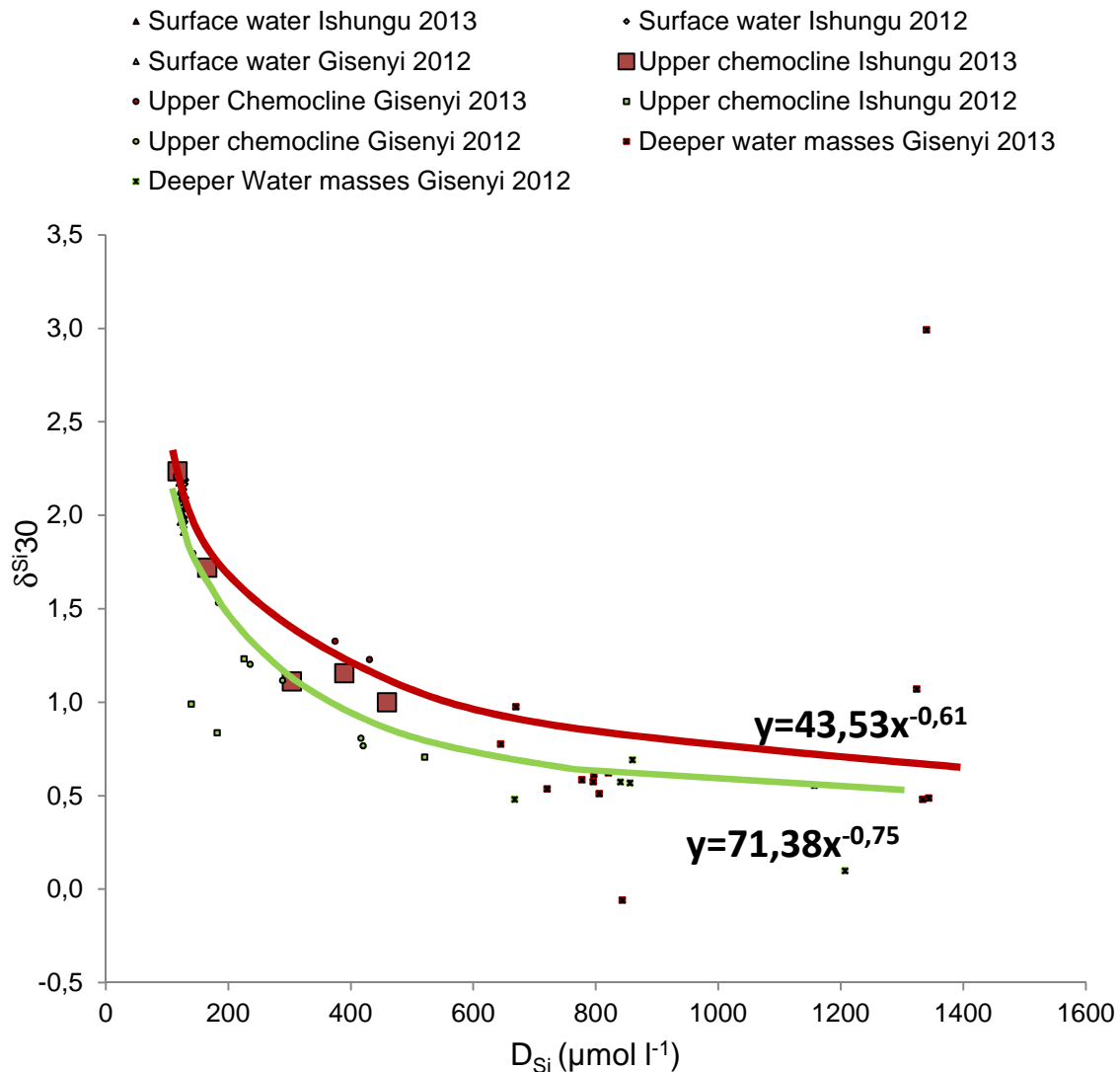


Figure 15:  $\delta^{30}\text{Si}$  vs  $D_{\text{Si}}$  diagram showing two distinct power “pseudo mixing curves” between the surficial and deeper water reservoirs in 2013 (red) and 2012 (green).

In the  $\delta^{30}\text{Si}$  vs  $D_{\text{Si}}$  diagram (Figure 15) both the 2012 and 2013 water samples fit two different “pseudo mixing curves” between the surface and deep waters end-members: power law relationships with two very different curvatures,  $\delta^{30}\text{Si} = 71.38(D_{\text{Si}})^{-0.753}$ , and  $\delta^{30}\text{Si} = 43.53(D_{\text{Si}})^{-0.613}$  respectively. The stronger curvature at the end of the dry season in 2012 reflect a larger diatom mineralization with lighter isotopic signatures at the low  $D_{\text{Si}}$  contents (<500ppm) compared to the dry season in 2013.

#### *Biogenic silica ( $B_{\text{Si}}$ )*

The  $B_{\text{Si}}$  observed in the epilimnion was about twice as large in 2012 as in 2013 in both Ishungu and Gisenyi (Figure 14) ranging from  $3.02 \mu\text{mol l}^{-1}$  to  $3.89 \mu\text{mol l}^{-1}$  and from  $1.69 \mu\text{mol l}^{-1}$  to  $2.19 \mu\text{mol l}^{-1}$  respectively in 2012, and from  $1.24 \mu\text{mol l}^{-1}$  to  $2.20 \mu\text{mol l}^{-1}$  and from  $0.71 \mu\text{mol l}^{-1}$  to  $1.32 \mu\text{mol l}^{-1}$  in 2013, respectively. At Kabuno Bay (0-9.5m), the situation is quite different because the  $B_{\text{Si}}$  was about 20% lower in 2012 than in 2013:  $6.18$  and  $8.35 \mu\text{mol l}^{-1}$  in 2012 and  $7.78$  and  $8.88 \mu\text{mol l}^{-1}$  in 2013 (Figure 16).

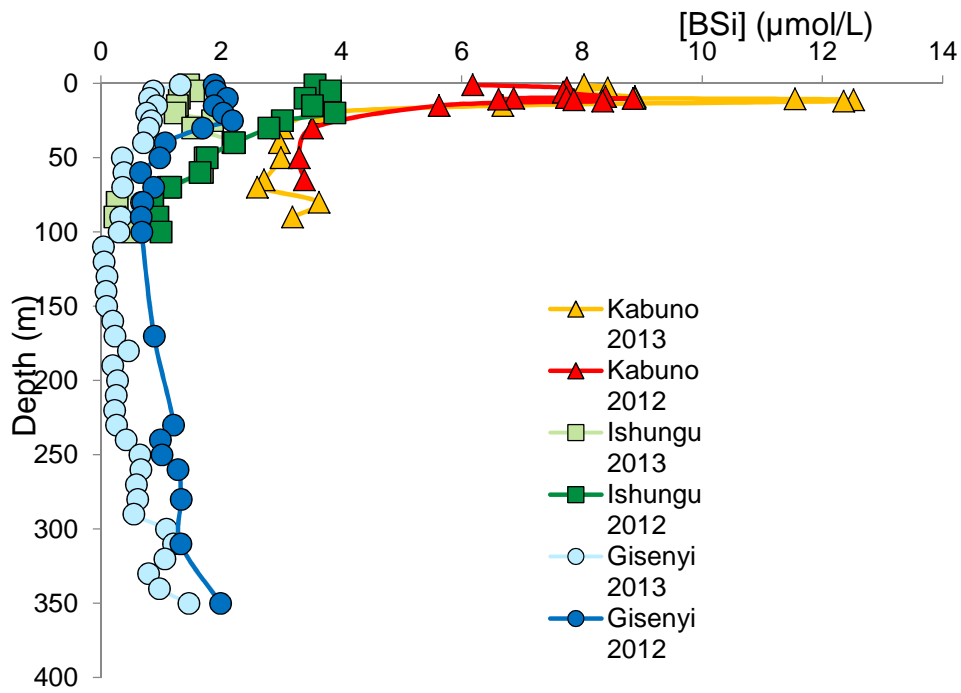


Figure 16: Depth related changes in BSi at Ishungu, Gisenyi and Kabuno in 2012 and 2013

*Incubation experiments*

The flux estimation at different depths through the 28 and 30 Si atoms gives very similar results which demonstrate the reproducibility of measuring diatom productivity and dissolution by isotope dilution. These rates indicate that the productivity was 4, 22 and 39 times higher in 2012 than in 2013 at Kabuno, Ishungu and Gisenyi, respectively (Figure 17). In 2012 dissolution rates were 5-10 times higher than the production rates, while they were 10 to 73 times higher in 2013. This predominance of the dissolution rate likely marks the step down of the nutrient supply to the euphotic zone at the closure of the dry season.

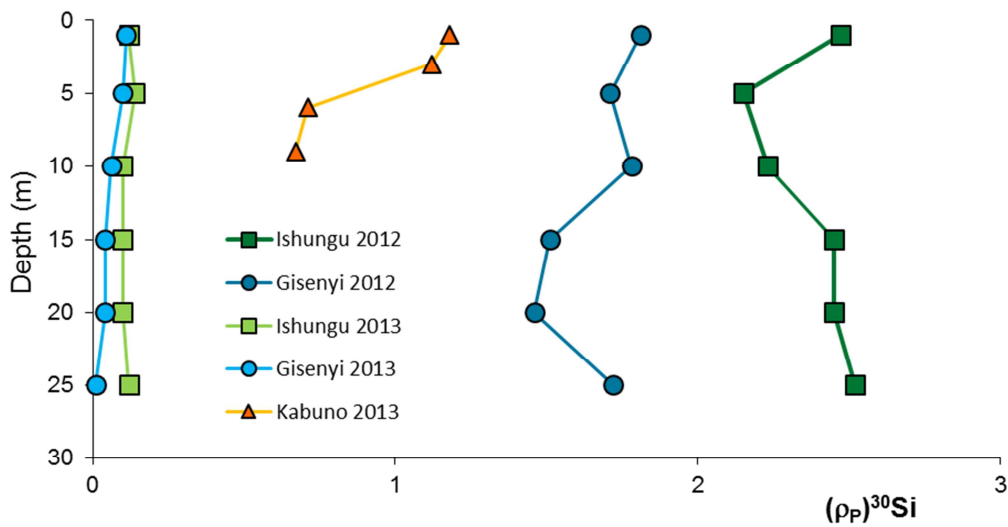


Figure 17: Depth related changes in flux rates of precipitation ( $\rho_p$ ) deduced from the  $^{30}\text{Si}$  atoms at Ishungu, Gisenyi and Kabuno

## Discussion

The ratios between the conservative elements could be used to identify the protolithic source from which the dissolved cations were extracted. In particular, the (Na+K)/Mg ratio is perfectly discriminant, because the  $(\text{Na}_2\text{O}+\text{K}_2\text{O})/\text{MgO}$  weight ratios should be very contrasted between the different kinds of surrounding rocks: Nyamulagira basanites (0.28-0.54); Muja picrites (0.05-0.09, Platz et al., 2004); Nyiragongo foidites ( $2.35\pm 1.20$ , Platz et al., 2004); crustal values (3.3). From there, it is clear that the very stable (Na+K)/Mg weight ratio in the Gisenyi basin around 2.3 (2004-07:  $2.24\pm 0.18$ ; 2012:  $2.39\pm 0.05$ ; 2013:  $2.26\pm 0.014$ ) points to a main source within the Nyiragongo foidites from the northern shoreline of the Main Basin. In contrast, the much lower values observed in the deep water (>30 m) from Kabuno Bay (2004-07:  $1.29\pm 0.54$ ; 2012:  $1.34\pm 0.04$ ; 2013:  $1.06\pm 0.05$ ) points to the closer source of the Nyamulagira and/or Muja volcanics which form the northern shoreline of Kabuno Bay.

The quite different geochemical signatures of the deep waters in Kabuno and Gisenyi demonstrate that the subaquatic deep hot inflows in these two segments of the lake are very contrasted. The the larger Sr/Ca (Figure 8), the strong positive Eu anomalies (Figure 10) and the low Ba/Si (Figure 16) in the Kabuno deep water suggest a strong geochemical control by geothermal anhydrite precipitation and are consistent with water inflows deriving from high temperature magmatic-derived hydrothermal fluids. Anhydrite tends to incorporate large quantities of Sr, but its mineral/water partition coefficient for Sr is lower than for Ca ( $0.4 < D_{\text{Sr}/\text{Ca}} < 0.8$ ) which results in fluid evolution to high Sr/Ca values (>15) with ongoing hydrothermal circulation and precipitation. Due to its retrograde solubility, anhydrite precipitates when the fluid is heated above 100°C. The temperature, pH, and redox conditions of the hydrothermal fluid are thus of particular importance to the potential fractionation of Eu relative to the other REEs. Eu can exist either as a divalent or trivalent ion, with the trivalent ion being closer in size to  $\text{Ca}^{2+}$  than the larger divalent ion. At high pressures and temperatures above 250°C, divalent Eu should predominate in most natural systems. Because of the insoluble character of  $\text{EuSO}_4$  within anhydrite Eu will be concentrated in the residual fluids, resulting in the pronounced Eu positive anomaly often observed in both black and white oceanic smokers. At lower temperature, since both divalent and trivalent Eu could coexist in the fluids, the impact of anhydrite on the fluid Eu anomaly will gradually decrease with the lowering temperature. The very high  $D_{\text{Sr}}$  in the Kabuno Basin is also indicative of high temperature inputs because the Si contents in a hydrothermal fluid drastically decrease with the temperature from about 13 mmol l<sup>-1</sup> at ~260°C down to 5 mmol l<sup>-1</sup> at ~180°C and to 3.2 mmol l<sup>-1</sup> at ~130°C. The sensibility of silica to temperature is so large that silica concentration in thermal waters has been widely used in geothermal exploration to infer temperatures of geothermal systems. Using the pressure sensitive silica geothermometer developed by Ragnarsdottir and Walther (1983), the silica contents of the Kabuno deep water would be compatible with hot thermal discharge at about 160°C. Our geochemical data thus confirm the very peculiar character of the Kabuno Bay which was already deduced from the dissolved gas composition as an indicator of large contribution of a sublacustrine CO<sub>2</sub>-rich mantle-derived discharge (Tassi et al. 2009). The conjugation of a negative Ce anomaly with a positive Eu anomaly is an exceptional feature. As far as we know, it cannot be explained by ongoing hydrothermal circulation and precipitation. Therefore we suggest that the Ce anomaly was a “fossil” characteristic feature of the recharge water

from which these hydrothermal fluids were generated. The most likely origin for this peculiar recharge is the Kabuno surface water itself because it bears an important Ce depletion due to the large Mn oxide precipitation at the oxic-anoxic interface. Therefore we assume that the Kabuno surface water constitutes the permanent recharge that feeds the hydrothermal hot springs which are discharged at different depths at the bottom of the Kabuno Bay. Because the deep water in the Kivu main basin also present significant negative Ce anomalies we surmise by analogy that the hot water inflows were there also constituted of recycled lake surface water. However it was actually equilibrated at a much lower temperature since the role of anhydrite in the hot spring activity was less pronounced as underlined by the much smaller changes in Sr/Ca (<20), the much smaller Ba/Si and the very low REE contents in the deep water. Our observation are very well in agreement with the data from Tassi et al (2009) which demonstrate a larger shift in the D-O isotopic data along the global meteoritic water line between the deep and surface water in Kabuno than in the main basin.

To account for the decadal changes in the Mn and P we have to refer to the rapid seasonal variation of the vertical position of the oxycline between the rainy (October-May) and the dry (June-September) season, as already proposed by Degens and Stoffers (1977) to account for the genesis of the manganese siderite in Lake Kivu. Indeed, a key feature of the lake is its very irregular shape which produces an unusually huge shoreline of about 1200 km long. This long shoreline coupled with an oxic-anoxic stratification that varies seasonally could induce a large dissolution-precipitation “bathtub ring” effect along the margins of all Kivu sub-basins that could trigger the observed Mn behavior. Below the oxycline, all particulate manganese (Mn oxides, Mn oxy-hydroxides) is dissolved in the water column, so that none reaches the bottom and the sediment is low in Mn (as shown by the sediment cores analyses). At the depth of the oxycline, during the dry season deeper mixing there is a strong enrichment in Mn oxide particulates due to quick oxygenation of the large quantity of the Mn dissolved in the upper chemocline. Reaction with the organic matter then converts these oxides to manganese carbonates (Mn siderites) during burial. At shallower depth, above the chemocline, the sediment are likely again low in manganese oxy-hydroxides because the oxygenated surface portion of the water column contains virtually no dissolved manganese. So, there is only a narrow zone between 40-60 m where the Mn-rich minerals could be precipitated and deposited as sediments on the shoreline. Accordingly, in 2012, the peak of particulate Mn ( $Mn_{Part}$ ) occurred at 50 m ( $Mn_{Part} = 346 \mu\text{mol l}^{-1}$ ) and 60 m ( $Mn_{Part} = 159 \mu\text{mol l}^{-1}$ ) at Gisenyi and Ishungu, respectively. Considering the extended Lake Kivu shoreline and assuming a slope of sediment of  $45^\circ$ , we could calculate that the amount of such a kind of Mn-rich sediment could be in the order of  $0.034 \text{ km}^3$  which is quite considerable considering the volume of water between 40 and 60 m depth ( $\sim 50 \text{ km}^3$ ). It is clear that we have potentially there a huge reservoir of Mn that could be reactivated in function of the water oscillation intensity: when these “oxic” minerals are not yet buried, they are readily sensitive to anoxic conditions and could thus be quickly re-dissolved when the oxycline is again stabilized at about 35 m during the rainy season. An indirect confirmation of the importance of such a process in Lake Kivu is given by the difference in dissolved REE between the Ishungu and the Gisenyi basins. The larger dissolution peak of REE and the stronger positive Ce anomaly (Figure 11) between 50 and 60 m in Ishungu point to larger oxide dissolution in this less deep more restricted basin which is consistent with a ratio of larger proportions of

oxide-rich sediments deposited in the 50-60 m interval recycled in a relatively much smaller local water volume at this depth interval compared to the Gisenyi basin.

This “bathtub ring” process could potentially have a strong impact on the long-term P availability and therefore the diatom productivity since P could be adsorbed in large quantity on the Mn and Fe oxides trapped in the “bathtub ring” sediments from which they could be released with the oxide dissolution. The significant negative correlation between P/Na and Mn/Na in Kabuno in 2013 demonstrates that the two processes are actually interdependent but are not directly coupled. Likewise, in Gisenyi and Ishungu, the peak of P growth relative to Na occurs at a depth very close but just below the peak of the positive Ce anomalies (70-80 m) which trace the dissolution of the Mn oxy-hydroxides. We cannot provide a straightforward explanation for this decoupling with our present data, but a very likely hypothesis could be that P is much closer linked to the Fe-oxide cycle than to the Mn-oxide cycle. Indeed, Mn and Ce undergo reductive dissolution under suboxic conditions unlike Fe which requires more extremely reducing conditions to undergo reductive dissolution at a deeper level.

Several results point to a greater primary productivity in 2012 than in 2013 within the main basin at Ishungu and Gisenyi:

1. The larger proportion of  $B_{Si}$  at both locations in 2012;
2. The larger flux rates of diatom precipitation at both locations in 2013;
3. A stronger P depletion of the mixolimnion and the upper chemocline at both locations in 2012;
4. A stronger Ba depletion in the mixolimnion at both locations in 2012;
5. A lack of significant change in  $D_{Si}$  and  $\delta^{30}Si$  between 2012 and 2013 in Ishungu.

The first three parameters provide direct reliable records of the instantaneous changes in the diatom productivity and their P main nutrient availability. As such they do not call for further discussion. In contrast, the last two proxies provide reliable records of the more global seasonal changes in the diatom productivity. Besides they could be easily recorded in the sedimentary column and they offer a way to quantify the past productivity. As such they require a more proper and detailed discussion below.

Our Ba profile mimics those found in the oceanic environments where dissolved Ba is generally depleted in the surface waters and enriched in deep waters with its concentration increasing along deep advective flowlines. In seawater, the Ba cycle is controlled by the Barite ( $BaSO_4$ ) precipitation and dissolution. Its precipitation is commonly associated with the decay of coccolithophore and diatom biomass, two phytoplankton groups that are not known to precipitate barite intracellularly. The decay process results in the localized development of micro-environments on organic particle surfaces, where Ba is concentrated via adsorption onto Fe-Mn-oxyhydroxides where the solubility product of barium ( $Ba^{+2}$ ) and sulfate ( $SO_4^{-2}$ ) exceeds the equilibrium constant of barite, causing spontaneous nucleation of barite microcrystals (Dehairs et al., 1992). This process is assisted by elevated concentrations of sulfate within sinking organic particles due to oxidation of organic-derived sulfur compounds such as amino acids or re-oxidation of  $H_2S$  produced through bacterial sulfate reduction. When some of these organic debris decompose they release the barite micro and

nanocrystals, which could be then partly dissolved. Since Ba cycles in a manner analogous to that of hard-part constituents of diatoms, dissolved Ba tends to correlate linearly with dissolved Si in much of the world oceans. Barite is relatively insoluble under oxidizing conditions and, hence, tends to be well preserved in the deep oceanic sediments where bottom waters are oxygenated. Despite the barite theoretical soluble character in oxygen-free conditions, the behavior of Ba in anoxic marine environment like as the Baltic Sea appears to be primarily imprinted by the formation and regeneration of Ba as it is in the open ocean (Falkner et al., 1993). The gradient of Ba change in the water column (0.036-4.39  $\mu\text{mol l}^{-1}$  in 2012 and 0.13-3.8  $\mu\text{mol l}^{-1}$  in 2013) are very much larger than those observed in other strongly anoxic environments: the Black Sea (0.19-0.50  $\mu\text{mol l}^{-1}$ , Falkner et al., 1993) and Framvaren Fjord (0.064-0.28  $\mu\text{mol l}^{-1}$ , Falkner et al., 1993). This probably endows a very unique character to the Lake Kivu diatom-barite-Ba cycle which is complicated by two other coeval factors: (1) the strong “bathtub” like Mn effect and (2) the hydrothermal controls of the Ba cycle. The importance of these “non-biogenic” controls of the Ba cycle are confirmed by (1) the lack of a positive correlation between the Ba content and the biogenic silica in the Gisenyi sediments; (2) the poor Ba-Si correlation in the Kabuno Bay (Figure 14). The quick change in the Ba vertical gradient between 2012 and 2013 is however interpreted as a quick response to the larger decaying diatom-derived organic matter in 2012 and its very quick and large mineralization all along the water column that released the barite which was then quickly dissolved. The strong change in the Ba concentrations between 2012 and 2013 demonstrate that within one year, the surface Ba content has been drastically increased by a factor of 4 while the deep Ba have decreased of about 15%. This is a strong evidence that over annual time scales the chemical stratification in Lake Kivu cannot be considered to be at a steady state in agreement with recently deduced temporal upward movements of thermoclines (Katsev et al., 2014). The different Si-Ba correlations and the larger scattering of the 2004-07 (Tassi et al., 2009) compared to ours may reflect some deep changes in the diatom–barite-Ba dynamic over the last decade.

Because an important seasonal peak of diatom productivity occurred in 2003 (Darchambeau et al., 2014), a rough estimate of the “interseasonal” isotopic mass fractionation factor between the Lake Kivu diatoms and the dissolved Si in the fresh water ( $\epsilon$ ) could be deduced from the Ruzizi large changes in  $D_{\text{Si}}$  and  $\delta^{30}\text{Si}$  observed between March and August 2003 at the Ruzizi outlet in Lake Tanganyika [cf. Alleman et al (2005) table 1], applying the following equation:

$$\epsilon = \left[ \frac{(\delta_{\text{Si}}^{30}) - (\delta_{\text{Si}}^{30})_0}{\ln f} \right] \quad \text{with } f = D_{\text{Si}} / (D_{\text{Si}})_0 \quad \text{Equation 1}$$

- $D_{\text{Si}}$ : Ruzizi dissolved Si in August 2003 [(92  $\mu\text{mol l}^{-1}$ ) cf. Alleman et al (2005) table 1].
- $(D_{\text{Si}})_0$ : Ruzizi dissolved Si in March 2003 [(145  $\mu\text{mol l}^{-1}$ ) cf. Alleman et al (2005) table 1]
- $(\delta_{\text{Si}}^{30})_0$ : Ruzizi  $\delta^{30}\text{Si}$  in August 2003 (+2.51‰) calculated from  $\delta^{29}\text{Si}$  (Alleman et al., 2005) assuming that  $\delta^{29}\text{Si}$  and  $\delta^{30}\text{Si}$  obey the terrestrial mass dependent equilibrium fractionation line ( $\delta^{30}\text{Si} = 1.93 \delta^{29}\text{Si}$ ).
- $\delta^{30}\text{Si}$ : Ruzizi  $\delta^{30}\text{Si}$  in March 2003 (+1.7 ‰) calculated from  $\delta^{29}\text{Si}$  (Alleman et al., 2005).

The calculated fractionation factor [ $\delta = -1.8 \text{ ‰}$ ] is within the range but slightly higher than those established from field studies in various environments: Lake Tanganyika [ $-1.1 \text{ ‰} \pm 0.4 (2\sigma)$ , Alleman et al., 2005], in the Southern Ocean [ $-1.3 \text{ ‰} \pm 0.4 (2\sigma)$ , Cardinal et al., 2007], in estuaries [ $-1.50 \text{ ‰} \pm 0.36 (2\sigma)$ , Sun et al., 2014]. This implies that the global seasonal diatom productivity in Lake Kivu could be efficiently monitored at the lake outflow by the Ruzizi River through monthly coupled measurements of  $D_{Si}$  and  $\delta^{30}Si$ . Our slight overestimate relative to field determinations is most likely explained by the fact that a part of the Ruzizi water could have been modified by the isotopic signatures of the Ruzizi tributaries even if its catchment area is small. So, for our further isotopic calculation, we still prefer to use the fractionation factor established by Alleman et al., (2005) in the close context of Lake Tanganyika.

The proportion of diatom produced in the surface water mass between 2012 and 2013 can be quantified at Ishungu using the equation:

$$B_{Si} = D_{Si} \left( e^{[(\delta_{Si}^{30})_0 - \delta_{Si}^{30}] / \epsilon} - 1 \right) \quad \text{Equation 2}$$

with the following parameters:

- $D_{Si}$ : average dissolved Si between 0 and 40m in September October 2012 ( $128 \mu\text{mol l}^{-1}$ ).
- $(\delta_{Si}^{30})_0$ : average  $\delta^{30}Si$  between 0 and 40 m in September October 2012 ( $+2.1 \text{ ‰}$ ).
- $\delta^{30}Si$ : average  $\delta^{30}Si$  between 0 and 40 m in August 2013 ( $+2.08 \text{ ‰}$ ).
- $\epsilon$ : Si isotopic fractionation by diatoms:  $-1.1 \text{ ‰}$  (Alleman et al., 2005).

The obtained diatom productivity is negative ( $-2.3 \mu\text{mol l}^{-1}$ ), but this negative value is very well in agreement with the incubation experiments in Ishungu because the average diatom dissolution rate ( $2.3 \mu\text{mol l}^{-1} \text{ d}^{-1}$ ) strongly exceeds the average production rate ( $0.11 \mu\text{mol l}^{-1} \text{ d}^{-1}$ ) showing that the balance is short of about  $-2 \mu\text{mol l}^{-1} \text{ d}^{-1}$ . This low productivity is also evidenced by the low range of total  $B_{Si}$  collected on the filters between 0 and 100 m in 2013:  $18 \mu\text{mol l}^{-1}$ .

At Kabuno Bay, the production was quite more active, as shown by the high measured  $B_{Si}$  ( $>8 \mu\text{mol l}^{-1}$ ) in 2013 and the significant decrease in  $D_{Si}$  ( $\Delta=73 \mu\text{mol l}^{-1}$ ), between 2012 and 2013. The proportion of diatom produced in the surface water mass between 2012 and 2013 can be quantified using equation 2, with the following parameters:

- $D_{Si}$ : average dissolved Si between 0 and 9m in September October 2012 ( $528 \mu\text{mol l}^{-1}$ ).
- $(\delta_{Si}^{30})_0$ : average  $\delta^{30}Si$  between 0 and 9m in September October 2012 ( $+1.3 \text{ ‰}$ ).
- $\delta^{30}Si$ : average  $\delta^{30}Si$  between 0 and 9m in August 2013 ( $+1.5 \text{ ‰}$ ).
- $\epsilon$ : Si isotopic fractionation by diatoms:  $-1.1 \text{ ‰}$  (Alleman et al., 2005).

The obtained diatom production ( $105 \mu\text{mol l}^{-1}$ ) is well in the range of the total  $B_{Si}$  collected on the filters between 0 and 90 m in 2013 ( $118 \mu\text{mol l}^{-1}$ ). This large diatom productivity in Kabuno relative to Ishungu and Gisenyi is likely a consequence of the large unusual inflow of P relative to Na in 2013. We cannot provide a straightforward explanation for this strong rapid inflow of P but it could result from either massive decomposition of organic matter from the large 2012 diatom bloom, from a change in the hot spring activity or from P release by the reduction of Fe-Mn-rich sediments.

The smooth increase in Si/Na between 50 and 100 m in the upper chemocline (70-100 m) is a clear evidence that the Si budget at those depths is controlled by the diatom rain dissolution. This is confirmed by the inverse relation between the increase in  $D_{Si}$  and the decrease in  $\delta^{30}Si$  vs  $D_{Si}$  diagram (Figure 12). This demonstrates that the upper chemocline is chemically very dynamic. Indeed, the isotopic heterogeneities found at the end of the dry season 2012 due to the high planktonic production are quickly removed by water mixing by the end of the following dry season. This contrasts with the surface and deeper reservoirs which are much more stable from one year to another, in agreement with the long residence time of the water below 260m deep (~870 years, Schmid et al., 2005). These power trends confirm previous results (e.g. Schmid et al., 2005 and reference therein) that indicate that the water within the lake is a blend of one deep source and lake surface water. They fit well with the presence of a negative Ce anomaly between 150 and 250m, because it demonstrates that the anomaly developed in the oxic layer has been transferred to the deepest layers.

The deeper reservoirs (>100 m) tend to display a very homogenous Si isotopic signature at about +0.5 ‰ despite the limited introduction of water with light (around 0 ‰ at 250-260 m) and heavy (>1 ‰ at 320-350 m) signatures. The subaquatic spring introduction around 250 m depth has been long recognized (Degens et al., 1973 and Schmid et al., 2005 and reference therein) and is therefore an active continuous input. The Si concentrations calculated by Pasche et al. (2009) for this spring was smaller than for the lake water and established to be around 660  $\mu\text{mol l}^{-1}$ . Such a low  $D_{Si}$  is indicative at a low temperature of about 80°C using the pressure sensitive silica geothermometer developed by Ragnarsdottir and Walther (1983). These low-T water inputs were supposed to be essentially meteoritic in origin and issued from the weathering of fresh volcanic rocks embedding the northern borders of lake Kivu (e.g. Pasche et al., 2009 and reference therein). This is corroborated by the (Na+K)/Mg ratios of all water layers. The very light Si isotopic signature is also very well in support of such a water derivation because fresh mantle-derived volcanic rocks such as those of the Virunga province are all characterized by a uniform slightly negative signature ( $\delta^{30}Si = -0.29 \pm 0.08$  ‰, Savage et al., 2010). With their very heavy signatures ( $1.07$  ‰ <  $\delta^{30}Si$  <  $+2.99$  ‰), the deeper spring inputs of the main basin and the Kabuno Bay are unlikely to derive from a direct basaltic dissolution. We could see two potential processes to account for those heavy signatures: (1) a kinetically controlled precipitation of amorphous silica within the hot springs; (2) the recycling of the the Kivu surface waters. Low temperature (<100 °C) amorphous silica deposition in a Si-rich hydrothermal fluid may kinetically create strongly negative  $\delta^{30}Si$  signatures ( $-0.1$  ‰ <  $\delta^{30}Si$  <  $-4$  ‰) in silica precipitates (Geilert et al., 2015). This precipitation may therefore increase the isotopic weight of the residual dissolved silica at the very neighborhood of the precipitated surface but is unlikely by itself to develop large positive Si isotopic anomalies on the running fluid if the initial fluid has a magmatic-derived signature close to 0 ‰. Another mechanism could be the mere recycling of the Kivu Lake surface water because it bears a very positive Si isotopic composition due to the diatom productivity. Our preferred mechanism to explain the very positive  $\delta^{30}Si$  is thus a combination of the two processes: the recycling of the surface Lake Kivu water associated to amorphous silica precipitations.

## Conclusions

- Our data confirm that most of the solutes of the Lake Kivu waters are mainly controlled by the hydrothermal alteration of the volcanics along the northern shoreline. These rock-water interactions take place in the Nyamulagira basanites and/or the Muja picrites in the Kabuno Bay and within the Nyiragongo foidites in the main Gisenyi basin.
- The most probable recharge source for these hydrothermal fluids is the surface water of the lake itself (locally mixed with magmatic-derived and meteoritic-derived fluids) as evidenced by the permanent negative Ce anomaly observed in the deep waters from the Kabuno and Gisenyi basins and the heavy Si isotopic signatures of some deep spring inputs at these two locations.
- The quite different geochemical signatures of the deep waters in Kabuno and Gisenyi demonstrate that the subaquatic deep hot inflows in these two segments of the lake are very contrasted. The strong positive Eu anomalies and the larger Sr/Ca in the Kabuno deep water suggest a strong geochemical control by geothermal anhydrite precipitation and are consistent with water inflows deriving from high temperature hydrothermal fluids (>200 °C). The anhydrite precipitation was much more limited in the Gisenyi hot inflows in agreement with much lower equilibration temperatures (<100 °C).
- The annual quick changes in Ba distribution and P/Na as well as the rapid  $\delta^{30}\text{Si} - D_{\text{Si}}$  re-equilibration of the upper chemocline after the diatom mineralization in 2012 demonstrate that the lake water mixing is more dynamic than previously thought. Moreover decadal changes in Na/K, Na/Mg, Si/Ba, dissolved Mn and Sr/Ca indicate that the chemical stratification in Lake Kivu is not in a steady state which in turn suggests that the residence time of most elements in deep waters is likely much smaller than the previous 800-100 years estimate from Schmid et al. (2005).
- We postulate that the strong P limitation that controls the diatom productivity throughout the year is dependent of a “bathtub ring” oxic-anoxic precipitation. The deposited oxy-hydroxydes could potentially release some P when the anoxic conditions of the rainy season mobilize the P stocked in the deep mixolimnion between 50 and 60 m. This mobilization could be dependent of two factors: (a) the intensity of the wind-induced water oscillation; (b) the morphology of the basin that controls the amount of oxy-hydroxide which could be deposited. The effect should therefore be larger in the restricted basin of Kabuno Bay and Ishungu Basin.
- The strong Si-Ba correlation and the strong Ba depletion of the surface waters in 2012 when the diatom productivity was larger (as demonstrated by larger  $B_{\text{Si}}$  and larger diatom precipitation rates) indicates that the Ba cycle is partly controlled by the Barite precipitation and dissolution consecutive to the decay of diatom biomass, which is known to precipitate barite intracellularly. However, due to other interference controls (Mn oxides, hydrothermal activity), the sedimentary  $\text{Ba}_{\text{Barite}}$  is unlikely to be useful as a proxy of the diatom paleoproductivity in Lake Kivu.
- Here we demonstrate that the changes in  $\delta^{30}\text{Si}$  vs  $D_{\text{Si}}$  are very sensitive to the global seasonal diatom productivity and mineralization in Lake Kivu. We suggest to monitor

the changes in  $\delta^{30}\text{Si}$  vs  $D_{\text{Si}}$  at the lake outlet in the Ruzizi river to quantify the global annual diatom productivity in the lake.

- The stable deep water Si isotopic signature at about +0.5 ‰ in the Gisenyi basin results from the addition of three sources: low-T meteoritic inputs with low Si isotopic signatures (0 ‰), diatom mineralization (~+1 ‰) and low-T hydrothermal recycling from the surface water (+3 ‰) in the decreasing order of magnitude.

### 2.2.1.5 Remote sensing

Time series of Lake Kivu Surface Water Temperature (LSWT) and Ocean Color (OC) products were produced from MODIS data. They cover the period 2002-2014. Raster georeferenced files and quick looks of daily and weekly-aggregated data were delivered as well as spatio-temporally aggregated Time Series (TS) in table format for the whole lake. We briefly present here the calibration and validation procedures implemented for deriving chlorophyll a and LSWT using *in situ* data and ARC-Lake dataset.

### Chlorophyll-a and K490 extraction from MODIS Terra and Aqua

The objective of this WP was to produce Time Series (TS) of Ocean Color (OC) products for Lake Kivu from MODIS images for the period 2002-2014.

#### *Satellite data preparation*

All available MODIS Level 1A data Reprocessing 5 (Feldman & McClain, 2014) covering the area of Lake Kivu have been downloaded from NASA Ocean Color server <http://oceancolor.gsfc.nasa.gov/>. SeaDAS v7.1 was used for the processing: extraction of geolocation information, computation of calibrated radiances and geophysical variables. For Visible (VIS) and Near-Infrared (NIR) channels we had to take extra care to define appropriate atmospheric correction for high altitude inter-tropical lakes. Terrain height correction was enabled when computing geolocation files and altitude was taken into account for computing Rayleigh radiance using external digital elevation model. Default stray light and cloud masking were disabled in order to preserve as many pixels as possible. We started processing from Level 1A in order to reduce the parallax effect and used already subset dataset to mitigate the data management aspect (data storage and processing time). Only Aqua data were used as the OBPG does not encourage the use of MODIS Terra data for OC processing due to on board sensor calibration problems (Franz et al., 2007). Level 2 products corresponding to each 5-minute granule were computed. They contain the following parameters: RS reflectance in all VIS wavelengths (Rrs), chl-a concentration computed using several algorithms, K490, sensor and solar zenith angles and other useful ancillary information such as quality flags. External MODIS cloudmask (35\_L2) from MODIS-Atmosphere group was also downloaded. It defines 4 quality levels: cloudy, probably cloudy, probably clear and clear.

#### *In situ dataset structuration, quality control and analysis*

*In situ* data from different stations have been integrated in databases structures and consistent quality control has been performed (wrong data identification, homogenization

between different Excel files formats, correction of station coordinates, completion of missing time and instrument information, homogenization of NoData coding, etc. ...). This step was needed to perform inter-comparison and validation of satellite data. In situ vertical profiles of water column have also been compared (vertical gradient) in order to detect inconsistencies and identify the most reliable in situ data to calibrate/validate the extraction of OC parameters and LSWT.

#### *OC calibration phase*

Important effort has been dedicated to select most appropriate bio-optical algorithm and atmospheric correction during a first calibration phase. It is important to remind that only small part of the signal recorded by the satellite sensor comes from the lake water i.e. Lw is small with respect to TOA radiance. This underlines the importance of atmospheric correction. The available in situ data together with the operational expectance of the RS contribution in this project did not allow the derivation of new sets of parameters for an atmospheric model specifically adapted to Lake Kivu. We thus reused existing models. SeaDAS allows applying different atmospheric corrections by defining different aerosol options (aer\_opt). In current version, 80 'fixed' aerosol models numbered from 0 to 79 are implemented (Ahmad et al., 2010). For information, these 'fixed' models are built according to 8 different values for relative humidity [30, 50, 70, 75, 80, 85, 90 and 95%] and 10 values for particle size (defined as fine mode fraction) [95, 80, 50, 30, 20, 10, 5, 2, 1 and 0%]. A variation of fine mode fraction will lead to higher differences in the computed Lw than a variation of relative humidity (McCarthy et al., 2012). SeaDAS aer\_opt parameters allows either to apply directly one of these 80 fixed models or to choose some other options numbered -1 to -10. Most of these options are variants of the iterative procedure described by Gordon & Wang (1994) using two NIR channels for selection of the most appropriate fixed models (or a combination of two of them). For example, option -2 (default) corresponds to multi-scattering with 2-band, RH-based model selection and iterative NIR correction and -10 corresponds to Multi-scattering with MUMM correction and MUMM NIR calculation. Several of these options and bio-optical algorithms for chl-a concentration computation (OC2, OC3, OC3C, OC3 with CDOM Morel correction, Morel, Carder, GSM, GIOP, MGIOP) were tested on Lake Kivu MODIS dataset. In situ surface chl-a concentration measurements and chl-a concentration from MODIS images has been matched applying the following filtering criteria: maximum time difference of 6h., 'clear' or 'probably clear' sky at selected pixel according to MODIS Atmosphere cloudmask, minimum coast distance of 1 km, maximum spatial distance of 4 km. In situ values have been associated either directly to the matched pixel value or the local median extracted in a 5-by-5 pixels window around this pixel to keep higher number of points in match-up. Certain aerosol model / bio-optical algorithm combinations result in a higher number of missing values of chl-a concentration. Only matching observations for which a value is given for each tested combination have been retained to compare their efficacy.

## **Results**

#### *Calibration/validation against in situ data*

The calibration for OC products extraction based on in situ chl-a data has been substantial. Only a few results are summarized in present report. After selecting surface, non-coastal chl-

a in situ measurements concomitant with clear sky (see match-up criteria in the methodological section), the number of available observations for calibration was considerably reduced.

R<sup>2</sup> is not in this case a reliable measure of performance of the tested algorithm. Figures 19 to 22 synthesize the comparison between all tested atmospheric algorithm combinations and in situ data following the recommendations of Campbell & O'Reilly (2006). Unfortunately our analysis does not permit to clearly identify a unique best combination. Results are sometimes contradictory for example using only one pixel values instead of the median in the neighborhood. In certain cases statistics can also be influenced by the low number of observations.

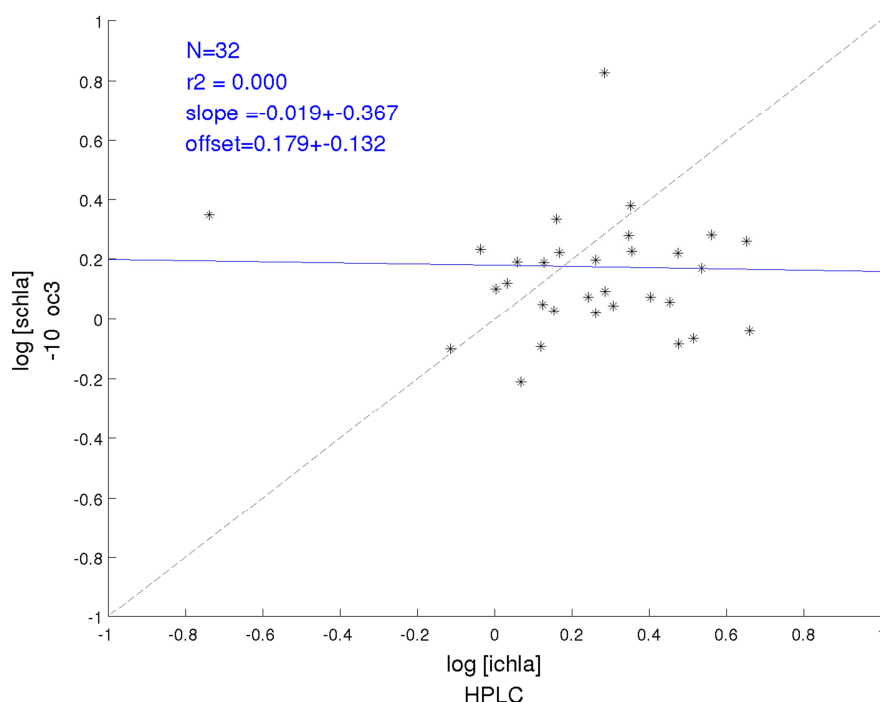
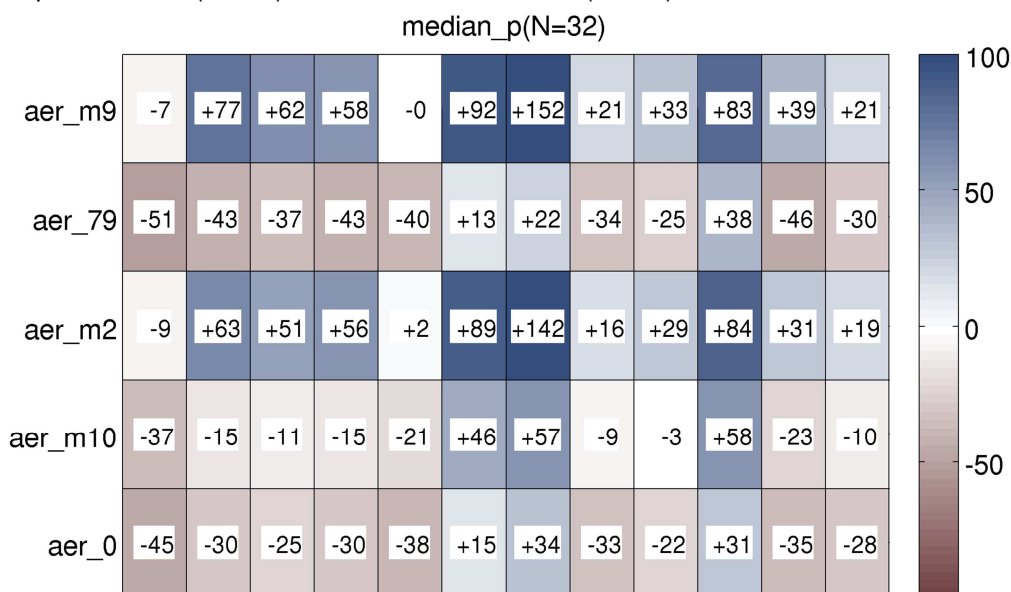


Figure 18 Relationship between MODIS Aqua OC3 algorithm and MUMM aer\_opt -10, median in a 5-by-5 pixel window (Y axis) and in situ HPLC values (X axis).



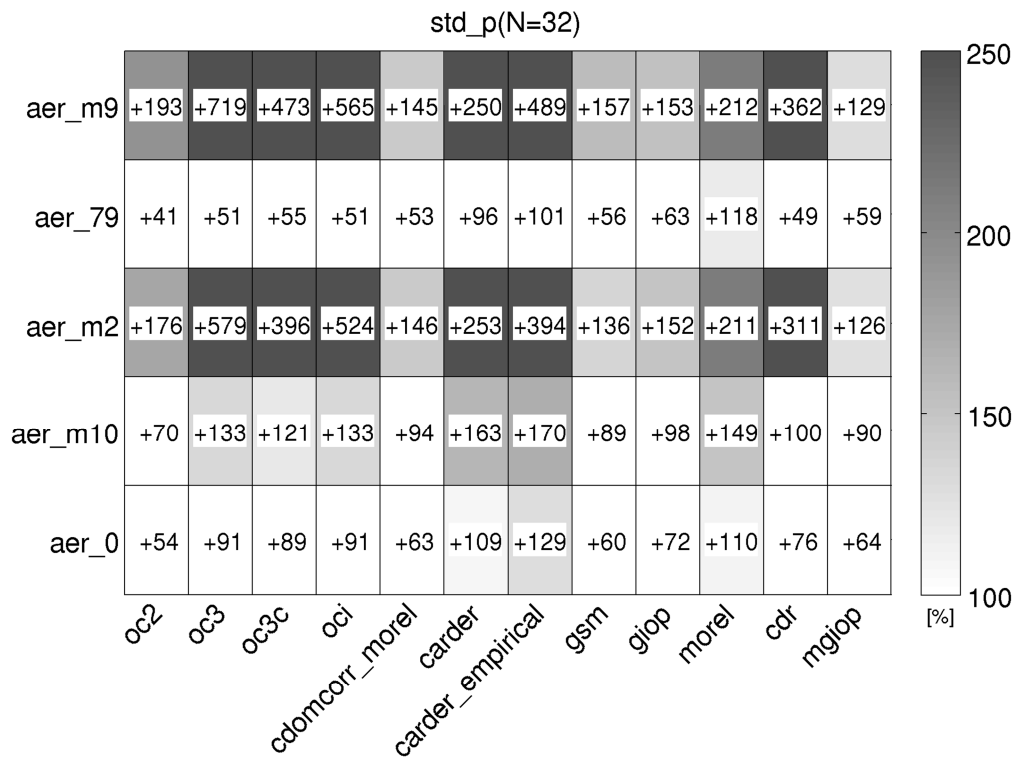


Figure 19. Median (bias) and standard deviation (imprecision) in % of the difference between in situ and MODIS Aqua values for 12 OC and 5 aerosol models (median value in 5-by-5 pixel) – N=32.

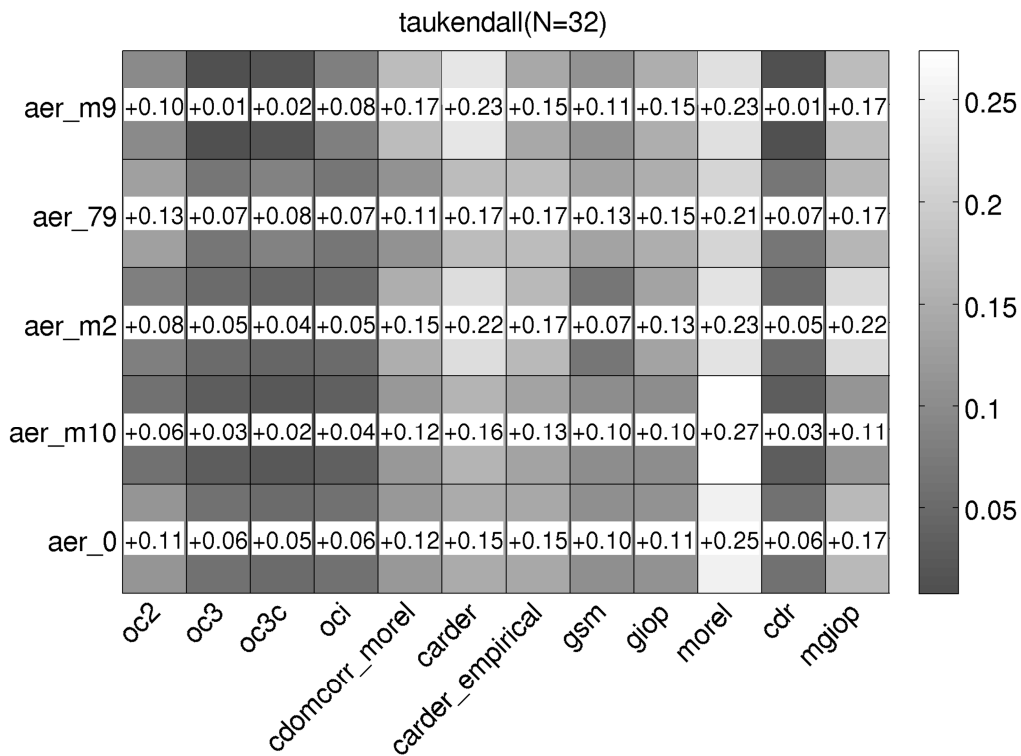


Figure 20. Rank correlation (Kendall Tau) between in situ and satellite values of chl-a concentration (median value in 5-by-5 pixels). A tau near 0 corresponds to low association between satellite and in situ.

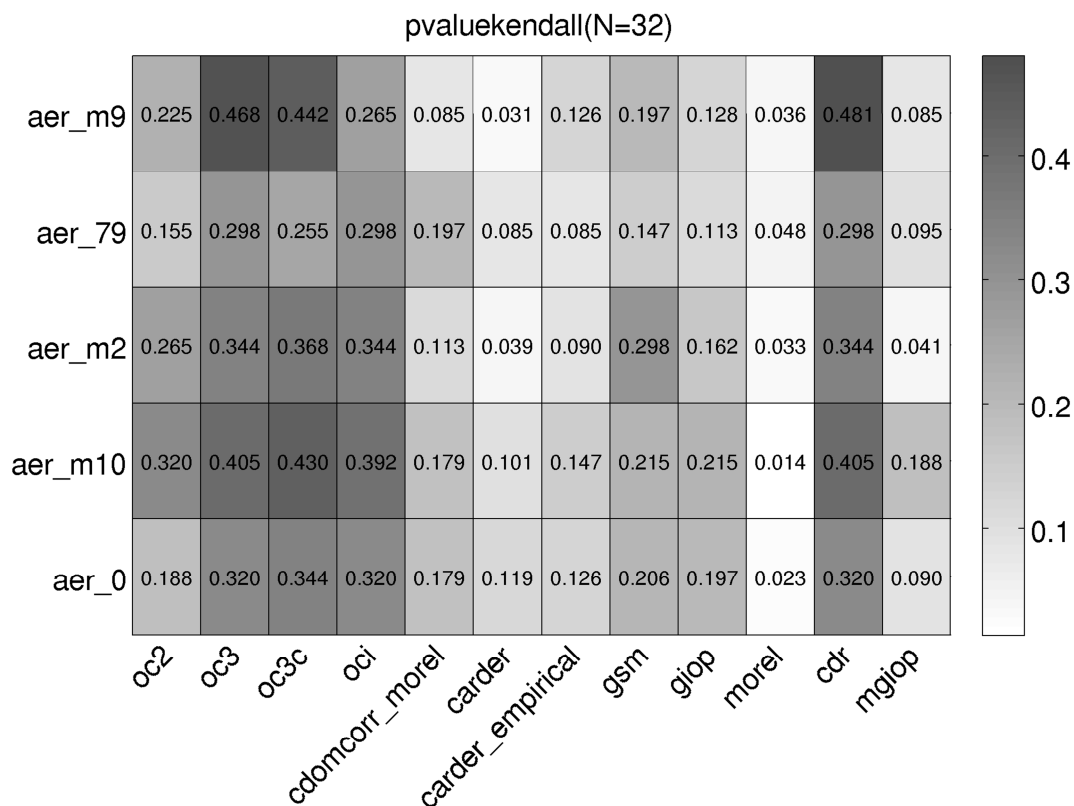


Figure 21. P-values associated to the Kendall Tau (statistical significance of the tau values). The association between in situ and RS chl-a concentration (median value in 5-by-5 pixels) is significant for some combinations at alpha level of 10%.

The range of chl-a concentration values from in situ (the ones in the match-up) data is very small (very few high values and no very high value). We noticed that satellite products tend to show an even smaller dispersion i.e. satellite data probably overestimate very low values and underestimate higher values (fig. 18 and fig. 22). Aerosol options -2 or -9 first appeared to give a higher range of values but it was noted that this was artificially produced by artifacts created during the atmospheric correction, giving rise quite often to incoherent spatial discontinuities (fig. 23). Moreover, another test performed on the 645 nm Rrs (fig. 24) shows that these options -2/-9 also tends to overestimate the contribution of atmosphere, giving rise to physically impossible negative reflectance values. From this figure, it can be observed that fixed model with high fine mode (21, 62, 73) also tends to overcorrect the atmospheric effect, at least during the dry season.

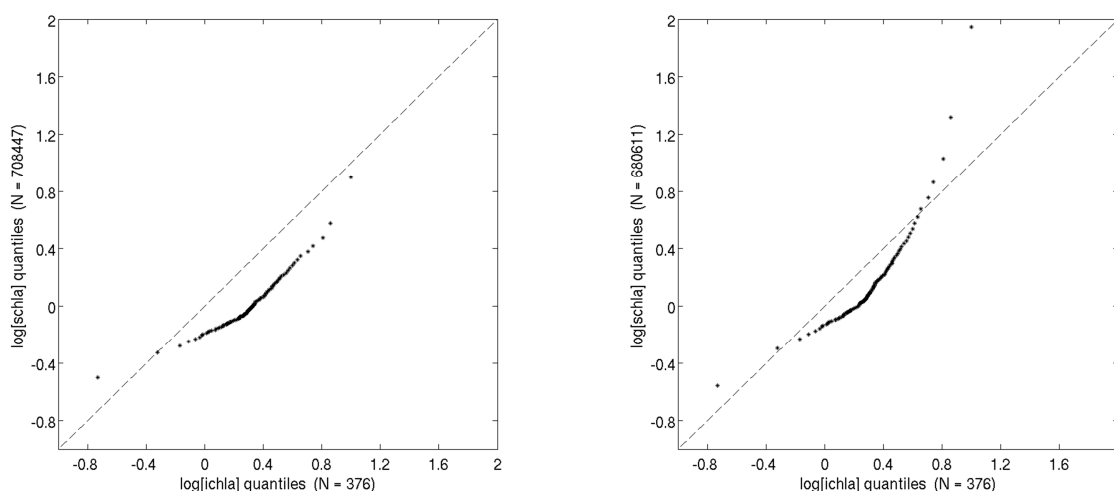


Figure 22 – Quantile-quantile plots comparing general distributions of satellite values (Y-axis - OC3 algorithm with aer\_opt 79 on the left and -10 on the right) and in situ chl-a values (X-axis). Not only matching observations were used but all pixels from 2002-2014 period from Lake Kivu and all surface chl-a in situ measurements.

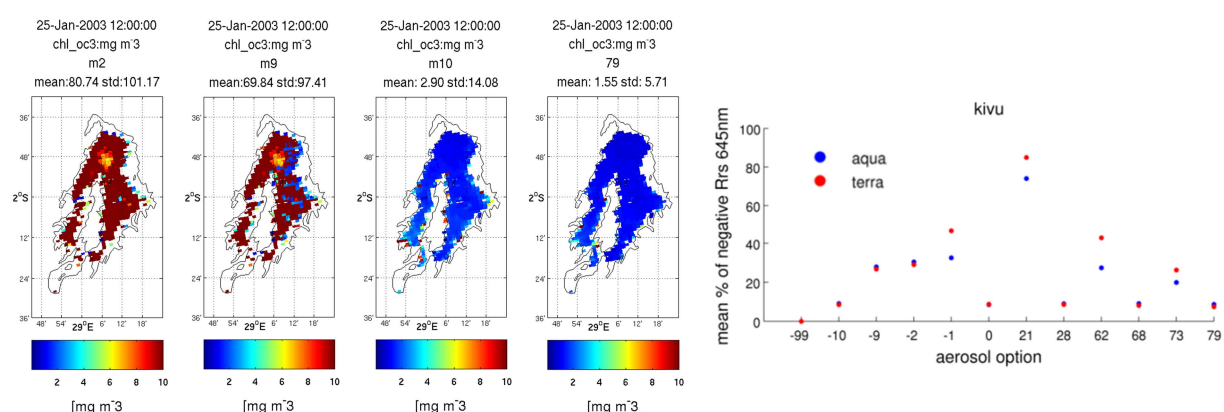


Figure 23 aer\_opt -2 and -9 (on the left) show unreliable spatial discontinuities in the computed chl-a concentration values. These discontinuities do not appear for options -10 and 79 (on the right).

Figure 24 Proportion of negative reflectance in band 645 nm based on a small number of clear sky images (mainly from May to September period, when clear sky is more frequent).

On the basis of these arguments, we produced the chl-a TS using OC3 algorithm with the two best-performing aerosol models for atmospheric correction: 79 (fixed model based on relative humidity of 90% and fine mode fraction of 0%) and -10 (multi-scattering with MUMM correction and MUMM NIR calculation). Considering bias and imprecision (fig. 9), we globally observed a lower effect of the bio-optical algorithm on the computed chl-a concentration values than the variation of aerosol model. This is not obvious considering Kendall Tau (fig. 20) and the corresponding p-values (fig. 21) that show significant association between in situ and remotely sensed values for some combinations. Finally the OC3 algorithm, the default algorithm for MODIS, was selected as we could not prove the global spatio-temporal superiority of some other based on in situ data. Some algorithms (usually the most complex) give more frequent no data values and some of them require to be parameterized while we do not have enough elements to automate that properly for each individual image. We are also comforted in this choice by the literature as Knox et al. (2014) considered appropriate for Lake Kivu this combination of the OC3 algorithm with the type of atmospheric correction very similar to aer\_opt 79 in the present report. This also confirms the previous choice of Horion et al. (2010) on Lake Tanganyika.

#### *Final dataset*

The final products in raster format and quicklooks give chl-a concentration at spatial resolution of 0.02 degrees for the whole lake with a daily and weekly temporal resolution for the period July 2002 – November 2014 with OC3 algorithm and the two mentioned aerosol options (79 and -10). Tables containing weekly spatio-temporally aggregated TS for the whole lake (fig. 25) were also produced. Due to the relatively small size of Lake Kivu coupled with the spatial resolution of MODIS and the high number of noisy or missing pixels due to very frequent cloud cover, no TS were extracted for smaller subregions of the lake. We realized a basic Seasonal Trend Analysis of two TS extracted at two points of the lake where temporal representativeness is the highest but the result of this analysis is not illustrated in the present report.

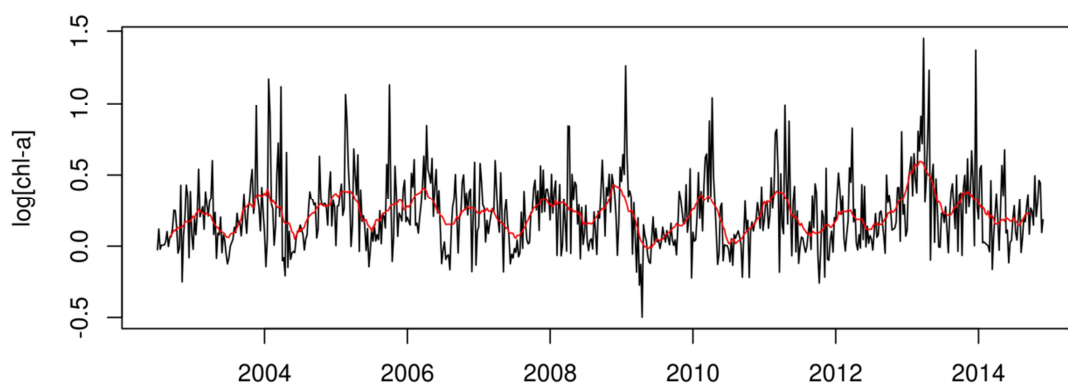


Figure 25. Weekly aggregated TS of log (chl-a concentration) with moving average of 13 weeks in red. Aggregated statistics shown is the third quartile of chl-a concentration values (OC3-aer\_opt -10) for all 'clear sky' pixels during the week for the whole lake. Cloudy pixels have been masked using threshold of 0.081 on cloud\_albedo computed in Seadas (i.e. not very constraining cloudmask) and chl-a concentration values greater than 40 $\mu$ g/L have also been masked.

From our calibration/validation process we can conclude that the uncertainty of absolute chl-a concentration values computed in one location and time from MODIS data cannot be considered as negligible, particularly for highest concentration values. However the obtained weekly aggregated TS demonstrate some physical coherence in time and space and can definitely be used in a relative and qualitative way. Furthermore the spatio-temporal aggregation greatly reduces the effect of local highly inaccurate values and can efficiently be exploited for association analysis with other environmental factors even if the amplitude of the variation from RS products is reduced. Noisiness still remains important even with more constraining cloud mask (fig.25). K490 TS has been computed but not used and distributed as its added value with respect to chl-a concentration is limited.

### Lake Surface Water Temperature (LSWT)

The objective of this WP was to produce TS of LSWT for Lake Kivu from MODIS images for the period 2002-2014.

#### *Satellite data preparation*

The same MODIS Level 1A dataset as for OC was used to derive LSWT. Level 2 products corresponding to each 5-minute granules were computed containing brightness temperature (BT) in different thermal IR channels, sensor and solar zenith angles and other useful ancillary information such as quality flags. To calibrate the LSWT model we used daytime and nighttime lake surface temperature of ARC-Lake dataset (MacCallum and Merchant, 2013), produced from (A)ATSRs acquisitions for the period 1991-2011 with a spatial resolution of 0.05 degrees and a temporal resolution of 3 days. More specifically, PLOBS3D and PLOBS3N datasets i.e. unaveraged per lake observations (from ENVISAT/AATSR only) were exploited. Coarser spatial and temporal resolution is the main disadvantage of ARC-Lake for our purpose. MODIS and ARC-Lake data fusion approach is thus justified. Furthermore we validated ARC-Lake data against existing in situ measurements to demonstrate its usefulness as a reference to produce specific model coefficients.

#### *LSWT computation*

Two methods were foreseen to derive LSWT model coefficients for MODIS/Terra and /Aqua sensors: using ARC-Lake dataset to adjust the coefficients of Coast-Watch-like models (semi-empirical) or Radiative Transfer Modeling (RTM) to simulate brightness temperature (Francois et al., 2002). RTM was not applied. The first method applies a triple (T37) window algorithm (McClain et al., 1985) with channels 3.96, 11.04 and 12.04  $\mu\text{m}$  for nighttime:

$$MCSST\_TRIPLE = a T_{11} + b (T_{3.96} - T_{12}) + c (T_{3.96} - T_{12})(\sec \theta - 1) + d$$

Non-linear (NL) split window algorithm (Walton et al., 1998) applied to thermal IR channels 11.04 and 12.04  $\mu\text{m}$  was used for daytime:

$$NLSST\_SPLIT = a T_{11} + b MCSST (T_{11} - T_{12}) + c (T_{11} - T_{12})(\sec \theta - 1) + d$$

where MCSST is estimated by:

$$MCSST\_SPLIT = a T_{11} + b (T_{11} - T_{12}) + c (T_{11} - T_{12})(\sec \theta - 1) + d$$

MODIS and ARC-Lake observations were matched using the following filtering criteria: time difference  $\leq 4$ h., spatial distance  $\leq 10$ km, distance to coast  $\geq 2$ km, external MODIS cloudmask clear or probably clear, cloud\_albedo flag from SeaDAS processing  $< 5.4\%$ , standard deviation in  $3 \times 3$  window of BT  $11 \mu\text{m}$  and  $12 \mu\text{m}$  channels  $< 0.05$  K (to avoid using too many undetected cloudy pixels). Equations coefficients were adjusted from the matching observations separately for Day/Night, Aqua/Terra, Yearly/Monthly by regressing MODIS BT against ARC-Lake LSWT. Due to the small size of Lake Kivu and the coarse spatial resolution of ARC-Lake and MODIS, we derived the LSWT model coefficients using data from Lake Tanganyika (from the CHOLTIC project). However validation was performed using Kivu dataset.

Several MATLAB and Python scripts have been written in order to automatize the processing.

### Cloud masking issue

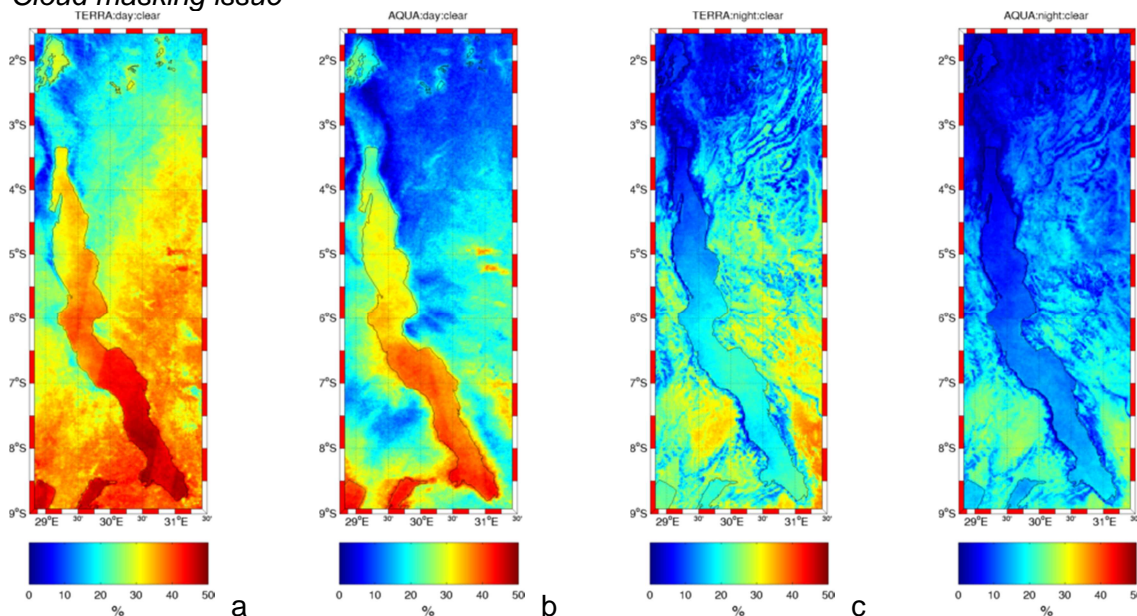


Figure 26 Frequency of clear pixels from MODIS cloudmask based on a subsample of 999 Aqua images (2003-2005) and 1025 Terra images (2004-2006). a) Terra daytime ( $\sim 8:30$ AM UTC); b) Aqua daytime (11:30AM UTC); c) Terra nighttime (8:30PM UTC) and d) Aqua nighttime (11:30PM UTC).

For both LSWT and OC, cloud masking was the critical step. Cloud frequency (Figure 6) shows a clear distinction between North and South but also between day and night that would also have direct consequences on the quality of derived products. Several test results demonstrate that even a dedicated MODIS cloudmask product is not accurate enough for the project purposes and cloud cover is sometimes underestimated leading for example to LSWT values lower than expected. We thus adapted cloud masking for the different concerns (derivation of LSWT coefficients or production of final LSWT/OC datasets) by applying more or less conservative simple thresholding methods.

### Derivation of new LSWT algorithm

We confirmed that ARC-Lake could be used as a reference dataset to produce regional coefficient by validating against *in situ* measurements. Indeed, using the MODIS/ARC-Lake match-up, default MODIS SST was compared to ARC-Lake temperature. From a detailed analysis of the residuals we decided to filter MODIS data using a threshold of 0.05 K on the local standard deviation in 3-by-3 window on brightness temperature in channel 11 $\mu$ m (BT11) and channel 12  $\mu$ m (BT12), before the derivation of new coefficients. This threshold is based on nighttime residual temperature and allows keeping enough points for analysis. In the same way, we defined threshold of 40° on satellite zenith angle. It can be noted that the association between MODIS and ARC-Lake is much better for nighttime (fig. 17 and fig. 18). Yearly coefficients already give good results and monthly coefficients do not improve substantially the quality of the association. Only one set of yearly coefficients has thus been used for the production of final dataset.

### Final dataset

All raster files, quicklooks and tables of spatio(-temporally) aggregated TS are available on a dedicated shared directory. The numerous figures and tables produced during calibration/validation phase of RS products computation are also available on request. Their publication in a report is not possible anyway because of their large number but they are essential to support our methodological choices and ensure the reproducibility of our research.

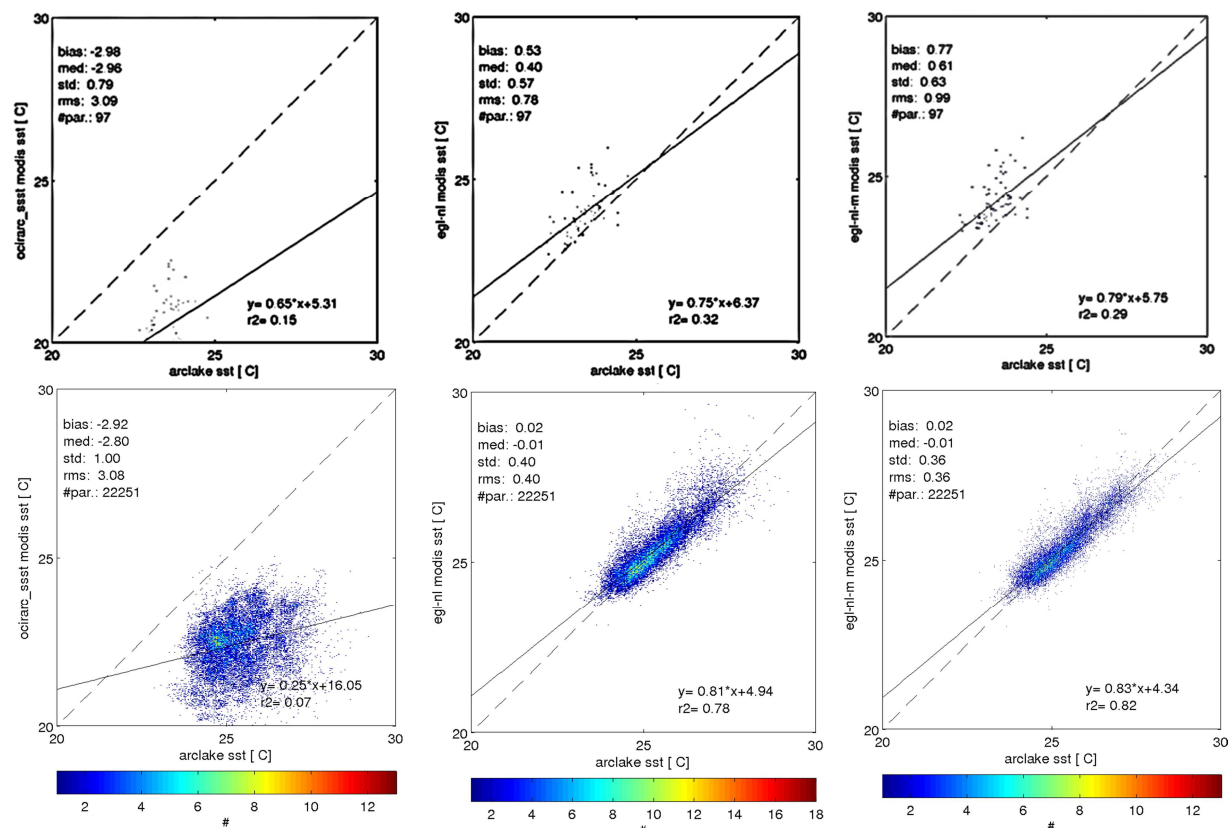


Figure 27 – Scatterplots correlating the daytime temperature of matching observations of ARC-Lake (X-axis) and MODIS Aqua (Y-axis). Top: Kivu. Bottom: Tanganyika (from CHOLTIC project) Left: default MODIS SST; centre: MODIS LSWT computed using monthly derived coefficients; right: MODIS LSWT computed new yearly derived coefficients (i.e. same coefficients for the whole series). Same threshold local standard deviation on BT11 and BT12 has been used but no threshold on satellite zenith angle.

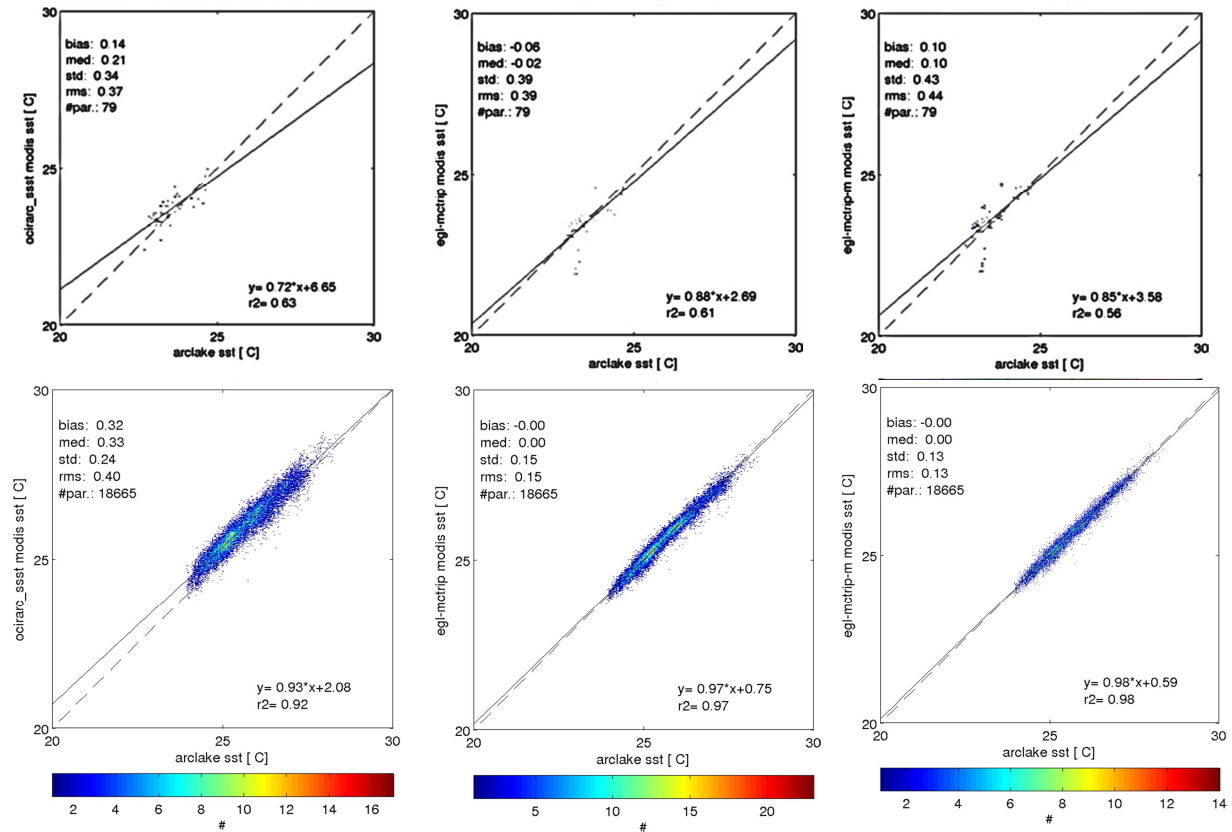


Figure 28. Same as Figure but for nighttime temperature.

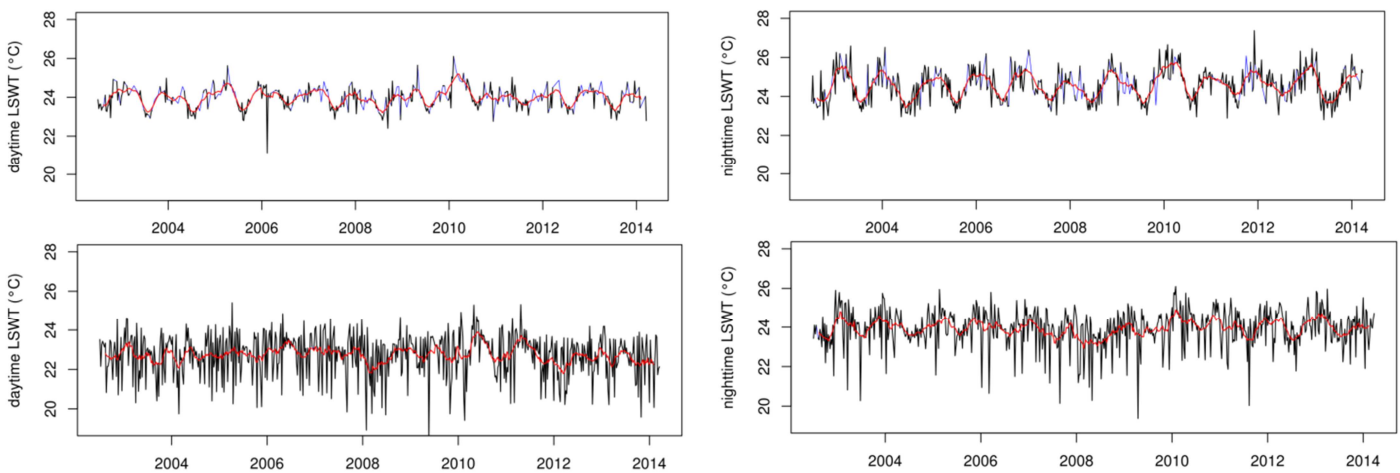


Figure 29– Weekly aggregated TS of daytime (left) and nighttime (right) LSWT in °C with moving average of 13 weeks in red and interpolated values in blue. Aggregated statistics is the median LSWT of all “clear sky” pixels during the week for the whole lake. On the figures below, cloudy pixels have been masked using a threshold of 0.081 on cloud\_albedo computed in Seadas. On the top, a more constraining cloudmask was used (threshold of 0.054 on cloud\_albedo computed in Seadas coupled with threshold of 0.12K on the local standard deviation in 3-by-3 window on Level 2 BT in channel 11 and channel 12 μm).

### 2.2.1.6 Fish surveys

Lake Kivu harbors a small number of fish species compared to other East African great lakes (Snoeks et al., 1997, 2012). Fish occupy the oxic layer, limited to the upper 60 m of the water column. Native fish include species of *Barbus*, *Clarias*, *Haplochromis*, as well as the *Nile Tilapia* (Snoeks et al., 1997). In 1959, *Limnothrissa miodon*, locally known as *Isambaza*, was intentionally introduced from Lake Tanganyika (Capart, 1959; Collart, 1960) and successfully colonized the pelagic part of Lake Kivu (Frank, 1989). The “Tanganyika sardine” became the most abundant species in the lake and has constituted the basis of a pelagic fishery for the population of the two surrounding countries.

During the running of EAGLES project, different activities aiming at the fisheries sustainable management were conducted, using , on the one hand, systematic collection of fishery statistics over the Rwandan side of Lake Kivu and, on the other hand, surveys of fish stocks over the whole lake using hydroacoustics.

### Fisheries statistics

A survey of fisheries was conducted for 3 years (October, 2011- December 2013). It involved fisheries ground mapping, the elaboration of a fisheries statistics recording system and data collection. Fish catch and fisheries facilities data were collected in all five basins following a field survey which helped in identifying fisheries sites and fisheries cooperatives. Geographic coordinates of fisheries facilities (fishing sites, selling points, cooperative offices, etc.) localities have been collected and interviews with fisheries officials have been conducted for more details on fisheries practices. Fish catch data were collected in 59 sites identified in the field survey period, and catches were recorded on a daily basis for 27 months, starting in October 2011. Fish catch data were recorded using a recording system which incorporated and integrated sparse data from diverse sources including fish catches on the market, catches consumed by fishermen and trimaran owners. With this system, daily catches ( $\text{kg d}^{-1}$ ) have been collected in the five basins of the Rwandan part of the lake. Recorded variables were daily catch per species, number of fishing units, number of fishermen, fish price on the market, and for some basin, fish size was measured.

The Lake Kivu fishing ground is made of 5 basins (districts) of different surface area (Fig. 30). These basins include, from north to south: Rubavu ( $47 \text{ km}^2$ ), Rutsiro ( $542 \text{ km}^2$ ), Karongi ( $200 \text{ km}^2$ ), Nyamasheke ( $225 \text{ km}^2$ ) and Rusizi ( $41 \text{ km}^2$ ). Among the 5 basins (Fig. 31), Nyamasheke has been identified to have the highest number of sites (27 sites) followed by Rusizi (10 sites), Karongi (9 sites), Rutsiro (9 sites) and Rubavu with the lowest (4 sites). During the data collection period, a total of 340 fishing units were operating in lake Kivu (Rwandan side). The average number of trimarans per site was 6, while the highest number of trimaran per site was observed in Rusizi zone (14 trimaran/site) followed by Rubavu (5 trimarans/site), Nyamasheke (4 trimarans/site), Rutsiro (4 trimarans/site) and the smallest was observed in Karongi (3 trimarans/site). The mean water surface area covered was  $17 \text{ km}^2$ , the smallest being observed in the Rusizi district ( $4 \text{ km}^2$ ) and the biggest in Rutsiro ( $55 \text{ km}^2$ ).

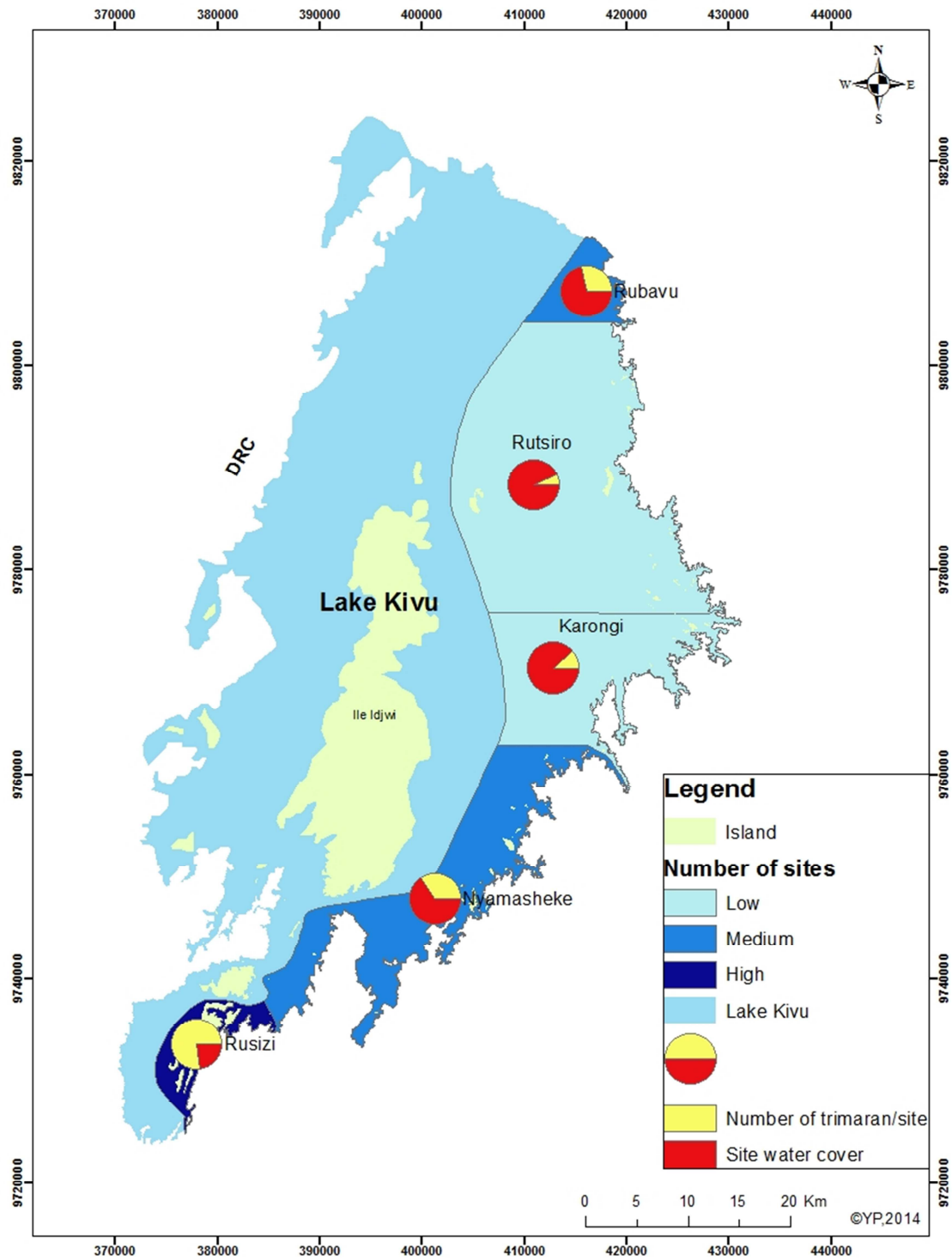


Fig. 30. Map of Lake Kivu, showing the five districts covered by the fishery survey in Rwanda. Note the difference in density of sites per district, and the variation of the number of fishing units per district, as well as the differences in lake area covered.

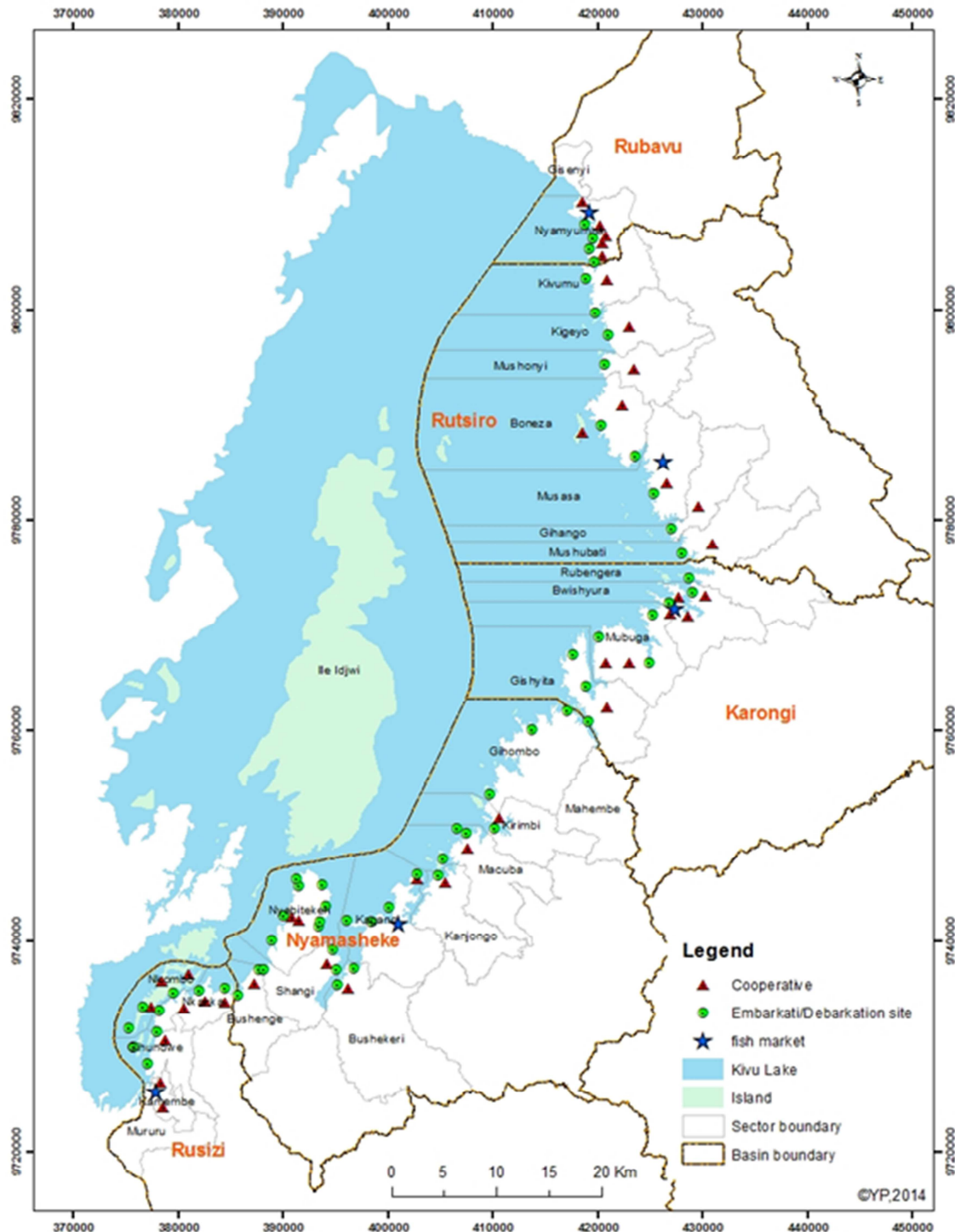


Fig. 31. Map of Lake Kivu, showing the distribution of the sites in which the fishery survey was conducted;

The Lake Kivu fisheries targets 5 major fish taxa (Fig. 32): including the “Tanganyika sardine” *Limnothrissa miodon*, *Haplochromis* spp., the recently introduced *Lamprichthys tanganicanus*, “Tilapia” (actually 3 species of *Oreochromis* and *Tilapia rendalli*) and *Clarias* spp. (*C. gariepinus* and *C. loiocephalus*). *Limnothrissa miodon* remains the dominant species in the catches the whole year round and across all basins.

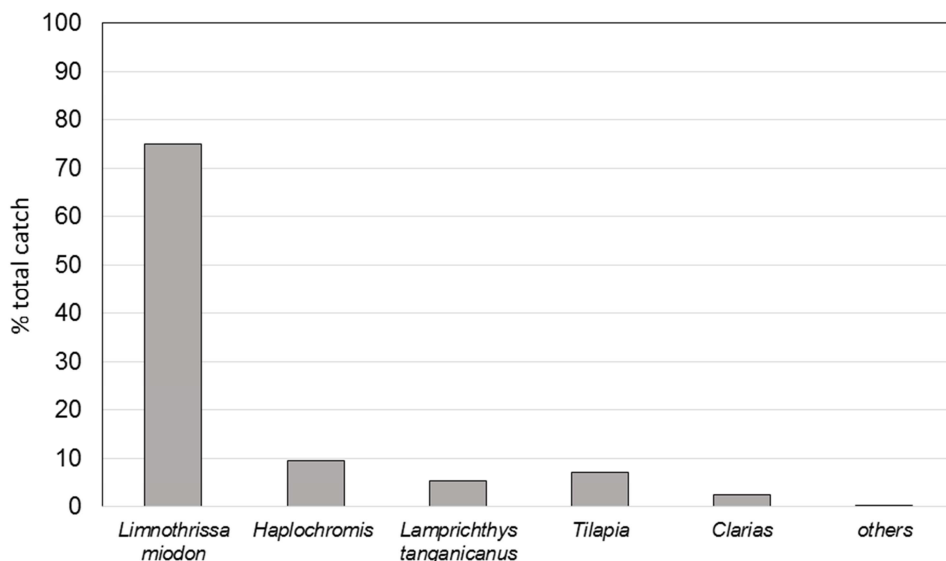


Fig. 32. Average composition of the fish catch in Lake Kivu during the survey (October 2011-December 2013)

The total catches for 2011 (October-December), 2012 and 2013 were 288.57 t, 700.64 t and 717.76 t respectively. The fish yield showed a substantial temporal variation (Fig. 33) with high catches in the rainy period of April to June in 2013 and the period following the fishing break (as per Rwandan policy), January to March in 2012. The monthly average total catch was 63.22 t, the highest catch was recorded in November 2011 and May, 2013 (84.37t) and the lowest in August, 2012 (8.65t). The CPUE (Fig. 34) didn't vary much except during the periods closer to the fisheries break, where before the break it fell down and slightly increased after the break. The average CPUE was 31.64 kg d<sup>-1</sup>; the highest value was observed in December 2011 (45.96 kg d<sup>-1</sup>) and the lowest is August 2013 (23.63 t).

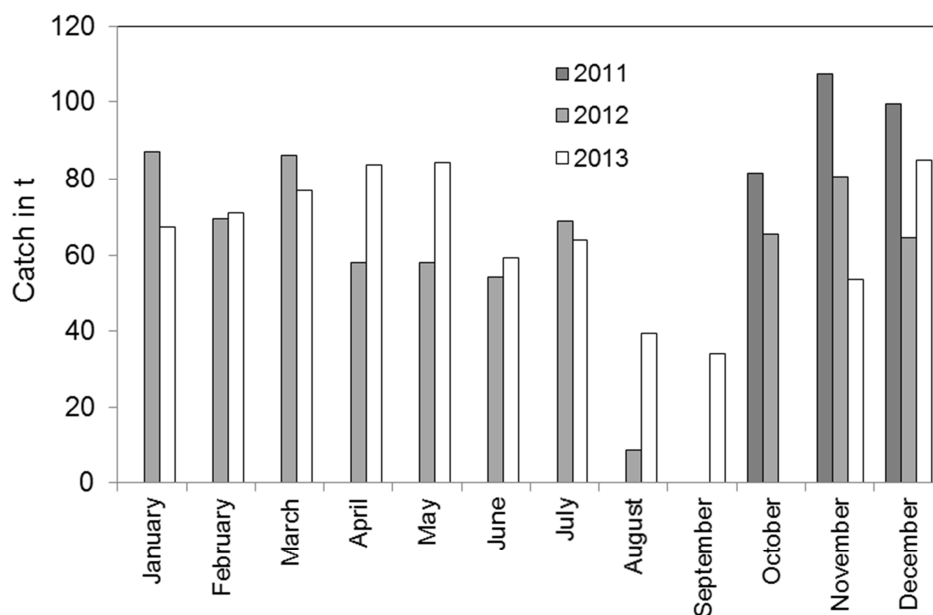


Fig. 33. Variation of the monthly fish catch in Lake Kivu during the survey (October 2011-December 2013)

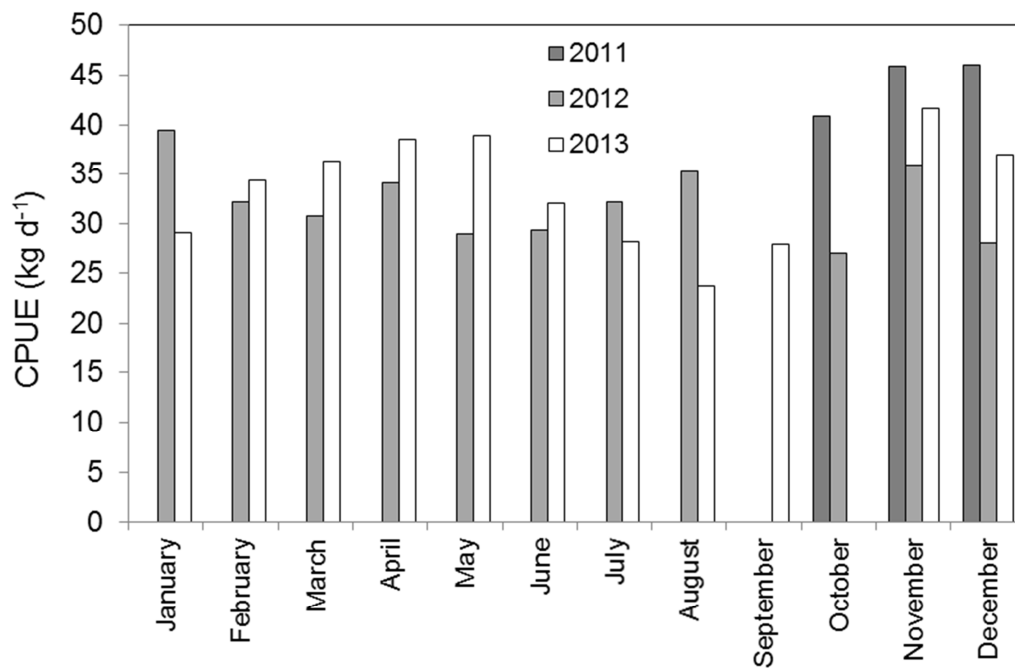


Fig. 34. Variation of the monthly CPUE (catch per unit effort) in Lake Kivu during the survey (October 2011-December 2013)

Fish catches varied among districts (Fig. 35), with high catches in the southern part of the lake (Nyamasheke basin), where in 2012 the total catch was 268.05 t and the CPUE 52.4 kg d<sup>-1</sup>. The total catch and the CPUE were generally higher in 2013 than in 2011 and 2012.

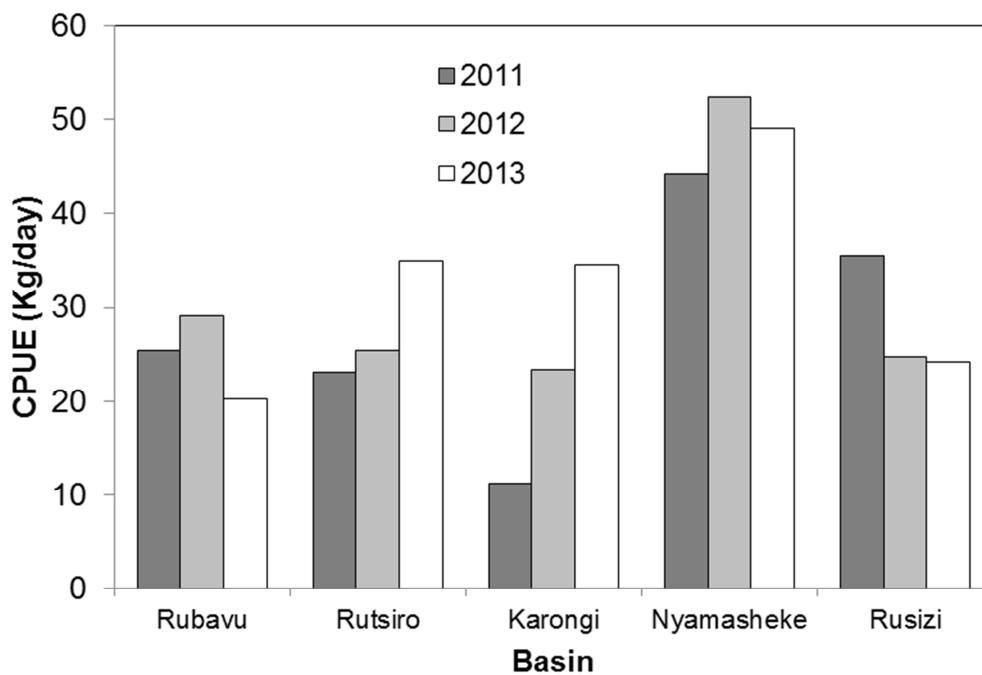


Fig. 35 Variation of CPUE among districts in Lake Kivu during the survey (October 2011-December 2013)

## Hydroacoustic surveys

The stock of Isambaza was estimated basing on two hydroacoustic surveys performed during the main dry season in July 2012 and July 2014. Previous survey works (February and July 2008) provided by Guillard et al. (2012) allowed us to explore if any major changes have occurred over this period.

Acoustics is a remote sensing technique with advantages over traditional fish sampling methods that include the ability to quickly sample nearly the entire water column, continuous areal coverage along a transect, and high data resolution (less than a meter vertically and tens of meters horizontally), and with no impact on fish. Limitations specific to acoustics include difficulty in determining fish species and the inability to acquire biological data such as age, sex, and diet. Fisheries acoustic surveys are typically integrated with other sampling methods, such as net catch and temperature data, to confirm target identity, to obtain biological data, and to estimate abundance. In Lake Kivu, acoustics can provide reliable fish stock estimates since more than 98% of the lake area, i.e. the pelagic part, is mostly inhabited by a single fish species.

For the surveys, the lake was divided into four basins (Fig. 36): north, east, south, west. Kabuno bay, located in the northeastern portion of the lake was not included in our study because the ecological conditions here are quite different from those found in the main lake.

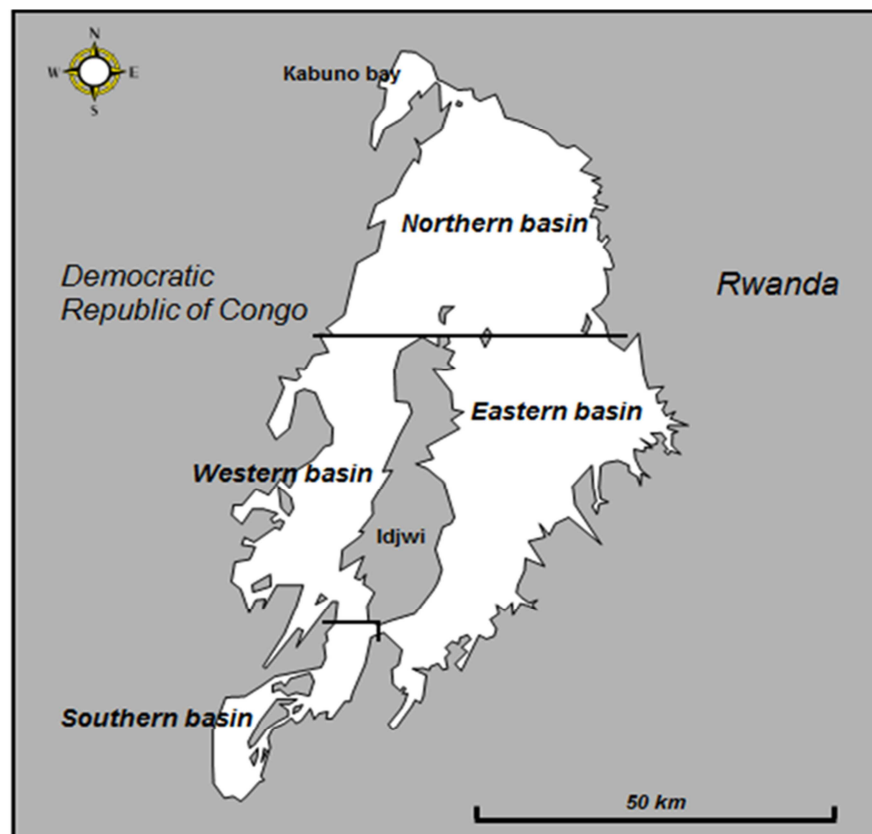


Figure 36: Map of Lake Kivu showing the different basins.

The four basins are morphologically different (Table 1) and are subject to strong winds in the dry seasons. The inshore zone, defined as areas where bathymetric depths are less than 50 m, represents a small portion (estimated at around 2%) of the total lake area.

Table 1: Basin characteristics

Basin	North	East	South	West	Inshore area
Estimated area (Km <sup>2</sup> )	900	900	97	320	50
Maximum depth(m)	489	400	225	105	50

### *Sampling design*

Two hydroacoustic surveys were performed, in July 2012 and July 2014, i.e. both during the dry season. For the first survey, only three basins located on the Rwandan part of the Lake were sampled due to lack of administrative authorization to move across water limits between the two countries. Thanks to collaboration with “Institut Supérieur Pédagogique” (ISP) of Bukavu, sampling the western part of the lake from the North to the South on the Congolese side was possible for the second survey.

Surveys were performed during daytime for security reasons. Routes (Fig. 37) were chosen to maximize the volume of water to be sampled. Some routes were shortened or modified due to adverse weather conditions, especially strong winds and heavy rains. Routes were predefined to ensure that each basin is sampled in order to obtain a sampling rate close to 6, as suggested by Aglen (1989). The distance covered for the two surveys was respectively 359 and 569 Km, equivalent to a sampling rate of 7.7 and 12.1. The predicted coefficient of variation based on the sampling rate (Aglen 1983, 1989) was respectively 18 and 14%. While analyzing data, we separated the samples acquired from the strictly pelagic area and the inshore one.

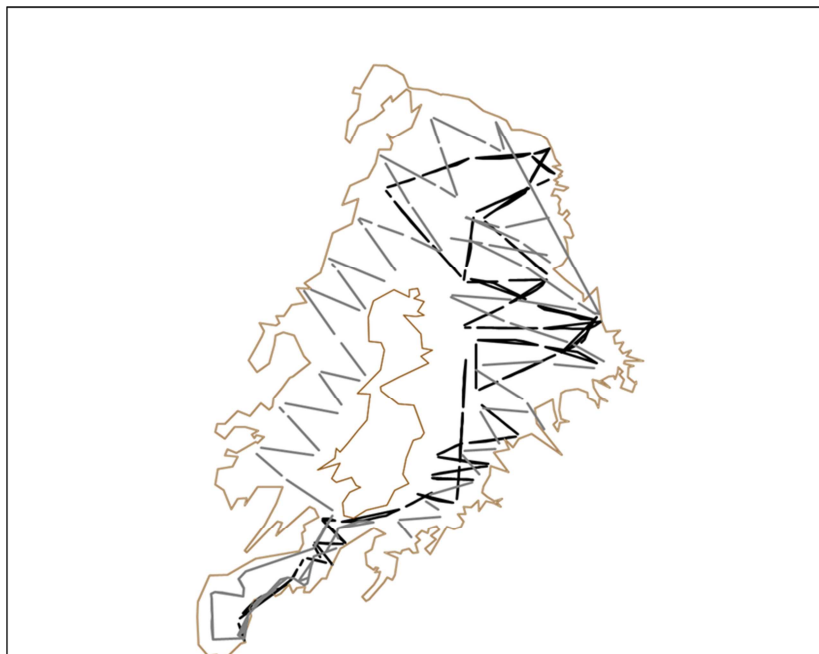


Figure 37. Routes sampled during the two surveys (Black lines: July 2012; grey lines: July 2014)

### *Equipment and analysis*

During these surveys, we used the echosounder Simrad EK60 equipped with a 70 kHz split-beam transducer with a half-power beam angle of 11°. A GPS system was used to record

boat positions. During data collection, the pulse duration was set at 0.256 ms (Godlewska et al., 2011) and the sampling rate was set at around 10 pulses per second and adapted to avoid false bottom echoes in certain depths. Sounder calibrations were performed before each survey in a protected bay following the standard protocol defined by Foote et al. (1987) and using the calibration software designed by SIMRAD (www.simrad.com). Data were collected using a research boat from at a mean speed of 7 km h<sup>-1</sup>. The transducer was aimed vertically by attaching it to a pole with deployment depth set at 0.7 m.

The detecting thresholds were set at -60 dB for single targets and -66 dB for echo integration data according to standard protocols (Parker-Stetter et al., 2009; CEN 2009). In our analysis, the sampled water column was divided into four layers each 15 m high (0-15 m; 15-30 m; 30-45 m and 45-60 m) so that results could be compared with previous studies (Lamboeuf, 1991, Guillard et al., 2012). The acoustic data were analyzed using the Sonar5-Pro software (Balk and Lindem, 2006) to calculate the total acoustic fish density in each depth layer and the acoustic size distributions. The Elementary Sampling Distance Unit (ESDU) was set at 1000 m. It follows that acoustic cells over which data were initially summarized measured 15 m in height and 1 km in length.

Density values were first expressed in acoustic energy "Sa" (m<sup>2</sup>.ha<sup>-1</sup>) reflected per layer and per unit area. All layer acoustic energy values were summed up by ESDU and the arithmetic mean was calculated for each basin and size classes in dB as a reflection index: the target strength "TS". The latter is an amount of energy reflected from an individual target. The Sa and TS measurements provide insight into the horizontal and vertical distributions of pelagic fish.

For size classes, we based our analysis on tracked fish, based on the merge of single echo detection to define a single fish (Balk & Lindem, 2006). To convert TS into the centimeter size, we used the equation:  $TS = 10^{((TS+62+0.9*LOG(Frequency))/19.1)}$  defined by Love (1971). TS data were grouped into two size classes (Table 2) basing on the maturity schedule of Isambaza in Lake Kivu (Kaningini et al. 1999).

Table 2. Length and TS equivalents of juvenile and adult Isambaza (*L. miodon*) according to Love (1971) and Kaningini et al. (1999)

Fish category	Juveniles	Adults
Target Strength(dB)	< - 48	- 48 < TS ≥ - 40
Size(Cm)	< 6.6	6.6 < Size ≥ 17.3

In order to calculate areal density of juveniles and adults, the total Sa of each cell had to first be apportioned to juvenile- (Sajuv.) and adult-(Saadult) sized fish based on their relative abundance in each cell. The following formulas were used:

$$Sajuv. = [(Tjuv. * \sigma_{juv.}) / ((Tjuv. * \sigma_{juv.}) + (Tadu * \sigma_{adu.}))] * Satot, \text{ and}$$

$$Saadu = Satot - Sajuv.;$$

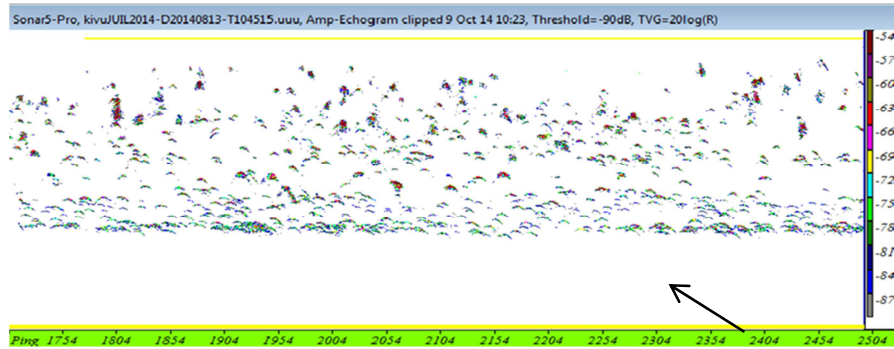
where Tjuv. and Tadu are the target counts of juvenile and adult in a given cell, respectively, and  $\sigma_{juv.}$  and  $\sigma_{adult.}$  are the mean equivalent surfaces of juvenile and adults in the cell,

respectively. Using  $S_a$  and TS data of each cell, we calculated the area density ( $\rho_a$ , fish·ha<sup>-1</sup>) of both juveniles and adults according to Simmonds & MacLennan (2005). Specifically, density of each size group was calculated by dividing the mean acoustic density ( $S_a$ , m<sup>2</sup>·ha<sup>-1</sup>) by the equivalent surface ( $\sigma$ ) defined as  $\sigma = 10^{(TS/10)} \cdot 4\pi$ .

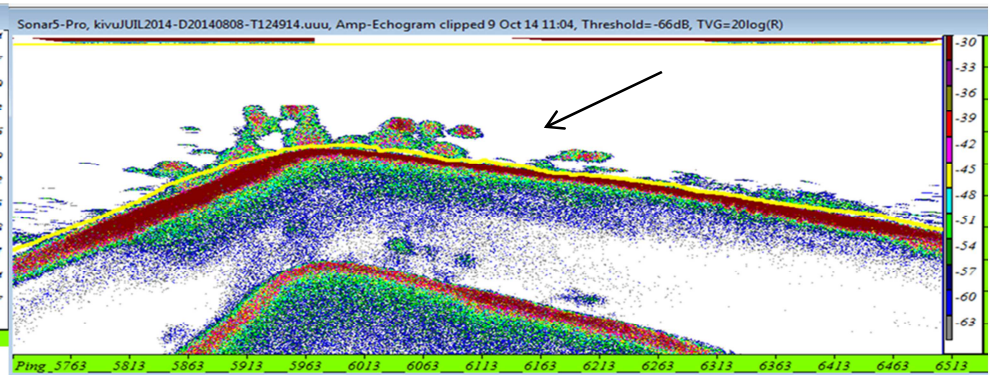
Areal biomass of each size group was calculated as the product of group areal density x group average mass. Average length was estimated from average TS with a TS-to-Length model (Love 1971). We converted average length to average mass using a length-to-weight relationship for Isambaza provided by Lamboeuf (1989):  $W$  (g) =  $0.055 * L$  (cm)<sup>2.27</sup>. We calculated the arithmetic means of  $S_a$  data to get the mean biomass values. We used the arithmetic mean as an estimator of the average for a basin assuming that the effort is distributed evenly without an initial statistical hypothesis (Smith, 1990). Furthermore, these estimates are similar to the estimators obtained by other methods of calculations if the sampling rate is close to that recommended by Aglen (1986) (Guillard and Vergés, 2007).

Observations made while sampling confirmed that no fish were detected below a depth of 60 m and close to the surface. Several types of structure were identified: individual fish (Fig. 28a) and more or less dense schools (Fig. 28b). Dense schools have been mainly observed in the inshore area or in adjacent pelagic zones. Significant density differences (Fig. 38c & d) were observed among the different basins and vertical layers.

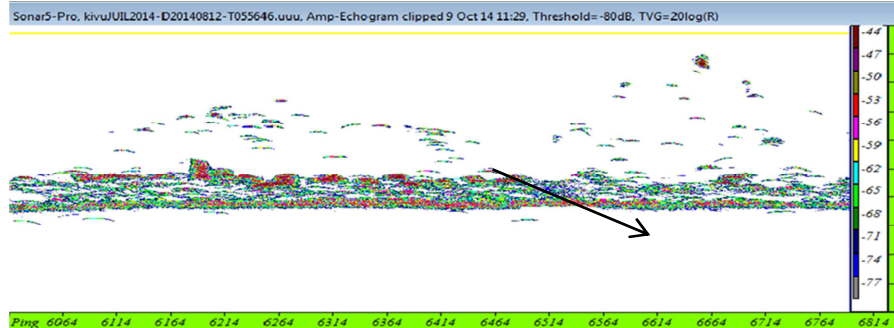
a. Echogram showing individual fish in the western basin in July 2014



b. Echogram showing fish schools on the bottom in the southern basin in July 2014



c. Echogram showing high fish density zone in the western basin in July 2014



d. Echogram showing low fish density zone in the northern basin in July 2014

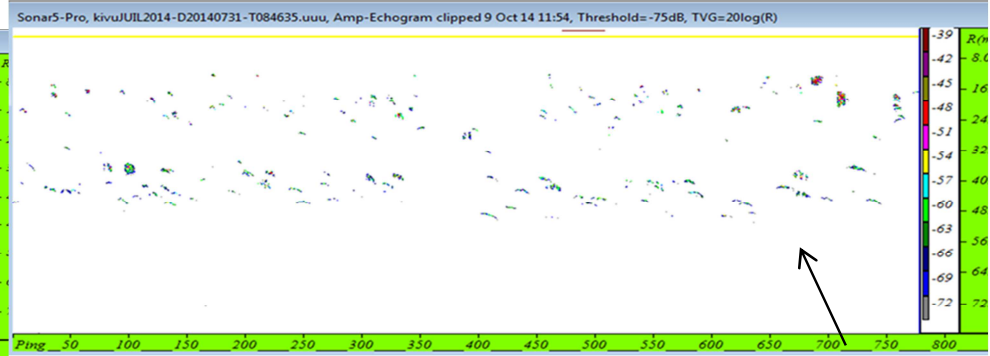


Figure 38: Example of echograms showing several types of fish structure

### Sa values

We calculated the mean  $S_{total}$  of each ESDU and of each layer. We then calculated mean  $S_{total}$  for each combination of survey and basin using the ESDUs as replicates. This analysis showed that mean  $S_{total}$  varied within basins, depth layers and surveys (Fig. 30). We ran ANOVA tests to assess the variability of the mean  $S_{total}$  among basins, surveys and depth layers. The mean  $S_{total}$  variability assessment concerned only the three sampled basins for the two surveys.

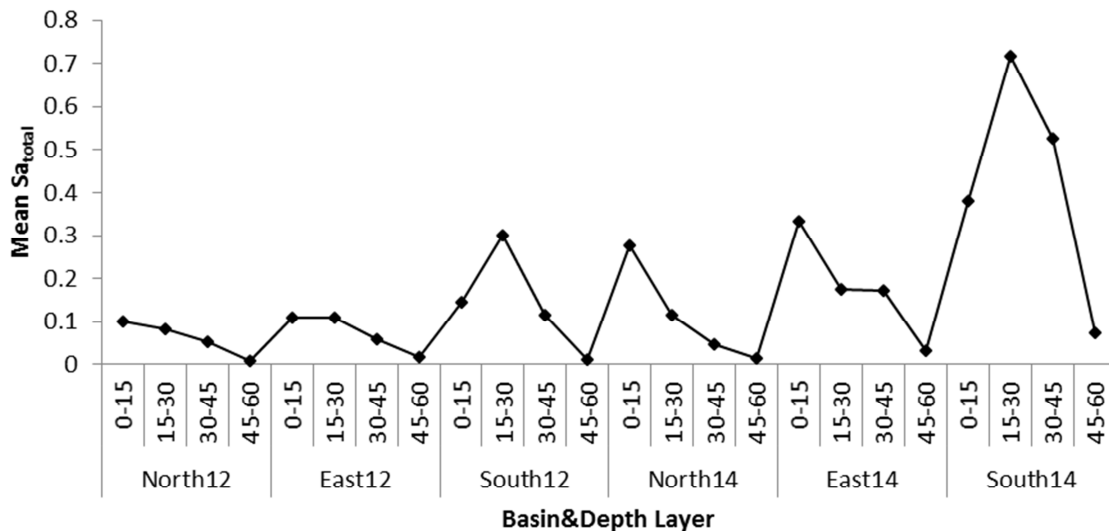


Figure 39. Variation of the mean  $S_{total}$  in the three basins for the two surveys

Fish were significantly more abundant in the southern basin than in the North and East for both surveys ( $P > 0.01$ ); with a highest fish density in the 15-30m depth layer. Fish were significantly more concentrated in the two upper -layers (0-15m and 15-30m) than in deeper layers of the water column ( $P > 0.05$ ) for both surveys in the three basins. Overall mean  $S_{total}$  values were significantly higher in July 2014 than in July 2012 ( $P > 0.01$ ).

### TS Results.

TS results have been divided into juveniles and adults fish according to studies conducted by Kaningini (1999) on the biology of *Limnothrissa miodon*. TS distributions were similar regardless of basins and surveys (Fig. 40). They are unimodal in the three basins for the two surveys.

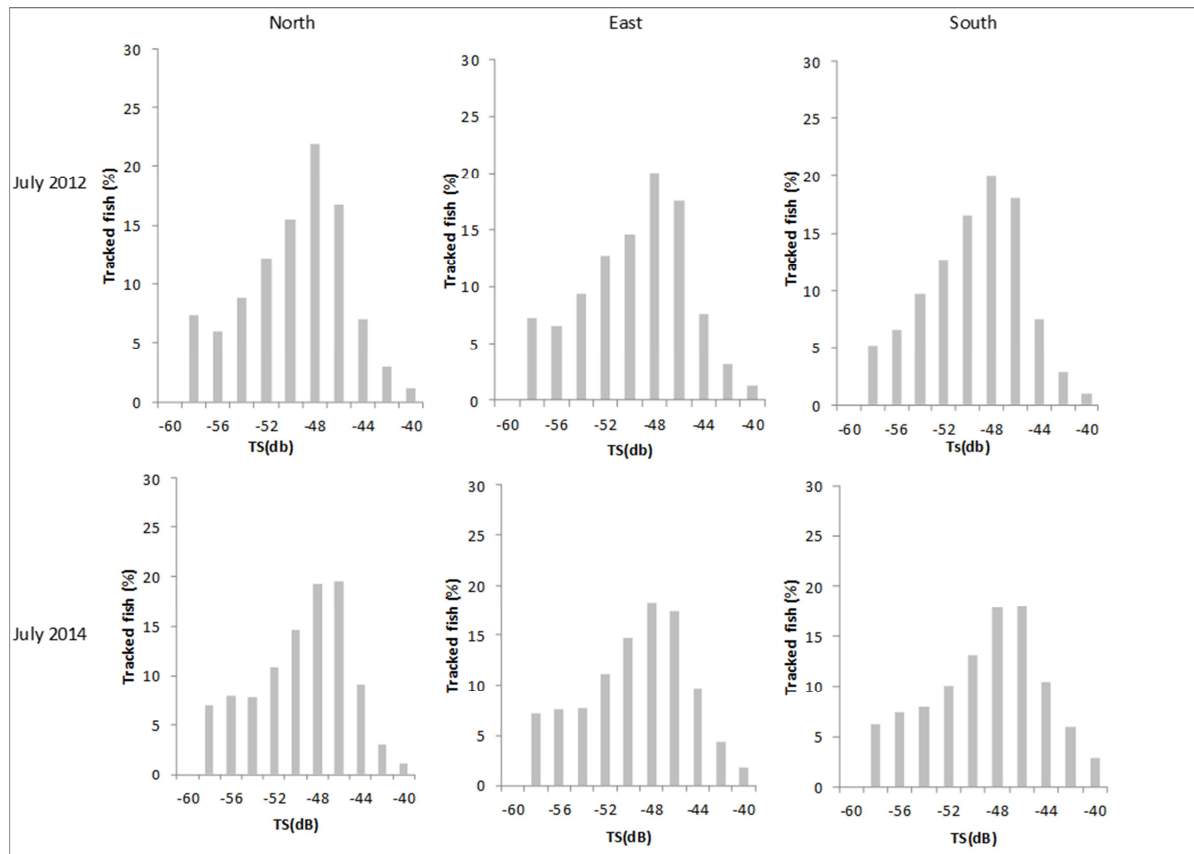


Figure 40. Acoustic size distributions of tracked fish in the three basins for the two surveys.

The fact of grouping TS data into juveniles and adults allowed us to make an easier comparison of their abundance in the three basins (Table 3). Juveniles were more numerous than adults in the three basins for the two surveys. There is no significant difference of abundance of the two categories of fish among basins.

Table 3: Number (%) of tracked juvenile and adult fish in the four basins

Survey	July 2012			July 2014			
	Nord	East	South	Nord	East	South	West
Juveniles	72	71	71	62	58	58	58
Adults	28	29	29	38	42	42	42

#### *Transformation of Sa into weight*

To transform the acoustic density into weight, we calculated first the areal density (number of individual fish/ hectare) and then the mean areal biomass ( $\text{kg ha}^{-1}$ ). The total biomass per basin was obtained by scaling up the mean biomass to the estimated area. Fish biomass for the whole lake was the sum of estimated fish biomass of all basins and the inshore area. As mentioned earlier, in July 2012, the western part of the lake could not be sampled. The total fish biomass for the western basin was estimated using the relative mean areal density ( $\text{kg.ha}^{-1}$ ) of the three basins by area.

Estimated fish biomass in the whole Lake was nearly 2.5 times higher in July 2014 than in July 2012, with 3398 and 1362 tons respectively.

Fish areal biomass ( $\text{kg}\cdot\text{ha}^{-1}$ ) varied in the different basins (table 4), the highest value was found in the southern and the western basin for the two surveys (Table 4).

Table 4: Fish areal biomass ( $\text{kg}\cdot\text{ha}^{-1}$ ) in the four basins of Lake Kivu

Basin	Nord	East	South	West
Jul 2012	4.98	6.15	11.94	
July 2014	9.95	15.56	37.39	20.35

### Discussion

The basic purpose of monitoring temporal dynamics of the fish stock on a whole lake scale is to provide relevant advice on the exploitation and sustainable management of the fishery. Living resources are limited but renewable, and fish stock assessment may be described as a tool enabling to determine the exploitation level that may in the long run give the reasonable yield in terms of weight from the fishery.

Stock assessment of the fish community in Lake Kivu in general and *Limnothrissa miodon* in particular was not well documented until recent surveys (Snoeks et al., 2012). The first estimates of whole-lake biomass of this fish species were provided by hydroacoustic surveys carried out at the end of the 1980s. They revealed a stock varying between 4 and 5000 tons (Lamboeuf, 1989) and 6 to 10000 tons (Lamboeuf, 1991). Some twenty years later, a whole-lake survey using similar methods was carried out by Guillard et al. (2012), leading to the conclusion that the stock of *L. miodon* in Lake Kivu had remained stable.

Our surveys conducted at day showed several types of fish structure, from aggregated schools to individual fish, similar to those observed by Guillard et al. (2012). Although no survey was conducted at night due to safety reasons, we observed during our daytime surveys a homogenous distribution of fish comparable to findings of previous studies (Guillard et al., 2012; Lamboeuf 1991); no or very few fish were detected near the surface and beyond 60 m depth.

*Limnothrissa miodon* was known as the only fish species inhabiting the pelagic zone of Lake Kivu until 2006, when a new species *Lamprichthys tanganicanus* was noticed in the fishermen catches for the first time (Masilya et al., 2011). An experimental fishing in the pelagic zone was conducted in June 2013 in the northern basin in order to assess a relative abundance of this species compared to that of *L. miodon*: less than 1% of *L. tanganicanus* were present in the catches. Then, the results of our surveys could not be biased by the presence of this new species in the pelagic zone of the lake.

Our results showed a variation of the fish stock in a two-year time interval. The reason for this difference could be explained with a long term analysis of other ecological, trophic parameters and the fishing effort. A possible cyclic pattern of the Isambaza stock could be possible, but this requires an analysis of a quite number of estimates data sets.

Fish were more abundant in the southern and the western basins; Guillard et al. (2012) noted a similar pattern, the same pattern was observed for the mean areal biomass, resulting from a combination of the acoustic density and acoustic size as described by Marshall (1991) based on CPUE results. The southern and the western basins share similar morphological characteristics (Marshall, 1991) providing optimal conditions for reproduction. However, other

limnological and fish biology data are required to enhance the explanation of the high productivity of these two parts.

Fish sizes were defined using tracked fish, their vertical distribution was homogenous within basin and among basins in accordance to results provided by previous studies (Lamboeuf, 1991 and Guillard et al., 2012). Proportions of juveniles were constantly higher than those of adults in the different basins for the eight surveys, similarly to findings of previous studies (Guillard et al., 2012; Kaningini, 1999).

Fish are mostly concentrated in the upper layers of the water column as the oxygen levels lower with depth in Lake Kivu. Isambaza also follows migration movement of the zooplankton, its main prey in Lake Kivu like other freshwater fish species (Mehner, 2012).

### *Conclusion*

Following its introduction in Lake Kivu, *Limnothrissa miodon* has successfully adapted to its new environment and became the most abundant fish species in the Lake. Its stock has gone through several changes with time; the present study showed a significant difference of stock estimates between two successive surveys. Compared to the previous surveys conducted in the same condition, the stock of *Limnothrissa miodon* seemed to have declined with time, but this assumption deserves to be confirmed by monitoring surveys on a longer period. Estimation of the fish stock should be complemented with the assessment of the fishing pressure to extend explanation of this stock decline in relation to time scales. The southern and the western basins are the most productive parts of the lake, fisheries managers should put more emphasis on the fishing monitoring in the four basins in an attempt to highlight factors affecting productivity in the different parts of the Lake as a result of an eventual unequal fishing effort.

## 2.2.2. Carbon pathways through the planktonic food web

### 2.2.2.1. Characterization of the different organic matter pools

DIC, DOC, POC and PN concentrations and their respective C ( $\delta^{13}\text{C}$ ) and N ( $\delta^{15}\text{N}$ ) stable isotope signatures were monitored in the mixed layer between January 2012 and May 2013. DIC concentrations were very high in the mixed layer (annual average at 10 m:  $11.942 \pm 0.223 \text{ mmol L}^{-1}$ ,  $n = 24$ ) and did not show any consistent seasonal pattern. Stable isotope analysis of DIC is a useful tool for understanding the fate of C in aquatic ecosystems and could provide information on the lake metabolism, defined as the balance between gross primary production and community respiration of organic matter. Primary producers preferentially incorporate the lighter isotopes ( $^{12}\text{C}$ ) into the biomass with the consequence that the heavier isotopes ( $^{13}\text{C}$ ) accumulate into the DIC pool, whereas mineralization releases  $^{13}\text{C}$ -depleted  $\text{CO}_2$  from the organic matter being respired, into the DIC pool. In Lake Kivu, the  $\delta^{13}\text{C}$ -DIC values were vertically homogeneous in the mixed layer but gradually decreased in the oxycline to reach minimal values at 70 m (Fig. 41a). Furthermore, we observed that  $\delta^{13}\text{C}$ -DIC values in the mixed layer increased linearly with time during the rainy season ( $r^2 = 0.79$ ,  $n = 12$ ), then suddenly decreased at the start of the dry season due to the vertical mixing with  $^{13}\text{C}$ -depleted DIC from deeper waters (Fig. 41b). Overall, the seasonal variability of  $\delta^{13}\text{C}$ -DIC in the mixed layer would suggest that photosynthetic  $\text{CO}_2$  fixation exceeds the respiration of organic matter, implying that the surface waters of Lake Kivu are net autotrophic, and hence that the microbial food web would be supported by autochthonous organic C sources. This observation confirms the recent study of Borges et al. (2014) who reported, based on a DIC mass balance approach, that the mixed layer of Lake Kivu was net autotrophic while acting as a source of  $\text{CO}_2$  to atmosphere driven by geogenic  $\text{CO}_2$  inputs.

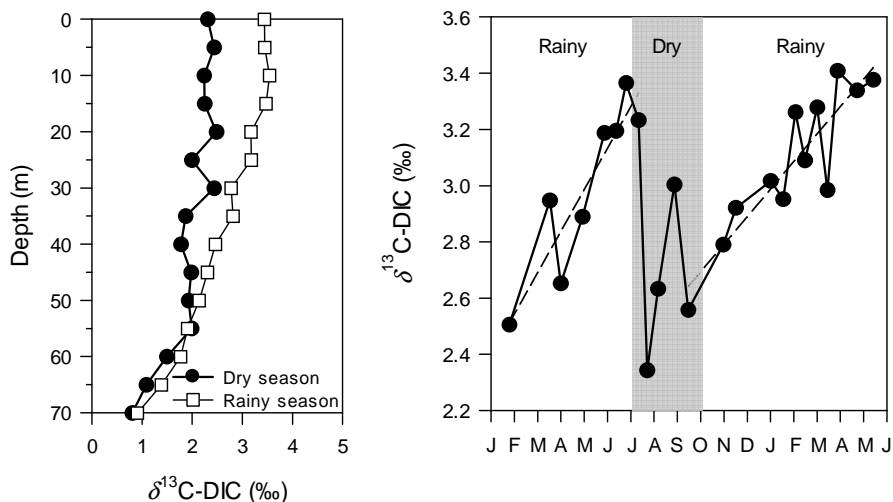


Figure 41: Depth profile of the  $\delta^{13}\text{C}$  of the dissolved inorganic carbon (DIC) pool in the mixolimnion during the dry (18/07/12) and the rainy (20/03/13) season and (b) temporal variation of the  $\delta^{13}\text{C}$ -DIC in the mixed layer of Lake Kivu between January 2012 and June 2013.

The concentration of POC was substantially higher in the mixed layer than below in the mixolimnion all over the year. During the dry season, however, POC concentrations in the oxycline (~50-65 m) were found to be as high as in the surface water (Fig. 42a). The isotopic signature of the POC pool stayed almost constant throughout the year in the mixed

layer (at 10 m:  $-23.8 \pm 0.8 \text{ ‰}$ ,  $n = 19$ ), but at the top of the oxic-anoxic transition,  $\delta^{13}\text{C}$ -POC values systematically decreased sharply (at the oxic-anoxic transition:  $-33.9 \pm 4.3 \text{ ‰}$ ,  $n = 19$ ) (Fig. 42b). The vertical position of this abrupt excursion toward more negative values closely followed the oxycline, and was therefore located deeper in the water column during the dry season. While DIC would be the major C source of the POC pool in the mixed layer, the important decrease of  $\delta^{13}\text{C}$ -POC values observed in the oxycline suggests that another  $^{13}\text{C}$ -depleted C source was actively incorporated into the biomass at the bottom of the mixolimnion. Such large  $^{13}\text{C}$  depletions of the POC pool in the water column have been reported by Blees et al. (2014), who measured  $\delta^{13}\text{C}$ -POC as low as  $-49\text{‰}$  in Lake Lugano, and they were related to high methanotrophic activity. In Lake Kivu, we showed that  $\text{CH}_4$  concentrations were found to decrease sharply at the oxic-anoxic transition, and the dissolved  $\text{CH}_4$  that reached the oxycline via turbulent diffusivity and vertical advection (Schmid et al. 2005) is known to be isotopically light, with a  $\delta^{13}\text{C}$  signature of approximately  $-60 \text{ ‰}$ . Therefore, the vertical pattern in  $\text{CH}_4$  concentrations and  $\delta^{13}\text{C}$ -POC values observed during this study suggests that a substantial part of  $\text{CH}_4$  was consumed and incorporated into the microbial biomass in the oxycline. Indeed, experiments carried out in Lake Kivu in February 2012 and September 2012 showed that microbial  $\text{CH}_4$  oxidation was significant in the oxycline (see the “aerobic methanotrophy” section of this document for further details).

The concentrations of the PN pool in the water column followed the same pattern as POC (Fig. 42c). The PN pool was larger in the mixed layer than below in the water column during most of year. However, higher PN concentrations were measured in the oxycline during the dry season (Fig. 42c).  $\delta^{15}\text{N}$ -PN values in the mixed layer oscillated between  $0 \text{ ‰}$  and  $1 \text{ ‰}$  during the rainy season but shifted toward significantly higher values during the dry season ( $3 \text{ ‰} - 4 \text{ ‰}$ ) (Fig. 43), reflecting the seasonal change in phytoplankton composition (shift between a dominance of cyanobacteria to diatoms).  $\delta^{15}\text{N}$ -zooplankton mirrored the seasonal variability of  $\delta^{15}\text{N}$ -PN in the mixed layer with a small time-shift, ranging between  $3 \text{ ‰} - 5 \text{ ‰}$  during the rainy season, then increasing at the start of dry season to reach a maximum of  $7.5 \text{ ‰}$  (Fig. 43). The  $\delta^{13}\text{C}$  signature of the zooplankton was on average  $-22.9 \pm 0.8 \text{ ‰}$  ( $n = 19$ ) and did not vary between seasons. The difference between  $\delta^{15}\text{N}$ -zooplankton and  $\delta^{15}\text{N}$ -PN ( $\Delta^{15}\text{NZoo-PN}$ ) was on average  $3.2 \pm 1.0 \text{ ‰}$  throughout the year while it was on average enriched in  $^{13}\text{C}$  ( $\Delta^{13}\text{CZoo-POC}$ ) by  $0.9 \pm 0.8 \text{ ‰}$ . In nature, comparison of the  $\delta^{15}\text{N}$  signature of consumers and their diet indicates that the  $\delta^{15}\text{N}$  value increases consistently with the trophic level, because of the preferential excretion of the isotopically lighter  $^{14}\text{N}$  (Montoya et al. 2002). However the C isotope fractionation consumers and diet is usually considered to be less than  $1 \text{ ‰}$  (Sirevag et al. 1977) The constant  $\delta^{15}\text{NZoo-PN}$  value found in Lake Kivu is within the range of trophic level enrichment between algae and *Daphnia magna* ( $\sim 2 \text{ ‰}$  to  $5 \text{ ‰}$ ) estimated in laboratory experiment (Adams and Sterner 2000),

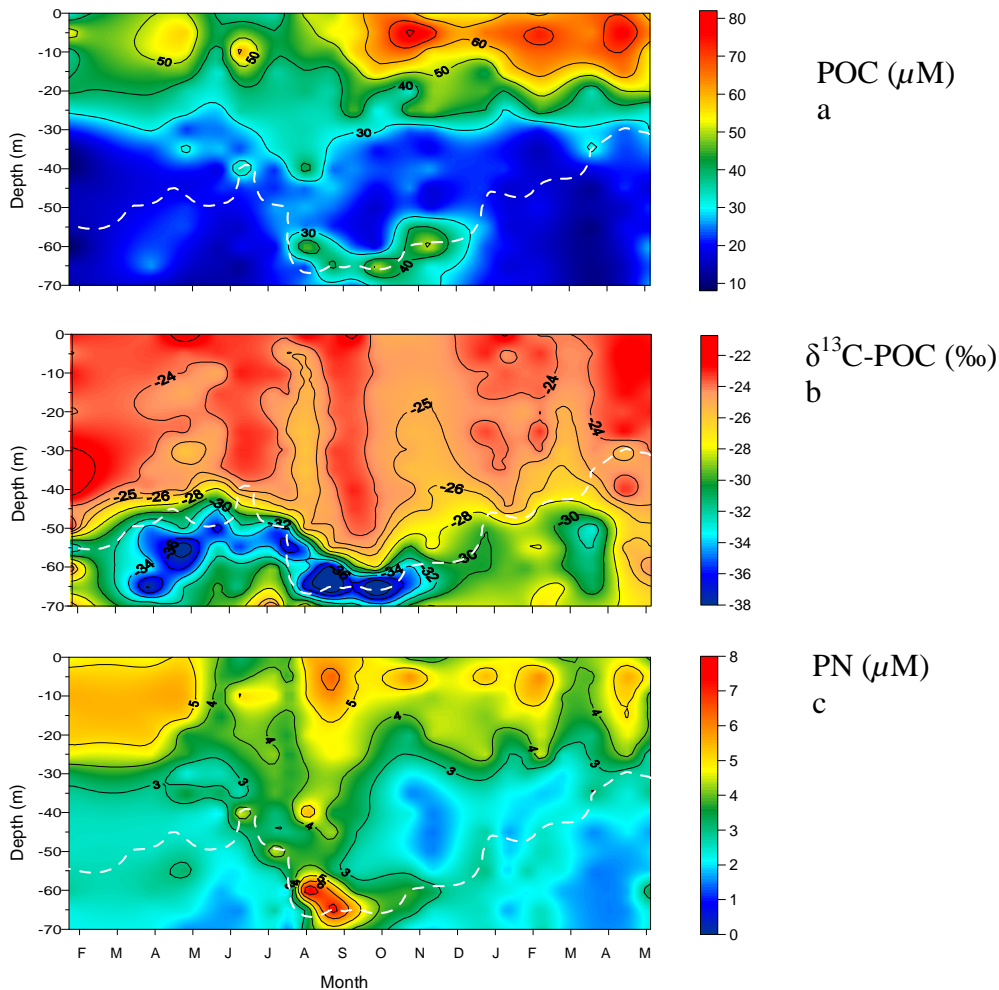


Figure 42: Temporal variability of (a) the particulate organic carbon (POC) concentration ( $\mu\text{mol L}^{-1}$ ), (b) the  $\delta^{13}\text{C}$  signature of the POC pool, and (c) the particulate nitrogen (PN) concentration ( $\mu\text{mol L}^{-1}$ ) in the mixolimnion of Lake Kivu, between February 2012 and May 2013.

and very close to the cross-system trophic enrichment value ( $3.4 \pm 1.0 \text{‰}$ ) proposed by Post (2002). Together with the slight enrichment in  $^{13}\text{C}$  compared with the autochthonous POC pool,  $\delta^{13}\text{C}$  and  $\delta^{15}\text{N}$  analysis suggests that zooplankton directly incorporate algal-derived organic matter in their biomass, and they would rely almost exclusively on this source of organic matter throughout the year. This is in general agreement with the very low allochthonous organic matter inputs from rivers in Lake Kivu (Borges et al. 2014).

The DOC concentration ( $142 \pm 20 \mu\text{mol C L}^{-1}$ ,  $n = 304$ ) and  $\delta^{13}\text{C}$ -DOC signature ( $-23.2 \pm 0.4 \text{‰}$ ,  $n = 304$ ) did not show any consistent variations with depth or time in the mixolimnion during all the sampling period. A vertical profile performed down to the lake floor revealed that the  $\delta^{13}\text{C}$ -DOC did not vary significantly in the monimolimnion either (vertical profile average:  $-23.0 \text{‰} \pm 0.2$ ,  $n = 18$ , Fig. 44).

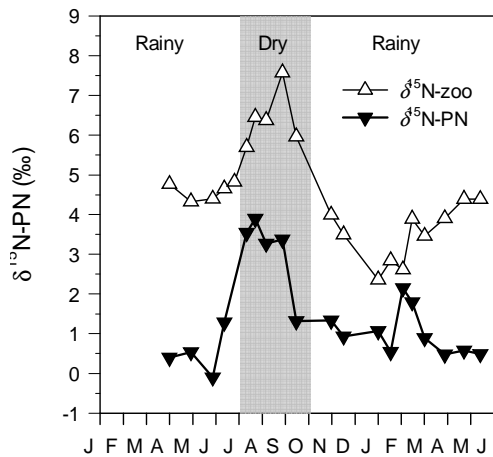


Figure 43: Temporal variability of the  $\delta^{15}\text{N}$  signature of the particulate nitrogen (PN) pool and zooplankton in the mixed layer

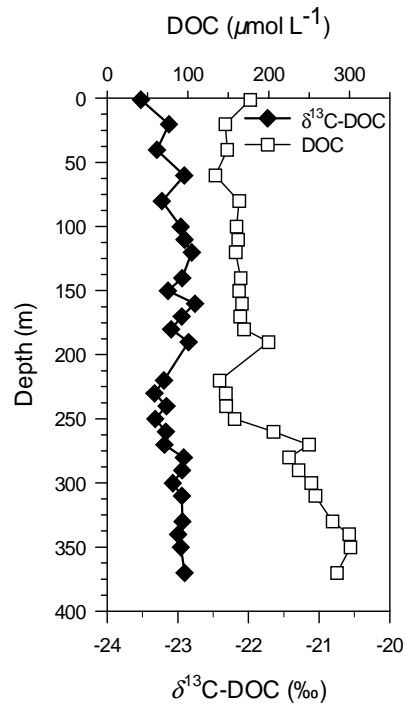


Figure 44: Vertical profile from the lake surface to the lake floor of the dissolved organic carbon (DOC) concentration ( $\mu\text{mol L}^{-1}$ ) and the  $\delta^{13}\text{C}$  signature of the DOC pool, in September 2013.

Despite the net autotrophic status of the mixed layer of Lake Kivu (see previous paragraph and Borges et al. 2014), the  $\delta^{13}\text{C}$  data indicate a difference in the origin of the POC and DOC pools in the mixed layer. Indeed, the  $\delta^{13}\text{C}$ -DOC showed very little variation and appeared to be vertically and temporally uncoupled from the POC pool in the mixed layer. A recent study (Morana et al. 2014, see also section 2.2.2.2. of this document for further details) demonstrated that phytoplankton extracellular release of DOC is relatively high in Lake Kivu, and the fresh and labile autochthonous DOC produced by cell lysis, grazing or phytoplankton excretion, that would reflect the  $\delta^{13}\text{C}$  signature of POC, is quickly mineralized by heterotrophic bacteria. Therefore, it appears that the freshly produced autochthonous DOC would contribute less than 1% of the total DOC pool (Morana et al. 2014), and as the standing stock of phytoplankton-derived DOC seems very small, it can be hypothesized that the bulk DOC pool is mainly composed of older, more refractory compounds that would reach the mixed layer through vertical advective and diffusive fluxes. Indeed, as described above, the  $\delta^{13}\text{C}$  signature of the DOC in the monimolimnion did not differ from the  $\delta^{13}\text{C}$ -DOC in the mixolimnion, suggesting that they share the same origin.

In summary, stable isotope data revealed large seasonal variability in the  $\delta^{15}\text{N}$  signature of the PN pool, most likely related to changes in the phytoplankton assemblage and to  $\text{N}_2$ -fixation. In contrast with the common observation that oligotrophic aquatic ecosystems tend to be net heterotrophic, the seasonality of  $\delta^{13}\text{C}$ -DIC is consistent with the mixed layer of Lake Kivu being net autotrophic, supporting the conclusions of Borges et al. (2014), based on DIC mass balance considerations. The  $\delta^{13}\text{C}$ -POC showed an important variation with depth due to the abundance of methanotrophic bacteria in the oxycline that fixed the lighter  $\text{CH}_4$ -derived C into their biomass. The  $\delta^{13}\text{C}$ -POC and  $\delta^{13}\text{C}$ -DOC appeared to be uncoupled vertically and

temporally, which suggests that the DOC pool was largely composed of relatively refractory compounds. Finally, the  $\delta^{13}\text{C}$  of zooplankton mirrored the  $\delta^{13}\text{C}$  signature of the autochthonous POC pool, and its  $\delta^{15}\text{N}$  signature followed the seasonal variability of the  $\delta^{15}\text{N}$ -PN pool in good agreement with the expected consumer-diet isotope fractionation. This suggests that zooplankton would rely throughout the year on algal-derived biomass as an organic C source. Finally, the detailed analysis of the stable isotope composition of diverse organic and inorganic components carried out during this study allowed to trace the organic matter dynamics in Lake Kivu during one seasonal cycle, and might be useful to improve the interpretation of sedimentary archives of this large and deep tropical lake.

#### **2.2.2.2. Significant production of DOC by phytoplankton in Lake Kivu and its uptake by heterotrophic prokaryotes**

In aquatic systems, the dissolved organic carbon (DOC) pool is a mixture of molecules in a continuum of biological lability, with components from different origins: allochthonous, in fresh waters mainly deriving from the watershed runoff, and autochthonous material produced in situ, such as DOC derived from phytoplankton extracellular release (DOCp) or cell lysis (Myklestad 2000). Both carbon (C) sources can be important to sustain the growth of heterotrophic prokaryotes but bacteria are highly selective towards the substrate they use (Sarmiento and Gasol 2012). In most aquatic systems, heterotrophic bacteria preferentially use labile freshly produced DOCp over more recalcitrant allochthonous compounds (Pérez and Sommaruga 2006). In Lake Kivu, time-course experiments were carried out in April 2009, October 2010 and June 2011 to quantify primary production, phytoplankton excretion, and the microbial uptake of freshly released dissolved organic carbon (DOCp).

These experiments showed that phytoplankton release of DOC is a significant process in Lake Kivu, where the PER (i.e. the fraction of primary production that is excreted by phytoplankton through the release of DOCp molecules) was ranging between 42 % and 64 %. Furthermore, the PER was found to be (1) significantly related to high light and low phosphate concentrations in the mixed layer, and (2) was comparatively higher in oligotrophic tropical lakes compared to their temperate counterparts. Both observations support the view that environmental factors play a key role in the control of phytoplankton excretion (Zlotnik & Dubinsky 1989). The experiments showed also that the DOCp standing stock was relatively small compared to the high rates of phytoplankton DOCp release (DOCp accounted for less than 1% of the total DOC pool), and the turnover times of the DOCp was therefore short (less than 3h). In other words, it showed that the consumption of DOCp was tightly coupled to its production, and hence only a small amount of DOCp accumulated in the water. This suggests that the DOCp pool was mainly composed of labile molecules, preferentially assimilated by heterotrophic prokaryotes over other organic C sources. These observations highlight the importance of a direct transfer of organic matter from phytoplankton to bacterioplankton in Lake Kivu.

#### **2.2.3. Carbon and nutrient cycling in the redoxcline of Lake Kivu**

Permanently stratified water bodies, such as Lake Kivu, are characterized by the presence of pelagic gradients in oxygen (oxycline) and redox species (redoxcline). These are usually

areas of intense biogeochemical activities, where chemolithoautotrophs and methanotrophs derive their energy from the oxidation of reduced species.

### **2.2.3.1. Aerobic methanotrophy**

The permanently stratified Lake Kivu is one of the largest freshwater reservoirs of dissolved methane ( $\text{CH}_4$ ) on Earth. Yet  $\text{CH}_4$  emissions from its surface to the atmosphere is several orders of magnitude lower than the  $\text{CH}_4$  upward flux to the mixed layer, suggesting that  $\text{CH}_4$  removal through microbial  $\text{CH}_4$  oxidation is an important process within the water column. A combination of natural abundance stable carbon isotope analysis ( $\delta^{13}\text{C}$ ) of several carbon pools and  $^{13}\text{CH}_4$ -labelling experiments was carried out during the rainy (February 2012) and the dry season (September 2012) to quantify (i) the contribution of  $\text{CH}_4$ -derived carbon to the biomass, (ii) the methanotrophic bacterial production (MBP). MBP rates within the oxycline were variable (from 0 to  $7.0 \mu\text{mol C L}^{-1} \text{d}^{-1}$ , Fig. 45), but during the two field campaigns, maximum values were always observed at the bottom of the oxycline, near the transition between oxic and  $\text{O}_2$ -depleted waters where the  $\text{CH}_4:\text{O}_2$  ratio is close to 1, suggesting that  $\text{CH}_4$  oxidation was mainly driven by oxic processes. Vertically integrated over the water column, the MBP was estimated at  $29.5 \text{ mmol m}^{-2} \text{d}^{-1}$  during the rainy season in the Northern Basin, and  $28.6 \text{ mmol m}^{-2} \text{d}^{-1}$  and  $8.2 \text{ mmol m}^{-2} \text{d}^{-1}$  during the dry season in the Southern Basin and the Northern Basin, respectively. These rates are comparable to the gross  $\text{CH}_4$  oxidation rate reported earlier by Jannasch (1975) in Lake Kivu ( $7.2 \text{ mmol m}^{-2} \text{d}^{-1}$ ) and the upward  $\text{CH}_4$  flux recently estimated ( $9.4 \text{ mmol m}^{-2} \text{d}^{-1}$ ) by Pasche et al (2009). Hence it appears that almost the entire upward  $\text{CH}_4$  flux was aerobically oxidized by the methanotrophic bacterial community in Lake Kivu.

An abundant methanotrophic biomass was found in the oxycline throughout the year, as revealed by the low  $\delta^{13}\text{C}$  signature of POC (Fig 42b). Isotope mixing calculations showed that between 4% and 6% of the POC in the mixolimnion (i.e. integrated over the mixolimnion depth) derived from  $\text{CH}_4$  incorporation into the biomass, but the contribution of  $\text{CH}_4$ -derived carbon to the POC pool could locally reach values as high as 50 %, as measured in the oxycline during the dry season. Areal MBP in Lake Kivu are equivalent to 16-60% of the mean annual phytoplankton primary production ( $49 \text{ mmol m}^{-2} \text{d}^{-1}$ , Darchambeau et al. 2014), suggesting that biomass production by methanotrophs has the potential to sustain a significant fraction of the pelagic food-web. However, it is still unclear to which extent the C fixed in the redoxcline by methanotrophs is transferred to higher trophic levels.  $\delta^{13}\text{C}$  analyses revealed that the contribution of  $\text{CH}_4$ -derived carbon to zooplankton biomass is insignificant. Furthermore,  $\delta^{13}\text{C}$  results from a 40 cm-long sediment core gathered in the Northern Basin of Lake Kivu (see section 2.2.4) showed that the  $\delta^{13}\text{C}$ -TOC in sediments ( $-24.5 \pm 0.9 \text{ ‰}$ ,  $n = 132$ ) varied little and was close to the  $\delta^{13}\text{C}$  signature of the POC in the mixed layer ( $-23.8 \pm 0.8 \text{ ‰}$ , see section 2.2.2.1.), suggesting that  $\text{CH}_4$ -derived carbon does not contribute significantly to the sedimenting OM flux.

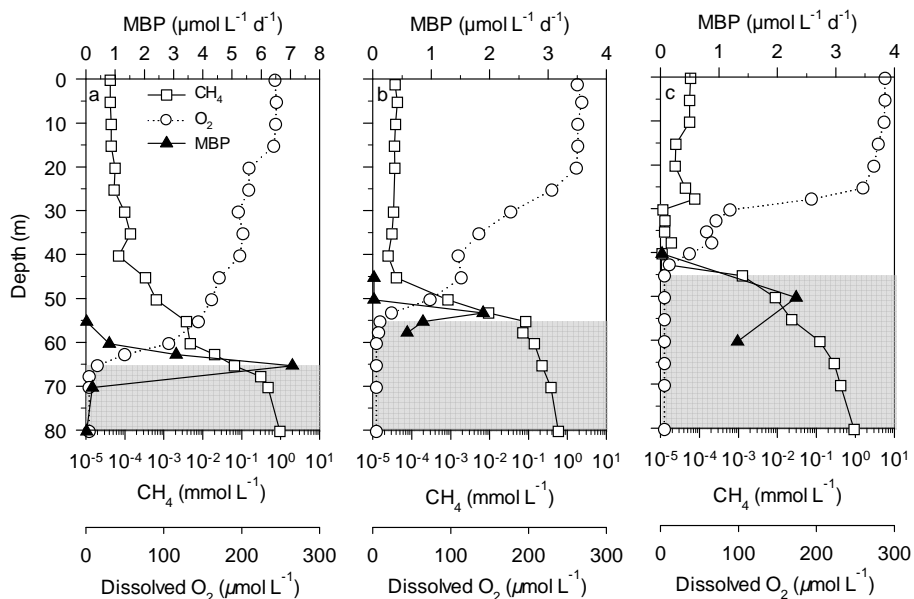


Figure 45: Vertical profiles of dissolved oxygen concentration (O<sub>2</sub>, μmol L<sup>-1</sup>), methane concentration (CH<sub>4</sub>, μmol L<sup>-1</sup>), and methanotrophic bacterial production rates (MBP, μmol L<sup>-1</sup> d<sup>-1</sup>) in the Southern Basin (a) and Northern Basin (b) in September 2012 and in the Northern Basin in February 2012 (c). The grey zone corresponds to waters with dissolved O<sub>2</sub> concentration < 3 μmol L<sup>-1</sup>.

Based on results gathered in small boreal lakes, some authors proposed that the relative contribution of methanotrophic bacteria to the total autotrophic production in a lake is related to its size (Kankaala et al. 2013). However, the results reported for the large (2370 km<sup>2</sup>) Lake Kivu do not fit with this general pattern, probably because of the permanent and strong stratification of its water column that on one hand promotes a long residence time of deep waters and the accumulation of CH<sub>4</sub>, and on the other hand leads to very slow upward diffusion of solutes, promoting the removal of CH<sub>4</sub> by bacterial oxidation as it diffuses to the surface.

### 2.2.3.2. Anaerobic methanotrophy

The results presented in the previous paragraph demonstrated that aerobic CH<sub>4</sub> oxidation is the main microbial process responsible of the CH<sub>4</sub> removal in the water column of Lake Kivu, but besides O<sub>2</sub>, a wide variety of others electron acceptors can be used by anaerobic organisms to oxidize CH<sub>4</sub> (anaerobic oxidation of methane, AOM). AOM can potentially occur with different electron acceptors: SO<sub>4</sub><sup>2-</sup> (SDMO), NO<sub>3</sub><sup>-</sup> (NDMO), Mn and Fe. The main basin of Lake Kivu shows high SO<sub>4</sub><sup>2-</sup> concentrations all year round, which are reduced into H<sub>2</sub>S at the top of anoxic waters. Our hypothesis is that this sulfate-reduction zone can potentially sustain the SDMO. Also, due to intense nitrification during the dry season, a NO<sub>3</sub><sup>-</sup> accumulation zone (nitracline) appears during the rainy season, at the oxic-anoxic interface, which can potentially sustain NDMO. In Kabuno Bay, high Fe and Mn concentrations could be used to oxidize CH<sub>4</sub> in anoxic waters.

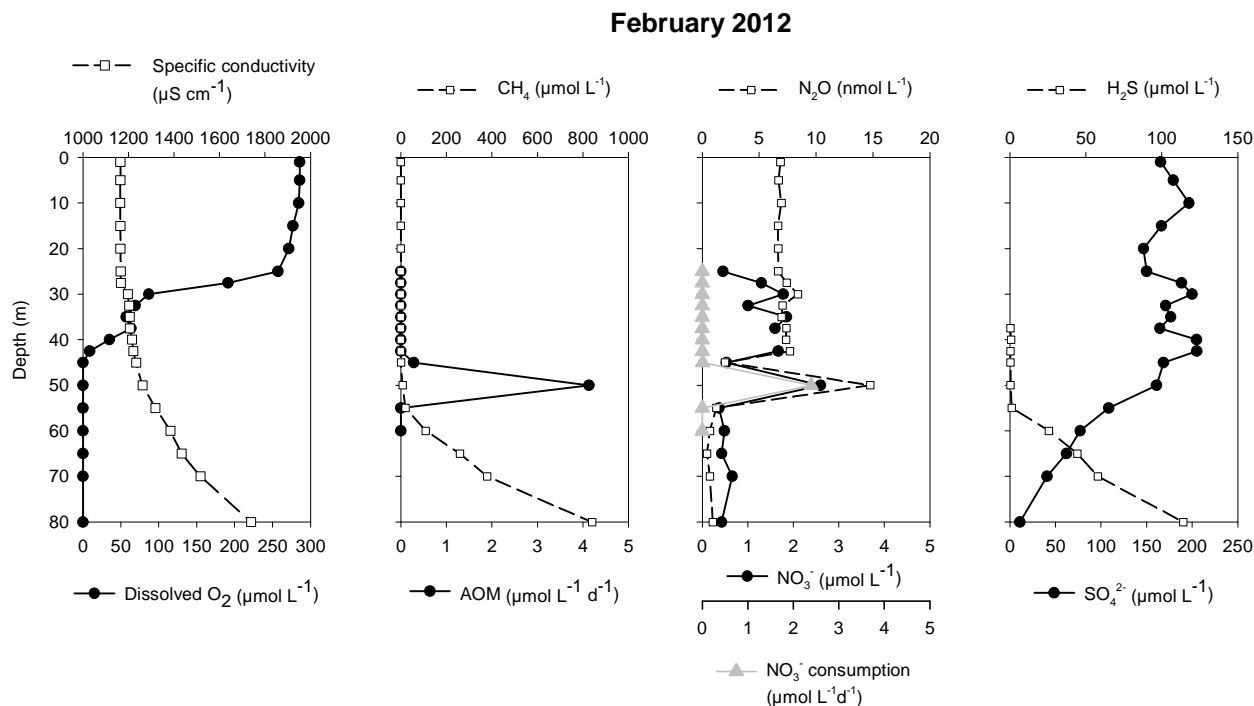


Figure 46: Specific conductivity ( $\mu\text{S cm}^{-1}$ ), dissolved  $\text{O}_2$  ( $\text{mg L}^{-1}$ ),  $\text{CH}_4$  concentration ( $\mu\text{mol L}^{-1}$ ), AOM rates ( $\mu\text{mol L}^{-1} \text{d}^{-1}$ ),  $\text{N}_2\text{O}$  concentration ( $\text{nmol L}^{-1}$ ),  $\text{NO}_3^-$  concentration ( $\mu\text{mol L}^{-1}$ ),  $\text{NO}_3^-$  consumption rates ( $\mu\text{mol L}^{-1} \text{d}^{-1}$ ),  $\text{H}_2\text{S}$  and  $\text{SO}_4^{2-}$  concentration ( $\mu\text{mol L}^{-1}$ , in the Northern Basin in February 2012.

AOM has been measured in the Northern Basin (off Gisenyi, Rwanda) during the 6 campaigns of Eagles: June 2011, February and September 2012, May and September 2013, and July 2014. Significant AOM rates were observed during all the campaigns, except in September 2012. AOM rates measured in February 2012, with dissolved  $\text{O}_2$ , specific conductivity,  $\text{CH}_4$ ,  $\text{N}_2\text{O}$ ,  $\text{NO}_3^-$ ,  $\text{H}_2\text{S}$  and  $\text{SO}_4^{2-}$  concentrations, and  $\text{NO}_3^-$  consumption rates are presented in Fig. 46 as an example. In February 2012, a small nitracline of  $\sim 3 \mu\text{mol L}^{-1}$  was observed in the top of anoxic waters. This nitracline co-occurred with a  $\text{NO}_3^-$  consumption peak of  $\sim 3 \mu\text{mol L}^{-1} \text{d}^{-1}$  and the AOM peak of  $\sim 4.5 \mu\text{mol L}^{-1} \text{d}^{-1}$  observed at 50 m. This suggests that NDMO could occur at this depth. However, the  $\text{NO}_3^-$  consumption rate is not sufficient to explain all the AOM rate observed, since  $7 \mu\text{mol L}^{-1} \text{d}^{-1}$  of  $\text{NO}_3^-$  are needed to consume  $4.5 \mu\text{mol L}^{-1} \text{d}^{-1}$  of  $\text{CH}_4$ . Thus, SDMO could also occur. In May 2013, September 2013 and July 2014 (not illustrated), NDMO was not possible, because the nitracline was either absent or located in the oxic waters. AOM peaks observed are thus hypothesized as SDMO.

### 2.2.3.3. Chemoautotrophic and anoxygenic photoautotrophic pathways of CO<sub>2</sub> fixation in the redoxcline of Lake Kivu

With the notable exception of Kabuno Bay, significant rates of anoxygenic photosynthesis were never measured in Lake Kivu during this study (June 2011, February 2012, and September 2012). This might be related to the very low light availability at the oxic-anoxic transition zone in the main basin of Lake Kivu. Indeed, considering a light attenuation coefficient of 0.26 m<sup>-1</sup> (Darchambeau et al. 2014), the light intensity at the oxic-anoxic transition zone was estimated at 6.66x10<sup>-3</sup> μmol photon m<sup>-2</sup> s<sup>-1</sup> in February 2012 and 3x10<sup>-5</sup> μmol photon m<sup>-2</sup> s<sup>-1</sup> in September 2012, well below the values reported in the chemocline of the Black Sea (~0.18 μmol photon m<sup>-2</sup> s<sup>-1</sup>) and Lake Matano (~0.12 μmol photon m<sup>-2</sup> s<sup>-1</sup>), where low-light adapted *Chlorobi* members (anoxygenic photoautotrophs) were identified (Marschall et al. 2010, Crowe et al. 2014).

In contrast, along with aerobic methanotrophy, chemoautotrophic CO<sub>2</sub> fixation pathways appeared to be significant processes in the redoxcline of Lake Kivu. During both the rainy (February 2012) and the dry (September 2012) season, significant CBP rates were measured at the oxic-anoxic transition zone as well as below the oxic-anoxic transition zone (hence, in O<sub>2</sub>-depleted waters). Maximal values were observed at the bottom of the mixolimnion (70 m) (1.43 μmol L<sup>-1</sup> d<sup>-1</sup>), in the counter-gradient of H<sub>2</sub>S/SO<sub>4</sub><sup>2-</sup> (Fig. 47). The maximal volumetric CBP rates measured in Lake Kivu were in the same range of values reported from H<sub>2</sub>S-rich marine redoxcline, such as the Black Sea (Grote et al. 2008), the Baltic Sea (Jost et al. 2008) and the Cariaco Basin (Taylor et al 2001). In these marine systems, the maximal chemoautotrophic activities were observed in sulfidic waters, well below the oxic-anoxic transition zone. In Lake Kivu, oxygen was also undetectable (< 3 μmol L<sup>-1</sup>) at most depths where significant chemoautotrophic production were measured, raising the question which electron acceptors are used by chemoautotrophic organisms in the lower zone of the redoxcline. As already pointed out (Darchambeau et al. 2014), the density gradient of the mixed layer is usually weak in Lake Kivu, and the stratification of the water column is rather unstable.

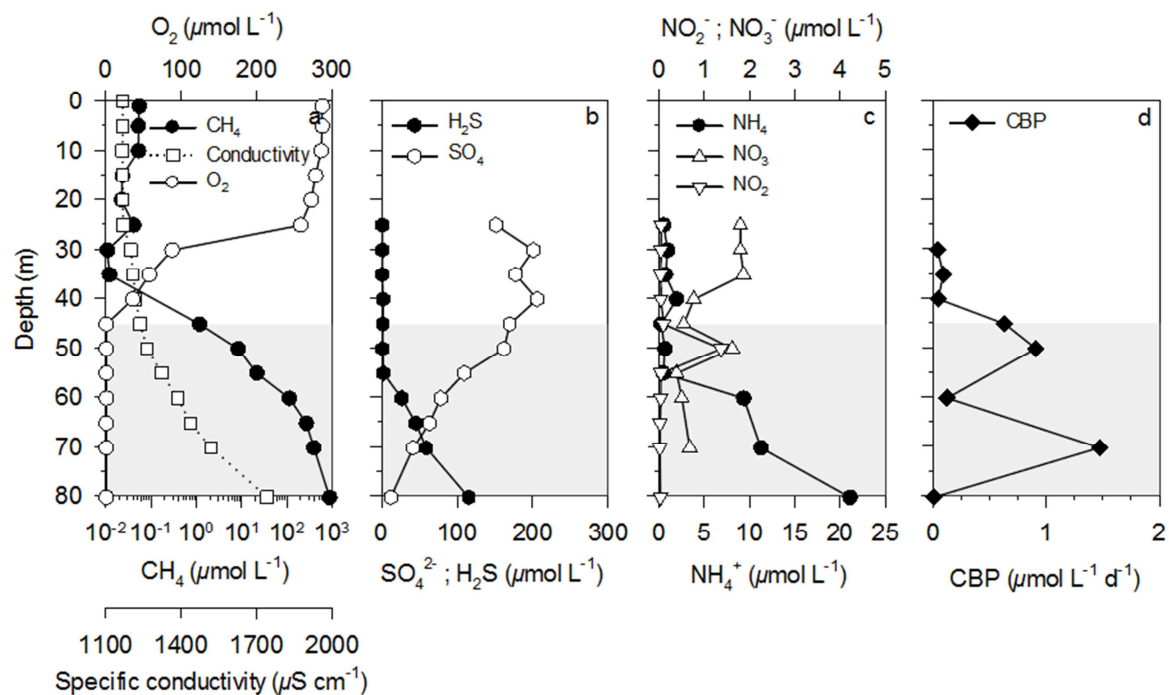


Figure 47: During the rainy season (February 2012) in the Northern basin, depth profile of (a) the conductivity ( $\mu\text{S cm}^{-1}$ ) and the concentration of dissolved  $\text{O}_2$  and  $\text{CH}_4$  ( $\mu\text{mol L}^{-1}$ ), (b) the concentration of  $\text{H}_2\text{S}$  and  $\text{SO}_4^{2-}$  ( $\mu\text{mol L}^{-1}$ ), (c) the concentration of  $\text{NH}_4^+$ ,  $\text{NO}_3^-$  and  $\text{NO}_2^-$  ( $\mu\text{mol L}^{-1}$ ), (d) the daily chemoautotrophic bacterial production rates ( $\mu\text{mol L}^{-1} \text{d}^{-1}$ ). Grey zone corresponds to the anoxic ( $< 3 \mu\text{mol L}^{-1}$ ) waters.

Episodic intrusion of dissolved  $\text{O}_2$  in the deeper part of the chemocline could therefore partly fuel aerobic  $\text{NH}_4^+$  or  $\text{H}_2\text{S}$  oxidation. However, in the absence of  $\text{O}_2$ , it is widely assumed that prokaryotes use the thermodynamically most favourable electron acceptors available in waters.  $\text{NO}_3^-$  could notably be used as an electron acceptor to reduce  $\text{H}_2\text{S}$  by autotrophic *Epsilonproteobacteria* members (*Sulfurimonas*, *Sulfuricurvum*), observed in high abundance in the bottom of the redoxcline in Lake Kivu (Inceoglu et al. 2015). Moreover, a putative linkage between  $\text{NO}_3^-$  reduction and  $\text{H}_2\text{S}$  oxidation has been indirectly evidenced in the  $\text{O}_2$ -depleted waters of Lake Kivu (see section below and Roland 2012). Integrated over the water column of the main basin of Lake Kivu, CBP was estimated at  $19.0 \text{ mmol m}^{-2} \text{ d}^{-1}$  and  $13.9 \text{ mmol m}^{-2} \text{ d}^{-1}$  during the rainy and dry season, respectively. Considering theoretical stoichiometries, the vertical diffusive and advective fluxes of the main electron donors ( $\text{NH}_4^+$ ,  $1.95 \text{ mmol m}^{-2} \text{ d}^{-1}$ ;  $\text{H}_2\text{S}$ ,  $0.61 \text{ mmol m}^{-2} \text{ d}^{-1}$ ) estimated in the main basin of Lake Kivu by Pasche et al. (2009) were largely insufficient to fuel the CBP rates measured during this study. It could imply that an intensive, yet cryptic, recycling of S- or N- redox species in the redoxcline must play an important role in Lake Kivu to sustain the chemoautotrophic demand, as suggested for the Black Sea (Murray et al. 1995) and the Cariaco basin (Taylor et al. 2001). Despite their biogeochemical significance in the water column, these processes would not have any clear *in situ* chemical expression because of the tight coupling between production and consumption of the chemical species used by the chemoautotrophs.

#### **2.2.3.4. Denitrification, anaerobic ammonium oxidation and dissimilative reduction of nitrate to ammonium**

Denitrification and anaerobic ammonium oxidation (anammox) have been quantified in June 2011 and February 2012. Dissimilative reduction of nitrate to ammonium (DNRA) has been quantified in February 2012. These measurements were made in the Northern Basin (off Gisenyi, Rwanda) and in the Southern Basin (Ishungu). In February 2012, a treatment with addition of H<sub>2</sub>S was performed, in order to determine the influence of H<sub>2</sub>S on denitrification and anammox rates. Rates of these three processes are shown in Fig. 48. A maximum denitrification rate of ~39 μmol L<sup>-1</sup> h<sup>-1</sup> was measured at 65 m, in the Northern Basin, in February 2012. In both stations, anammox rates were relatively low compared with denitrification rates, since the maximum anammox rate, without H<sub>2</sub>S added, was estimated to 1.7 nmol NO<sub>3</sub><sup>-</sup> L<sup>-1</sup> h<sup>-1</sup>, in the Southern Basin in February 2012. Some studies have suggested an inhibitory effect of H<sub>2</sub>S on anammox (Dalsgaard et al. 2003, Jensen et al. 2008, 2009). However, other studies conducted in wastewater bed reactors showed that anammox bacteria tolerate H<sub>2</sub>S and even that H<sub>2</sub>S stimulates anammox (Kalyuzhnyi et al. 2006, Jung et al. 2007). The study of Wenk et al. (2013) on Lake Lugano also showed that anammox bacteria were only active when H<sub>2</sub>S was added. Here, we also show that anammox was strongly stimulated by the addition of H<sub>2</sub>S, since anammox rates increased up to 31 nmol NO<sub>3</sub><sup>-</sup> L<sup>-1</sup> h<sup>-1</sup>. Also, denitrification rates increased with the addition of H<sub>2</sub>S at the depths of 50 and 55 m in the Northern Basin, and at 50 m in the Southern Basin, suggesting the occurrence of chemolithotrophic denitrification (denitrification coupled with the oxidation of H<sub>2</sub>S). However, at 60 and 65 m depth, in the Northern Basin, the addition of H<sub>2</sub>S was found to inhibit denitrification.

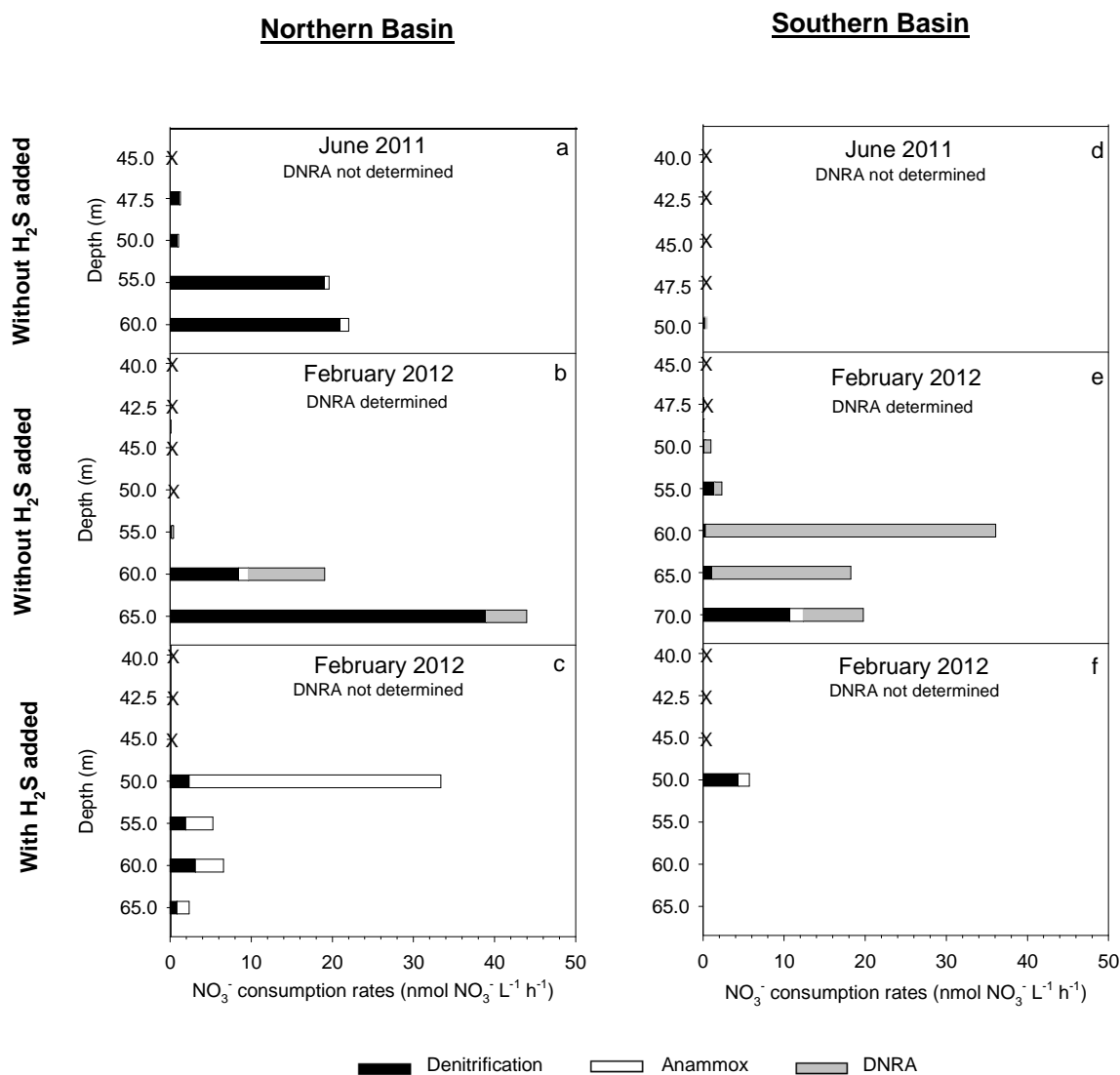


Figure 48: Denitrification (black), anammox (white) and DNRA (grey) with and without H<sub>2</sub>S added (nmol NO<sub>3</sub><sup>-</sup> L<sup>-1</sup> h<sup>-1</sup>), in the Northern Basin (a-c) and in the Southern Basin (d-f), for the campaigns of June 2011 (a and d) and February 2012 (b, c, e and f).

These observations are difficult to explain. A normal expectation would have been that the addition of H<sub>2</sub>S does not stimulate denitrification at these depths, because H<sub>2</sub>S is naturally present at non-negligible concentrations (25 and 45 μmol L<sup>-1</sup> at 60 and 65 m, respectively). Our hypothesis is that there is a competition for substrates with DNRA bacteria at high H<sub>2</sub>S concentrations. For a long time, authors reported an inhibition of denitrification when H<sub>2</sub>S were present (e.g. Jorgensen 1989,

Joye and Hollibaugh 1995, An and Gardner 2002) but it is now established that denitrification can be coupled with the oxidation of H<sub>2</sub>S (chemolithotrophic denitrification). So, it seems that the apparent inhibition of denitrification at high H<sub>2</sub>S concentrations could be due to a substrate competition with DNRA. Indeed, several studies suggest that DNRA can be enhanced at high H<sub>2</sub>S concentrations (e.g. Brunet and Garcia-Gil 1996, Rysgaard et al. 1996, Sayama et al. 2005) and become, in this case, more competitive than denitrification. We did not measure DNRA with the addition of H<sub>2</sub>S during this study but DNRA measurements without H<sub>2</sub>S added allow us to suggest a competition between these two processes. At both stations, higher denitrification rates correspond to lower DNRA rates (Fig. 49), consistent with substrate competition between denitrification and DNRA (NO<sub>3</sub><sup>-</sup>,

organic matter,  $\text{H}_2\text{S}$ ). DNRA rates were not enhanced where  $\text{H}_2\text{S}$  were naturally high (deep waters), in both stations, so we can hypothesize that natural  $\text{H}_2\text{S}$  concentrations (below  $50 \mu\text{mol L}^{-1}$ ) are not sufficient to allow DNRA to become more competitive than heterotrophic/chemolithotrophic denitrification or simply to inhibit the two last steps of denitrification.

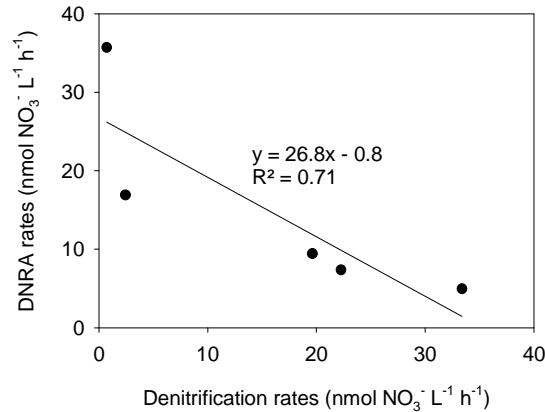


Figure 49: Correlation between DNRA and denitrification rates (nmol  $\text{NO}_3^- \text{L}^{-1} \text{h}^{-1}$ ) during both stations and both campaigns.

### 2.2.3.5. The importance of methanotrophy and chemoautotrophy in the ecosystem functioning of Lake Kivu

Methanotrophy and chemoautotrophy in the pelagic redoxcline may affect the ecological functioning of Lake Kivu in several ways. First, these processes might represent alternative sources of autochthonous OM for higher trophic levels, besides oxygenic photosynthesis carried out by phytoplankton in the surface waters. They could also exert an indirect control on phytoplankton production by limiting the amount of inorganic nutrient that reach the illuminated surface waters. This seems to be especially important in the large East African Rift lakes where internal nutrient loading via upward fluxes is of major importance for phytoplankton growth (Kilham and Kilham 1990; Pasche et al. 2009). For instance, assuming that methanotrophic and chemoautotrophic uptake of dissolved inorganic phosphorus (DIP) follows Redfield stoichiometry (C:P = 106:1), DIP uptake in the redoxcline would have approximated  $0.29 \text{ mmol m}^{-2} \text{ d}^{-1}$  and  $0.40 \text{ mmol m}^{-2} \text{ d}^{-1}$  in February and September 2012, respectively. This DIP uptake flux is higher than the upward DIP flux of  $0.08 \text{ mmol m}^{-2} \text{ d}^{-1}$  estimated by Pasche et al. (2009), highlighting the strength of the constraint they might exert on nutrient availability in the mixed layer, but also suggesting that a substantial amount of DIP is actively recycled in the redoxcline to sustain the chemoautotrophic demand. Secondly, aerobic  $\text{CH}_4$  oxidation and chemoautotrophic processes would participate substantially to the  $\text{O}_2$  consumption in the water column, and hence they would contribute to the seasonal uplift of the oxycline observed after the re-establishment of the thermal stratification during the rainy season. Shallower oxic zone during the rainy season might have several implications for the ecological functioning of Lake Kivu. Among them, the habitat compression endured by pelagic zooplankton species as a result of hypoxia would reduce the extent of vertical migration, and might thus significantly increase the predation pressure on larger zooplankton individuals during the rainy season (Isumbusho et al. 2006).

## 2.2.4. Sediment core retrieval – new cores and analyses

### 2.2.4.1. Materials and methods

#### *Sediment core retrieval*

Five lake sediment cores (Kivu-G1 to Kivu-G5) were collected during the first field campaign (June 2011) at two closely located sites off Gisenyi where the influence from the littoral zone and catchment area was expected to be minimal. In September 2013 and August 2014, additional sediment cores (Kivu-G7 and Kivu-G8) were taken at the same location for pollen analyses and non-destructive core scanning respectively. All cores were taken using a UWITEC gravity corer. Cores Kivu-G4, Kivu-G5 and Kivu-G7 were subsampled for sedimentological, biogeochemical and microfossil analyses in the field, while core Kivu-G8 was kept and transported intact to Belgium. Core Kivu-G4 was selected as the master core on which the majority of the analyses were performed.

#### *Non-destructive core scanning*

The Kivu-G8 core was opened laterally and analysed using a Geotek core scanner equipped with a spectral camera. The ratio between the absorption maximum of carotenoids (450 nm) and that of chlorophyll a (670 nm) was used to align the core with the Kivu-G4 core based on the total carotenoid content measured using high performance liquid chromatography (see below) as well as with the percentage of benthic diatoms counted. The core was subsequently analyzed using a medical CT scanner (Siemens SOMATOM Definition Flash) in order to detect sediment deformations and identify mass transport deposits (MTD).

#### *Geochronology*

The chronology of the sediments was obtained using a combination of three approaches. First, the activities of  $^{210}\text{Pb}_{\text{xs}}$ ,  $^{226}\text{Ra}$  and  $^{137}\text{Cs}$  were measured in the surface sediments of the Kivu-G4 core using a low background, high efficiency  $\gamma$  detector (CANBERRA) equipped with a Cryo-Cycle (CANBERRA) (Schmidt et al. 2014). Calibration was achieved using certified reference materials (IAEA-RGU-1; IAEA-RGTh; SOIL-6). Activities are expressed in  $\text{mBq g}^{-1}$  and errors are based on 1 SD counting statistics. Excess  $^{210}\text{Pb}$  ( $^{210}\text{Pb}_{\text{xs}}$ ) was calculated by subtracting the activity supported by its parent isotope,  $^{226}\text{Ra}$ , from the total  $^{210}\text{Pb}$  activity in the sediment. We have used the CIC (constant initial concentration) model (Robbins and Eglinton 1975; Bolliet et al. 2014), which assumes a steady initial  $^{210}\text{Pb}_{\text{xs}}$  concentration at the sediment surface, to calculate the age of measured depths.

Secondly, the age-depth model guided us to select depths in which we screened for the presence of pollen from the non-native trees *Eucalyptus* spp., *Cupressus* spp. and *Pinus* spp. Focus was put on the following depths in the Kivu-G7 core: 2-3 cm, 3-4 cm, 6-7 cm and 11-12 cm. *Eucalyptus* was first introduced around 1920, while *Cupressus* and *Pinus* spp. were introduced after 1948 (MINITERE 2003). The minimal dates of appearance of these pollen in the sediments were calculated by adding the ages of maturity (i.e. start of pollen production) of *Eucalyptus*, *Cupressus* and *Pinus* (i.e. 3.3 yr, 7.1 yr and 15.5 yr, respectively; Verdú 2002) to the year of introduction.

Thirdly, the sediments below 20 cm depth were screened for the presence of terrestrial macrofossils for  $^{14}\text{C}$  dating in the Kivu-G7 core. At 38.25 cm depth a thorn was found and

picked out of the sediment. The thorn was rinsed with milli-Q water and sent to the BETA radiocarbon facility. The  $^{14}\text{C}$  age was calibrated using CALIB 7.0 and the IntCal13 calibration curve (Reimer et al. 2013).

### *Geochemical analyses*

The sediments from core Kivu-G4 were analyzed from depth 0.125 cm to depth 6.125cm (with a 0.25 cm resolution) for major ( $\text{SiO}_2$ ,  $\text{P}_2\text{O}_5$ ,  $\text{K}_2\text{O}$ ,  $\text{CaO}$ ,  $\text{MnO}$ ,  $\text{Fe}_2\text{O}_3$  tot,  $\text{TiO}_2$ ) and trace element (Sc, V, Cr, Co, Ni, Cu, Zn, Ga, Ge, Rb, Sr, Y, Zr, Nb, Cs, Ba, La, Ce, Pr, Nd, Eu, Sm, Gd, Dy, Ho, Er, Yb, Lu, Hf, Ta, W, Pb, Th, U) by ICP-MS and HR-ICP-MS, respectively. In order to get precise and reproducible results despite the very limited weight of available matter, each sample was placed in suspension in some distilled water in order to collect all available sediment matter on a filter. This enabled us to weight each sample correctly with the filter. In order to avoid any loss of sample during the further dissolution procedure, we had to proceed to the element analyses after a full dissolution of both the filter with the sediments. The average precision for trace elements is on average at 5% at a  $2\sigma$  level. The major elements did not sum up to 100% because we were unable to analyze the large proportion of  $\text{CO}_2$  present within the carbonates. The Ce and Eu anomalies were calculated as  $\text{Ce}/\text{Ce}^* = \text{Ce}/(\text{La} \cdot \text{Pr})^{1/2}$  and  $\text{Eu}/\text{Eu}^* = \text{Eu}/(\text{Sm} \cdot \text{Gd})^{1/2}$ .

The concentration of amorphous silica was estimated by applying a wet alkaline digestion method on the filters. Aluminum released during the digestion was used to correct for concomitant dissolution of lithogenic particles following the method of Ragueneau et al. (2005). A known fraction of the filter was submitted to a first digestion in 0.2 mol L<sup>-1</sup> NaOH at 100°C for 40 min. At the end of this first leach, all the  $\text{BSi}$  and some lithogenic Si were supposed to be dissolved. Si and Al concentrations ( $[\text{Si}]_1$  and  $[\text{Al}]_1$ ) in the supernatant were then analyzed by high-resolution inductively coupled plasma mass spectrometer (HR-ICP-MS). After rinsing and drying, the filter was submitted to a second digestion step, identical to the first, allowing us to determine a  $(\text{Si}/\text{Al})_2$  ratio characteristic of the lithogenic particles present on the filter. This ratio is then used to correct the concentration of Si in biogenic silica form as follows:  $[\text{BSi}] = [\text{Si}]_1 - [\text{Al}]_1 \times (\text{Si}/\text{Al})_2$ . A third digestion step was added to the original method to verify that no BSi was left after the first leach.  $(\text{Si}/\text{Al})$  ratios should therefore be similar in the supernatants after the second and the third leaches. In a few cases in which all the BSi was not dissolved on the first attempt, the procedure was started over with a smaller filter fraction. Uncertainty on BSi measurements with the method from Ragueneau et al. (2005) is ca. 10% but depends on the importance of the correction. Note that the presence of Al within opal is not taken into account and could lead to a slight underestimation of [BSi]. If the Al/Si is in the range of those measured in *Aulacoseira* sp. (Al/Si ratio of 0.027) which is the dominant diatom species in the Congo River, it would induce an underestimation of only ca. 4% of the measured BSi.

Total carbon (TC), total organic carbon (TOC) and total nitrogen (TN) concentrations as well as  $\delta^{13}\text{C}$  and  $\delta^{15}\text{N}$  measurements were performed in the laboratory of the Department of Earth and Environmental sciences (KUL, Belgium) using an Elemental Analyzer - Isotope Ratio Mass Spectrometer (Thermo Flash HT/EA with Delta V Advantage). In summary, aliquots of 0.5 to 1 mg, 1 to 2 mg and 3 to 5 mg of dry samples were packed into silver capsules for TC,

TOC and TN analyses, respectively. Samples intended for TOC analyses were decarbonated by acid treatment using 40 µl of HCl 8 %, and dried at 60°C. This treatment was repeated twice prior to EA-IRMS analysis. Standards consisted of IAEA-N2, IAEA-C6, acetanilide, aspartic acid and leucine.  $\delta^{13}\text{C}$  analyses of total inorganic carbon (TIC) were made by direct acidification ( $\text{H}_3\text{PO}_4$ ) of dried sediment samples in helium-flushed 12 mL exetainer vials, followed by injection in the EA-IRMS. For calibrations we used LSVEC and either NBS-19 or IAEA-CO-1.

Total inorganic carbon (TIC) was calculated from TOC and TC based on the isotope mass balance principle using the following equation:

$$\delta^{13}\text{C}_{\text{TIC}} * \% \text{TC} = \delta^{13}\text{C}_{\text{TOC}} * \% \text{TOC} + \delta^{13}\text{C}_{\text{TIC}} * \% \text{TIC}$$

The calcium and phosphorus content of bulk sediment samples was determined following the techniques used by Fagel et al. (2005). Aliquots of 250 mg of dried sediment samples were mechanically crushed through a 100-200 µm mesh and then digested in alkaline solution of Lithium metaborate using a Pt crucible at 1000 °C for 1 h. After a night of dissolution in nitric acid, the residue was analyzed for Ca, Ti, Fe and P by Inductively Coupled Plasma Atomic Emission Spectrometry (ICP-AES; Thermo Optek Iris Advantage, Royal Museum for Central Africa, Tervuren, Belgium).

#### *Microfossil and pollen analysis*

Samples for pollen analysis were prepared according to standard pollen extraction techniques (Faegri et al., 1989), which included sieving at mesh size 212 µm, KOH (10%) treatment, acetolysis, heavy liquid separation (density: 2.0) with sodium polytungstate, and mounting in glycerin jelly.

The samples for microfossil analysis were prepared following a slightly modified protocol of Renberg (1990) and embedded in Naphrax®. The slides were screened under an Axioplan 2 light microscope. Digital pictures of the different diatom species were taken using an Axiophot module and an Axiocam camera.

#### *Phytoplankton and bacterial pigment analyses*

Pigments were analyzed only on the core GIS-KV11-4 and were normalized to dry weight. Pigment extraction was performed according to standard protocols (Wright et al. 1991; Reuss and Conley 2005). A precise quantity (between 0.2 and 0.5 g) of freeze-dried sediment samples was treated with 5 ml HPLC grade acetone in 14 ml tubes with screw caps. Samples were extracted for 24 hours in cool and dark conditions after which they were shaken for 5 hours and allowed to settle. They were subsequently ultrasonicated on ice-bath for 15 minutes and centrifuged for 15 minutes under 4500 rpm always in dark conditions. A volume of 1.7 ml of the extract for each sample was mixed to 0.3 ml of nanopure water, transferred to a dark glass and kept frozen until HPLC analyses following the procedures of Descy et al. (2005) and Sarmiento and Descy (2008).

HPLC analysis was carried out using the Wright *et al.* (1991) gradient elution method, with a Waters system comprising a Waters 996 PDA detector and a Waters 470 fluorescence detector. Calibration was made using commercial external standards (DHI, Denmark).

Identification of pigments was checked against a library of pigment spectra, obtained by diode array acquisition of chromatograms from pure pigment solutions and from acetone extracts of pure cultures of algae. Chromatograms processing was done with the Waters Empower software.

#### 2.2.4.2. Results and discussion

##### *X-ray imaging of core Kivu-G8*

The X-ray scanning revealed that between the bottom of the core Kivu-G8 and 34 cm depth, the sediment is alternating between light and dark lamina (Fig.50). From 34 to 23 cm depth the sediment is dark and heavily disturbed, which suggests that this layer corresponds to a mass transport deposit (MTD). From 23 to 21 cm depth a whitish layer with fine laminations is present, which is interrupted at 21.5 cm depth by a dark lamina. From 21-16 cm depth the sediment has a darker color with poor lamination. Between 16 and 14 cm the sediments color is getting lighter and weak lamination can be observed. From 14 to 11 cm depth the sediment is tilted with fine whitish laminations. Between 11 and 9 cm the sediment is still tilted and abruptly changes to a dark color without lamination. At 9 cm the sediment changes abruptly to a white layer which is disturbed and includes fish bones. Tilted lamina following the fish bones suggest that these bones caused the perturbation and the lamination was formed around them. Without the bones, this layer would probably be laminated.

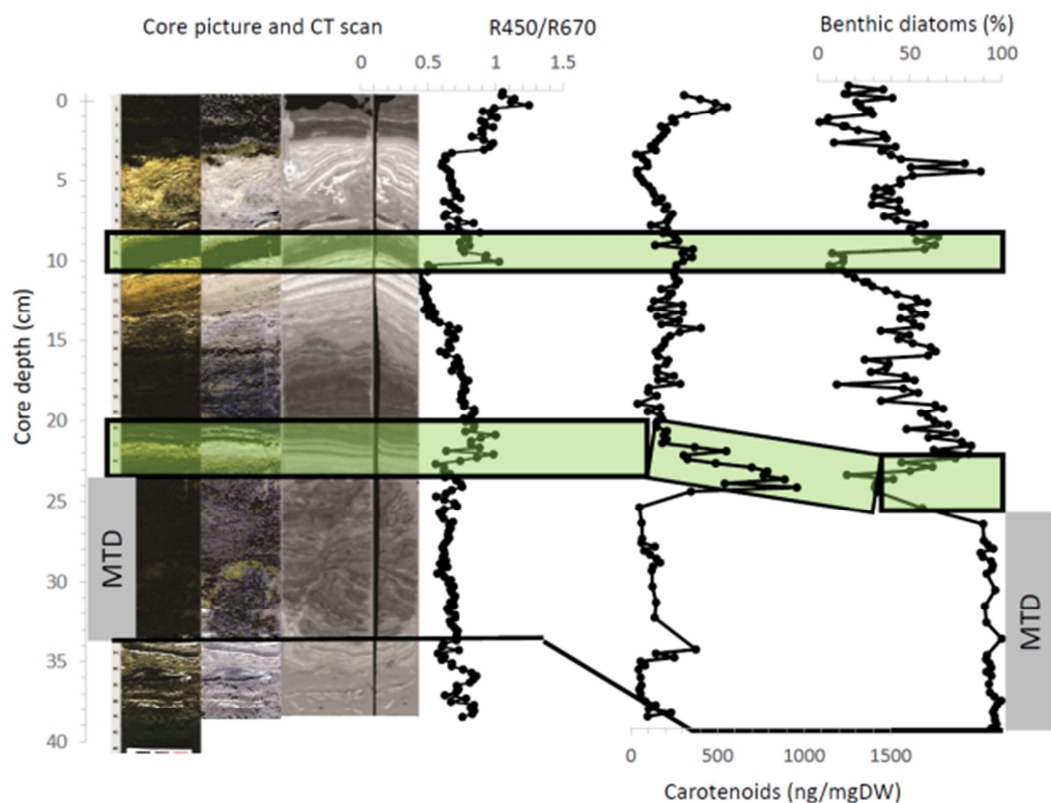


Fig.50: Geotek and CT scan showing the mass transport deposit (MTD) between 34 and 23 cm depth in the Kivu G8 core. Based on the between the reflection at 450 and 670 nm and the total carotenoid content, the MTD in the Kivu G4 could be tentatively put between 26 and 40 cm. This zone corresponds to the sediments which are dominated by benthic diatoms.

The Kivu-G8 core could be tentatively aligned with the Kivu-G4 core based on the pigment and diatom analyses. This alignment suggests that between 40 and 27 cm a mass transport deposit is present. It follows that these sediments cannot be used for environmental reconstructions.

### Geochronology

The three different approaches for dating revealed three different averaged sedimentation rates. Based on the  $^{210}\text{Pb}$  dating and the model using a constant initial concentration (CIC) the average sedimentation rate equalled 0.13 cm/yr (Fig. 51)

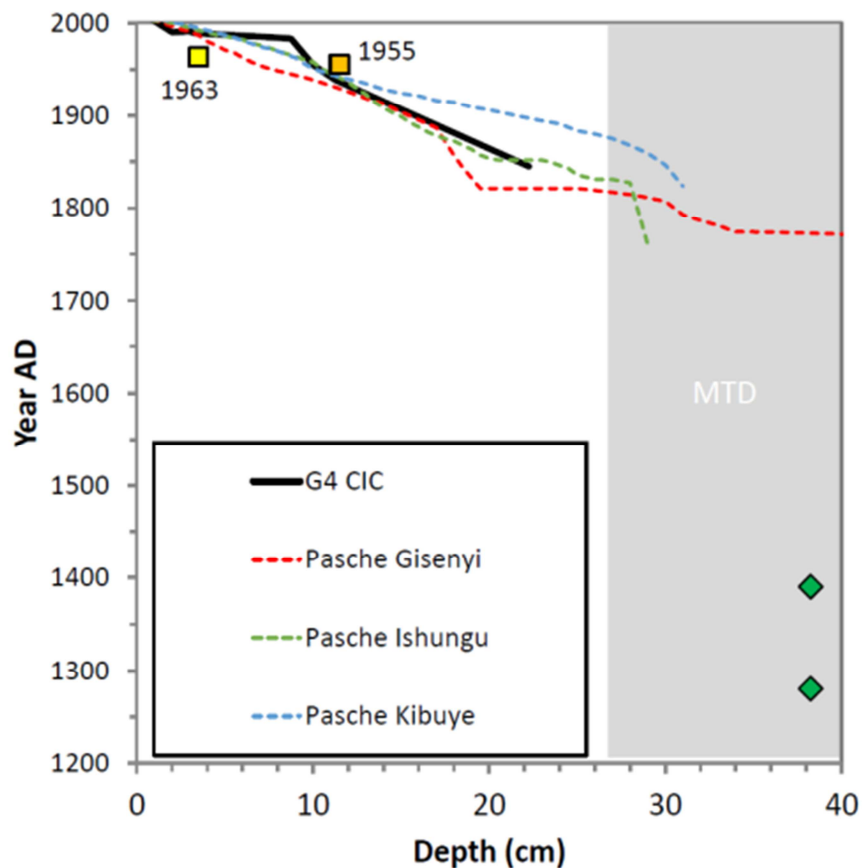


Fig. 51: Age depth model based on  $^{210}\text{Pb}$  dating of the Kivu-G4 core (full black line) and the  $^{210}\text{Pb}$  based age depth models of Pasche et al. (2010) (dotted line) for comparison. The pollen dates represent the earliest occurrence of *Pinus* (1963) and *Cupressus* (1955). The upper and lower calibrated  $^{14}\text{C}$  dates of the thorn found at 38.25cm are denoted by the green diamond. The Mass Transport Deposit (MTD) is indicated with the grey rectangle.

These age estimations were similar to those found by Pasche et al. (2009). Pollen of *Eucalyptus* and *Pinus* were found at 2-3 cm depth of *Cupressus* and *Pinus* at 3-4 cm and of *Eucalyptus* and *Cupressus* at 6-7 cm depth. At 11-12 cm depth only *Cupressus* occurred. It follows that the 3-4 cm sediment slice cannot have been formed before AD 1963 and the 11-12 cm not before AD 1955 (Fig. 51). The latter observation suggests a sedimentation rate of at least 0.19 cm/yr for the top 11 cm of the core, which contradicts with the dates obtained using the  $^{210}\text{Pb}$  measurements. The wooden thorn was found at 38.25 cm depth. It has a calibrated  $^{14}\text{C}$  date of 560-670 cal yr BP old (1280-1390 AD). This results in an average

sedimentation rate of 0.06-0.07 cm/yr, which is far below that obtained using  $^{210}\text{Pb}$  dating and based on the pollen. As the thorn was found in the MTD, we suggest it was derived from sediments that were deposited somewhere after 1280-1390 AD, but prior to ca. 1800 AD (extrapolation of sediment age at 27 cm depth based on the  $^{210}\text{Pb}$ -based sedimentation rate). Due to the uncertainty related with the dating of the core, the changes in the proxy records are summarised and discussed in relation to sediment depth.

### *Geochemistry*

Major and trace elements were used to quantify the respective proportions of clays and carbonates (e.g. Rb/Sr versus CaO, fig 52 and 53), the hydrothermal-derived carbonate precipitates (e.g. positive Ce anomaly  $\text{Ce}/\text{Ce}^*$ , negative Eu anomaly  $\text{Eu}/\text{Eu}^*$ , the low chondrite normalized  $\text{La}_N/\text{Yb}_N$  ratio, high Ba content; Fig. 52), and the changes in the detrital source from normal crustal-derived components ( $\text{La}_N/\text{Yb}_N \sim 8$ ;  $\text{Th}/\text{U} \sim 1$ ) to alkaline volcanic-derived Virunga-like sources (nephelinitic;  $\text{La}_N/\text{Yb}_N \sim 15-25$ ;  $\text{Th}/\text{U} > 2.3$ ).

From 40 to 21.75 cm depth, the sediment is characterized by a large carbonate fraction with low biogenic silica (Fig. 52) and very low clay detrital components ( $\text{Rb}/\text{Sr} < 0.05$ ). The carbonate phase incorporates large quantities of Strontium ( $780 < \text{Sr} < 1820 \text{ppm}$ ). This high Sr content could be triggered either by the influx of a buoyant hydrothermal plume within the lake as suggested by Ross et al. (2015) or by the meteoric dissolution of the Sr-rich ( $1600 < \text{Sr} < 3200 \text{ppm}$ ) nephelinites that form the largest fraction of the Nyiragongo volcanics (Platz et al., 2004) or by a combination of both factors. Considering the very low Ba content and the lack of an Eu anomaly, a direct hydrothermal source is unlikely. In contrast, the significant Ce anomalies  $0.69 < \text{Ce}/\text{Ce}^* < 0.88$  between 40 and 29.5 cm which drastically contrast with smaller or the lack of such anomalies from 29 cm to the top sediment ( $0.91 < \text{Ce}/\text{Ce}^* < 1.01$ ) indicate a change in the oxic/anoxic conditions. Cerium is a well-known redox-sensitive rare earth element and its potential paleo-redox value in the hydrosphere is long been established (Elderfield 1990 for an overview). The origin of a distinctive Ce negative anomaly in the water column may be interpreted as follows. Oxidation precipitation of insoluble  $\text{Ce}^{4+}$  oxide must occur through the oxygenated portion of the upper water column. This could reflect large influx of oxygen-rich Sr-rich meteoric water into the lake. The subsequent decrease in the Ce anomaly may reflect either a reduction of these surface water influxes and/or an upwelling invasion of deep suboxic water towards the surface water. If this second hypothesis is realistic, this might have impacted the shallow water biosphere and might have led to the partial extinction of the surface water diatom productivity. Alternatively and more likely, the Ce anomalies between 40 and 29.5 cm are related to the deposition of oxygenated sediments from the littoral zone, as suggested by the high amount of benthic diatoms and the disturbed nature of the sediments in this part of the cores (Fig. 50).

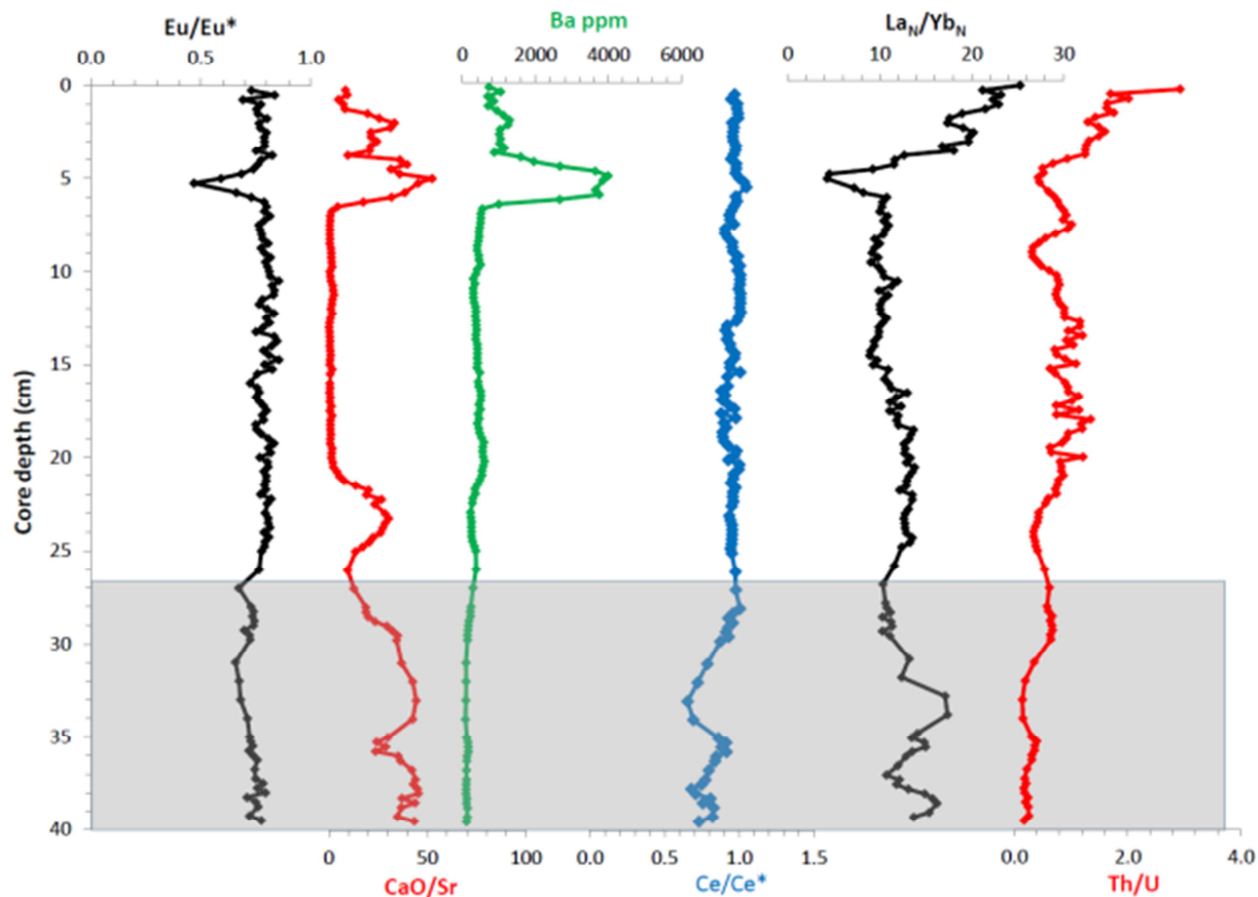


Figure 52: Variations in the Europium anomaly ( $\text{Eu}/\text{Eu}^*$ ),  $\text{CaO}/\text{Sr}$ , Ba, the Ce anomaly ( $\text{Ce}/\text{Ce}^*$ ), the chondrite normalized  $\text{La}/\text{Yb}$  ratio and  $\text{Th}/\text{U}$

From 21.75 cm to 7 cm depth, there is a significant proportion of biogenic silica (>3wt %) with a peak between 14 and 10 cm which reflects a period of diatom blooms. This is in agreement with the total diatom biomass as assessed using microscopy and the external added marker (Fig.53). This event is accompanied by a significant (but variable) influx of Rb-rich Sr-poor crustal-derived detrital clays ( $\text{Rb}/\text{Sr} > 0.1$ ). The low  $\text{La}_N/\text{Yb}_N$  and  $\text{Th}/\text{U}$  suggest that the Virunga volcanic-derived detrital sources might have been limited relative to the other crustal-derived detrital sources from the west and east of the lake. This may suggest that a part of the diatom blooms have been related to surface nutrient inputs.

At 5 cm the detrital, the normal carbonate precipitations and the biogenic silica production are abruptly interrupted by a precipitate of hydrothermal origin. The hydrothermal character of the deposit is evidenced by the sudden appearance of deep negative Eu anomalies ( $0.47 < \text{Eu}/\text{Eu}^* < 0.73$ ) associated with high Barium contents ( $1900 < \text{Ba} < 4000 \text{ ppm}$ , cf Fig. 52) and very high  $\text{CaO}/\text{Sr}$  ratios (Fig. 52). This demonstrates that a plume-like hydrothermal fluid has been suddenly mixed to the normal Kivu Lake water. This event marks a drastic change in the lake sedimentation with the appearance of sedimentary components showing high  $\text{La}_N/\text{Yb}_N$  and  $\text{Th}/\text{U}$  ratios. This change in the detrital source from normal crustal-derived components ( $\text{La}_N/\text{Yb}_N \sim 8$ ;  $\text{Th}/\text{U} \sim 1$ ) to alkaline volcanic-derived Virunga-like sources (nephelinitic;  $\text{La}_N/\text{Yb}_N \sim 15-25$ ;  $\text{Th}/\text{U} > 2.3$ ) clearly suggests strong inputs of Virunga volcanic ashes in the very modern sedimentation.

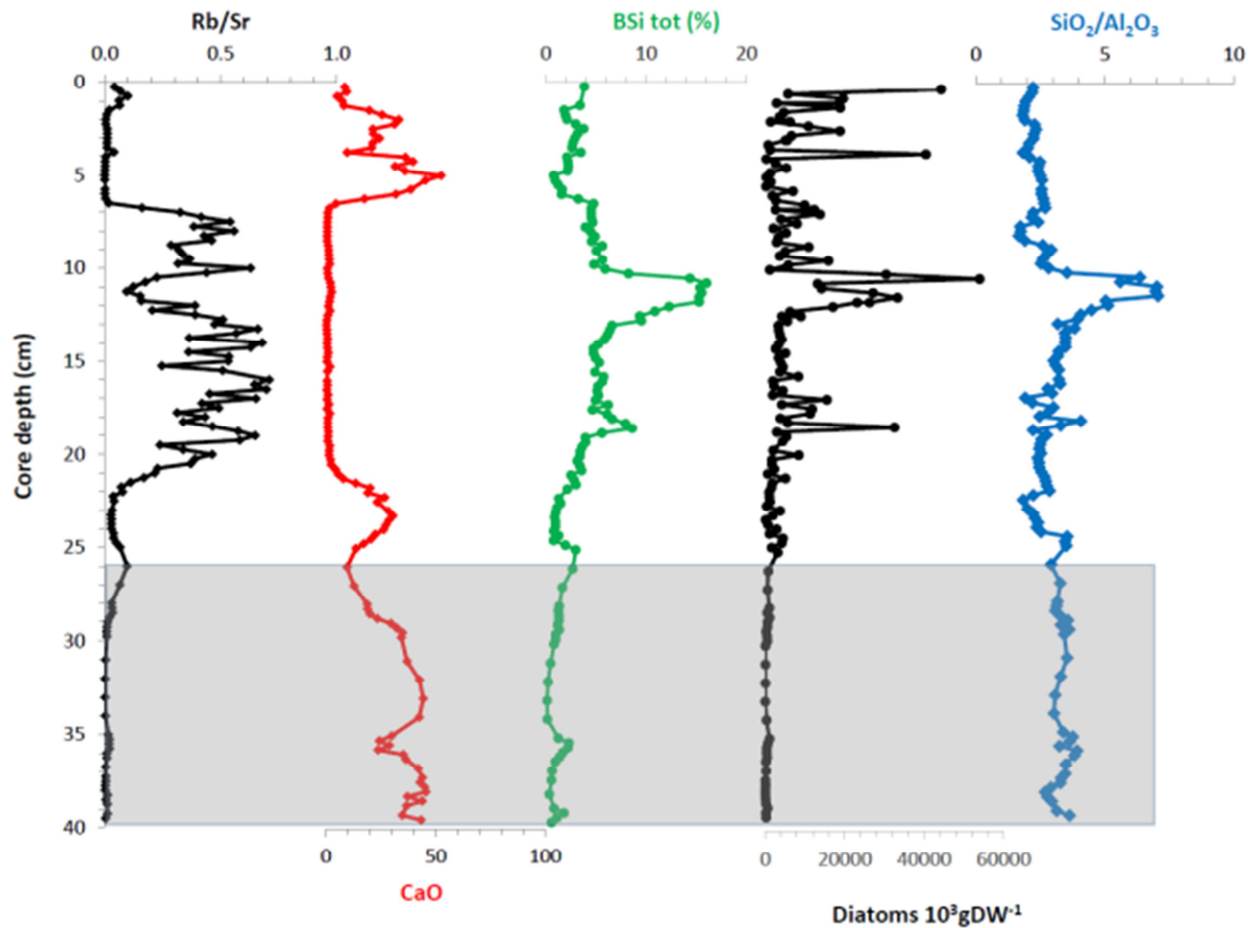


Figure 53: Variations in Rb/Sr, CaO, Biogenic silica, total diatom abundance and  $\text{SiO}_2/\text{Al}_2\text{O}_3$  versus depth. The grey rectangle denotes the mass transport deposit.

#### *Diatoms and fossil pigments*

A total of 52 diatom taxa could be identified from which 33 occurred at least once at a relative abundance exceeding 2%. Between 40 and 27 cm, the diatom composition is dominated by *Encyonema muelleri* and other benthic species. This zone was not used for environmental reconstruction as it is very likely a mass transport deposit.

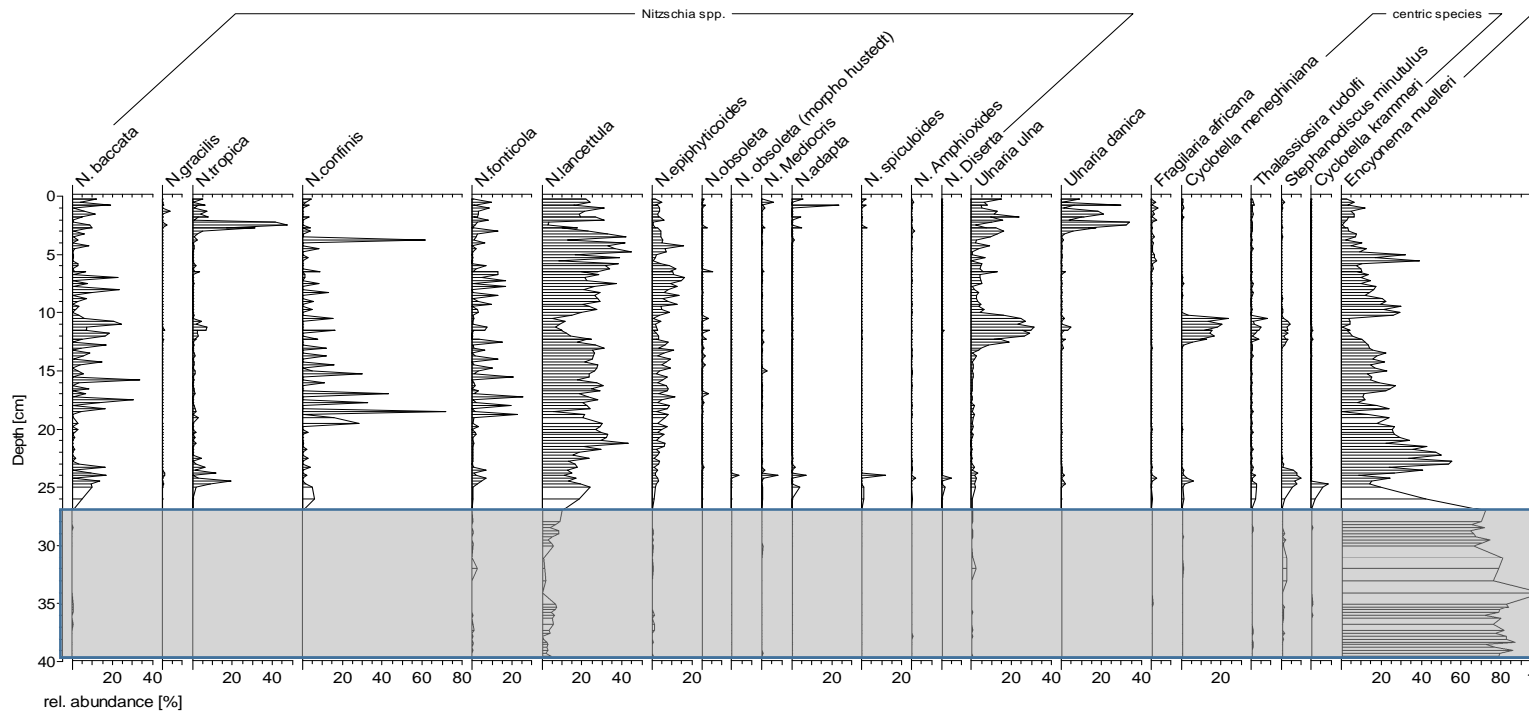


Figure 54: Diatom relative abundance in the Kivu-G4 core. Only diatoms exceeding a relative abundance of 2% in at least 1 sample were included. The mass transport deposit is indicated with the grey bar. The bars correspond with the analysed depth. Among the benthic diatoms, only the most abundant, *Encyonema muelleri*, is presented.

From 27 cm onwards, species belonging to the genus *Nitzschia* are generally the most dominant taxa, while centric diatoms and species belonging to *Ulnaria* are co-dominant at some depths.

When grouped according to the ecological groups discerned by Kilham et al. (1986) based on optimal Si/P ratios (centric species grouped), five significant zones could be identified in the upper 27 cm (Fig. 55) based on a CONISS analysis and a broken stick model. While no pigments specific for diatoms were identified, the zonation of the pigment stratigraphy (Fig. 56) followed more or less that of the diatoms.

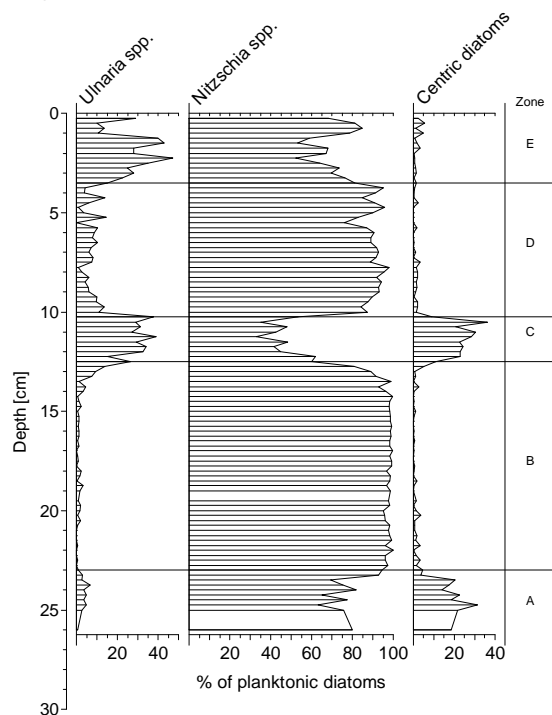


Figure 55: Summary of the diatoms present in the Kivu-G4 core grouped according to the ecological classification by Kilham et al. (1986) based on optimal Si/P ratios (centric species grouped). Only the upper 27 cm sediments are shown.

*Nitzschia spp.* is the most abundant group in zone A (between 26 and 23.5 cm), while centric diatoms are sub-dominant and *Ulnaria spp.* are present, but at relatively low relative abundances. The abundance of centric diatoms decreases towards the end of this zone. Diatom zone A is characterized by relatively high amounts of total chlorophylls and total carotenoids (Fig. 56). The high amounts of zeaxanthin,  $\beta$ -carotene and echinenone suggest high abundance of cyanobacteria. The green algal pigment lutein is also present, but its high correlation with zeaxanthin suggests that an isomerization might have occurred, casting doubt on the specificity of this marker in the sediment. The bottom part of Zone A is furthermore enriched with isorenieratene, pointing to the presence of green sulphur bacteria. In this zone the OC:P is also high, while the total diatom abundance and the biogenic silica content are relatively low. Combined, this suggest that the lake was relatively productive and characterised by a relatively stable lake water column, in which cyanobacteria were abundant. The inorganic carbon content is relatively high in the upper sediments of this zone and remains high in the next zone.

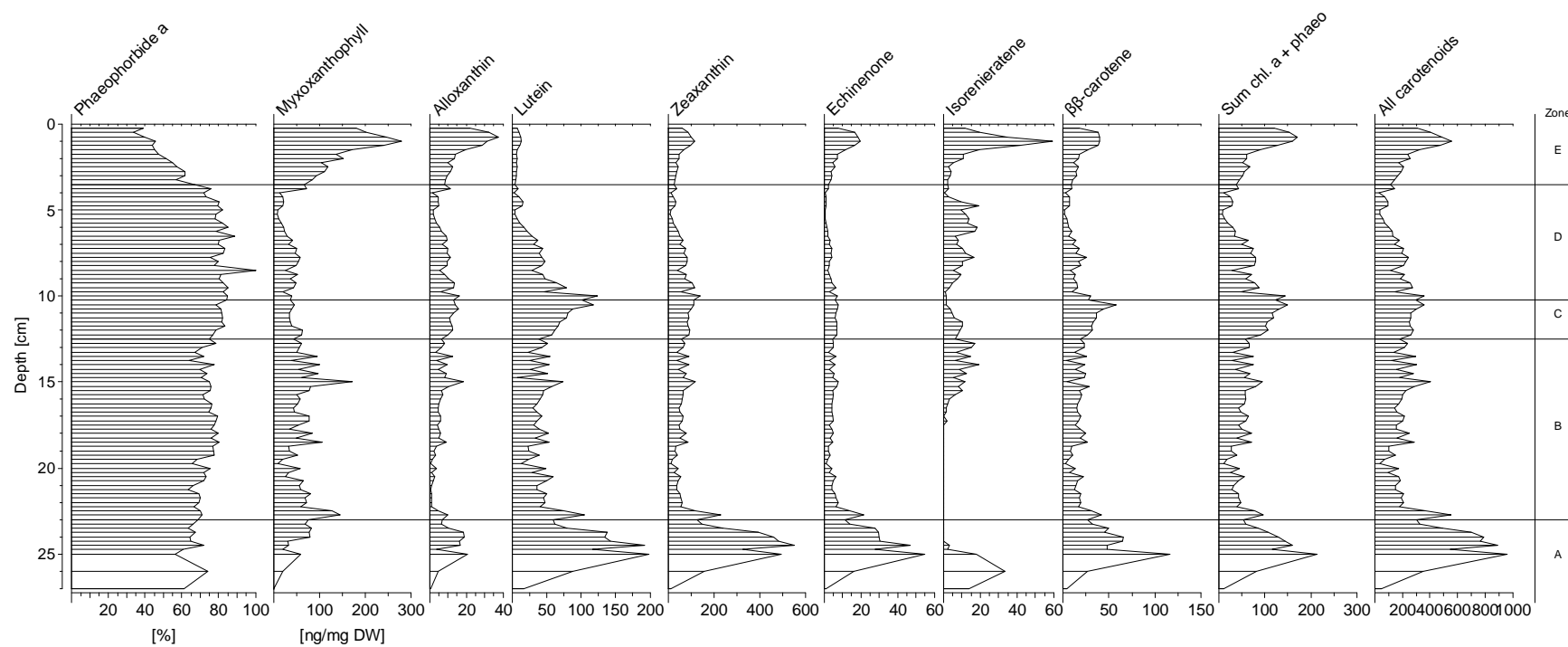


Figure 56: Pigment stratigraphy and the zonation based on the diatoms (Fig. 55). Only the upper 27 cm are shown.

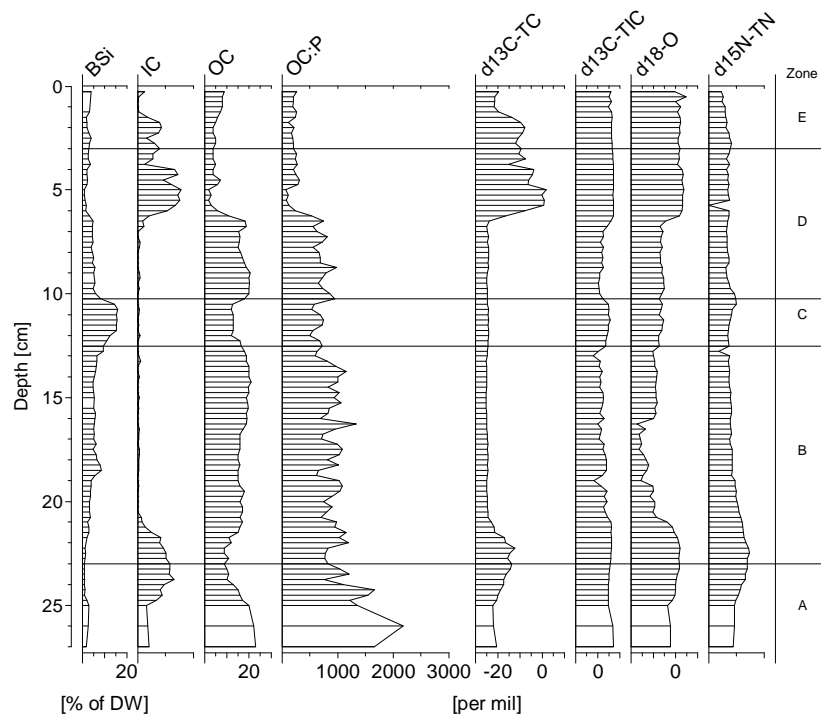


Figure 57: Biogeochemical proxies on the Kivu-G4 core showing biogenic silica (BSi), inorganic carbon concentration (Ic, in % of DW), organic carbon concentration (OC, in % of DW), the organic carbon over phosphorus ratio (OC:P), the stable carbon isotope signature ( $\delta^{13}\text{C}$ ) of the total carbon ( $\delta^{13}\text{C}\text{-TC}$ ) and of the inorganic carbon ( $\delta^{13}\text{C}\text{-TIC}$ ), and the  $\delta^{15}\text{N}$  of the total nitrogen ( $\delta^{15}\text{N}\text{-TN}$ ). The zones are based on the diatom community structure (Fig.55).

In Zone B (23.25-12.5 cm), the diatom communities consist of almost exclusively *Nitzschia* spp. The relatively low amount of total chlorophyll a and carotenoid concentration suggests a moderate primary production. This is however not in agreement with the bulk organic carbon content which is high in this zone (Fig. 57). The myxoxanthophyll concentration is relatively high, suggesting a relatively high abundance of cyanobacteria.

In Zone C (12.25 – 10.25 cm) the three ecological groups (centric taxa, *Ulnaria* spp. and *Nitzschia* spp) are nearly equally present. This zone corresponds with a high biogenic silica content and a total diatom abundance (Fig. 53), suggesting a high diatom production. Also the total chlorophyll a and carotenoid concentration are relatively high as well as the lutein content and remain high until the beginning of diatom zone D. Combined this suggests that the primary production in this zone was dominated by diatoms as well as green algae.

In zone D (10 – 4.75 cm), *Nitzschia* spp. are again dominant, while *Ulnaria* spp. are present at a relative abundance that are intermediate between zone B and C. The total chlorophyll and carotenoid concentration decrease in this zone, which is in agreement with a decrease in the bulk organic carbon content (Fig. 57). The inorganic carbon content increases from ca. 6 cm onwards and remains relatively high in the beginning of the next zone.

Zone E (4.5 – 0 cm) is characterized by the dominance of *Nitzschia* spp. and a relatively high abundance of *Ulnaria* spp. Myxoxanthophyll and alloxanthin are relatively high suggesting a contribution of cyanobacteria and cryptophytes to the planktonic primary production. The amount of phaeophorbide decreases towards the top of this zone, which suggests ongoing

degradation of chlorophyll a with depth. The high abundance of isorenieratene suggests a relatively high biomass of green sulphur bacteria, hence indicating stratification conditions which generated anoxia in part of the euphotic layer.

A detailed comparison between our data and those in Pasche et al. (2009) was complicated due to the large uncertainties associated with the age-depth models, both in our study as well as those in previous ones. Patterns in inorganic carbon deposition in the G4 core were more or less similar to those previously obtained from a sediment core from near Gisenyi, with increased concentrations being situated between 25 and 21 cm and between 7 and 3.5 cm (Pasche et al. 2009). The most recent increase in carbonate deposition as well as changes in diatom community structure were previously attributed to (i) the introduction of the non-native planktivorous fish, (ii) eutrophication, and/or (iii) hydrological changes and increased lake water mixing (Pasche et al. 2009). However, our results suggest that the history of the lake might be more complex, and that changes in carbonate deposition and the autotrophic community structure are not always in-phase. More in particular, we observed high diatom and biogenic silica concentrations, as well as significant differences in diatom community structure compared with the rest of the core between ca. 13 and 10 cm; a period when the carbonate content is relatively low and constant. By contrast, when the carbonate deposition is high between 5 cm until c. 3.5 cm, no significant changes in the diatom community structure are evident. It follows that the carbonate deposition in the lake – at least the most recent one – is related to hydrothermal events rather than changes in the ecology of the lake. This is also evidenced by the sudden appearance of deep negative Eu anomalies ( $0.47 < \text{Eu}/\text{Eu}^* < 0.73$ ) associated with high Barium contents ( $1900 < \text{Ba} < 4000 \text{ ppm}$ , cf Fig. 52) and very high CaO/Sr ratios (Fig. 52).

## **2.3. LABORATORY STUDIES (2011-2014)**

### **2.3.1 Diatom cultures**

#### *Material and methods*

During 3 field campaigns, 20 L of lake water from 3 different sites in Lake Kivu (Gisenyi, Ishungu and Kabuno) and several smaller lakes in the same region were sieved over a plankton net (mesh size = 10  $\mu\text{m}$ ). The samples were stored in the dark at 5°C and sent to Belgium. A total of 22 monoclonal strains were established from these samples and cultured in standardized Guillard's WC culture medium (Guillard, 1975) at 23°C. These strains were morphologically (light microscopy) and molecularly characterized. Strains from samples from two additional campaigns were isolated and grown in lake water, because some taxa (long *Nitzschia* spp.) appeared to be extremely difficult to culture. DNA of the isolated strains was extracted following Muyzer et al. (1993). Sequencing was based on the species-level markers LSU rDNA and rbcL and alignment with sequences published on GenBank allowed the reconstruction of a rooted phylogenetic tree.

### *Results*

A ranking of different diatom species along a Si:P gradient was presented by Kilham et al. (1986). *Ulnaria ulna* is postulated to perform best at high Si:P molar ratios, while *Nitzschia bacata* performs best at intermediate and *Stephanodiscus* spp. best at low Si:P ratios (Kilham et al. 1986). Although this ranking is still to be verified in laboratory experiments, it is widely used among paleolimnologists. We aim at the validation of this ranking to increase the value of these species as paleolimnological proxies. A total of 22 diatom strains were isolated and identified as species belonging to *Ulnaria* spp. Molecular markers (rbcL and LSU) and light microscopy identified the strains to the same genus. The major problem encountered was the lack of living strains from *Nitzschia bacata* and *Stephanodiscus* spp., the two other taxa commonly used as Si:P indicator. Although *Nitzschia bacata* is reported to be very abundant in Lake Kivu (Sarmiento et al. 2007), no living specimens were found in the field samples. *Stephanodiscus* spp. have not been reported in Lake Kivu anymore. Due to the difficulties for growing African diatoms, we were unable to perform the laboratory experiments.

## 2.4. DATA ANALYSIS AND MODELING

### 2.4.1 Statistical data analysis

Phytoplankton composition and biomass for the period 2002-2014 in the Ishungu basin are presented in Darchambeau et al. (2014) (Fig. 58). The community was dominated by cyanobacteria, diatoms and cryptophytes. A seasonal peak, with a biomass higher than 100 mg Chla m<sup>-2</sup>, was observed at the end of the dry season (August-September) in 2003, 2004, 2008 and 2012. A lower dry season peak was observed in 2006, 2007, 2009, 2011 and 2013. By contrast, cyanobacteria developed best during the rainy season, from October to May. Cryptophytes were present throughout the year. The inter-annual variability of phytoplankton biomass was relatively high, with the lowest mean annual biomass observed in 2005 with 53 mg Chla m<sup>-2</sup> and the highest in 2008 with 119 mg Chla m<sup>-2</sup>. The inter-annual coefficient of variation from 2002 to 2014 was 24 %. The dry season (from June to August) was generally characterized by a deeper mixed layer, although this pattern was not consistent over the years (Fig. 58C). The depth of the euphotic zone, Z<sub>eu</sub>, ranged between 8.3 – 28.5 m (median, 17.6 m) (Fig. 58D). The highest transparencies were observed at the end of the rainy season, in June, and sometimes in July and August, depending on the year (Fig. 58E). The daily primary production was calculated based upon *in situ* observed and modeled photosynthetic parameters from 2002 to 2008 (Fig. 58F). The mean observed daily primary production was 0.620 g C m<sup>-2</sup> d<sup>-1</sup> (range, 0.142-1.924). Annual primary productions were calculated from modeled values. The mean annual primary production from 2002 to 2008 was 211 g C m<sup>-2</sup> y<sup>-1</sup> (Darchambeau et al. 2013a). The inter-annual variation was important (coefficient of variation from 2002 to 2008, 24 %), with a minimum value of 138 g C m<sup>-2</sup> y<sup>-1</sup> in 2005 and a maximum value of 258 g C m<sup>-2</sup> y<sup>-1</sup> in 2003.

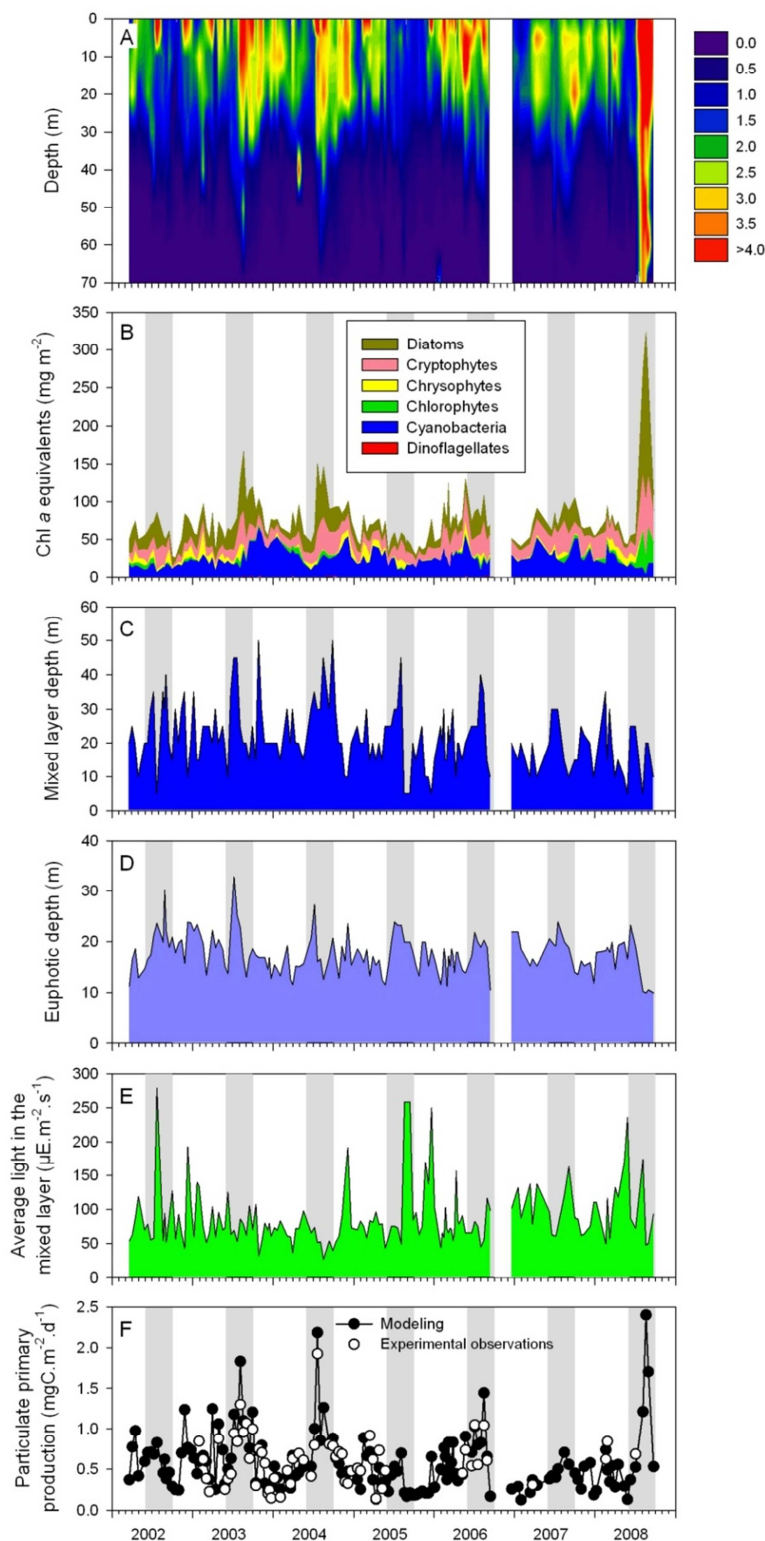


Figure 58: (A) Vertical distribution of phytoplankton biomass (Chlorophyll a,  $\text{mg m}^{-3}$ ), (B) areal chlorophyll a concentrations and biomass composition from marker pigment analysis in Lake Kivu, (C) depth of the mixed layer, (D) depth of the euphotic layer, (E) average light in the mixed layer, (F) daily depth-integrated primary production with photosynthetic parameters estimated from in situ  $^{14}\text{C}$  incubations (white circles) or with photosynthetic parameters calculated from equations 5 and 6 (black circles with lines), during the 2003-2008 period, in Lake Kivu, Ishungu station (southern basin) (Darchambeau et al. 2014).

It was also found that the importance of the annual phytoplankton biomass peak was negatively correlated to the stability of the water column during the season preceding the bloom (Darchambeau et al. 2013b). This suggests that the importance of the annual bloom is not driven by weather conditions during the mixing period but by the stratifying conditions prevailing several months earlier. Statistically highly significant correlations between intra- and inter-annual variations of water column stability, phytoplankton biomass and tropical ocean climate indices, including the Western Tropical Indian Ocean (WTIO) sea surface temperature (SST) anomaly index, the Dipole Mode Index (DMI), the Southern Ocean Index (SOI) and the El Niño-Southern Oscillation (ENSO), were also observed (Fig. 59, Darchambeau et al. 2013b).

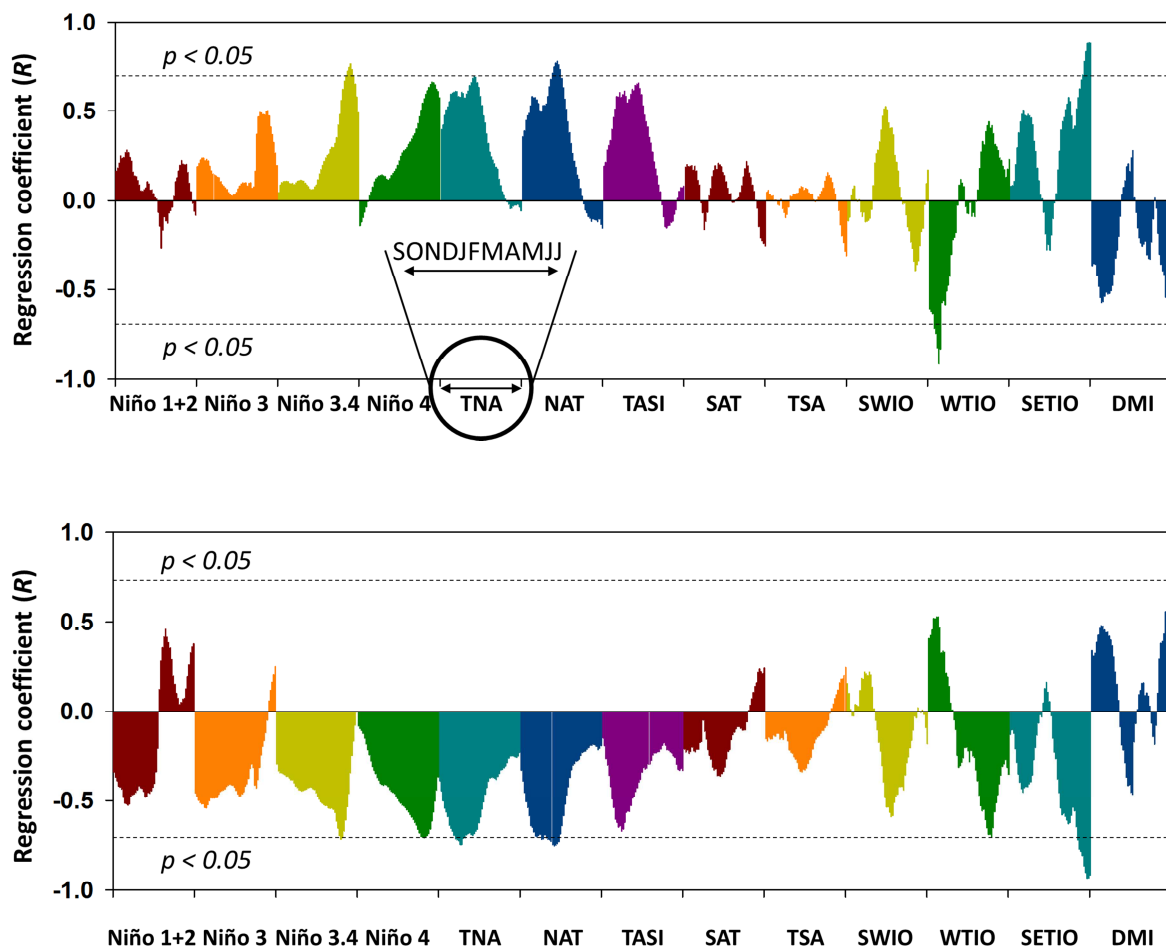


Figure 59: (Above) Regression coefficient ( $R$ ) of ordinary least squares Pearson linear regressions between (Above) the dry season (August) Schmidt's stability index of the 0-60 m water column or (Below) annual dry season (August) chlorophyll a peak and 9-week moving averages of several ocean climate indices. Time lags from 0 to 12 months before the dry season peak were evaluated. From Darchambeau et al. 2013b.

## 2.4.2 Modelling of present conditions

Here we present several modeling studies on climate in the African Great lakes region, with a focus on Lake Kivu hydrodynamics and on the impact of the lakes on the regional climate. Most of this research has been published (see 5). A related publication, not presented here, concerns the present wind regime over Lake Tanganyika (Docquier et al., in review.).

### 2.4.2.1 Climate simulations for the period 1999-2008

#### Standalone FLake simulations

Owing to the strong contrast in albedo, roughness and heat capacity between land and water, lakes significantly influence the surface-atmosphere exchange of moisture, heat and momentum (Mironov et al., 2010). Some effects of this modified exchange are (i) the dampening of the diurnal temperature cycle and lagged temperature response over lakes compared to adjacent land, (ii) enhanced winds due to the lower surface roughness, (iii) higher moisture input into the atmosphere as lakes evaporate at the potential evaporation rate, and (iv) the formation of local winds, such as the lake/land breezes (Lauwaet et al., 2011).

Given its good compromise between physical realism and computational efficiency, FLake has become a landmark in representing lakes within atmospheric models (Thiery et al., 2014a). However, this model has never been thoroughly evaluated for tropical conditions. Therefore the ability of the one-dimensional lake model FLake to represent the mixolimnion temperatures for tropical conditions was tested for three locations in East Africa: Lake Kivu, Lake Tanganyika's northern and southern basins. Meteorological observations from surrounding automatic weather stations were corrected and used to drive FLake, whereas a comprehensive set of water temperature profiles served to evaluate the model at each site.

At each location, three simulations were conducted. First, FLake was integrated with observed meteorological values from an automatic weather station on the shore of Lake Kivu (AWS 1) and using the average observed value for water transparency  $k$  (hereafter referred to as "raw"). However, analysis of wind observations from an automatic weather station offshore Gisenyi (AWS Kivu) which was installed in September 2012 in the framework of the EAGLES project (Figure ) showed that wind velocities are significantly higher over the lake compared to land data. A second AWS-driven simulation (hereafter referred to as "control") was therefore conducted wherein wind velocities were allowed to vary within specific upper (from AWS Kivu) and lower (from AWS 1) bounds until the observed mixing regime is reproduced. Besides wind velocity,  $k$  was also allowed to vary within bounds  $\bar{k} - \sigma_k$  and  $\bar{k} + \sigma_k$ , but this correction had only little effect on the model skill. Finally, FLake was integrated using the global reanalysis product ERA-Interim data from the nearest grid cell as forcing (hereafter referred to as "ERA-Interim").

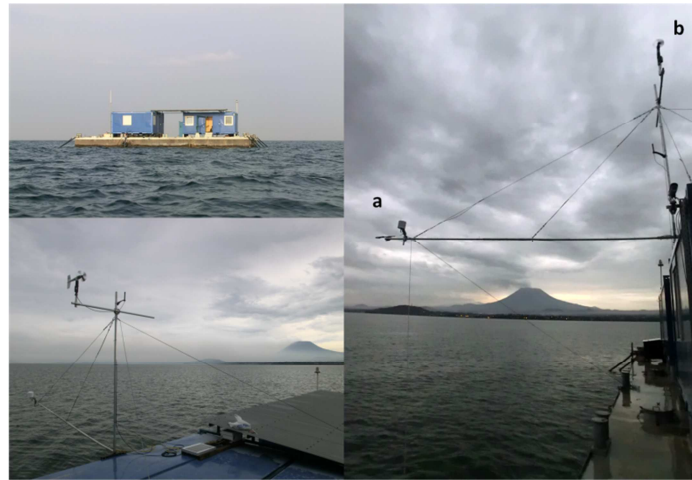


Figure 60: The EAGLES Automatic Weather Station on Lake Kivu after its installation, 8 October 2012 (© Wim Thiery).

Comparing modelled and observed water temperatures of Lake Kivu near the surface (5 m) shows that the timing of the near-surface seasonal cycle is well represented by the raw, control and ERA-Interim simulations (Figure a). However, whereas it shows a small negative bias compared to the observations, only the control integration grasps the correct magnitude of the seasonal temperature range. The overestimation of the temperature seasonality in the raw and ERA-Interim simulations is reflected by 5 m Brier Skill Score (BSS) of -0.36 and -2.13, respectively, compared to only -0.26 for the control case. At a depth of 60 m, both the raw and ERA-Interim integration predict a year-round constant temperature of 3.98 °C, the temperature of maximum density, resulting in a cold bias of about 19 °C. At the bottom, the lake's thermal structure is reproduced only by the control simulation (BSS = -0.17; 61b).

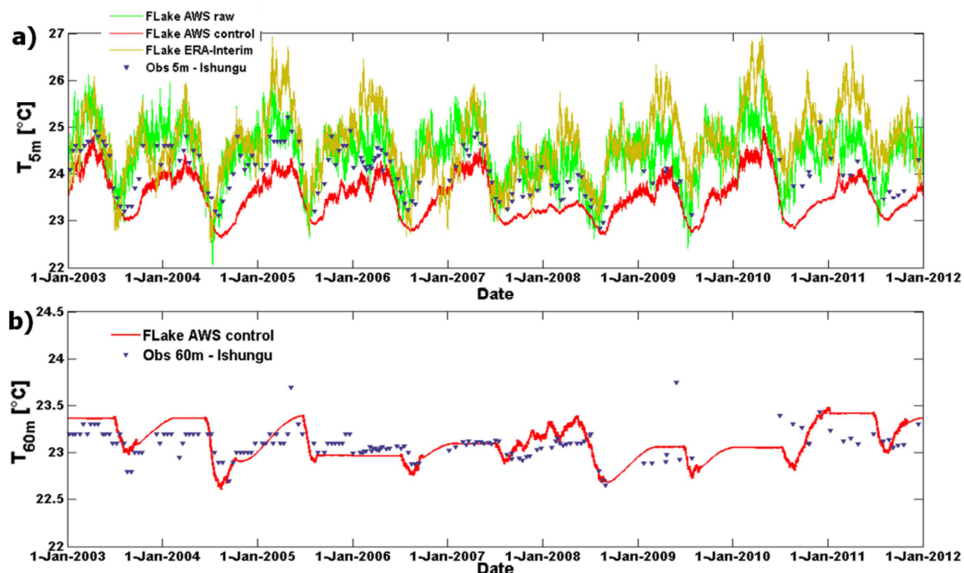


Figure 61: Modelled and observed temperature evolution at Ishungu (Lake Kivu) at (a) 5 m, and (b) 60 m depth. FLake temperatures at 60 m predicted by the raw and ERA-Interim integration are omitted as they are constant at 3.98 °C.

Once a year, during the dry season (from June to August), the mixed layer depth at Ishungu extends down to approximately 60 m. At this depth, the upwelling of deep, saline waters ( $0.5 \text{ m yr}^{-1}$ ; Schmid and Wüest, 2012) equilibrates with mixing forces. The result is a strong salinity gradient from 60 m downwards. During the remainder of the year, stratified conditions dominate, with the mixed layer depth varying between 10 and 30 m (Figure a). The raw simulation does not reproduce this mixing seasonality, but instead predicts permanently stratified conditions and a complete cooling down to  $3.98 \text{ }^\circ\text{C}$  from 30 m downwards. On the other hand, with wind velocity corrected for the land effect and  $k$  tuned to  $0.32 \text{ m}^{-1}$ , the control simulation closely reproduces the mixing regime at Ishungu (Figure 62b). In this case, also the lower stability, indicated by the observations near the end of 2006 and during 2008 and 2009, is captured by this control simulation, although it is somewhat overestimated in 2008 with a predicted year-round mixing down to  $\sim 55 \text{ m}$ . Note however that, due to the lower stability during these years, the effect on the near-surface water temperatures is limited. Furthermore, also the late onset of the stratification in early 2007 is represented by the model.

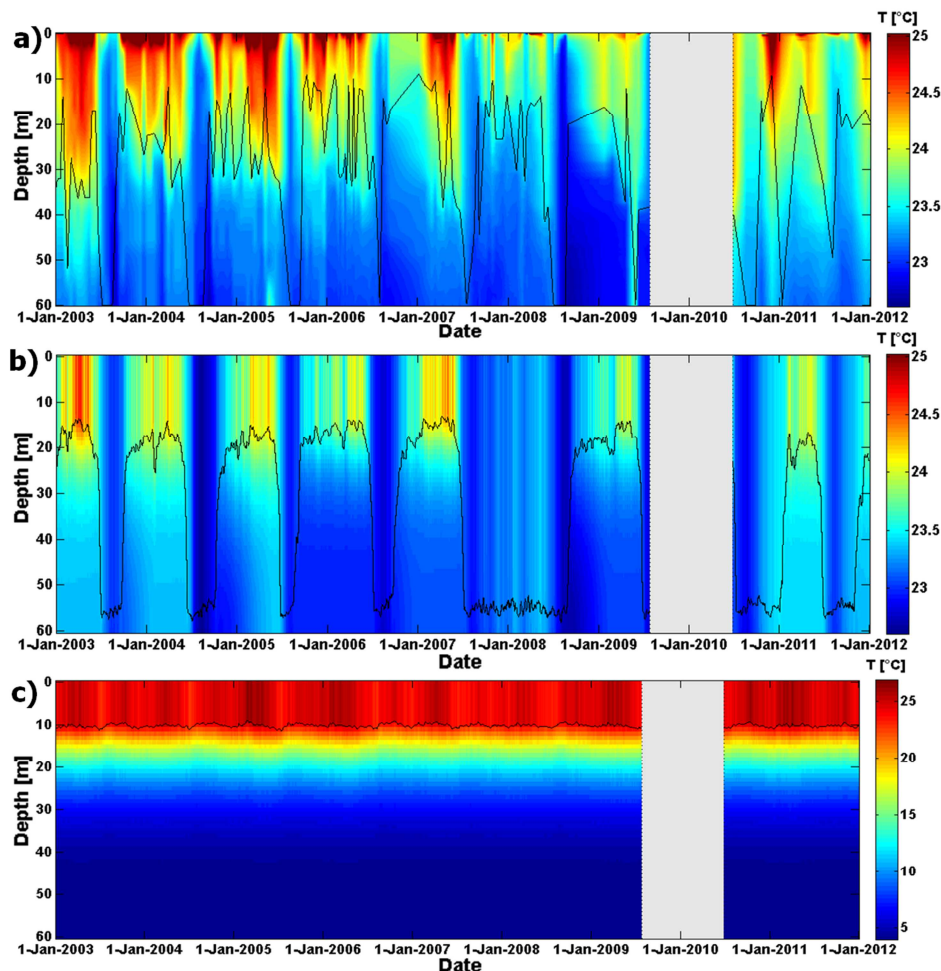


Figure 62: Lake water temperatures ( $^\circ\text{C}$ ) at Ishungu (Lake Kivu) (a) from observations, (b) as predicted by the AWS-driven FLake-control, and (c) as predicted by FLake-ERA-Interim. The black line depicts the weekly mean mixed layer depth. Note the different colour scaling in (c). The lake water temperatures for the raw simulation are not shown as they strongly resemble the predictions of the ERA-Interim simulation.

Finally, feeding FLake with ERA-Interim derived near-surface meteorology does not succeed in reproducing the mixing regime. Instead, this simulation predicts permanently stratified conditions and a complete cooling down to 3.98 °C, the temperature of maximum density, from 30 m downwards (Figure c). The low and constant mixed layer depth generates near-surface temperature fluctuations found too strong on seasonal time scales (Figure a). Similar to the raw integration, the inability of the ERA-Interim integration to produce deep mixing is primarily due to the predicted values for the wind velocity, which are 33% lower compared to the control run average wind velocity and 49% lower compared to wind speeds from AWS Kivu (measured over the lake surface during 59 days in October-November 2012). Underlying reasons for this deviation are (i) the fact that the lake surface covers only a fraction of the selected ERA-Interim grid box, and (ii) the higher uncertainty of this product in central Africa owing to the sparse observational data coverage in this region (Dee et al., 2011).

The strong response of the modelled water temperatures to forcing fields calls for a systematic study of the sensitivity of the model to different sources of error. Hereafter, results of FLake's sensitivity to variations in external parameters and meteorological forcing data are presented.

At 5 m depth, the different sensitivity experiments for variations in external parameters produce similar values for centered root mean square error ( $RMSE_c$ ), correlation coefficient ( $r$ ), and BSS (Figure a). Only the seasonal temperature variability is closer to reality in the control simulation. At 30 m, already some changes to this pattern can be noticed (Figure b), but only at 60 m the differences fully emerge, with a clear reduction in predictive skill for the simulations with  $k$  decreased (increased) to the lowest (highest) observed values at Ishungu (Figure c). Higher water transparency leads to deeper mixing, as solar radiation penetrates down to the interface between mixed layer and thermocline and therewith enhances the mixed layer depth.

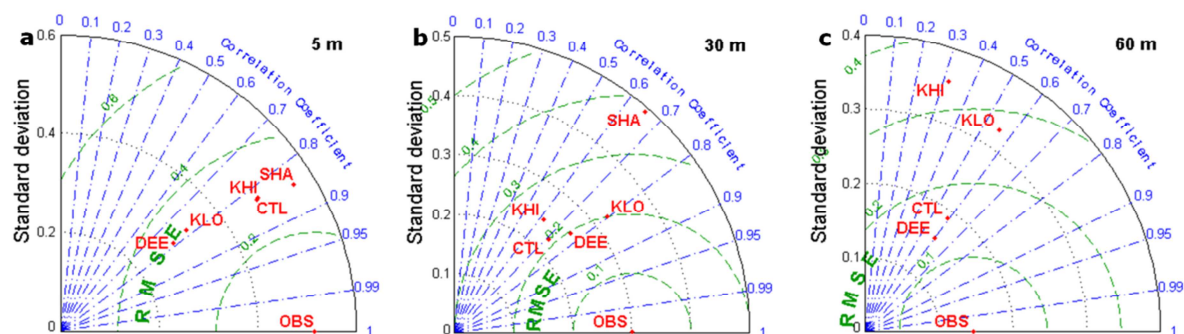


Figure 63: Taylor diagram indicating model performance for water temperature at (a) 5 m, (b) 30 m and (c) 60 m depths for different external parameter values at Ishungu (January 2003 – December 2011). Standard deviation  $\sigma$  (°C; radial distance), centred Root Mean Square Error  $RMSE_c$  (°C; distance apart) and Pearson correlation coefficient  $r$  (azimuthal position of the simulation field) were calculated from the observed T-profile interpolated to a regular grid (1 m increment) and corresponding midday FLake profile. OBS: observations, CTL: control, SHA (DEE): model lake depth set to and 30 m (120 m), KHI (KLO): downward light attenuation coefficient  $k$  set to the highest (lowest) observed value at Ishungu. Note that model performance indicators at 60 m cannot be calculated for the SHA integration.

Sensitivity experiments for perturbations in meteorological reveal a marked sensitivity of FLake results to variations in wind speed (Figure a-b). Generally, when wind velocities increase (decrease), mechanical mixing reaches deeper (less deep) into the lake, causing a cooling (warming) of the mixed layer for the same energy budget. For Lake Kivu, at some point the increased wind velocity however provokes a regime switch from seasonally mixed conditions to (almost) permanently mixed conditions. This switch, illustrated by the sharp decrease in vertically integrated BSS in Figure a-b along the y-axis, is already reached before the wind velocity is enhanced or decreased by 0.4 standard deviation. When combined in pairs, errors may compensate each other and still generate adequate model predictions.

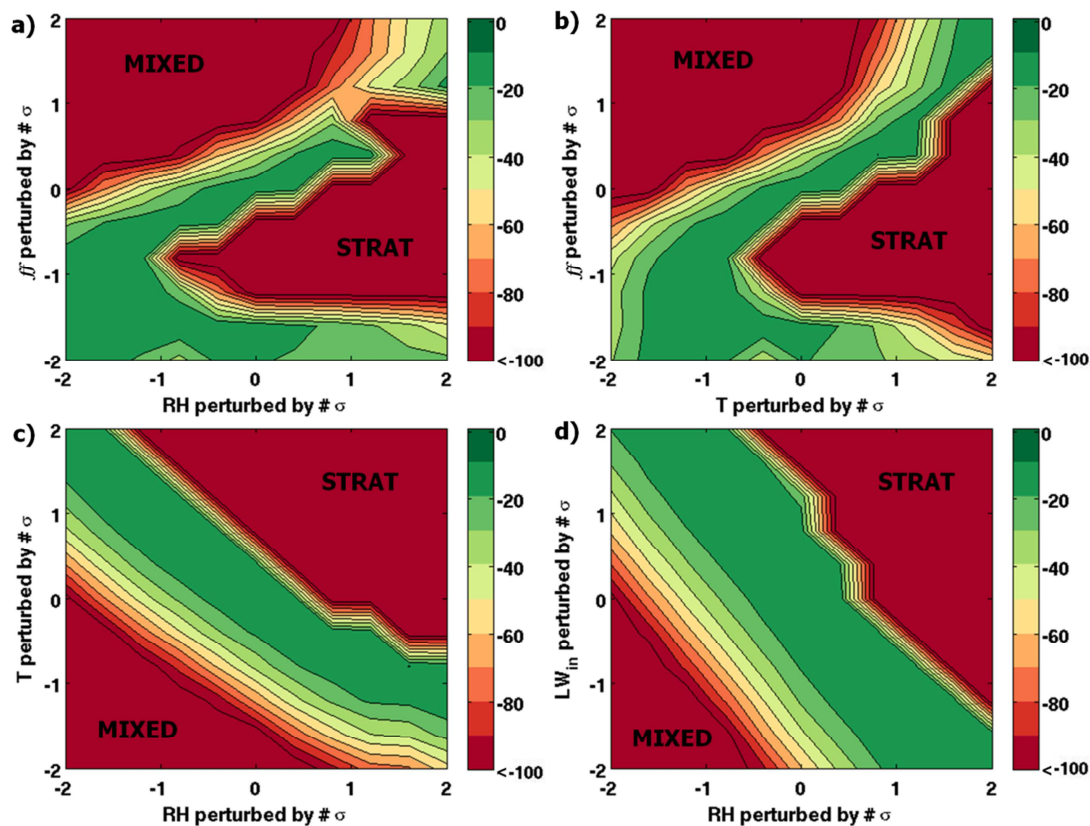


Figure 64: Vertically averaged Brier Skill Scores (BSS) of water temperature profiles (0 – 60 m; 1 m vertical increment) at Ishungu from 4 sensitivity experiments, wherein pairs of forcing variables recorded at AWS 1 were perturbed by proportions of their respective standard deviations  $\sigma$ . Perturbed forcing variables are wind velocity ( $ff$ ), Relative humidity (RH), air temperature (T) and incoming long-wave radiation ( $LW_{in}$ ). Generally, values for BSS range from +1 (perfect prediction) to  $-\infty$  (no relation between observation and prediction). Permanently stratified (STRAT) and fully mixed conditions down to 60 m (MIXED) are indicated.

This has important implications for the applicability of FLake to the study of tropical lake-climate interactions. When FLake is interactively coupled to an atmospheric model, it may very well be that e.g. the near-surface wind velocities serving as input to FLake does not fall within the narrow range for which it predicts a correct mixing regime. However, the only FLake variable which directly influences the atmospheric boundary layer is mixed layer temperature, the variable from which the exchange of water and energy between the lake

and the atmosphere is computed. In this study, predictions for this variable were found to be robust, even when modelled bottom temperature values are biased. We may therefore suppose that for tropical conditions, a coupled model system will not be much affected by the strong sensitivity of FLake's deepwater temperatures to wind speed values, for instance. Finally, FLake was used to attribute the seasonal mixing cycle at Lake Kivu to variations in the near-surface meteorological conditions. It was found that the annual mixing down to 60 m during the main dry season is primarily due to enhanced lake evaporation and secondarily due to the decreased incoming long wave radiation, both causing a significant heat loss from the lake surface and associated mixolimnion cooling.

### **LakeMIP-Kivu**

The Lake Model Intercomparison Project (LakeMIP) is an initiative wherein different one-dimensional lake-models are compared through their application to one location (Thiery et al., 2014b). In the past, this initiative has focused on numerous lakes such as Lake Sparkling, Valkea-Kotinen and Kossenblatter, each time resulting in an international peer-reviewed publication (Stepanenko et al., 2010; 2013; 2014). The unique limnology of meromictic Lake Kivu, with the importance of salinity and subsurface springs in a tropical high-altitude climate, presents a worthy challenge to the seven models involved in LakeMIP. Meteorological observations from two automatic weather stations are used to drive each of these seven models (Hostetler, CLM4-LISSS, LAKEoneD, LAKE, SimStrat, FLake and MINLAKE2012), whereas a unique dataset, containing over 150 temperature profiles recorded since 2002, is used to assess the model performance. Simulations are performed over the freshwater layer only (60 m) and over the average lake depth (240 m), since salinity increases with depth below 60 m in Lake Kivu and some lake models do not account for the influence of salinity upon lake stratification.

All models are able to reproduce the mixing seasonality in Lake Kivu (Figure ) as well as the magnitude and seasonal cycle of the lake enthalpy change (Figure 67). However, Hostetler, CLM4-LISSS and SimStrat clearly display lower water temperatures, suggesting an underestimation of heat entering the lake (Figure 5b, d). Since this affects the whole water column, it cannot be primarily due to differences in the mixing processes, but is likely due to a different surface energy exchange. Furthermore, in the top 5 m of the water column, LAKE predicts a slightly unstable stratification (Figure 5e). This can be ascribed to a numerical precision artefact of the fully implicit time stepping scheme employed in this model. For each iteration, the numerical procedure solves the temperature conductance equation including radiative heating, and using a Dirichlet top boundary condition. The temperature profile will therefore contain its temperature maximum close to the surface - instead of at the surface - with the abundance of this maximum depending on the eddy conductance at the top layers calculated by the  $k-\epsilon$  scheme. Hence, in LAKE the top boundary conditions of the  $k-\epsilon$  parameterisation might be inappropriate to successfully simulate the mixing at the top of water column.

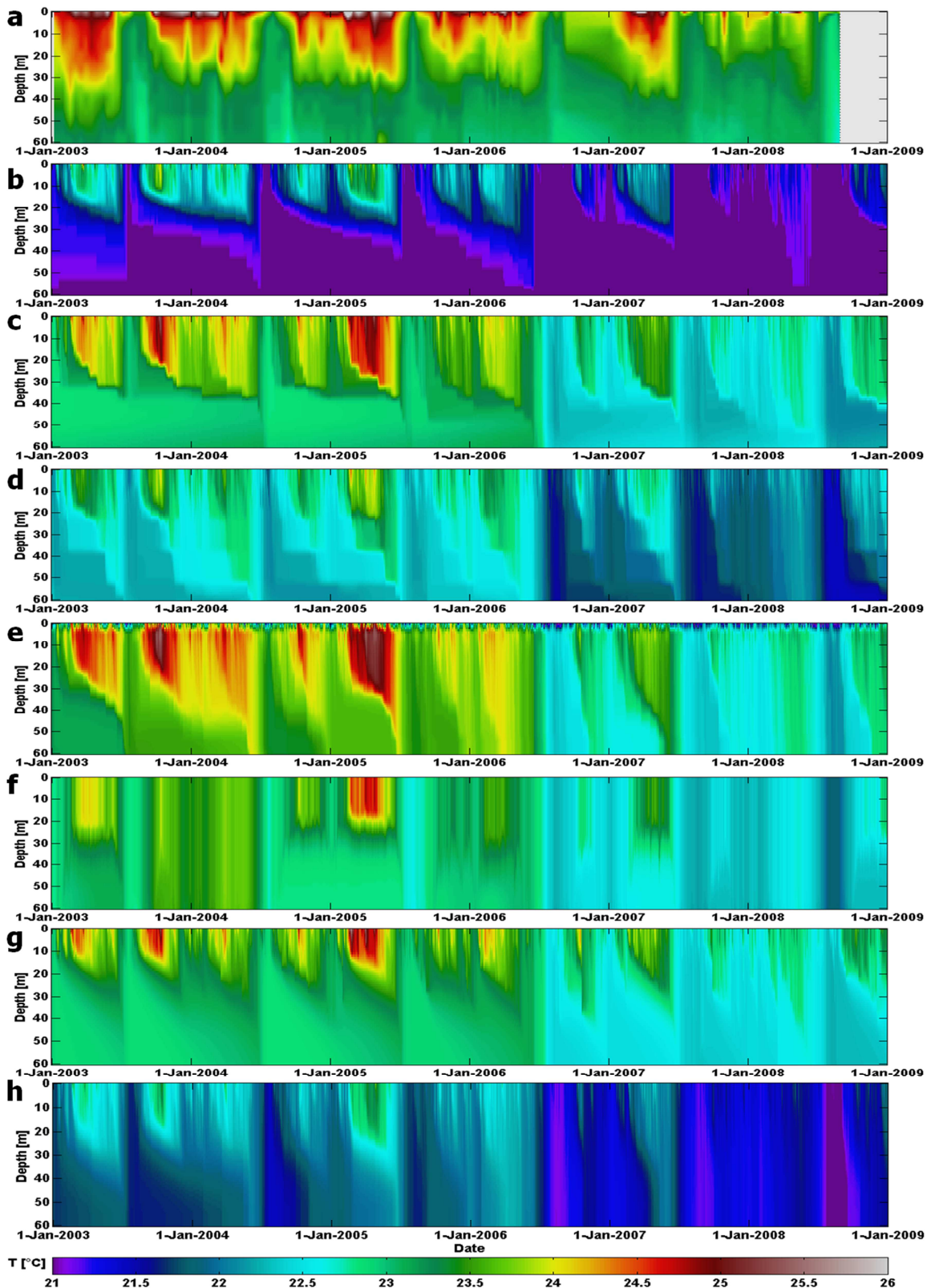


Figure 65: Lake water temperatures (°C) at Ishungu (Lake Kivu), 2003 - 2008: (a) from observations, and as predicted by the models: (b) Hostetler, (c) LAKEoneD, (d) SimStrat, (e), LAKE, (f) FLake, (g) MINLAKE2012, (h) CLM4-LISSS.

Vertical profiles of the BSS (1 m vertical increment, BSS below -20 were set to -20) indicate that the skill decreases with depth in all models (Figure 66a). Since the BSS accounts for the effect of a systematic bias, BSS for Hostetler, CLM4-LISS and SimStrat quickly reach low values. But although Hostetler and SimStrat both depict a cold bias, they most successfully reproduce seasonal and interannual lake water temperature variability. On the other hand, towards deeper layers both LAKE and, to a lesser extent, FLake depict reducing skill compared to other models (Figure 5). For LAKE, the overestimation of the observed variance can probably be explained by a higher sensitivity of LAKE to wind velocity relative to other models, whereas for FLake, this might be ascribed to the fully mixed conditions predicted during the 2003-2004 wet season: in both cases this increases the deep water temperature variability during the integration period (Figure 5).

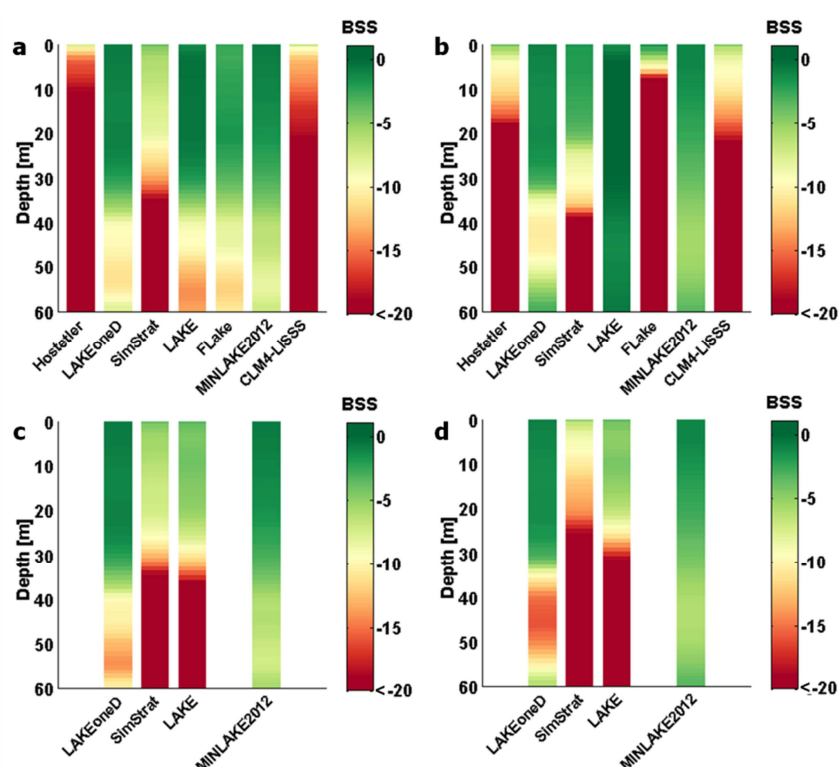


Figure 66: Brier Skill Score (BSS) vertical profiles at Ishungu (Lake Kivu), calculated per 1 m vertical increment over the respective integration period, for (a) the WS Kamembe 60 m, (b) the WS Bukavu 60 m, (c) the WS Kamembe 240 m and (d) the WS Bukavu 240 m integrations. Note that Hostetler, FLake and CLM4-LISS were not applied in the 240 m depth experiment.

Differences between the models can be ascribed to variations in the treatment of the radiative forcing and the computation of the turbulent heat fluxes. Fluctuations in wind velocity and solar radiation explain inter-annual variability of observed water column temperatures. The good agreement between the deep simulations and the observed meromictic stratification also shows that a subset of models is able to account for the salinity- and geothermal-induced effects upon deep water stratification. At the same time, this study also revealed a number of strengths and weaknesses for the different groups of models.

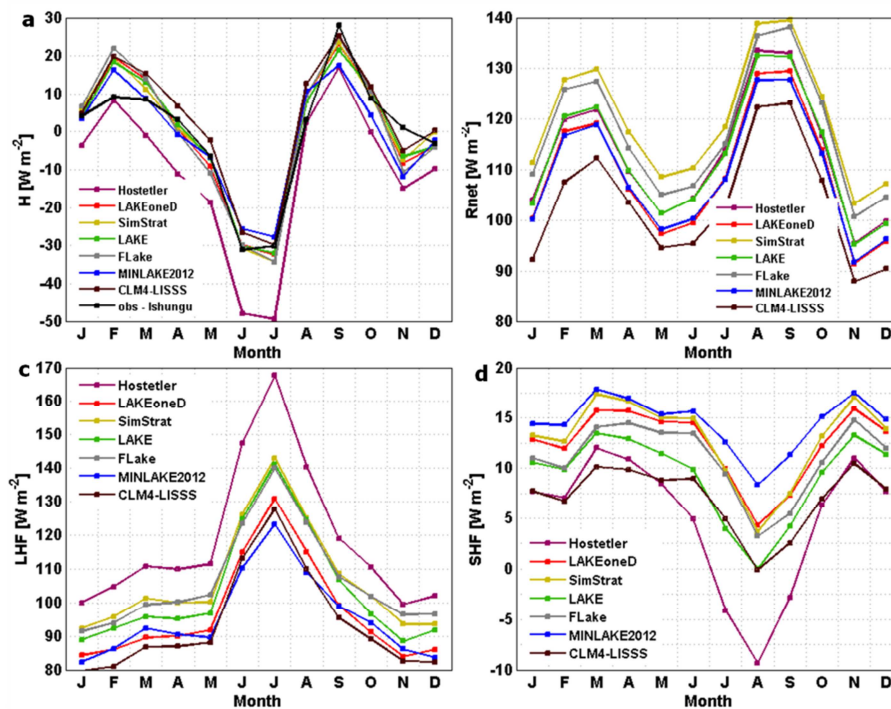


Figure 67: Monthly average lake energy balance components ( $\text{W m}^{-2}$ ) at Ishungu (Lake Kivu), 2003 - 2008, calculated by model's surface flux routines. Components are (a) lake enthalpy change  $H$ , (b) net radiation  $R_{\text{net}}$ , (c) latent heat flux  $LHF$ , and (d) sensible heat flux  $SHF$ .

First, while FLake is computationally the most efficient and depicts good predictive skill in the control simulation compared to other models, water temperatures towards the bottom of Lake Kivu's mixolimnion are found sensitive to modifications in the forcing fields and model configuration. Further research is needed to address the ability of FLake to represent weakly stratified lakes. However, since near-surface temperatures, in contrast to near-bottom temperatures, are more robust, the model remains a good candidate in applications where a quick and reliable computation of lake surface temperatures is important.

Second, given their limited computational expense, the Hostetler-based models (Hostetler and CLM4-LISSS) are also attractive candidates to represent lake processes within atmospheric models. Although both models predict colder water temperatures compared to observations, they correctly reproduce the observed variability, and a model calibration can potentially correct for the small systematic bias.

Third, the more comprehensive lake models, i.e. MINLAKE2012 and the  $k$ - $\epsilon$  models SimStrat, LAKE and LAKEoneD, not only capture the variability of Lake Kivu's mixolimnion and therewith the effects of the meteorological controls on mixing, they also succeed in reproducing the effect of salinity and dissolved gases on the stratification. Sometimes, individual models react stronger to a certain forcing than other models, such as the heating in the lowest layers of LAKEoneD in response to the imposed geothermal heat flow (deep simulation), or the marked response to wind stress in LAKE. However, altogether, the considered comprehensive lake models are suited to investigate hydrodynamic processes occurring within large, deep lakes, and therewith make way for further studies of, for instance, biogeochemical cycling within these lakes.

### **The impact of the African Great Lakes on the regional climate**

Although the African Great Lakes (AGL) are important regulators for the East African climate, their influence on atmospheric dynamics and the regional hydrological cycle remains poorly understood (Thiery et al., 2015a). We aim to assess this impact by comparing a regional climate model simulation which resolves individual lakes and explicitly computes lake temperatures to a simulation without lakes. The Consortium for Small-scale Modeling regional climate model (COSMO-CLM), coupled to the Freshwater Lake model (FLake) and Community Land Model (CLM), hereafter referred to as COSMO-CLM<sup>2</sup>, is used to dynamically downscale a CORDEX-Africa (Coordinated Regional Climate Downscaling Experiment) simulation to 7 km grid spacing for the period of 1999-2008. Efforts were made to enhance the realism of the simulations, by accounting for (i) a model set-up and land surface model suited for tropical conditions, (ii) a horizontal grid resolution effectively resolving individual lakes and complex topography, unprecedented for climate simulations in this region, and (iii) a state-of-the-art one-dimensional lake model capable of reproducing tropical Lake Surface Water Temperatures (LSWT).

A comprehensive evaluation of COSMO-CLM<sup>2</sup> shows an adequate representation of precipitation and LSWT; the model reproduces the most important spatial patterns, including enhanced over-lake precipitation, absolute LSWT values and LSWT gradients within and between lakes (Figure ). The phase and amplitude of the mean annual cycle are also similar to observations, although the amplitude is overestimated for LSWT (Figure ) and precipitation is underestimated during April and the main dry season. The remaining LSWT biases are ascribed to an underestimation of the mixed layer depth and the absence of three-dimensional circulation in the larger lakes.

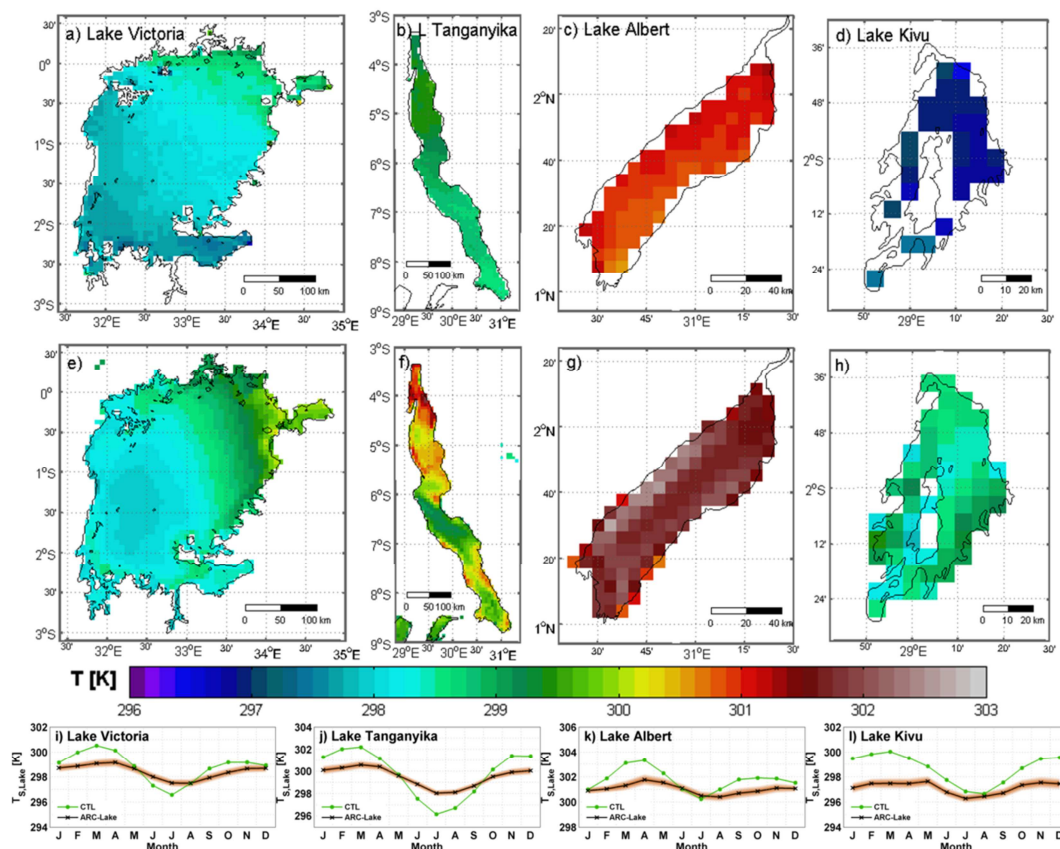


Figure 68: 1999-2008 observed lake surface water temperatures LSWT [K] from the ARC-Lake dataset (top panels) and modelled LSWT from the COSMO-CLM<sup>2</sup> control (CTL) simulation (central panels) for (a,e) Lake Victoria, (b,f) Lake Tanganyika, (c,g) Lake Kivu and (d,h) Lake Albert. (i-l) Lake-averaged observed (black line) and modelled (green line) monthly mean LSWT including observational error estimate as provided with the product (red shading).

Furthermore, the mean annual cycles of net shortwave and longwave radiation at the surface, sensible and latent heat flux and cloud cover are mostly simulated within the margins of observational uncertainty (Figure ). Finally, we show that our simulation largely outperforms a state-of-the-art reanalysis product (ERA-Interim) for most of the considered variables, especially precipitation and LSWT, whereas the added value relative to a state-of-the-art, continent-scale RCM simulation (COSMO-CLM CORDEX-Africa evaluation simulation) is evident for precipitation, LSWT and net surface shortwave radiation.

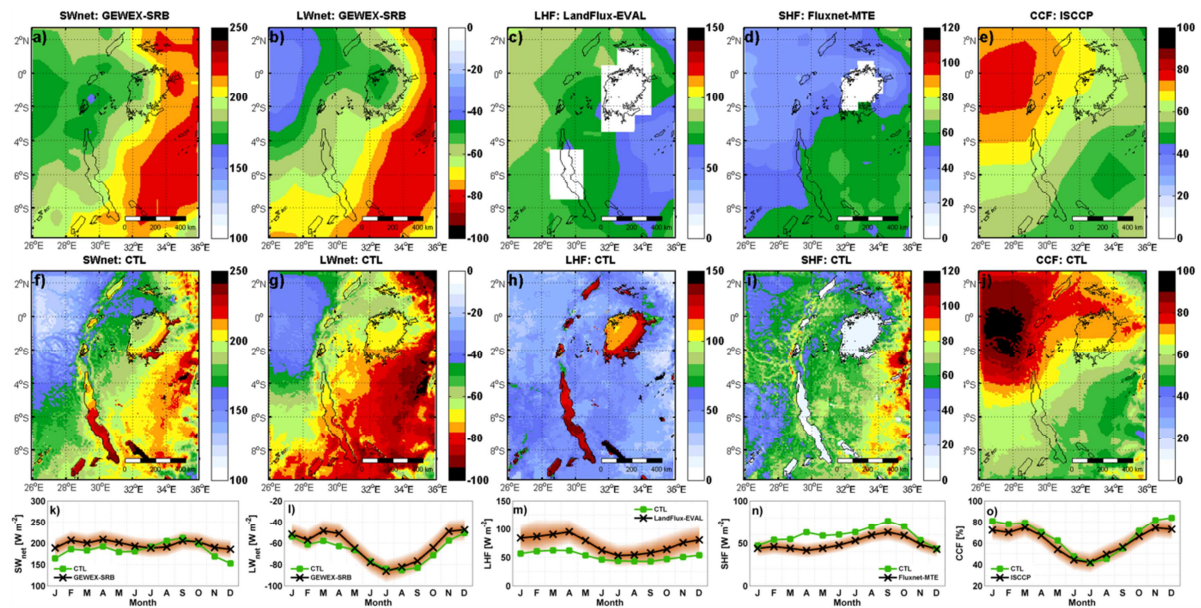


Figure 69: Observed and modelled annual mean maps (top and central panels, respectively), and domain-averaged seasonal cycles (lower panels) for (a,f,k) net shortwave radiation at the surface  $SW_{net}$  [ $W m^{-2}$ ], (b,g,l) net longwave radiation at the surface  $LW_{net}$  [ $W m^{-2}$ ], (c,h,m) latent heat flux LHF [ $W m^{-2}$ ], (d,i,n) sensible heat flux SHF [ $W m^{-2}$ ] and (e,j,o) percent cloud cover CCF [%]. Both observational products and model output are shown for the respective measurement periods (a,e: 1999-2008; b,c: 1999-2007; d: 1999-2005). For the white areas in (c) and (d), no data is available. The red shading around the observed annual cycle (black line) indicates the observational uncertainty as provided with the products.

The AGL significantly reduce offshore near-surface air temperature by about  $-0.57$  K, with maxima in excess of  $-1.50$  K (Figure 70). The cooling effect is advected across the lake shores within dynamic and orographic constraints, and is found to be strongest at the end of the main dry season, when the land surface warms faster than the water surface and the lake-land temperature contrast reaches a maximum.

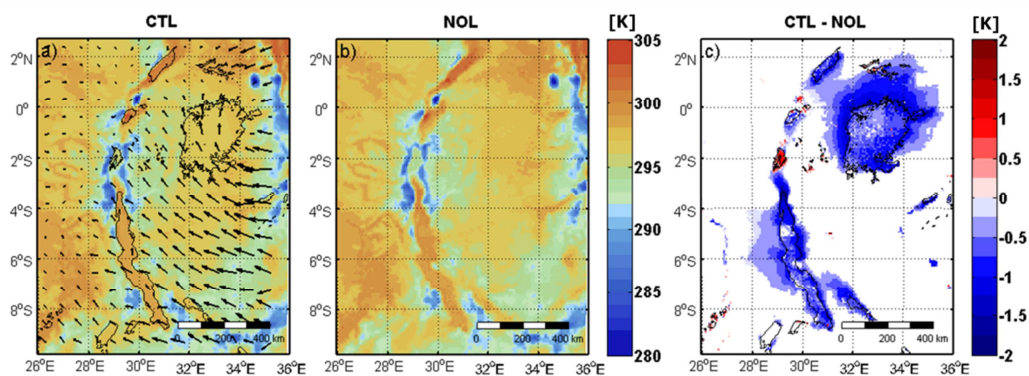


Figure 70: Impact of the AGL on 2 m air temperature  $T_{2m}$ . Shown are annual mean  $T_{2m}$  [K] for the (a) control (CTL) and (b) nolakes (NOL) simulations, and (c) statistically significant changes at the 5% significance level (CTL-NOL; two-tailed t-test) over the period 1999-2008. Temporally averaged 10 m wind vectors from the control simulation are shown in (a).

The four major AGL also enhance precipitation by  $+732$  mm  $yr^{-1}$  (+87 %) over their surface, and even  $+1373$  mm  $yr^{-1}$  (+145 %) over Lake Kivu (Figure ). All lakes together annually evaporate  $222$  km<sup>3</sup> of water into the atmosphere. In contrast to the near-surface temperature impact, the precipitation change is highly restricted to the lake areas. Both for temperature and precipitation, the mean effect masks a pronounced diurnal pattern: the temperature

signal exhibits strong cooling during daytime and moderate warming during nighttime over the lakes, whereas precipitation is enhanced mostly at night and during early morning.

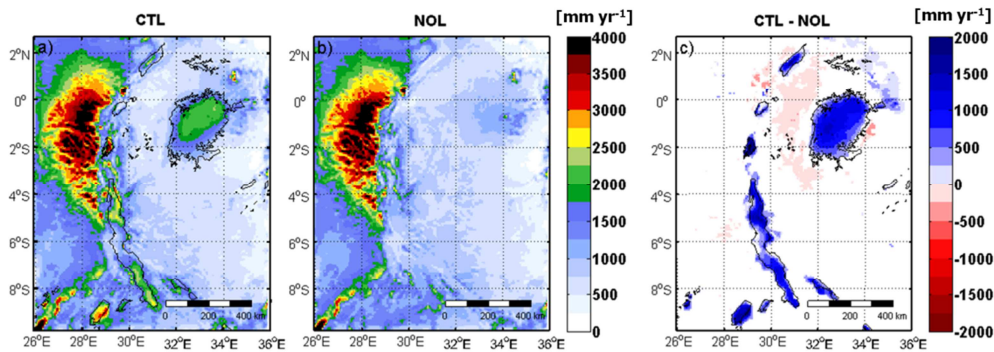


Figure 71: Impact of the AGL on precipitation P. Shown are annual mean P [ $\text{mm yr}^{-1}$ ] for the (a) control (CTL) and (b) nolakes (NOL) simulations, and (c) statistically significant changes at the 5% significance level (CTL-NOL; two-tailed t-test) over the period 1999-2008.

Decomposition of the lake-induced surface temperature increase over the AGL shows that reduced albedo has a moderate warming influence (+5.91 K), while reduced sensible heating enhances surface temperatures even more (+8.64 K; Figure 72a). For the most part, their effect is compensated by the enhanced lake evaporation, responsible for -12.21 K cooling. The apparent contradiction between surface and near-surface temperature change is cleared by considering day- and nighttime separately: daytime heat storage in the lake and reduced upward sensible heat flux dominate the near-surface air temperature change, whereas the nighttime warming determines the surface temperature signal.

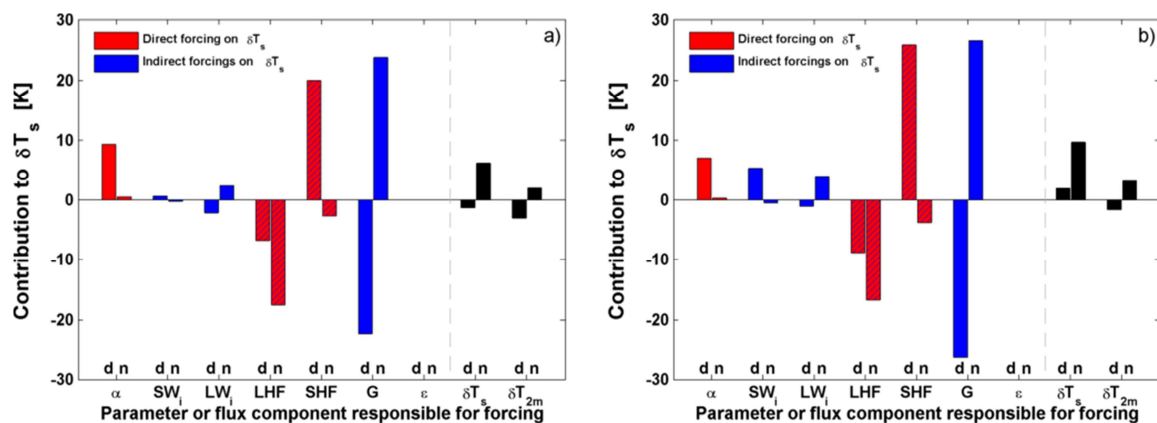


Figure 72: Lake-induced individual direct (red), indirect (blue) and mixed (hatched) contributions to  $\delta T_s$  shown separately for 09-18 UTC ("daytime", shown as d) and from 21-06 UTC ("nighttime", shown as n) for (a) lake pixels only and (b) Lake Kivu only (all units K). Individual direct (red), indirect (blue) and mixed (hatched) contributions to  $\delta T_s$  are shown for (b) the whole domain and (d) lake pixels only (all units K). Each contributing factor is indicated by its corresponding responsible parameter or flux component, with  $\alpha$  denoting the change in  $T_s$  caused by a modified albedo,  $SW_i$  by changing incoming shortwave radiation,  $LW_i$  by changing incoming longwave radiation, LHF by changing evapotranspiration, SHF by changing sensible heat flux due to modified aerodynamic resistance, and temperature gradient, G by changing subsurface heat flux and  $\epsilon$  by changing emissivity. Finally, the AGL impact on  $T_{2m}$  is also shown.

Lake Kivu constitutes an interesting exception, given the positive  $T_{2m}$  anomaly and strong precipitation increase generated by its presence (Figure 70, Figure ). The reasons for this behaviour become apparent when applying the surface energy balance decomposition method to this lake alone. Over Lake Kivu, daytime  $T_s$  increases as SHF is strongly dampened during this time (+25.81 K contribution to  $\delta T_s$ ; Figure 72b). Furthermore, the lake presence lowers daytime cloud cover and therewith enhances solar radiation input. Both effects are only partly compensated by changes in other contributions to  $\delta T_s$  (Figure 72b: G,  $\alpha$ , LHF). At night, the heat release from Lake Kivu is modelled to be more effective relative to the other AGL, further strengthening the nighttime warming influence. The different response of the various surface energy balance components is likely caused by the high-altitude of Lake Kivu (1463 m a.s.l.) relative to other AGL. In our simulation, the surface layer over Lake Kivu is predicted to be very unstable, with an average 3.4 K temperature difference between the lake surface and 2 m level (relative to 1.7 K, 1.7 K and 1.2 K over Lake Victoria, Lake Tanganyika and Lake Albert, respectively). Overall, the absence of daytime  $T_s$  cooling and strong nighttime  $T_s$  warming in CTL relative to NOL causes Lake Kivu to display a general warming influence upon the near-surface air. In addition, the strong nighttime warming intensifies the dynamical response to lake presence, leading to enhanced atmospheric column destabilisation and associated precipitation production.

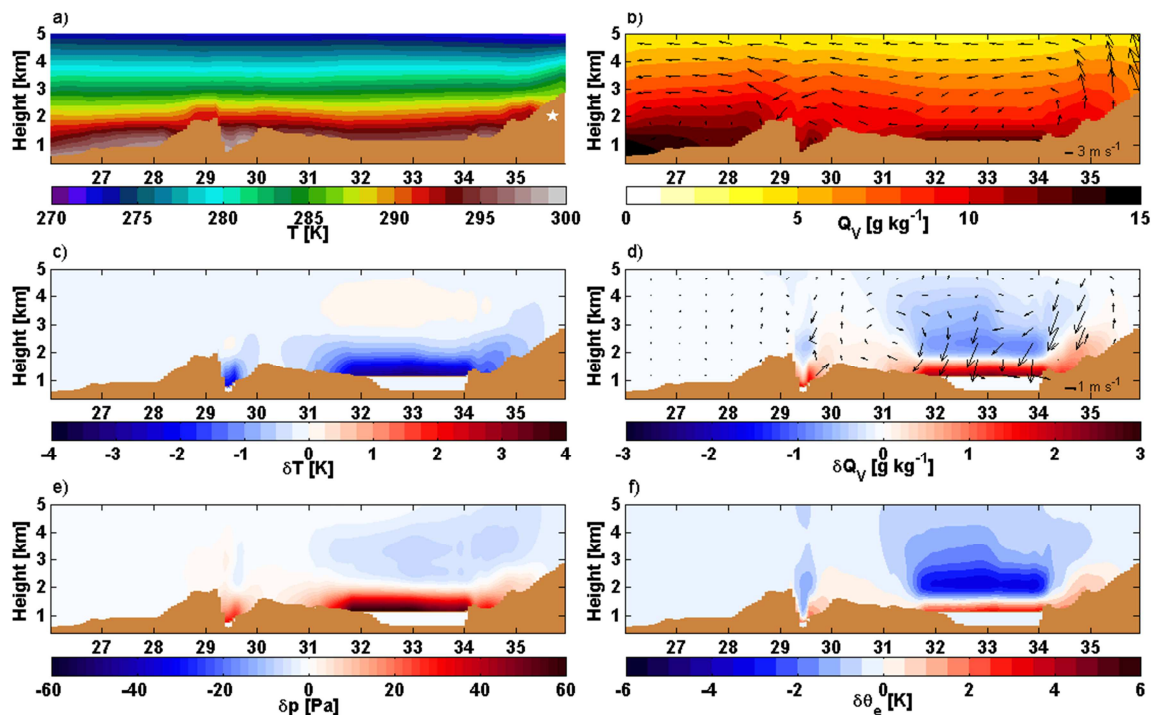


Figure 73: Vertical cross sections along the transect through Lake Victoria for the 10-year reference climatologies (CTL, 1999-2008) from 09-18 UTC (“daytime”) of (a) air temperature  $T$  [K] and (b) specific humidity  $Q_v$  [ $\text{g kg}^{-1}$ ] including longitudinal circulation climatology, and for the mean change due to lake presence (CTL minus NOL) in (c) air temperature  $\delta T$  [K], (d) specific humidity  $\delta Q_v$  [ $\text{g kg}^{-1}$ ] due to heat low-induced net convergence at lower levels, as indicated by arrows, (e) pressure  $\delta p$  [Pa], and (f) equivalent potential temperature  $\delta \theta_e$  [K]. Lake depth and vertical wind velocity were height-exaggerated by factor 10 and 200, respectively. The white star in (a) denotes the Kenyan Rift Valley mountains.

Finally, analysis of the dynamical response using day- and nighttime cross sections over lake Victoria highlights the importance of circulation changes induced by the lake-land temperature contrast. During daytime, the lake breeze transports cold air across the lake borders and generates over-land updrafts and over-lake subsidence (Figure ). This secondary circulation stabilizes the atmosphere above  $\sim 1.5$  km and therewith effectively suppresses convection from the unstable surface layer (Figure f).

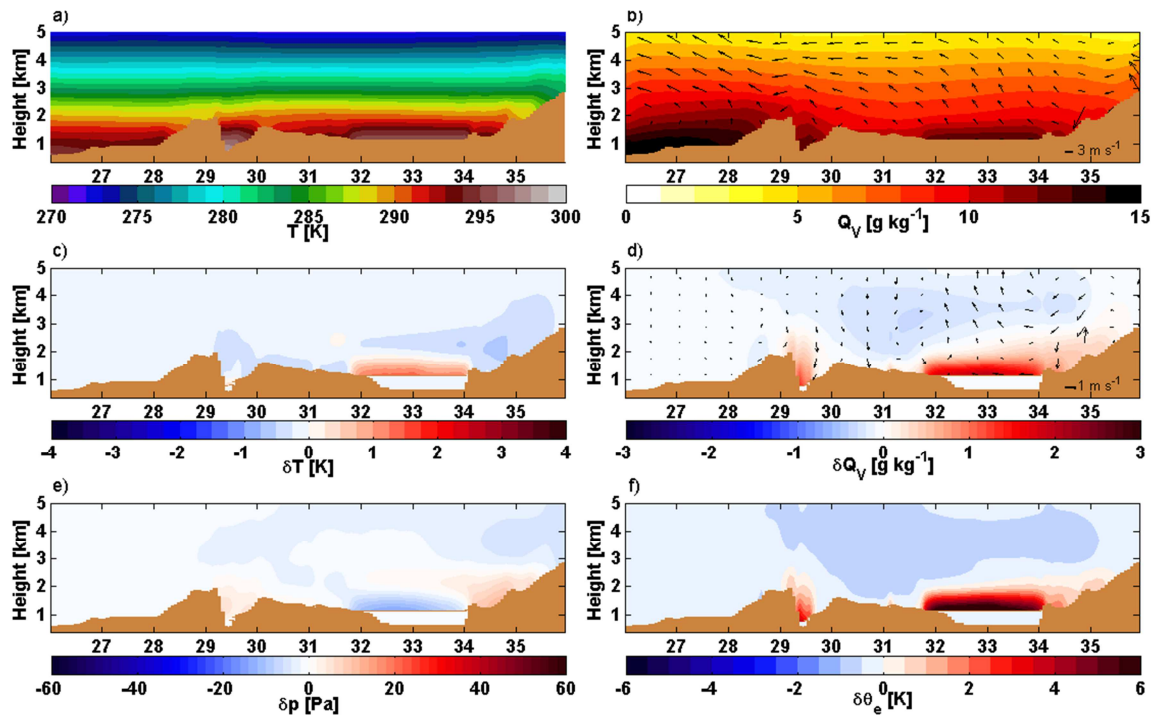


Figure 74: Same as Figure , but from 21-06 UTC (“nighttime”).

At night, the thermal inertia of the lake surface generates a positive temperature anomaly and a pressure deficit, and maintains the daytime evaporation rates, inputting large amounts of moisture into the boundary layer (Figure ). These three effects together cause a strong destabilization of the lower atmosphere. As the land breeze and secondary circulation subsequently induce near-surface convergence and the lifting of these highly unstable air masses (Figure d), strong convection is triggered and precipitation is released over the lake (Figure ; Figure ). On the eastern shore, complex topography and associated gravity currents superimpose on this pattern, generating a somewhat different response especially during daytime.

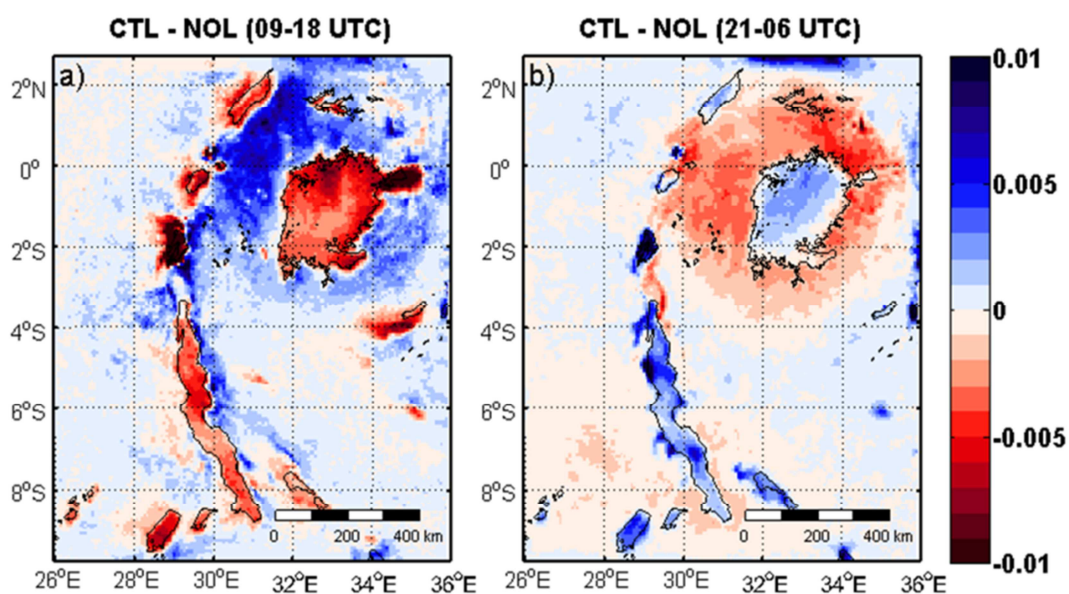


Figure 75: 1999-2008 mean change in convective mass flux density at cloud base height [ $\text{kg m}^{-2} \text{s}^{-1}$ ] induced by lake presence, for (a) 09-18 UTC (“daytime”) and (b) 21-06 UTC (“nighttime”).

#### 2.4.2.2 Lake hydrodynamics and ecological simulations for the period 2002-2013

The coupled one-dimensional (1D) hydrodynamic-ecosystem model DYRESM–CAEDYM (Yeates and Imberger 2004, Romero et al. 2004) was used as a model platform for developing ecological and biogeochemical modeling of L. Kivu ecosystem. The hydrodynamic Kivu model was coupled to an adapted version of CAEDYM. Boundary forcing was given by Muvundja et al. (2009) for river inputs, by Schmid et al. (2005) for deep spring inputs and by the regional atmospheric model CCLM (T4.2.1) for meteorological data. The dynamics of two phytoplankton communities (diatoms and non nitrogen-fixing cyanobacteria) were simulated. Calibration and validation of the hydrodynamic model were carried out on the 2002-2013 period, using the data of the updated Kivu database.

The Lake Kivu ecological model reproduced the seasonal stratification of the mixolimnion in Lake Kivu during the period 2002-2013 (Fig. 76) and seasonal nutrient upwelling (Fig. 77).

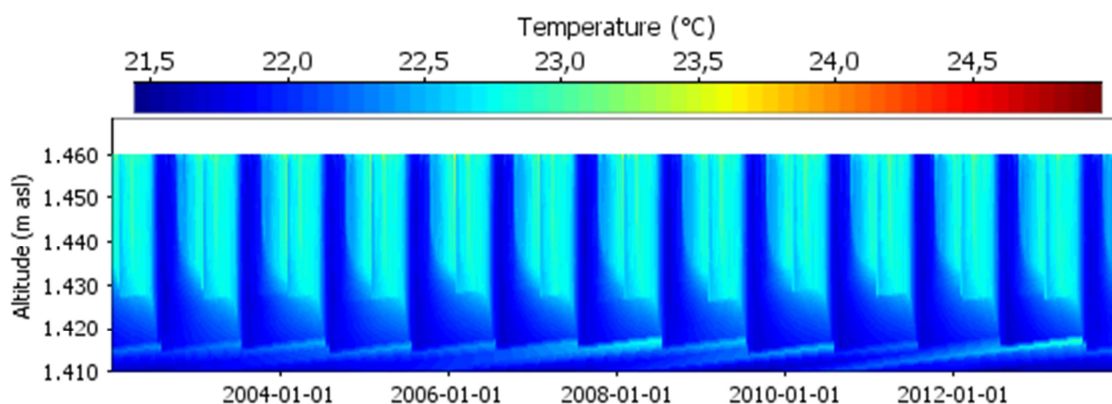


Figure 76: Lake temperature in the mixolimnion during the 2002-2013 period simulated by the DYRESM-CAEDYM coupled model developed for Lake Kivu.

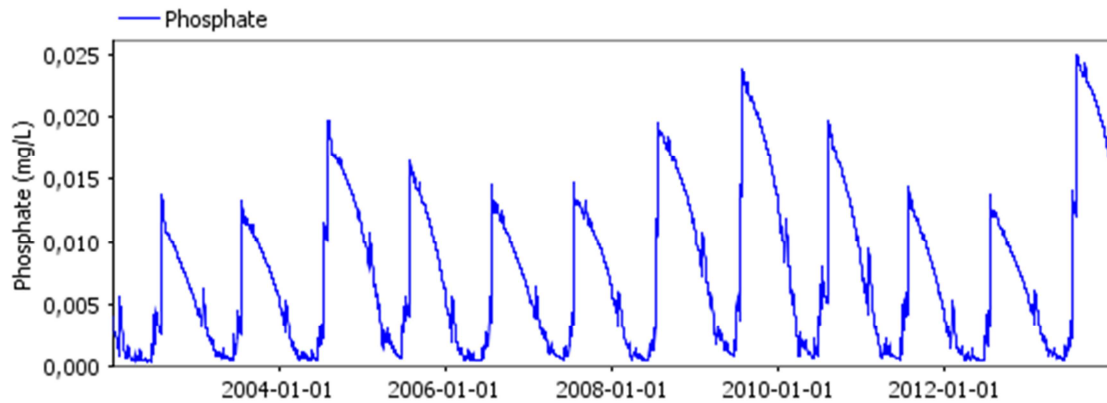


Figure 77: Phosphate concentrations in the surface of Lake Kivu during the 2002-2013 period simulated by the DYRESM-CAEDYM coupled model developed for Lake Kivu.

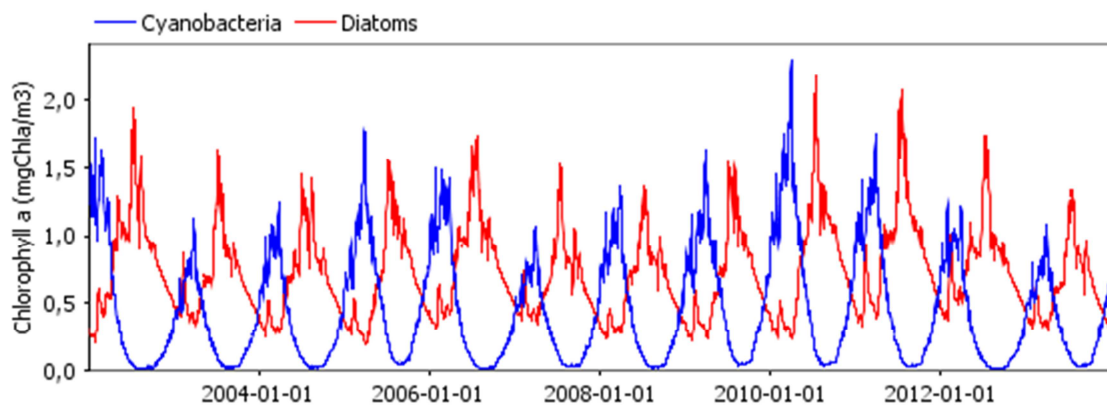


Figure 78: Diatoms and cyanobacteria biomass (in Chlorophyll a units) at 10 m during the 2002-2013 period simulated by the DYRESM-CAEDYM coupled model developed for Lake Kivu.

A diatom bloom developed during the dry season and were slowly replaced by cyanobacteria when nutrient became limiting during the thermally-stratified rainy season (Fig. 78).

## 2.4.3 Past changes

### 2.4.3.1 Past climate and ecology

Work is ongoing to derive historical climatological information. Modelled precipitation amounts from an ensemble of historical Global Climate Model (GCM) simulations are retrieved from the Earth System Grid Federation (ESGF) data nodes and used to compute a number of drought indicators (e.g. Standardised Precipitation Index, Aridity Index). Given the predominant control of relative humidity on mixing dynamics in Lake Kivu discovered during this project (sect. 2.4.2.1), temporal variations in dryness constitute the most likely source of fluctuations in ecosystem functioning. The spread of the ensemble will additionally provide an estimate of the model uncertainty of the drought signal. In addition to indices, the SANDRA weather type classification (see sect. 2.4.4.2 for a full description) will be applied to the model output, enabling the attribution of the historical variations to either local changes (e.g. lake-land breeze, evapotranspiration) or large-scale dynamical changes (e.g.

reduced/enhanced oceanic influence). This work will be continued after the termination of the project.

## **2.4.4 Prediction of future changes & ecosystem responses**

### **2.4.4.1 Climate projections**

#### **Future precipitation changes in East Africa – A circulation based approach.**

The East African region is highly dependent on precipitation due to its water-fed agricultural system. At the same time, the region experiences a high interannual variability regarding precipitation amounts. Consequently, there is a strong need to predict how precipitation amounts will evolve under climate change in this region.

Africa is the least studied continent of the world in terms of climate variability. The current lack of understanding of the physical and dynamical processes hampers the comprehension of the variability and changes in the climate and how these changes are likely to impact agro-ecological sectors that are of major importance for a large population (Otieno and Anyah, 2012; Shongwe et al., 2011). Part of the interannual variability in precipitation over East Africa is related to sea surface temperature perturbations over the Equatorial Pacific (El Niño Southern Oscillation) and Indian Ocean (Indian Ocean Dipole) (Anyah and Semazzi, 2009; Nicholson, 1996; Omondi et al., 2012, 2013). However, a large part remains unexplained and a lot of research is still necessary.

Here we investigate how precipitation amounts and its interannual variability will change in the future. First, an overview of the changes in mean precipitation that are expected over the region are discussed. An ensemble of 15 regional climate models – retrieved from the CORDEX project – is used and two periods are analysed: the historical period 1981-2010 and the future period 2071-2100 (RCP 8.5 scenario). The mean daily precipitation amount for the historical period is calculated over all simulations and compared to the mean daily precipitation amounts of the future. Statistical significant changes at the 1 % significance level are calculated using the Kolmogorov-Smirnov two-sided test based on yearly precipitation averages for every pixel.

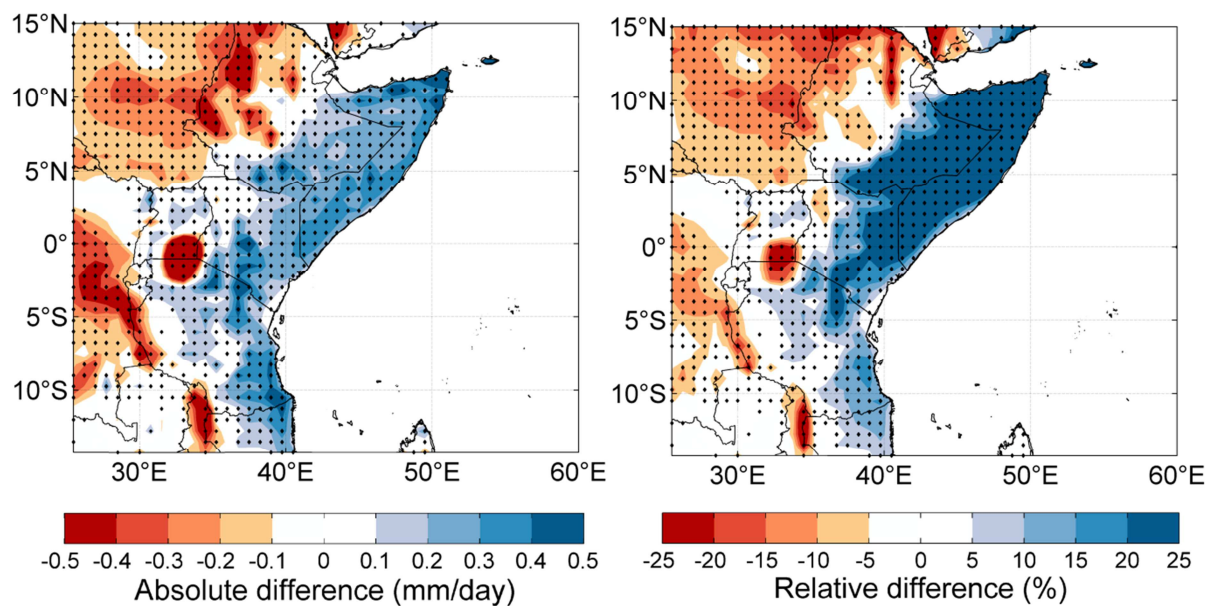


Figure 76: Precipitation changes between 1981-2010 and 2071-2100 (RCP8.5). Statistical significance at the 1 % level is shown by the black diamonds.

In general, precipitation increases are found over the coastal areas and highest relative increases are expected over Somalia and the southern parts of Ethiopia (Figure ). Precipitation amounts over these areas are fairly low and limited to certain periods every year. Absolute increases higher than 0.5 mm/day therefore result in relative increases of more than 25 %. Also Kenya (+10 % to +25 %) and coastal Tanzania (+5 % to +15 %) are projected to become wetter. The more inland regions of DR Congo show a drying in the future projection (-5 % to -10 %), just like the northern parts of the study area i.e. southern Sudan and the mountainous areas of Ethiopia (-5 % to -15 %).

A few very distinct drying areas are notable in the south-western part of the study area (Figure ). These correspond with the different lakes that are present over the region. Lake Victoria (located in the southern part of Uganda), Lake Tanganyika (located at the border of Tanzania and DR Congo) and Lake Malawi can easily be detected. Lake Victoria shows the most remarkable drying with respect to absolute numbers, but since a lot of precipitation takes place here, the relative change is of the same order as for the other lakes (-20 % to -25 %).

For the lake areas, strong decreases in precipitation are expected. First of all it must be noted that current regional climate models do not explicitly account for lake presence by using a lake model (60 % of the models in the ensemble have a lake model). These lakes are represented by a two-layered one-dimensional structure. Although the model's lake bottom temperatures were found very sensitive to perturbations in external parameters and forcing fields, lake surface temperature predictions are judged to be robust (Thiery et al., 2014a, 2014b; ). Remaining biases in the lake surface temperatures, but especially limitations in the atmospheric convection parameterization, explain the precipitation bias observed over the lakes, although observational products for precipitation are also characterised by large uncertainty over the African Great lakes (Thiery et al., 2015a; sect. 4.2.1.3.). Previous research at high resolution (0.0625°) using a two dimensional lake

representation (FLake) has shown a significant decrease in average precipitation over the African Great Lakes under the RCP8.5 scenario (Thiery et al., 2015b). This corresponds with our findings and puts extra confidence in the decrease obtained in the results.

The results obtained here confirm earlier findings. The Intergovernmental Panel on Climate Change (IPCC) Fifth Assessment Report (AR5) states that latest CMIP5 research found an increase in mean annual precipitation under RCP8.5 over most East Africa (excluding southern Sudan and the Ethiopian Highlands) (Niang et al., 2014). This has also been confirmed in earlier research using CMIP3 (Moise and Hudson, 2008; Shongwe et al., 2011). A drying of the eastern part of DR Congo is not found and most research also project a wetting for that part of Africa. This is contradictory with our results, however it must be noted that these areas showed serious evaluation biases. The results can therefore not be trusted fully over this area.

Furthermore, the precipitation change signal is subdivided into two components: a thermodynamic (including local and mesoscale changes) and a synoptic component. To execute such a subdivision, a bottom-up strategy is used. Instead of only considering precipitation amounts, pressure patterns are analysed. Pressure patterns are classified in typical circulation types using the COST733Class software (Philipp et al., 2014). From this, a weather atlas for the region is constructed, relating atmospheric circulation to observed precipitation patterns (Figure ). Furthermore, changes in precipitation amounts between the historical and future period for the same circulation types can now be calculated. These changes represent the thermodynamic fraction of the change in total precipitation (including the local and mesoscale). Further, the amount of days from the historical and future period that are classified to certain circulation types can be reconstructed and changes in the relative occurrence of circulation types can be calculated. By relating these changes in occurrences to precipitation the synoptic part of the total change in precipitation over the region is achieved.

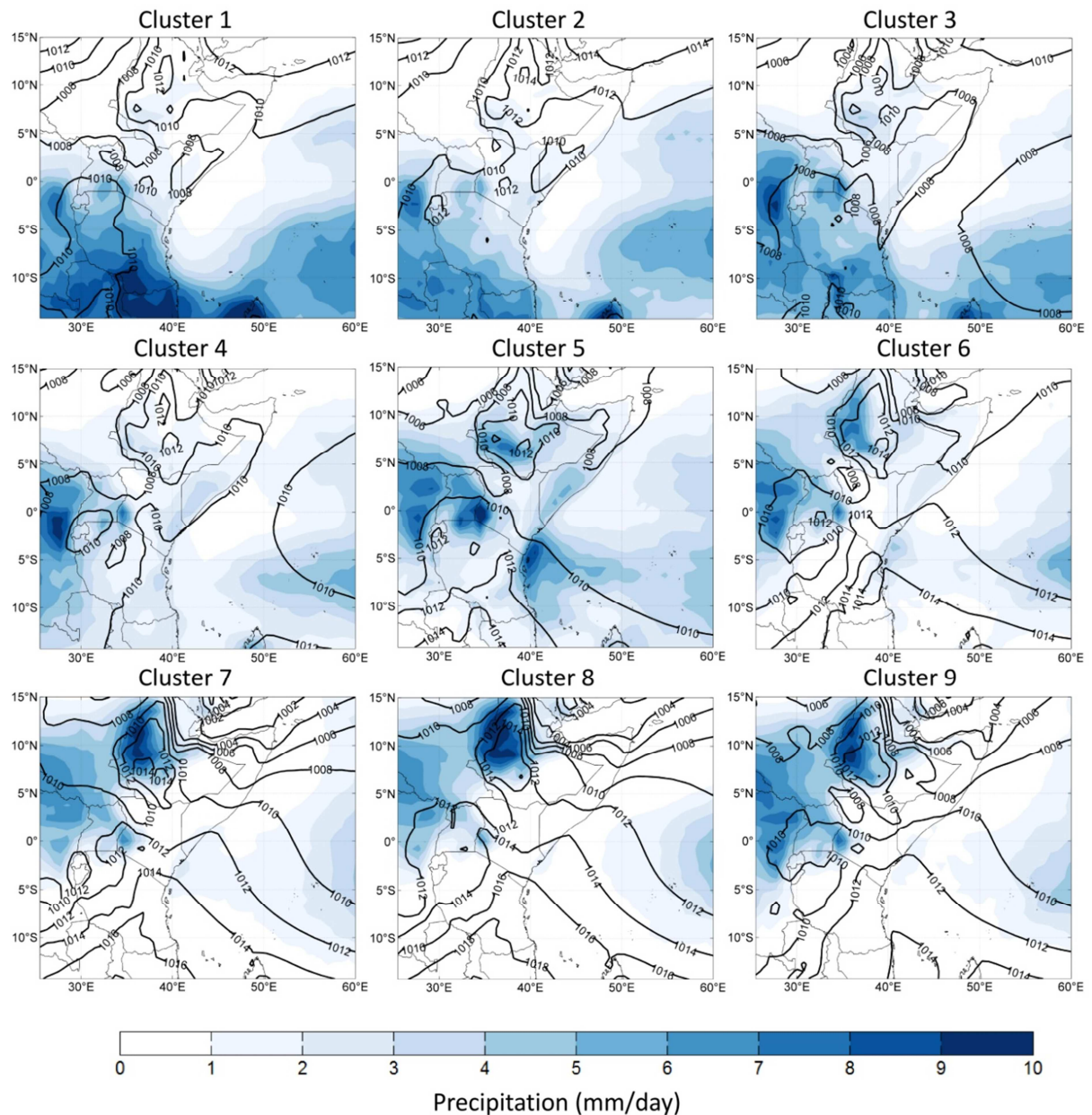


Figure 77: Weather atlas for East Africa.

This subdivision of the total precipitation change signal allows to obtain the drivers behind the changes. Thermodynamic (including local and mesoscale) changes are related to e.g. enhanced precipitation due to an increase of moisture content in the atmosphere regarding the Clausius-Clapeyron relation, cloud feedbacks, evaporation changes,... Synoptic changes are related to changes in large-scale atmospheric drivers and are associated to changes in the frequency of certain circulation types on the climatic time scale. A subdivision of the precipitation change signal in both components gives a good idea of the importance of the different drivers behind the changes, which is not yet available in current research.

The thermodynamic (local and mesoscale) contribution reaches 80 % of the total precipitation change signal, while the synoptic component only contributes 20 % (Figure a; Figure ). The thermodynamic component has the same pattern as the total precipitation

change. Precipitation increases over the coastal regions and decreases over the Ethiopian Highlands, southern Sudan and the eastern part of DR Congo.

In contrast, the (small) changes that are present in the synoptic component show an opposite result compared to the thermodynamic component. A drying is taking place over the southern part of the continental study area, while a wetting of southern Sudan and the Ethiopian Highlands is projected.

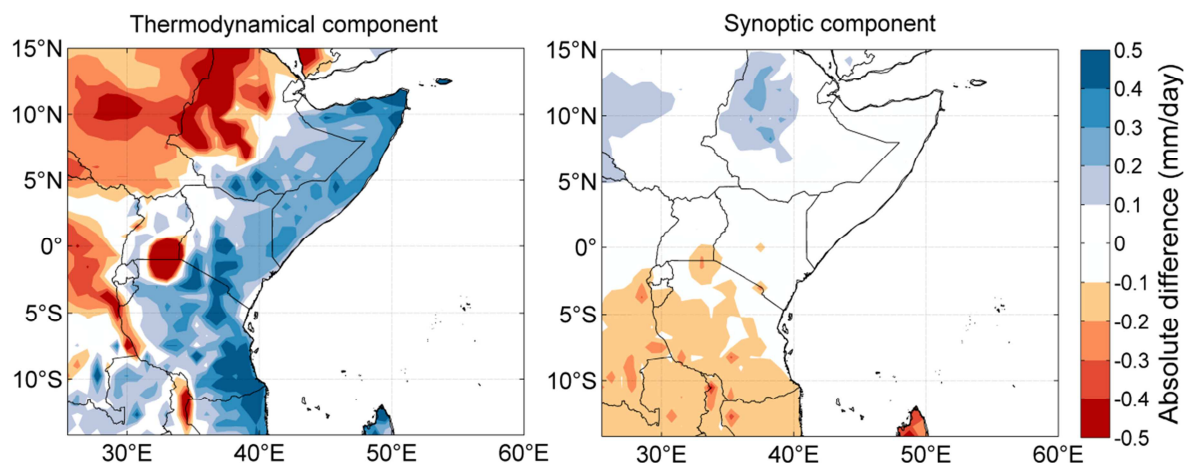


Figure 78: Absolute contribution of the components determining the change in precipitation between 1981-2010 and 2071-2100.

The precipitation changes over the lakes were attributed to the thermodynamic component. This suggests that the changes in precipitation over the lakes are induced by changes in mesoscale circulation or local moisture availability. This corresponds with the work of Thiery et al. (2015b). Under a climate change scenario, the land areas warm more quickly than the lakes. This enhances a pressure gradient in which a lake breeze may occur and reduces the nighttime land breeze. Moisture is transported away from the lakes into mainlands during daytime while less moisture is advected during nighttime, decreasing moisture and precipitation amounts over the lake area.

In general it is stated that changes in precipitation over East Africa are not related to large-scale dynamics, like e.g. sea surface temperature changes, despite their current important influence on interannual precipitation variability. This is a very important conclusion and has to be taken into account in future research concerning precipitation changes over East Africa. A publication on this topic is currently in preparation (Souverijns et al., 2015).

#### 2.4.4.2 Effects of methane exploitation

The effects of uncontrolled CH<sub>4</sub> harvesting on the lake ecosystem were examined using the calibrated DYRESM-CAEDYM model (see 2.4.2.2). The effect of a 140 MW industrial plant was simulated with a starting exploitation year in 2012. The methane was harvested from the Upper Resource Zone (320 m) and degassed waters were released in surface.

A rapid community shift is observed: cyanobacteria rapidly disappeared and diatoms dominated at high biomass (up to 25  $\mu\text{g Chla} / \text{L}$ ) (Fig. 79). The important increase of phytoplankton biomass resulted in a significant drop of oxygen concentration in the deeper layers of the mixolimnion. The resulting biozone was then limited to the first 10 meters of the water column (Fig. 80).

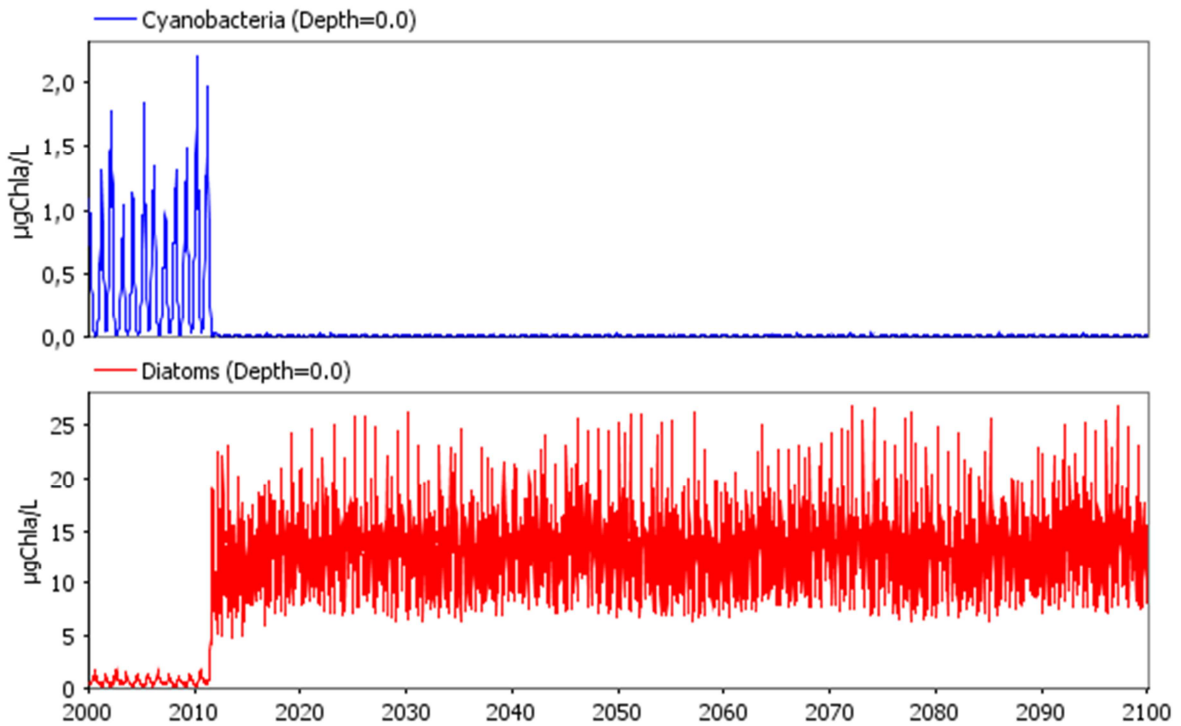


Fig. 79: Simulated effect of a 140 MW  $\text{CH}_4$  exploitation plant starting in 2012 on phytoplankton communities.

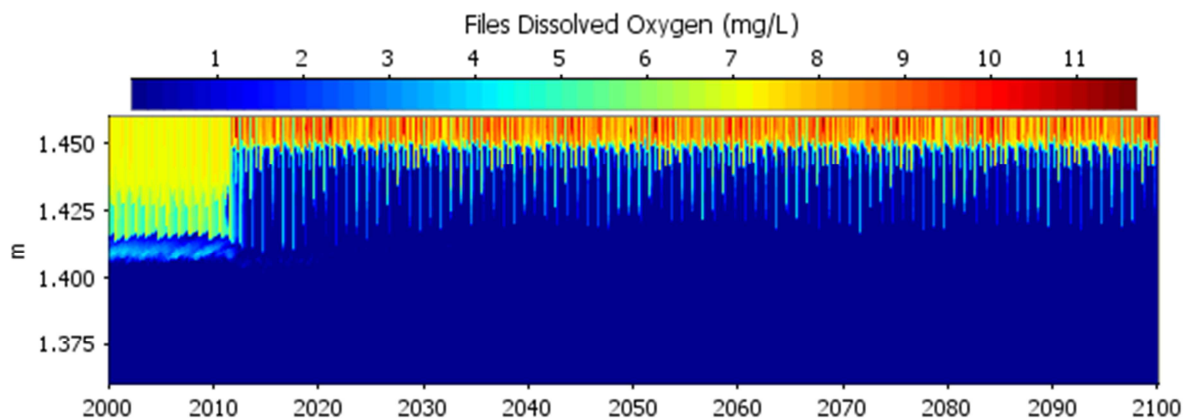


Fig. 80: Simulated effect of a 140 MW  $\text{CH}_4$  exploitation plant starting in 2012 on oxygen budget in the mixolimnion.

Consequently, an uncontrolled  $\text{CH}_4$  exploitation at industrial scale in Lake Kivu will result into a dramatic shift of phytoplankton communities and a rapid decline of ecosystem services including fish productivity and fisheries.

### 3. POLICY SUPPORT

The EAGLES project has provided several outputs relevant to the management of Lake Kivu and other East African great lakes. The first key output of EAGLES is relevant to the lake's monitoring and management in a context of environmental changes driven by climate change and aquatic resources exploitation. Two work packages of the project, WP1 (exploitation of existing data) and WP2 (acquisition of new data) have contributed to provide data and insight on the status of the lake ecosystem, that is developed in the top 60 m of the water column. A significant step for dissemination of the knowledge was the publication of a book in May 2012, devoted to a synthesis on limnology and biogeochemistry of Lake Kivu (Descy, Darchambeau and Schmid, 2012). This book is an effective output of EAGLES WP1, making the scientific studies on Lake Kivu since the 1930s accessible to a large audience, including the authorities in charge of the lake management. Hereafter, we present the main aspects pertaining to sustainable exploitation of the lake, derived from the book published in 2012 and from the results presented in this report. Most of these aspects were presented at a seminar involving the stakeholders from both surrounding countries, Rwanda and Democratic Republic of the Congo, held in Gisenyi, Rwanda, July 30-31, 2015. The presence of key people involved in the lake's management, monitoring and research allows to consider the EAGLES presentation at this meeting as a local end-users meeting (see the report on this meeting in annex 2)

#### **Fisheries yield and management**

All African great lakes still have active fisheries that provide proteins to the surrounding population and income for the fishermen and for people involved in the economy around the fishery. In Lake Kivu, the fishery is essentially based on one species, *Limnothrissa miodon*, locally called *sambaza* or *isambaza*, which was successfully introduced from Lake Tanganyika in the 1950s. So far, the status of the fishery was incompletely known, based on studies carried out at the end of the 1980s (by the FAO project Isambaza) in the northern part of the lake and from studies conducted only in the southern part of the lake, mainly in the Bukavu Bay. Under EAGLES, two types of fish studies were conducted: fish statistics surveys, conducted in the Rwandese part of the lake from 2011 through 2013, and two hydroacoustic survey on the entire lake, conducted in the dry seasons 2012 and 2014. These two surveys followed two first surveys conducted in 2008 during the CAKI project supported by FRS-FNRS. The most recent hydroacoustic surveys have confirmed the conclusions from the two first ones (Guillard et al., 2012), i.e. that the total sardine stock seems unchanged since the FAO assessments of the late 1980s, suggesting that the sambaza fishery is sustainable and hasn't collapsed as predicted by Dumont (1986). Still, the sardine production is lower than expected initially: instead of the expected 35000 tons, the present production is around 10000 tons. Several explanations to this low yield are the oligotrophic status of Lake Kivu and the status of the water column that restricts fish distribution to the top 30-40 m oxic layer for most of the year. Also, the production of zooplankton, on which the sardines feed, is low for most of the year, with a short peak in the dry season, following the phytoplankton peak.

Several results of the present report have confirmed these data and added new information on the pelagic food web of Lake Kivu. Regarding the low fish production, it is not, despite predictions based on previous studies (Dumont, 1986), related to low zooplankton production. Indeed, on an annual basis, zooplankton production ( $\sim 20 \text{ g C m}^{-2} \text{ y}^{-1}$ ) is about 1/10<sup>th</sup> of phytoplankton production, and zooplankton biomass is in the same range as in the other great Rift lakes of similar trophic status (L. Tanganyika, L. Malawi). By contrast, the estimated fish production, estimated from the whole-lake fish stock, is much lower than expected, indicating that the reason for the low sardine yield lies at the zooplankton-fish interface. What happens is still hypothetical, however, but several possible reasons can be advocated, largely drawn from the results of the limnological, planktological and geochemical studies carried out during EAGLES and former projects:

- The relatively low water transparency (maximum euphotic zone depth: 28 m) may reduce the efficiency of fish predation, as large zooplankton migrate downward during the day (Isumbisho, 2006); additionally, fish has no access to the oxygen-depleted 40-60 m zone during the long rainy season;
- Zooplankton biomass is unevenly distributed throughout the year, being very low during the rainy season, probably from lower and P-depleted phytoplankton biomass, often dominated by cyanobacteria, which are low-quality food for zooplankton (Masilya, 2012); it is likely that survival of fish larvae and juveniles is strongly dependent on the availability of zooplankton;
- Zooplankton production depend on phytoplankton production which may vary by a factor of 2 from year to year (Darchambeau et al., 2014); geochemical studies presented above confirm that variation of primary productivity can be substantial, depending on the degree of P limitation;
- A substantial size fraction of the phytoplankton biomass may not be edible by zooplankton: for instance, diatoms comprise mostly long, needle-like, species (Sarmiento et al., 2006);
- The microbial food web is important, leading to low trophic efficiency as a large part of phytoplankton production is consumed by bacteria, with substantial respiration losses (Morana et al. 2014, this report);

Therefore, as those likely limitations are strong constraints on the sardine yield, there is little hope that the production of the pelagic fishery can be improved. All the available evidence points to the fact that “natural” fish production may vary strongly in Lake Kivu as well as in other great Rift lakes, depending on variations in the regional climate (see below possible consequences of climate change). Hence, the regulation of the fishery, on both parts of the lake, should take into account those natural, climate-related, variations, by adapting the fishing effort to the fish production that could be predicted from monitoring the planktonic resources. Therefore we recommend to pursue surveys fish stock and the fishery (see below), and to try to establish relationships between fish production and plankton availability.

Additional useful information has been provided by the fishery survey conducted in the Rwandese part of the lake. A first important information from the fishery statistics in that

*Limnothrissa miodon* (the sambaza) remains the major species caught in the pelagic zone of Lake Kivu, despite the fear that the recently introduced *Lamprichthys tanganicanus* would become a competitor of the sambaza for food and would threaten the pelagic fishery. If *Limnothrissa* and *Lamprichthys* adults do compete for large zooplankton and have significant niche overlap (Masilya et al. 2011), it seems that *Lamprichthys* did not invade the pelagic zone but preferred the littoral zone. The fishery survey conducted in Rwanda also shows seasonal variations of the catches that may be related to resource-dependent variations in the sardine stock, rather than resulting from overexploitation. The fact that the catches are greatest at the beginning of the rainy season, after reduced catches in the dry season months, may result from greater abundance of large zooplankton following the phytoplankton peak, allowing growth to the young fish. Hence, the variation of the catches over the year should be seen as a natural phenomenon depending on the lake functioning, and not a result of poor fishery management. However, it should be stressed that lake-wide fishery management is desirable but is presently impossible as fisheries statistics are totally absent for the Congolese waters. Therefore we recommend to establish fisheries surveys over the whole lake: this study has demonstrated the feasibility of catch data collection in the Rwandese waters, as well as the feasibility of getting data on the whole-lake stock assessment thanks to the use of hydroacoustics and with the collaboration of technicians and scientists from both surrounding countries. However, it remains necessary, for a sound fishery management, to relate the data from the fisheries surveys and from the hydroacoustic surveys. Moreover, as effects from variations of climate-driven plankton productivity are expected, the data from the fish surveys should be examined together with the data on weather, limnology and plankton. This was beyond the scope of this study, but the existence of the various data bases (CTD data, phytoplankton, fish, over-lake weather station) allows exploring relationships and looking at seasonal and interannual variations, and perhaps to develop predictions of the fish yield, which may be useful for regulating the sardine fishery in order to ensure its sustainability.

In addition to variations of the lake's productivity related to climate variability, an impact of the large-scale methane exploitation is expected. Several scenarios of the extraction of methane from the deep waters of Lake Kivu were reviewed and tested by mathematical simulation by Wüest et al. (2012). In the extraction process, the water drawn from the deep "resource zone" is degassed and reinjected at a given depth. This reinjection is needed for two main reasons: first, the salinity gradient within the lake must be maintained; second, the water that contains large amounts of salt and nutrients cannot be released into the surface waters where they would result in severe alteration of water quality and ecosystem status. Moreover, the reinjection depth is critical, as any enrichment of an intermediate layer will ultimately affect the surface, as the sublacustrine sources result in an upwelling of the water and the dissolved substances. Despite the recommendations for plant operation are to re-inject the degassed water in sufficiently deep layers, one cannot be certain that plant operation will not affect the lake's ecosystem, both near the plants and far away from them, as physical and chemical changes will likely occur in the deep strata all over the lake. A key output of the EAGLES project has been to provide data bases on limnological and planktological data, covering more than a decade, that are a reference for the status of the lake's mixolimnion. In addition, EAGLES has contributed to the monitoring of greenhouse

gasses, of organic matter sedimentation and of various geochemical parameters. Several key biogeochemical processes were intensively studied during EAGLES, thereby contributing to improved knowledge of ecological and geochemical functioning of the lake.

In the context of methane extraction, the main recommendation can be made:

- To pursue the monitoring of the limnological and planktological parameters, in order to detect changes in the surface waters near the plants and in the main monitoring sites (off Gisenyi and at Ishungu)
- To reinforce the hydroacoustic surveys, in order to follow the fish stocks and the fish distribution in the water column, that depends strongly on the position of the oxycline in the mixolimnion.

**Remote sensing (RS)** can also be recommended for monitoring future changes affecting seasonal cycles and trends. Aggregated time series (weekly for the whole lake) of ocean color (providing estimates of surface chlorophyll a) and LSWT (allowing estimates of the surface temperature of the lake) clearly show the seasonal cycles. Therefore, RS could be used for assessing long term trends under several conditions. First, the period of analysis should be increased using next generation of satellite sensors, provided that an accurate cross-calibration with MODIS can be demonstrated. Second, this should be realized on the area with the highest temporal representativeness (i.e. the eastern basin) provided that this area can be considered as representative of the lake behavior.

### **Modelling of past and present conditions**

The quantification of the lake effect and its study through the surface energy balance and dynamical framework improves the scientific understanding of climate processes in East Africa. The strong imprint of the lakes on the hydrological cycle additionally highlights the vulnerability of local communities to lake-induced precipitation and storm activity. On the short term, we therefore recommend the installation of early warning systems for over-lake thunderstorms (or their improvement at locations where they are already present). This may, for instance, be achieved through operational numerical weather prediction systems capable of accounting for the relevant lake-atmosphere interactions. Such prediction systems should moreover operate at sufficiently high resolution to resolve the relevant mesoscale atmospheric processes. Insights from our analyses may thereby provide useful information for improving the skill of these predictions systems.

The climate model projections for the end-of-the-century underline the major role for Lake Victoria in modulating precipitation changes (2.4.4). Under a high-emission scenario (RCP8.5), over-lake extreme precipitation may intensify up to three times faster towards 2071-2100 relative to 1981-2010 compared to the projected change over the surrounding land (after isolation from the mean change). In the context of climate change and lake-induced weather hazards, we therefore strongly recommend the development of climate change adaptation strategies in the African Great Lakes region, in particular measures aiming at enhanced navigation safety for the fishermen operating on their surface.

Climate change has been identified as the main cause of the decrease of the oxygen content of the oceans since the warming of surface waters leads to an increased difference in water density that reduces the vertical penetration of oxygen (Keeling and Garcia 2002). In the East African region, records of air temperature show that temperature has risen by 0.5-0.7°C during the 20th century, consistently with the global increase pattern (O'Reilly et al. 2003). In consequence, climate warming has been recently found to strengthen the vertical stratification and to affect the ecological functioning of another large and deep East African lake, the neighboring Lake Tanganyika (Verburg and Hecky 2009). It is still unclear how climate change would affect Lake Kivu specifically, but it could be hypothesized that more stable stratification conditions would further reinforce the importance of methanotrophy and chemoautotrophy in the redoxcline, which might ultimately lead to (1) an even more pronounced uplift of the oxycline toward shallower waters during the rainy season, and (2) an increased physical (density gradient) and biological (methanotrophy and chemoautotrophy) constraint on the upward inorganic nutrient fluxes. Together, they might accentuate the nutrient limitation in the mixed layer and therefore negatively affect the phytoplankton productivity, as recently suggested in Lake Tanganyika and Lake Malawi (Verburg and Hecky 2009). The simulation of the effects of methane extraction, with the operation of a 140 MW power plant, has indeed shown that depletion of oxygen would likely occur in the mixolimnion, along with a substantial increase of chlorophyll a and a shift in phytoplankton composition.



#### **4. DISSEMINATION AND VALORISATION**

In addition to the specific scientific publications and to the communications in scientific meetings, the information contained in the book “Lake Kivu: Limnology and geochemistry of a tropical great lake” has been widely disseminated: since its online publication on April 25, 2012, there has been a total of 3,825 chapter downloads for the eBook on SpringerLink (Book performance report 2014, June 2015).

Several meetings were organized for general project planning and coordination among the various work packages. Three follow-up committees were organized, one with the local partners in Kigali (July 2011) and two with external European members in Brussels (December 2011 and March 2003). Several presentations were made during these meetings and reports with recommendations were produced. Just before the submission of the present report, a presentation of the main results of the project was made in Gisenyi (Rwanda, in the presence of representatives and stakeholders from Rwanda and Democratic Republic of the Congo. This allowed to reach many more people than in the case of the follow-up committee, and we consider this presentation as an equivalent to a local end-users committee.

Contacts were established with other relevant national and international programs: a notable example was the coordination with the “Biological Baseline of Lake Kivu”, financed by the Belgian technical Cooperation (BTC), which consisted in designing a monitoring program of the lake for collected reference data before the large-scale exploitation of methane for energy production in Rwanda. Also, several European and North-American scientists and students were invited in the field missions, thereby extending the approaches to complementary disciplines, as geophysics, sedimentology, geochemistry and microbial ecology. The EAGLES members participated in various scientific meetings to ensure data and information exchange among the partners and among national and international scientific communities, thereby ensuring dissemination of the project outputs.



## 5. PUBLICATIONS

### 5.1 Publications of the teams

#### 5.1.1 Peer review (published and in press)

1. Abril G., S. Bouillon, F. Darchambeau, C. R. Teodoru, T. R. Marwick, F. Tamoo, F. O. Omengo, N. Geeraert, L. Deirmendjian, P. Polsemaere & A.V. Borges (2015) Technical Note: Large overestimation of pCO<sub>2</sub> calculated from pH and alkalinity in acidic, organic-rich freshwaters, *Biogeosciences*, 12(1):67-78.
2. Balagizi C.M., F. Darchambeau, S. Bouillon, M.M. Yalire, T. Lambert & A.V. Borges (2015) River geochemistry, chemical weathering and atmospheric CO<sub>2</sub> consumption rates in the Virunga Volcanic Province (East Africa), *Geochemistry, Geophysics, Geosystems (G-Cubed)*, doi:10.1002/2015GC005999
3. Borges A.V., C. Morana, S. Bouillon, P. Servais, J.-P. Descy & F. Darchambeau (2014) Carbon cycling of Lake Kivu (East Africa): net autotrophy in the epilimnion and emission of CO<sub>2</sub> to the atmosphere sustained by geogenic inputs, *PlosOne*, 9(10): e109500. doi:10.1371/journal.pone.0109500
4. Borges A.V., G. Abril, B. Delille, J.-P. Descy & F. Darchambeau (2011) Diffusive methane emissions to the atmosphere from Lake Kivu (Eastern Africa), *Journal of Geophysical Research – Biogeosciences*, 116, G03032, doi:10.1029/2011JG001673
5. Borges A.V., S. Bouillon, G. Abril, B. Delille, D. Poirier, M.-V. Commarieu, G. Lepoint, C. Morana, W. Champenois, P. Servais, J.-P. Descy & F. Darchambeau (2012) Variability of carbon dioxide and methane in the epilimnion of Lake Kivu, In *Lake Kivu: Limnology and biogeochemistry of a tropical great lake* (J.-P. Descy, F. Darchambeau, M. Schmid, Eds), pp 47-66, *Aquatic Ecology Series*, Springer
6. Borges AV, Darchambeau F, Teodoru CR, Marwick TR, Tamoo F, Geeraert N, Omengo FO, Guérin F, Lambert T, Morana C, Okuku E & Bouillon S (2015) Globally significant greenhouse gas emissions from African inland waters, *Nature Geoscience*, 8, 637–642, doi:10.1038/NGEO2486
7. Darchambeau F, Isumbisha M, Descy J-P (2012) Zooplankton of Lake Kivu. In *Lake Kivu, Limnology and Biogeochemistry of a Tropical Great Lake*. Springer, *Aquatic Ecology Series*, Vol. 5, 107-126 (P1 & P4)
8. Darchambeau, F., Sarmiento, H. & Descy, J. P. 2014. Primary production in a tropical large lake: The role of phytoplankton composition. *The Science of the total environment*. 473-474, 178-188, p. 178-188
9. Descy J-P, Darchambeau F, Schmid M (2012) Lake Kivu Research: Conclusions and Perspectives. In *Lake Kivu, Limnology and Biogeochemistry of a Tropical Great Lake*. Springer, *Aquatic Ecology Series*, Vol. 5, 181-190 (P1 & P4)
10. Descy J-P, Darchambeau F, Schmid M (2012) Lake Kivu: Limnology and geochemistry of a tropical great lake. *Aquatic Ecology Series*, Vol. 5, Springer. 190 pp. (P1 & P4)
11. Guillard J, Darchambeau F, Mulungula PM, Descy J- P (2012) Is the fishery of the introduced Tanganyika sardine (*Limnothrissa miodon*) in Lake Kivu (East Africa) sustainable? *Journal of Great Lakes Research* 38: 524-533. (P1, P4 & P8)
12. Inceoğlu Ö, M Llíros, SA Crowe, T Garcia-Armisen, C Morana, F Darchambeau, AV Borges, JP Descy, P Servais (2015) Vertical distribution of functional potential and active microbial communities in meromictic Lake Kivu, *Microbial Ecology*, doi:10.1007/s00248-015-0612-9
13. Inceoglu, O., Llíros, M., Garcia-Armisen, T., Crowe, S.A., Michiels, C., Darchambeau, F., Descy, J.P. & Servais, P. (2015). Distribution of bacterial and archaeal communities in meromictic tropical Lake Kivu (Africa). *Aquatic Microbial Ecology*. 74: 215-233
14. Llíros M, Descy J-P, Libert X, Morana C, Schmitz M, Wimba L, Nzavuga-Izere A, García-Armisen T, Borrego C, Servais P, Darchambeau F (2012) Microbial Ecology of Lake Kivu. In *Lake Kivu, Limnology and Biogeochemistry of a Tropical Great Lake*. Springer, *Aquatic Ecology Series*, Vol. 5, 85-105 (P1, P3 & P4)
15. Llíros M, T García-Armisen, F Darchambeau, C Morana, X Triadó-Margarit, Ö Inceoglu, C M Borrego, S Bouillon, P Servais, AV Borges, J-P Descy, DE Canfield & SA Crowe (2015) Pelagic photoferrotrophy in a modern ferruginous basin, *Scientific Reports* 5, doi:10.1038/srep13803
16. Loïselle, S., Cózar, A., Adgo, E., Ballatore, T., Chavula, G., Descy, J-P., Harper, D. M., Kansiiime, F., Kimirei, I., Langenberg, V., Ma, R., Sarmiento, H., Odada, E. & Descy, J-P. 2014. Decadal trends and common dynamics of the bio-optical and thermal characteristics of the African Great Lakes. *PLoS ONE*. 9, 4, e93656
17. Masiya MP, Darchambeau F, Isumbisha M, Descy J-P (2011). Diet overlap between the newly introduced *Lamprichthys tanganyicus* and the Tanganyika sardine in Lake Kivu, Eastern Africa. *Hydrobiologia* 675: 75–86.
18. Morana C, H Sarmiento, J-P Descy, JM Gasol, AV Borges, S Bouillon & F Darchambeau (2014) Production of dissolved organic matter by phytoplankton and its uptake by heterotrophic prokaryotes in large tropical lakes, *Limnology and Oceanography*, 59(4), 1364-1375
19. Morana C, AV Borges, FAE Roland, F Darchambeau, J-P Descy, S Bouillon (2015a) Methanotrophy within the water column of a large meromictic tropical lake (Lake Kivu, East Africa), *Biogeosciences*, 12, 2077-2088

20. Morana C, F Darchambeau, F Roland, AV Borges, F Muvundja, Z Kelemen, P Masilya, J-P Descy & S Bouillon (2015b) Biogeochemistry of a large and deep tropical lake (Lake Kivu, East Africa): insights from a stable isotope study covering an annual cycle, *Biogeosciences*, 12, 4953–4963
21. Morana C, FAE Roland, SA Crowe, M Llirós, AV Borges, F Darchambeau & S Bouillon (2015c) Chemoautotrophy and anoxygenic photosynthesis within the water column of Lake Kivu, in preparation
22. Roland FAE, S Crowe, AV Borges, B Thamdrup, L De Brabandere & F Darchambeau (2015a) Denitrification, anaerobic ammonium oxidation and dissimilatory nitrate reduction to ammonium in an East African Great Lake, in preparation
23. Roland FAE, F Darchambeau, C Morana, M Llirós & AV Borges (2015b) Methane and nitrous oxide time-series in the epilimnion of a meromictic tropical large lake (Lake Kivu, East-Africa), submitted
24. Sarmiento H, Darchambeau F, Descy J-P (2012) Phytoplankton of Lake Kivu. In *Lake Kivu, Limnology and Biogeochemistry of a Tropical Great Lake*. Springer, Aquatic Ecology Series, Vol. 5, 67-83.
25. Sarmiento, H., Amado, A. M. & Descy, J-P. 2013. Climate change in tropical fresh waters (comment on the paper 'Plankton dynamics under different climatic conditions in space and time' by de Senerpont Domis et al.) *Freshwater Biology*. 58, 10, p. 2208-221
26. Stoyneva, MP, Descy, J.-P. Balagué V, Compère P, Leitao M and Sarmiento H (2012). The queer *Tetraëdron minimum* from Lake Kivu (Eastern Africa): is it the result of a human impact? *Hydrobiologia* 698:273-283
27. Thiery W, Davin E, Panitz H-J, Demuzere M, Lhermitte S and Van Lipzig NPM (2015) The impact of the African Great Lakes on the regional climate. *Journal of Climate* 28: 4061–4085.
28. Thiery W, Martynov A, Darchambeau F, Descy J-P, Plisnier P-D, Sushama L, van Lipzig NPM (2014a) Understanding the performance of the FLake model over two African Great Lakes, *Geosci. Model Dev.* 7: 317-337.
29. Thiery, W, Stepanenko, VM, Darchambeau, F, Fang, X, Jöhnk, KD, Li Z, Martynov A, Mironov D, Perroud M, Subin ZM, van Lipzig NPM (2014b) LakeMIP Kivu: evaluating the representation of a large, deep tropical lake by a set of one-dimensional lake models, *Tellus A* 66, 21390.

## 5.2 Co-publications

### 5.2.2 Others

- **Master thesis**

- Balagzi C (2012) Géochimie des eaux continentales de la Province Volcanique des Virunga (Afrique de l'Est), University of Liège, 79 pp. (P4)
- De Saedeleer K (2013) Contribution relative des archées (Thaumarchaeota) et des bactéries ( $\beta$ - &  $\gamma$ -Proteobacteria) au processus de nitrification dans le lac Kivu (Rift Est Africain). MSc thesis, University of Namur, 79 pp. (P1)
- Herman M (2012) Inferring recent environmental changes in Lake Kivu by a study of sediments. MSc thesis, KU Leuven, 83 pp. (P3)
- Laenen F (2011) Modélisation physique et biogéochimique du lac Kivu, MSc. thesis, ULg, 116 pp. (P4)
- Montante L (2012) Abondance et diversité microbiennes liées à l'oxydation du méthane dans le lac Kivu (Afrique de l'Est). MSc thesis, University of Namur, 85 pp. (P1)
- Roland F (2012) Contribution à la description du cycle de l'azote au sein des eaux superficielles du lac Kivu (Afrique de l'Est). MSc thesis, Université de Liège, 57 pp. (P4)
- Schmitz M (2012) Implication des populations microbiennes dans le cycle de l'azote au lac Kivu (Afrique de l'Est), MSc. thesis, University of Namur, 83 pp. (P1)

- **PhD Theses**

- Balagizi C.M. (2015) Water geochemical investigation in the Nyiragongo and Nyamulagira volcanic fields: implications for Lake Kivu water chemistry, *Seconda Università degli Studi di Napoli*
- Masilya M. (2011) Ecologie alimentaire comparée de *Limnotherissa miodon* et de *Lamprichthys tanganicanus* au lac Kivu (Afrique de l'Est). Thèse de doctorat, PUN, Namur, 212 p
- Morana C. (2014) Exploring the carbon cycle in a large tropical lake (Lake Kivu, East Africa): from the cellular to the ecosystem level, KU Leuven
- Muvundja A.F. (2015). Hydrological variability and biogeochemistry of particulate organic matter in a large tropical rift lake, Lake Kivu (East Africa). PhD thesis, University of Namur, 190 p. + appendices.
- Thiery W (2015) Present and future impact of the African Great Lakes on the regional climate, KU Leuven, 198 p.

• **International colloquium**

1. Balagazi C, F Darchambeau, M Kasereka, S Bouillon, M Yalire and AV Borges, Geochemistry of continental rivers of the Virunga Volcanic Province, East Africa, AVCOR-2013, Active Volcanism & Continental Rifting with special focus on the Kivu Rift Zone, Gisenyi, Rwanda, 12-15 November 2013, oral presentation
2. Borges AV, Abril G, Delille B, Bouillon S, Descy J-P, Darchambeau F (2011) Variability of methane in the epilimnion of Lake Kivu. Paper presented at International Symposium on Soil Organic Matter 2011 Organic matter dynamics – from soils to oceans. Leuven, Belgium (P1, P3 & P4)
3. Borges AV, Abril G, Delille B, Descy J-P, Darchambeau F (2011) Variability of methane in the epilimnion of Lake Kivu. Geophysical Research Abstracts, 13:EGU2011-10360 (P1 & P4)
4. Borges AV, Abril G, Morana C, Bouillon S, Darchambeau F (2012) Variability of methane in the epilimnion of Lake Kivu. Geophysical Research Abstracts, 14:EGU2012-7485-1 (P1, P3 & P4)
5. Borges AV, Bouillon S, Morana CDT, Servais P, Descy J-P, Darchambeau F (2013) Carbon cycling in the epilimnion of Lake Kivu (East Africa): surface net autotrophy and emission of CO<sub>2</sub> to the atmosphere sustained by geogenic inputs. Geophysical Research Abstracts, 15:EGU2013-9572 (P1, P3 & P4)
6. Borges AV, CDT Morana, S Bouillon, J-P Descy & F Darchambeau, Carbon cycling of Lake Kivu (East Africa): net autotrophy in the epilimnion and emission of CO<sub>2</sub> to the atmosphere sustained by geogenic inputs, European Geosciences Union, General Assembly, Vienna, Austria, 27 April – 2May 2014
7. Borges, A.V.; Bouillon, S. Teodoru, C. Descy, J.P.; Lambert, T. Darchambeau, F. Inorganic and organic carbon spatial variability in the Congo River during high waters (December 2013) and low waters (June 2014), ASLO Aquatic Sciences Meeting February 22-27, 2015, Granada, Spain, oral
8. Crowe SA, DE Canfield, A Sturm, RP Cox, SJ Hallam, M Lliros, C Jones, O Ulloa, F Darchambeau, A Borges, T Garcia-Armisen, S Katsev, Rates of microbial sulfur oxidation in low oxygen environments, 46th international Liège colloquium, Low oxygen environments in marine, estuarine and fresh waters, 5-9 May 2014, Liège, Belgium
9. Darchambeau F (2011) Potential impacts of methane extraction on lake ecosystem. Paper presented at International Workshop on the Monitoring and Development of Lake Kivu gas resource. Rubavu, Rwanda (P4)
10. Darchambeau F, Borges AV, Sarmento H, Leporcq B, Isumbisha PM, Alunga G, Masilya PM, Descy J-P (2013) Teleconnections between ecosystem productivity and climate indices in a tropical great lake. Geophysical Research Abstracts, 15:EGU2013-9919-1 (P1 & P4)
11. Darchambeau F, Roland F, Crowe SA, De Brabandere L, Lliros M, García-Armisen T, Inceoglu O, Michiels C, Servais P, Morana CDT, Bouillon S, Meysman F, Veuger B, Masilya PM, Descy J-P, Borges AV (2013) Denitrification, anammox and fixed nitrogen removal in the water column of a tropical great lake. Geophysical Research Abstracts, 15:EGU2013-12761 (P1, P3 & P4)
12. Darchambeau F, Muvundja Amisi F, Morana C, Leporcq B, Rugema E, Descy J-P, Bouillon S (2015). Fate and downward fluxes of phytoplankton pigments in a deep tropical lake. ASLO meeting, Granada, February 2015.
13. Descy, J.-P. (2011). A summary of the ecological knowledge on Lake Kivu and the ongoing research projects. XXth AIOL Congress, Lecce, Italy.
14. Descy, J.-P., H. Sarmento P. Isumbisha, P. Masilya, A.V. Borges, C. Morana, M. Lliros, P. Servais, J. Guillard and F. Darchambeau. Lake Kivu: food web structure and energy flows. SIL Congress, Budapest, August 2013.
15. García-Armisen T, Inceoglu O, Lliros M, Crowe S, Darchambeau F, Morana C, Bouillon S, Borges A, Descy J-P, Servais P. (2012) Vertical stratification and functional guilds in the bacterial community of Lake Kivu (East Africa). Paper presented at 14th International Symposium on Microbial Ecology. Copenhagen, Denmark (P1, P3 & P4)
16. Jöhnk K., et al. (2015) Workshop Integrated modelling of lakes in the climate system, on Parameterization of Lakes in NWP and CMs (Evora, PT), oral presentation
17. Lliros M, Darchambeau F, García-Armisen T, Morana C, Plasencia A, Gich F, Leporcq B, Delille B, Borges AV, Isumbisha P, Casamayor EO, Borrrego CM, Descy J-P (2011) Microbial diversity and processes in Lake Kivu (East Africa). Paper presented at 12th Symposium on Aquatic Microbial Ecology (P1, P3 & P4)
18. Lliros M, García-Armisen T, Crowe SA, Darchambeau F, Morana C, Michiels C, Schmitz M, de Saedeleer K, Montante L, Roland F, Thiery W, Bouillon S, Borges A, Servais P, Descy J-P. (2012) Opening the archaeal box in a oligotrophic freshwater environment." Paper presented at 14th International Symposium on Microbial Ecology. Copenhagen, Denmark (P1, P3, P4 & P7)
19. Lliros M, O Inceoglu, T Garcia-Armisen, JC Auguet, C Morana, F Darchambeau, SA Crowe, S Bouillon, P Servais, AV Borges, J-P Descy, Ammonia Oxidising Archaea in the OMZ of a freshwater African Lake, 46th international Liège colloquium, Low oxygen environments in marine, estuarine and fresh waters, 5-9 May 2014, Liège, Belgium
20. Masilya PM, Isumbisha M, Kaningini M, Lepoint G, Darchambeau F, Descy J-P (2011) The recent introduction of *Lamprichthys tanganicanus* in Lake Kivu (Eastern Africa): a threat for the pelagic fishery? Paper presented at Aquatic Ecosystem Health & Management Society 10th conference The Aquatic Ecosystem Puzzle: Threats, Opportunities & Adaptation, Siena, Italy (P1 & P4)

21. Michiels C, Darchambeau F, Roland F, Morana C, Lliros M, Garcia-Armisen T, Thamdrup B, Borges A, Bouillon S, Canfield D, Servais P, Descy J-P & Crowe S, NO<sub>3</sub>- Reduction is Fe-Dependent in a Ferruginous Chemocline, Goldsmith, 08 - 13 June 2014, Sacramento, USA
22. Morana C, A.V. Borges, F. Darchambeau, F. Roland, L. Montante, J.-P. Descy & S. Bouillon, Methanotrophy and chemoautotrophy within the redox gradient of a large and deep tropical lake (Lake Kivu, East Africa), European Geosciences Union, General Assembly, Vienna, Austria, 27 April – 2 May 2014
23. Morana C, AV Borges, F Darchambeau, F Roland, L Montante, JP Descy & S Bouillon, Methanotrophy and chemoautotrophy within the redox gradient of a large and deep tropical lake (Lake Kivu, East Africa), 46th international Liège colloquium, Low oxygen environments in marine, estuarine and fresh waters, 5-9 May 2014, Liège, Belgium
24. Morana C, F Darchambeau, F Muvundja, F Roland, Z Kelemen, M-V Commarieu, B Leporcq, G Alunga, P Masiya, J-P Descy, AV Borges & S Bouillon, Carbon cycling in a large, meromictic tropical lake (Lake Kivu, East Africa): insights from seasonal monitoring of biogeochemical depth profiles, 46th international Liège colloquium, Low oxygen environments in marine, estuarine and fresh waters, 5-9 May 2014, Liège, Belgium
25. Morana C, F Darchambeau, F Muvundja, F Roland, Z Kelemen, M-V Commarieu, B Leporcq, G Alunga, P Masiya, J-P Descy, AV Borges & S Bouillon, Carbon cycling in a large, meromictic tropical lake (Lake Kivu, East Africa): insights from seasonal monitoring of biogeochemical depth profiles, European Geosciences Union, General Assembly, Vienna, Austria, 27 April – 2 May 2014
26. Morana C, H Sarmiento, J-P Descy, JM Gasol, AV Borges, S Bouillon & F Darchambeau, Production of dissolved organic matter by phytoplankton and its uptake by heterotrophic prokaryotes in large tropical lakes, European Geosciences Union, General Assembly, Vienna, Austria, 27 April – 2 May 2014
27. Morana C, Sarmiento H, Bouillon S, Gasol JM, Descy J-P, Darchambeau (2012) Dissolved primary production and heterotrophic prokaryote reassimilation in a large oligotrophic tropical lake (Lake Kivu, Eastern Africa). Paper presented at 2012 ASLO Aquatic Sciences Meeting, Shiga, Japan (P1, P3 & P4)
28. Roland F, F Darchambeau, SA Crowe & AV Borges, Anaerobic methane oxidation in two tropical freshwater systems, 46th international Liège colloquium, Low oxygen environments in marine, estuarine and fresh waters, 5-9 May 2014, Liège, Belgium
29. Roland F, F Darchambeau, SA Crowe & AV Borges, Anaerobic methane oxidation in two tropical freshwater systems, European Geosciences Union, General Assembly, Vienna, Austria, 27 April – 2 May 2014
30. Roland F., A. V. Borges, S. Crowe & F. Darchambeau, Contribution to the description of the nitrogen cycle in Lake Kivu, AVCOR-2013, Active Volcanism & Continental Rifting with special focus on the Kivu Rift Zone, Gisenyi, Rwanda, 12-15 November 2013, poster
31. Roland F., F. Darchambeau & A. V. Borges, Methane cycle and methane oxidation in Lake Kivu and Kabuno bay, AVCOR-2013, Active Volcanism & Continental Rifting with special focus on the Kivu Rift Zone, Gisenyi, Rwanda, 12-15 November 2013, oral presentation
32. Souverijns N, Thiery W, Demuzere M, van Lipzig, N (2015) Present and future precipitation variability over the East African region using CORDEX simulations (COSMO-CLM) and its relation with circulation patterns, EGU general assembly (Vienna, AT), oral presentation
33. Souverijns N, Thiery W, Demuzere M, van Lipzig, N (2015) Present and future precipitation variability over the East African region using CORDEX simulations (COSMO-CLM) and its relation with circulation patterns, COSMO User Seminar poster (Offenbach am Main, DE), poster
34. Thiery W, Davin E, Panitz H-J, Lhermitte S, van Lipzig N (2014) Climate change intensifies hazardous thunderstorms over Lake Victoria, Swiss climate summer school (Grindelwald, CH), poster
35. Thiery W, Davin E, Panitz H-J, Lhermitte S, Demuzere M, van Lipzig N (2015) Influence of the African great lakes on the regional climate, EGU general assembly (Vienna, AT), oral presentation
36. Thiery W, Davin E, Panitz H-J, Lhermitte S, van Lipzig N (2015) Modeling the influence of the African Great Lakes on the regional climate, ASLO aquatic Sciences meeting (Granada, ES), poster
37. Thiery W, Davin E, Panitz H-J, Lhermitte S, van Lipzig N (2015) Present and future impact of the African Great Lakes on the regional climate, COSMO User Seminar poster (Offenbach am Main, DE), oral presentation
38. Thiery W, Davin E, Panitz H-J, Lhermitte S, Demuzere M, van Lipzig N (2015) Present and future impact of the African Great Lakes on the regional climate, Workshop on Parameterization of Lakes in NWP and CMs (Evora, PT), oral presentation
39. Thiery W, Davin E, Panitz H-J, Lhermitte S, van Lipzig N (2014) The impact of the African Great Lakes on the regional climate in a dynamically downscaled CORDEX simulation, EGU general assembly (Vienna, AT), poster
40. Thiery W, Davin E, Panitz H-J, Lhermitte S, van Lipzig N (2014) The impact of the African Great Lakes on the regional climate in a dynamically downscaled CORDEX simulation, COSMO User Seminar poster (Offenbach am Main, DE), oral presentation
41. Thiery W, Davin E, Seneviratne SIS, Lhermitte S, van Lipzig N (2015) Hazardous thunderstorms over Lake Victoria: climate change and early warnings, Swiss climate summer school (Ascona, CH), poster
42. Thiery W, Davin E, Seneviratne SIS, Lhermitte S, van Lipzig N (2015) Amplification of extreme precipitation response to climate change over Lake Victoria, EGU general assembly (Vienna, AT), oral presentation

43. Thiery W, Martynov A, Darchambeau F, Plisnier P-D, Descy J-P, van Lipzig N (2013) Understanding the performance of the FLake model over the African Great Lakes. EGU general assembly (Vienna, AT).
44. Thiery W, Martynov A, Darchambeau F, Plisnier P-D, Descy J-P, van Lipzig N (2013) Understanding the performance of the FLake model over the African Great Lakes. COSMO User Seminar poster (Offenbach am Main, DE).
45. Thiery W, Martynov A, Darchambeau F, Plisnier P-D, Descy J-P, van Lipzig N (2012) Testing the representation of the African Great lakes in COSMO's lake module (FLake). CLM assembly (Leuven, BE).
46. Thiery W, Martynov A, Darchambeau F, Plisnier P-D, Descy J-P, van Lipzig N (2012) Testing the representation of the African Great lakes in COSMO's lake module (FLake). Workshop on Parameterization of Lakes in NWP and RCM (Helsinki, FI).
47. Thiery W, Martynov A, Darchambeau F, Plisnier P-D, Descy J-P, van Lipzig N (2012) Testing the representation of the African Great lakes in COSMO's lake module (FLake): Evaluation, model sensitivity and controlling variables. Meteoclim (Liège, BE).
48. Thiery W, Martynov A, Darchambeau F, Plisnier P-D, Descy J-P, van Lipzig N (2012) Evaluating COSMO's lake module (FLake) for an East-African lake using a comprehensive set of lake temperature profiles. EGU general assembly (Vienna, AT).
49. Thiery W, Martynov A, Darchambeau F, Plisnier P-D, Descy J-P, van Lipzig N (2012) Evaluating COSMO's lake module for an East-African lake using a comprehensive set of lake temperature profiles. COSMO User Seminar poster (Offenbach am Main, DE).
50. Thiery W, Panitz, H-J, van Lipzig N (2013) LakeMIP Kivu & the impact of the African Great Lakes on the regional climate. Open Water Symposium (Etterbeek, BE).
51. Thiery W, Panitz, H-J, van Lipzig N (2013) The impact of the African Great Lakes on the regional climate in a dynamically downscaled CORDEX simulation. AGU Fall Meeting (San Fransisco, USA),
52. Thiery W, Panitz, H-J, van Lipzig N (2013) The impact of the African Great Lakes on the regional climate in a dynamically downscaled CORDEX simulation. CORDEX 2013 International Conference on Regional Climate (European Commission, BE).
53. Thiery W, Panitz, H-J, van Lipzig N (2013) The impact of the African Great Lakes on the regional climate in a dynamically downscaled CORDEX simulation. CLM General Assembly (Zürich, CH).
54. Thiery W, Stepanenko V, Darchambeau F, Joehnk K, Martynov A, Mironov D, Perroud M, van Lipzig N (2013) LakeMIP Kivu: Evaluating a set of one-dimensional lake models over a large tropical lake. EGU general assembly (Vienna, AT).
55. Thompson K, Lliros M, Borrego C, Kenward P, Darchambeau F, Borges A, Canfield D & Crowe S, New Insights into Iron-Based Photosynthesis, Goldsmith, 08 - 13 June 2014, Sacramento, USA



## **6. ACKNOWLEDGEMENTS**

This research on Lake Kivu, in addition to the funding by BELSPO benefited from various grants and fellowships. A FRS-FNRS project (MICKI, Microbial Ecology in Lake Kivu) allowed participation of scientists and students, as well as complementary analyses that contributed to the biogeochemical studies. An FWO PhD fellowship enabled additional model simulations and analyses contributing to the climate studies. Part of this research contributed to the European Research Council starting grant project AFRIVAL (African river basins: Catchment-scale carbon fluxes and transformations, 240002). Luc André, Wim Vyverman and Jean-Pierre Descy are members of the Royal Academy of Overseas Sciences, Belgium.



## 7. REFERENCES

- Abraham K., S. Opfergelt, F. Fripiat, A.-J. Cavagna, J. T.M. de Jong, S. Foley, L. André, D. Cardinal. (2008).  $^{30}\text{Si}$  and  $^{29}\text{Si}$  determinations on BHVO-1 and BHVO-2 reference materials with a new configuration on a Nu Plasma Multi Collector ICP-MS, *Geostandards and Geoanalytical Research*, 32, 193-202
- Adams, T. S., & Sterner, R. W. (2000). The effect of dietary nitrogen content on trophic level  $^{15}\text{N}$  enrichment. *Limnology and Oceanography*, 45: 601-607.
- Aglen, A. (1989). Empirical results on precision-effort relationships for acoustic surveys. – ICES CM/30: 28 p.
- Ahmad Z., Franz B.A., McClain Ch.R., Kwiatkowska E.J., Werdell J., Shettle E.P. & Holben B.N. (2010). New aerosol models for the retrieval of aerosol optical thickness and normalized water-leaving radiances from the SeaWiFS and MODIS sensors over coastal regions and open oceans. *Applied Optics* 49, 29.
- Akkermans T, Thiery W, van Lipzig NPM (2014). The regional climate impact of a realistic future deforestation scenario in the Congo Basin. *Journal of Climate* 27, 2714-2734.
- Alleman L.Y., D. Cardinal, C. Cocquyt, P.-D. Plisnier, J.-P. Descy, I. Kimirei, D. Sinyianza and André L. (2005). Silicon isotopic fractionation in Lake Tanganyika and its tributaries. *J.Great Lakes Res.*, 31, 509-519.
- An, S. and Gardner, W. S. (2002). Dissimilatory nitrate reduction to ammonium (DNRA) as a nitrogen link, versus denitrification as a sink in a shallow estuary (Laguna Madre/Baffin Bay, Texas). *Marine Ecology Progress Series* 237: 41-50.
- Anyah RO and Semazzi F (2009) Idealized simulation of hydrodynamic characteristics of Lake Victoria that potentially modulate regional climate. *International journal of climatology* 29: 971–981: doi:10.1002/joc.
- Balk, H & Lindem, T. (2006). Sonar 4, Sonar 5, Sonar 6 – Post-processing Systems. Operator Manual. University of Oslo, Norway, 427p.
- Bergamino N., Horion S., Stenuite S., Cornet Y., Loiselle S., Plisnier P.-D. & Descy J-P. (2010). Spatio-temporal dynamics of phytoplankton and primary production in Lake Tanganyika using a MODIS based bio-optical time series. *Remote Sensing of Environment* 114, 4, 772–780.
- Blees, J., Niemann, H., Wenk, C. B., Zopfi, J., Schubert, C. J., Kirf, M. K., et al. (2014). Micro-aerobic bacterial methane oxidation in the chemocline and anoxic water column of deep south-Alpine Lake Lugano (Switzerland). *Limnology and Oceanography* 59: 311-324.
- Bolliet T., Jorissen F.J., Schmidt S., Howa H. (2014). Benthic foraminifera from Capbreton Canyon revisited; faunal evolution after repetitive sediment disturbance. *Deep Sea research part II : Topical studies in oceanography* 104 : 319-334.
- Borges, A.V., Morana, C., Bouillon, S., Servais, P., Descy, J-P., & Darchambeau, F. (2014). Carbon cycling of Lake Kivu (East Africa): Net autotrophy in the epilimnion and emission of CO<sub>2</sub> to the atmosphere sustained by geogenic inputs. *PloS one* DOI: 10.1371/journal.pone.0109500
- Borges, AV, Abril G, Delille, B, Descy, J-P and Darchambeau, F. Diffusive methane emissions to the atmosphere from Lake Kivu (Eastern Africa). *Journal of Geophysical Res*, 116, G03032.
- Brunet, R. C. and Garcia-Gil, L. J. (1996). Sulfide-induced dissimilatory nitrate reduction to ammonia in anaerobic freshwater sediments. *FEMS Microbiology Ecology* 21(2): 131-138.
- Campbell J.W. & O'Reilly J.E. (2006). Metrics for Quantifying the Uncertainty in a Chlorophyll Algorithm : Explicit equations and examples using the OC4.v4 algorithm and NOMAD data. *Papers from the Ocean Color Bio-optical Algorithm Mini-Workshop* 748 (27-29 September 2005).
- Capart, A. (1959). A propos de l'introduction du Ndakala (*Stolothrissa tanganicae*) dans le lac Kivu. (About the introduction of Ndakala (*Stolothrissa tanganicae*) into Lake Kivu. In French.). *Bulletin Agricole du Congo Belge et du Ruanda-Urundi* 50(4): 1083–1087.
- Cardinal D., Savoye N., Trull T.W., Dehairs F., Kopczynska E.E., Fripiat F. and André L. (2007). Silicon isotopes in size-fractionated diatoms in the spring Southern Ocean suggest latitudinally-varying isotopic fractionation. *Marine Chemistry*, 106,48-62.
- Cardinal, D., Alleman L., De Jong J., Ziegler K., and André L. (2003) Silicon isotopic composition of silicon measured by multicollector plasma source mass spectrometry in dry plasma mode. *Journal of Analytical Atomic Spectrometry*, 18,213-218.

- Collart, A. (1960). L'introduction du *Stolothrissa tanganicae* (Ndagala) au lac Kivu. (The introduction of *Stolothrissa tanganicae* to Lake Kivu. In French.). Bulletin Agricole du Congo Belge 51(4): 975–985.
- Crowe, S. A., Maresca, J. A., Jones, C., Sturm, A., Henny, C., Fowle, D. A., Cox, R. P., DeLong, E. F. & Canfield, D. E. (2014). Deep-water anoxygenic photosynthesis in a ferruginous chemocline. *Geobiology*, 12: 322-339.
- Dalsgaard, T., Canfield, D. E., Petersen, J., Thamdrup, B. and Acuña-González, J. (2003). N<sub>2</sub> production by the anammox reaction in the anoxic water column of Golfo Dulce, Costa Rica. *Nature* 422(6932): 606-608.
- Darchambeau, F., Sarmiento, H., & Descy, J-P. (2014). Primary production in a tropical large lake: The role of phytoplankton composition. *Science of the Total Environment*, 473: 178-188.
- Davin, E. L. & Seneviratne, S. I. (2012). Role of land surface processes and direct radiation partitioning in simulating the European climate. *Biogeosciences* 9, 695-1707.
- Dee, D. P., Uppala, S. M., Simmons, A. J., Berrisford, P., Poli P., Kobayashi, S., Andrae, U., Balmaseda, M. A., Balsamo, G., Bauer, P., Bechtold, P., Beljaars, A. C. M., van de Berg, L., Bidlot, J., Bormann, N., Delsol, C., Dragani, R., Fuentes, M., Geer, A. J., Haimberger, L., Healy, S. B., Hersbach, H., Hólm, E. V., Isaksen, L., Källberg, P., Köhler, M., Matricardi, M., McNally, A. P., Monge-Sanz, B. M., Morcrette, J.-J., Park, B.-K., Peubey, C., de Rosnay, P., Tavolato, C., Thépaut, J.-N., and Vitart, F. (2011). The ERA-Interim reanalysis: Configuration and performance of the data assimilation system, *Q. J. Roy. Meteor. Soc.*, 137, 553–597,.
- Degens, E.T., and Stoffers. P. 1977. Phase boundaries as an instrument for metal concentration in geological systems. In: D.D. Klemm and H-J. Schneider, Eds., *Time and Strata-Bound Ore Deposits*. Springer-Verlag, New York, Heidelberg, Berlin" p.25-45.
- Degens, ET, von Herzen RP, Wong HK, Deuser WG, Jannasch HW (1973) Lake Kivu: structure, chemistry and biology of an east African rift lake. *Geol Rundsch* 62 (1): 388-404.
- Dehairs F., Baeyens W., and Goeyens L. (1992) Accumulation of suspended barite at mesopelagic depths and export production in the Southern Ocean. *Science* 258, 1332–1335.
- Descy J.-P., F. Darchambeau, M. Schmid (2012). *Lake Kivu: Limnology and Biogeochemistry of a tropical great lake*. Aquatic Ecology Series, Springer, 190 p
- Descy, J.-P., Hardy, M.-A., Stenuite, S., Pirlot, S., Leporcq, B., Kimirei, I., Sekadende, B., Mwaitega, S.R. & Sinyenza, D. (2005). Phytoplankton pigments and community composition in Lake Tanganyika. *Freshwater Biology* 50(4):668-684.
- Elderfield H. (1990). Tracers of ocean paleoproductivity and paleochemistry: an introduction. *Paleoceanography* 5: 711-717.
- Fægri K., Kaland P.E., Krzywinski K. (1989). *Textbook on pollen analysis*. John Wiley & sons, 3208 pp.
- Falkner, K.K., Klinkhammer, G.P Bowers, T.S, Todd, J.F, Lewis, B.L, Landing, W.M., Edmond J.M. (1993). The behavior of barium in anoxic marine waters. *Geochim. Cosmochim. Acta*, 57, 537-554
- Feldman G.C. & McClain Ch.R., 2014. *Ocean Color Web, MODIS Aqua and Terra v6*. NASA Goddard Space Flight Center. Eds. Kuring, N., Bailey, S. W. Access on Decembre 2014. <http://oceancolor.gsfc.nasa.gov/>
- Fogel, M. L., & Cifuentes, L. A. (1993). Isotope fractionation during primary production, p 73-98. In M. H. Engel & S. A. Macko (eds.), *Organic geochemistry*, Plenum Press, New York
- Foot et al.: Foote KG, Knudsen H, Vestnes G. (1987). Calibration of acoustic instruments for fish density estimation: a practical guide. ICES Cooperative Research Report 144.
- Godlewska M, Colon M, Jóźwik A, Guillard J. (2011). How pulse lengths impact fish stock estimations during hydroacoustic measurements at 70 kHz. *Aquat Living Resour.* 24:71–78.
- François Chr., Brisson A., Le Borgne P. & Marsouin A. (2002). Definition of a radiosounding database for sea surface brightness temperature simulations - Application to sea surface temperature retrieval algorithm determination. *Remote Sensing of Environment*, 81: 309-326.
- Frank V. (1989). Mission d'évaluation de la réussite de l'introduction des Isambaza au lac Kivu (Octobre-Novembre 1976). (Evaluation mission of the success of the introduction of Isambaza to Lake Kivu. (October–November, 1976) In French.) Séminaire : Trente ans après l'introduction de l'Isambaza au lac Kivu. (Seminar: 30 years after the introduction of Isambaza to Lake Kivu. In French.) *Projet RWA/87/012*: 1–3.

- Franz B.A., Kwiatkowska E.J., Meister G. & McClain Ch.R., 2007. Utility of MODIS-Terra for Ocean Color Applications. Proc. SPIE 6677, 14 p.
- Fripiat F., Corvaisier R., Navez J., Elskens M., Shoemann V., Leblanc K., André L., Cardinal D. (2009) Measurements of production-dissolution rates of marine biogenic silica by <sup>30</sup>Si-isotope dilution using a high resolution sector field ICP-MS. *Limnology and oceanography: Methods*, 7, 470-478.
- Geilert, S., Vroon, P.Z., Keller, N.S. Gudbrandsson, S., Stefánsson, A. van Bergen M. J. (2015). Silicon isotope fractionation during silica precipitation from hot-spring waters: Evidence from the Geysir geothermal field, Iceland. *Geochim. Cosmochim. Acta*, 164, 403-427
- Gordon H.R. & Wang M., 1994. Retrieval of water-leaving radiance and aerosol optical thickness over the oceans with SeaWiFS: a preliminary algorithm. *Applied Optics*, 33, 3, 443-452.
- Grote, J., Jost, G., Labrenz, M., Herndl, G. J., & Jürgens, K. (2008). Epsilonproteobacteria represent the major portion of chemoautotrophic bacteria in sulfidic waters of pelagic redoxclines of the Baltic and Black Seas. *Applied and Environmental Microbiology*, 74: 7546-7551.
- Guillard J. et Vergès C. (2007). The Repeatability of Fish Biomass and Size Distribution Estimates obtained by Hydroacoustic Surveys Using Various Survey Designs and Statistical Analyses. *International Review of Hydrobiology*, 92, 6: 605–617.
- Guillard, J., Darchambeau, F., Masiya, P., Mulungula, C.D. and Descy, J.P. (2012). Is the fishery of the introduced Tanganyika sardine (*Limnothrissa miodon*) in Lake Kivu (East Africa) sustainable? *Journal of Great Lakes Research* 38 (2012): 524–533.
- Horion S., Bergamino N., Stenuite S., Descy J.-P., Plisnier P.-D., Loisel S.A. & Cornet Y. (2010). Optimized extraction of daily bio-optical time series derived from MODIS/Aqua imagery for Lake Tanganyika, Africa. *Remote Sensing of Environment* 114, 781-791.
- Hughes H.J., Delvigne, C., Korntheuer, M., de Jong, J., André L., Damien Cardinal D. (2011) Controlling the mass bias introduced by anionic and organic matrices in silicon isotopic measurements by MC-ICP-MS. *Journal of Analytical Atomic Spectrometry*, 26, 1892-1896.
- Hughes, H.J., Sondag, F., Santos, R.V., André, L. and Cardinal D. (2013). The riverine silicon isotope composition of the Amazon Basin. *Geochimica Cosmochimica Acta*, 121, 637-651.
- Isumbiso, M., Sarmiento, H., Kaningini, B., Micha, J-C., & Descy, J-P. (2006) Zooplankton of Lake Kivu, East Africa, half a century after the Tanganyika sardine introduction. *Journal of Plankton Research*, 28: 971-989
- Jannasch, H. W. (1975). Methane oxidation in Lake Kivu (central Africa), *Limnol. Oceanogr.*, 20: 860–864
- Jensen, M. M., Kuypers, M. M. M., Lavik, G. and Thamdrup, B. (2008). Rates and regulation of anaerobic ammonium oxidation and denitrification in the Black Sea. *Limnology and Oceanography* 53(1): 23-36.
- Jensen, M. M., Petersen, J., Dalsgaard, T. and Thamdrup, B. (2009). Pathways, rates, and regulation of N<sub>2</sub> production in the chemocline of an anoxic basin, Mariager Fjord, Denmark. *Marine Chemistry* 113(1-2): 102-113.
- Jorgensen, K. S. (1989). Annual Pattern of Denitrification and Nitrate Ammonification in Estuarine Sediment. *Applied and Environmental Microbiology* 55(7): 1841-1847.
- Jost, G., Zubkov, M. V., Yakushev, E., Labrenz, M., & Jurgens, K. (2008). High abundance and dark CO<sub>2</sub> fixation of chemolithoautotrophic prokaryotes in anoxic waters of the Baltic Sea. *Limnology and Oceanography*, 53: 14-22.
- Joye, S. B. and Hollibaugh, J. T. (1995). Influence of sulfide inhibition of nitrification on nitrogen regeneration in sediments. *Science* 270(5236): 623-625.
- Jung, J. Y., Kang, S. H., Chung, Y. C. and Ahn, D. H. (2007). Factors affecting the activity of anammox bacteria during start up in the continuous culture reactor. *Water Science and Technology*. 55: 459-468.
- Kalyuzhnyi, S., Gladchenko, M., Mulder, A. and Versprille, B. (2006). DEAMOX-New biological nitrogen removal process based on anaerobic ammonia oxidation coupled to sulphide-driven conversion of nitrate into nitrite. *Water Research* 40(19): 3637-3645.
- Kaningini, B. (1995). Etude de la croissance, de la reproduction et de l'exploitation de *Limnothrissa miodon* au lac Kivu, bassin de Bukavu (Zaïre). Thèse de Doctorat en Sciences, Biologie, F.U.N.D.P., Facultés des Sciences, Namur, 166 p.

- Kaningini, B., Micha, J.C. Vandenhaute, J., Platteau, J.P., Watongoka, H., Mélard, C., Wilondja, M.K. and Isumbisha, M. (1999). Pêche du Sambaza au filet maillant dans le lac Kivu. Presses Universitaires de Namur, Namur, 187 p.
- Kankaala, P., Bellido, J. L., Ojala, A., Tulonen, T., & Jones, R. I. (2013). Variable production by different pelagic energy mobilizers in boreal lakes. *Ecosystems*, 16: 1152-1164.
- Katsev, S, Aaberg, A.A., Crowe, S.A. & Hecky, R.E. (2014) Recent warming of Lake Kivu. *Plos one*, vol 9, issue 10, 1-7.
- Keeling, R. F., & Garcia, H. E. (2002). The change in oceanic O<sub>2</sub> inventory associated with recent global warming. *Proceedings of the National Academy of Sciences*, 99: 7848-7853.
- Kilham P., Kilham S. S. and Hecky R. E. (1986) Hypothesized resource relationships among African planktonic diatoms. *Limnol. Oceanogr.*, 31: 1169-1181.
- Kilham, P., & Kilham, S. S. (1990). Endless summer: internal loading processes dominate nutrient cycling in tropical lakes. *Freshwater Biology*, 23: 379-389.
- Knox A, Bertuzzo E, Maria L, Odermatt D, Verrecchia E & Rinaldo A (2014). Optimizing a remotely sensed proxy for plankton biomass in Lake Kivu. *International Journal of Remote Sensing* Vol 35, n°13, 5219-5238.
- Lamboeuf M. (1989). Estimation de l'abondance du stock d'Isambaza (*Limnothrissa miodon*), résultats de la prospection acoustique de septembre 1989. RWA/87/012/DOC/TR/20.
- Lamboeuf M. (1991). Abondance et répartition du *Limnothrissa miodon* du lac Kivu, résultat des prospections acoustiques d'avril 1989 à juin 1991. RWA/87/012/DOC/TR/46.
- Lauwaet, D., van Lipzig, N. P. M., Van Weverberg, K., De Ridder, K., Goyens, C. (2011). The precipitation response to the desiccation of Lake Chad, Q. J. Roy. Meteor. Soc., 138, 707-719, DOI:10.1002/qj.942.
- Loiselle, S., Cózar, A., Adgo, E., Ballatore, T., Chavula, G., Descy, J-P., Harper, D. M., Kansime, F., Kimirei, I., Langenberg, V., Ma, R., Sarmiento, H., Odada, E. & Descy, J-P. (2014). Decadal trends and common dynamics of the bio-optical and thermal characteristics of the African Great Lakes. *PLoS ONE*. 9, 4, e93656
- Love R.H. (1977). Target strength of an individual fish at any aspect. *Journal of the Acoustical Society of America* 72:1397-1402.
- MacCallum S. & Merchant C.J. (2013). ATSR Reprocessing for Climate Lake Surface Water Temperature: ARC-Lake, University of Edinburgh. <http://datashare.is.ed.ac.uk/handle/10283/88> (last consultation 26/5/2015).
- Marschall, E., Jogler, M., Henssge, U., & Overmann, J. (2010) Large-scale distribution and activity patterns of an extremely low-light adapted population of green sulphur bacteria in the Black Sea. *Environmental Microbiology*, 12:1348-1362
- Marshall, B. E. (1991). Seasonal and annual variations in the abundance of the clupeid *Limnothrissa miodon* in Lake. *Journal of Fish Biology* 39: 641-648.
- McCarthy S.C., Gould R.W. Jr., Richman J., Kearney C. & Lawson A. (2012). Impact of Aerosol Model Selection on Water-Leaving Radiance Retrievals from Satellite Ocean Color Imagery. *Remote Sensing*, 4, 3638-3665.
- McClain E.P., Pichel W.G. & Walton C.C., (1985). Comparative performance of AVHRR-based multichannel sea surface temperatures. *Journal of Geophysical Research: Oceans*, 90: 11587-11601.
- Mehner Thomas (2012). Diel vertical migration of freshwater fishes: proximate triggers, ultimate causes and research perspectives. *Freshwater Biology*, vol.: 57 (7): 1342-1359.
- MINITERE (2003). Stratégie Nationale et Plan d'action pour la conservation de la biodiversité au Rwanda. 81 pp.
- Mironov, D., Heise, E., Kourzeneva, E., Ritter, B., Schneider, N., and Terzhevik, A. (2010). Implementation of the lake parameterisation scheme FLake into the numerical weather prediction model COSMO, *Boreal Environ. Res.*, 15, 218-230,
- Moise AF and Hudson DA (2008) Probabilistic predictions of climate change for Australia and southern Africa using the reliability ensemble average of IPCC CMIP3 model simulations. *Journal of Geophysical Research: Atmospheres* 113(15): 1–26: doi:10.1029/2007JD009250.
- Montoya, J. P., Carpenter, E. J. & Capone, D. G. (2002). Nitrogen fixation and nitrogen isotope abundances in zooplankton of the oligotrophic North Atlantic. *Limnology and Oceanography*, 47: 1617–1628.

- Morana C., Sarmiento H., Descy, J-P., Gasol, J. M., Borges, A. V., Bouillon, S., & Darchambeau, F. (2014). Production of dissolved organic matter by phytoplankton and its uptake by heterotrophic prokaryotes in large tropical lakes. *Limnology and Oceanography*, 59: 1364-1375.
- Murray, J. W., Codispoti, L. A., & Friederich, G. E. (1995). Oxidation-reduction environments: the suboxic zone in the Black Sea. p. 157-176. In C. P. Huang, C. R. O'Melia, and J. J. Morgan (eds), *Aquatic chemistry: Interfacial and interspecies processes*. American Chemical Society: *Advances in Chemistry Series*, 244
- Muvundja F et al (2009) Balancing nutrient inputs to Lake Kivu. *J Great Lakes Res* 35:406-418.
- Myklestad, S. M. (2000). Dissolved organic carbon from phytoplankton, p. 111-148. In P. Wangersky [ed], *Marine chemistry*. Springer.
- Nayar, A. (2009). A lakeful of trouble. *Nature* 460 : 321-323
- Niang I, Ruppel O, Abdrabo M, Essel A, Lennard C, Padgham J, et al. (2014) Africa. In: Barros VR, Field C., Dokken DJ, Mastrandrea MD, Mach KJ, Bilir TE, et al. (eds) *Climate Change 2014: Impacts, Adaptation, and Vulnerability. Part B: Regional Aspects. Contribution of Working Group II to the Fifth Assessment Report of the Intergovernmental Panel on Climate Change*. Cambridge, United Kingdom and New York, NY, USA: Cambridge University Press, 1199–1265.
- Nicholson S (1996) A review of climate dynamics and climate variability in Eastern Africa. In: Johnson TC and Odada E. (eds.) *Limnology, Climatology and paleoclimatology of the East African lakes*. Amsterdam: CRC Press, 25–56.
- Omondi P, Awange JL, Ogallo L a., Okoola R a. and Forootan E (2012) Decadal rainfall variability modes in observed rainfall records over East Africa and their relations to historical sea surface temperature changes. *Journal of Hydrology*. Elsevier B.V. 464-465: 140–156: doi:10.1016/j.jhydrol.2012.07.003.
- Omondi P, Ogallo L, Anyah R, Muthama JM and Ininda J (2013) Linkages between global sea surface temperatures and decadal rainfall variability over Eastern Africa region. *International Journal of Climatology* 33(8): 2082–2104: doi:10.1002/joc.3578.
- O'Reilly, C. M., Alin, S. R., Plisnier, P. D., Cohen, A. S., & McKee, B. A. (2003). Climate change decreases aquatic ecosystem productivity of Lake Tanganyika, Africa. *Nature*, 424(6950), 766-768.
- Otieno VO and Anyah RO (2012) CMIP5 simulated climate conditions of the Greater Horn of Africa (GHA). Part I: contemporary climate. *Climate Dynamics* 41(7-8): 2081–2097: doi:10.1007/s00382-012-1549-z.
- Panitz H-J et al. (2014) COSMO-CLM (CCLM) climate simulations over CORDEX Africa Domain: analysis of the ERA-Interim driven simulations at 0.44° and 0.22° resolution. *Climate Dyn.* 41, 2081-2097.
- Parker-Stetter S. L., Rudstam L. G., Sullivan P. J. & Warner D. M. (2009). Standard operating procedures for fisheries acoustic surveys in the Great Lakes. *Great Lakes Fisheries Commission Special Publication*, 2009-01.
- Parkhurst, DL, 1995 User's guide to PHREEQC- a computer program for speciation, reaction path, advective-transport, and inverse geochemical calculations. *Water resources investigations report 95-4227*. US Geological Survey, Earth Sciences Information Section, 151 pp.
- Pasche N, Alunga G, Mills K, Muvundja F, Ryves DB, Schurter M, Wehrli B, Schmid M (2010) Abrupt onset of carbonate deposition in Lake Kivu during the 1960s: response to recent environmental changes. *J Paleolimnol* 44: 931-946.
- Pasche, N., Dinkel, C., Müller, B., Schmid, M., Wüest, A., & Wehrli, B. (2009). Physical and bio-geochemical limits to internal nutrient loading of meromictic Lake Kivu. *Limnology and Oceanography*, 54:1863-1873.
- Pérez, M. T., and R. Sommaruga (2006). Differential effect of algal- and soil-derived dissolved organic matter on alpine lake bacterial community composition and activity. *Limnology & Oceanography* 51: 2527-2537.
- Philipp A, Beck C, Huth R and Jacobeit J (2014) Development and comparison of circulation type classifications using the COST 733 dataset and software. *International Journal of Climatology*: doi:10.1002/joc.3920.
- Platz Th., Foley S. & André L. (2004) Low-pressure fractionation of the Nyiragongo volcanic rocks, Virunga Province, D. R. Congo. *Jour. of Volc. and geothermal Research* 136: 269-295
- Post, D. M. (2002). Using stable isotopes to estimate trophic position: models, methods, and assumptions. *Ecology*, 83: 703-718.

- Ragnarsdottir K.V. & Walther, J.V., 1983. Pressure sensitive "silica geothermometer" determined from quartz solubility experiments at 250°C. *Geochim. Cosmochim. Acta* 47, 941-946
- Ragueneau O., Savoye N, Del Amob Y., Cottenc J., Tardiveaua B., Leynaerta A. (2005). A new method for the measurement of biogenic silica in suspended matter of coastal waters: using Si:Al ratios to correct for the mineral interference. *Continental Shelf Research* 25: 697–710.
- Reimer PJ, Bard E, Bayliss A, Beck JW, Blackwell PG, Bronk Ramsey C, Buck CE, Cheng H, Edwards RL, Friedrich M, Grootes PM, Guilderson TP, Hafliadason H, Hajdas I, Hatté C, Heaton TJ, Hoffmann DL, Hogg AG, Hughen KA, Kaiser KF, Kromer B, Manning SW, Niu M, Reimer RW, Richards DA, Scott EM, Southon JR, Staff RA, Turney CSM, van der Plicht J. 2013. IntCal13 and Marine13 radiocarbon age calibration curves 0–50,000 years cal BP. *Radiocarbon* 55(4):1869–1887.
- Renberg I (1990) A procedure for preparing large sets of diatoms slides from sediment cores. *Journal of Paleolimnology*, 4: 87-90.
- Reuss, N., Conley, D.J., (2005). Effects of sediment storage conditions on pigment analyses. *Limnol. Oceanogr.: Methods* 3:477-487
- Roland, F. (2012). Contribution à la description du cycle de l'azote au sein des eaux superficielles du lac Kivu (Afrique de l'Est). MSc thesis, Université de Liège, Belgium [Contribution to the description of the nitrogen cycle in the mixolimnion of Lake Kivu (East Africa)]
- Romero JR et al (2004) One- and three- dimensional biogeochemical simulations of two differing reservoirs. *Ecol Model* 174:143-160
- Ross K.A., Schmid M., Ogorka S., Muvundja F.A., Anselmetti F.S. (2015). The history of subaquatic volcanism recorded in the sediments of Lake Kivu; East Africa. *Journal of Paleolimnology* 54: 137-152
- Rysgaard, S., Risgaard-Petersen, N. and Sloth, N. P. (1996). "Nitrification, denitrification, and nitrate ammonification in sediments of two coastal lagoons in Southern France." *Hydrobiologia* 329(1-3): 133-141.
- Sarmiento, H. & J.-P. Descy (2008). Use of marker pigments and functional groups for assessing the status of phytoplankton assemblages in lakes. *J. Appl. Phycol.*, 20:1001–1011.
- Sarmiento, H., Amado, A. M. & Descy, J-P (2013). Climate change in tropical fresh waters (comment on the paper 'Plankton dynamics under different climatic conditions in space and time' by de Senerpont Domis et al.,) *Freshwater Biology*. 58, 10, p. 2208-2221
- Sarmiento, H., and J. M. Gasol (2012). Use of phytoplankton-derived dissolved organic carbon by different types of bacterioplankton. *Environmental Microbiology* 14: 2348-2360.
- Sarmiento, H., Isumbisho, M. & Descy, J.-P (2006). Phytoplankton ecology of Lake Kivu (Eastern Africa). *Journal of Plankton Research*, 28 (9), 815-829.
- Sarmiento, H., Isumbisho, M., Stenuite, S., Darchambeau, F., Leporcq, B., & Descy, J- P. (2009). Phytoplankton ecology of Lake Kivu (eastern Africa): biomass, production and elemental ratios. *International Association of Theoretical and Applied Limnology*, 30: 709-713.
- Sarmiento, H., Leitao, M., Stoyneva, M., Couté, A., Compère, P., Isumbisho, M., & Descy, J-P. (2007). Species diversity of pelagic algae in Lake Kivu (East Africa). *Cryptogamie-Algologie*, 28, 245:269.
- Savage, P.S, Georg, R.B., Armytage, R.M.G., Williams H.M., Halliday, A.N., 2010. Silicon isotope homogeneity in the mantle. *Earth Planet. Sci. Lett.* 295, 139–146.
- Savijärvi, H. and Järvenoja, S.: Aspects of Fine-Scale Climatology Over Lake Tanganyika as Resolved by a Mesoscale Model, *Meteorol. Atmos. Phys.*, 73, 77-88, 2000.
- Sayama, M., Risgaard-Petersen, N., Nielsen, L. P., Fossing, H. and Christensen, P. B. (2005). Impact of bacterial NO<sub>3</sub> - transport on sediment biogeochemistry. *Applied and Environmental Microbiology* 71(11): 7575-7577.
- Schmid M. and Wüest A. (2012). Stratification, mixing and transport processes in Lake Kivu. In Descy J.-P., F. Darchambeau, M. Schmid: *Lake Kivu: Limnology and Biogeochemistry of a tropical great lake. Aquatic Ecology Series*, Springer, p.13-29.
- Schmid, M., Halbwegs, M., Wehrli, B., & Wüest, A. (2005). Weak mixing in Lake Kivu: new insights indicate increasing risk of uncontrolled gas eruption. *Geochemistry, Geophysics, Geosystems*, 6(7).

- Schmidt S., Howa H., Diallo A., Martin J., Cremer M., Duros P., Fontanier C., Deflandre B., Metzger E., Mulder T. (2014). Recent sediment transport and deposition in the Cap-Ferret Canyon, South-East margin of Bay of Biscay. *Sea research part II : Topical studies in oceanography* 104 : 134-144.
- Shongwe ME, van Oldenborgh GJ, van den Hurk B and van Aalst M (2011) Projected Changes in Mean and Extreme Precipitation in Africa under Global Warming. Part II: East Africa. *Journal of Climate* 24(14): 3718–3733: doi:10.1175/2010JCLI2883.1.
- Sirevåg, R., Buchanan, B. B., Berry, J. A., & Troughton, J. H. (1977). Mechanisms of CO<sub>2</sub> fixation in bacterial photosynthesis studied by the carbon isotope fractionation technique. *Archives of Microbiology*, 112:35-38.
- Snoeks J, Kaningini B, Masilya M, Nyinawamwiza L, Guillard J. (2012). Fishes in Lake Kivu: Diversity and Fisheries. In: Descy J-P, Darchambeau F, Schmid M (eds.). *Lake Kivu-Limnology and biogeochemistry of a tropical great Lake*. Aquatic Ecology series, Springer 5, 127-149
- Snoeks, J., De Vos, L. & Thys Van Den Audenaerde, D. (1997). The ichthyogeography of Lake Kivu. *South African Journal of Science* 93: 579–584.
- Spigel, R. H. and G. W. Coulter (1996). Comparison of hydrology and physical limnology of the East African Great Lakes: Tanganyika, Malawi, Kivu and Turkana (with reference to some North American Great Lakes). *The limnology, climatology and paleoclimatology of the East African Lakes*. T. C. Johnson and E. O. Odada. Amsterdam, Gordon & Breach Publ.: 103-139.
- Stenuite, S., S. Pirlot, M.-A. Hardy, H. Sarmiento, A.-L. Tarbe, B. Leporcq and J.-P. Descy (2007). Phytoplankton production and growth rate in Lake Tanganyika: evidence of a decline in primary productivity in recent decades. *Freshwater Biol* 52: 2226-2239.
- Stepanenko, V. M., Goyette, S., Martynov, A., Perroud, M., Fang, X. and Mironov, D. (2010). First steps of a Lake Model Intercomparison Project: LakeMIP. *Boreal Environ. Res.* 15, 191-202.
- Stepanenko, V. M., Jöhnk, K., Machulskaya, E., Mironov, D., Perroud, M., Subin, Z., Nordbo, A. and Mammarella, I. (2013). Simulation of surface energy fluxes and stratification of a small boreal lake by a set of one-dimensional models. *Tellus A* 66, 21389.
- Stepanenko, V. M., Martynov, A., Jöhnk, K. D., Subin, Z. M., Perroud, M., Fang, X., Beyrich, F., Mironov, D. and Goyette, S. (2012). A one-dimensional model intercomparison study of thermal regime of a shallow turbid midlatitude lake. *Geosci. Model Dev.* 6, 1337-1352.
- Stoyneva, M. P., J. P. Descy, V. Balagué, P. Compère, M. Leitaó, H. Sarmiento (2012). The queer Tetraëdron minimum from Lake Kivu (Eastern Africa): is it a result of a human impact?" *Hydrobiologia* 698:273-283. DOI 10.1007/s10750-012-1092-2
- Sun, X., Olofsson, M., Anderson, P.S., Bryan, F., Legrand, C., Humborg, C., Mörrth, C-M. (2014) Effects of growth and dissolution on the fractionation of silicon isotopes by estuarine diatoms. *Geochim. Cosmochim. Acta*, 130, 156-166.
- Tassi, F., Vaselli, O., Tedesco, D., Montegrossi, G., Darrah, T. and co-authors. 2009. Water and gas chemistry at Lake Kivu (DRC): geochemical evidence of vertical and horizontal heterogeneities in a multibasin structure. *Geochim. Geophys. Geosy* 10 DOI: 10.1029/2008GC002191
- Taylor, G. T., Iabichella, M., Ho, T. Y., Scranton, M. I., Thunell, R. C., Muller-Karger, F., & Varela, R. (2001). Chemoautotrophy in the redox transition zone of the Cariaco Basin : A significant midwater source of organic carbon production. *Limnology and Oceanography*, 46: 150-155.
- Thiery W, Davin E, Panitz H-J, Demuzere M, Lhermitte S and Van Lipzig NPM (2015a) The impact of the African Great Lakes on the regional climate. *Journal of Climate* 28: 4061–4085.
- Thiery W, Davin E, Seneviratne S, Panitz H-J, Bedka K, Demuzere M, et al. (2015b) Present and future impact of the African Great Lakes on the regional climate. *COSMO User Seminar*. Offenbach am Main, 36.
- Thiery W, Martynov A, Darchambeau F, Descy J-P, Plisnier P-D, Sushama L, et al. (2014a) Understanding the performance of the FLake model over two African Great Lakes. *Geoscientific Model Development* 7: 317–337: doi:10.5194/gmd-7-317-2014.
- Thiery W, Stepanenko VM, Fang X, Jöhnk KD, Li Z, Martynov A, et al. (2014b) LakeMIP Kivu: Evaluating the representation of a large, deep tropical lake by a set of one-dimensional lake models. *Tellus A: Dynamic Meteorology and Oceanography* 66: 21390: doi:10.3402/tellusa.v66.21390.

- Tierney, J. E., M. T. Mayes, N. Meyer, C. Johnson, P. W. Swarzenski, A. S. Cohen and J. M. Russell (2010). Late-twentieth-century warming in Lake Tanganyika unprecedented since AD 500. *Nature Geoscience* 3(6): 422-425.
- Verburg, P. and Hecky, R. E (2003). Wind patterns, Evaporation and Related Physical Variables in Lake Tanganyika, East-Africa, *J. Great Lakes Res.*, 29, 48-61,.
- Verburg, P., & Hecky, R. E. (2009). The physics of the warming of Lake Tanganyika by climate change. *Limnology and Oceanography*, 54: 2418-2430
- Verdú, M. (2002). Age at maturity and diversification in woody angiosperms. *Evolution* 56: 1352-1361
- Walton C.C., Pichel W.G., Sapper J.F. & May D.A. (1998). The development and operational application of nonlinear algorithms for the measurement of sea surface temperatures with the NOAA polar-orbiting environmental satellites. *Journal of Geophysical Research: Oceans*, 103: 27999-28012.
- Wenk, C. B., Bleses, J., Zopfi, J., Veronesi, M., Bourbonnais, A., Schubert, C. J., Niemann, H. and Lehmann, M. F. (2013). Anaerobic ammonium oxidation (anammox) bacteria and sulfide-dependent denitrifiers coexist in the water column of a meromictic south-alpine lake. *Limnology and Oceanography* 58(1): 1-12.
- Wright, S.W., Jeffrey, S.W., Mantoura, R.F.C., Llewellyn, C.A., Bjornland, T., Repeta, D. and Welschmeyer, N. (1991). Improved HPLC method for the analysis of chlorophylls and carotenoids from marine phytoplankton. *Mar. Ecol. Prog. Ser.* 77, 183-196.
- Yeates PS, Imberger J (2004) Pseudo two-dimensional simulations of internal and boundary fluxes in stratified lakes and reservoirs. *Inter J River Basin Management* 1:297-319
- Zlotnik, I., and Z. Dubinsky. (1989). The effect of light and temperature on DOC excretion by phytoplankton. *Limnology and Oceanography* 34: 831-839.

## **ANNEXES**

**ANNEX 1 : COPY OF THE PUBLICATIONS**

**ANNEX 2 : MINUTES OF THE FOLLOW-UP COMMITTEE MEETINGS**